



GRIGORE T. POPA UNIVERSITY OF
MEDICINE AND PHARMACY IASI

An insight into the evolving role of cardiovascular imaging techniques in clinical practice

Habilitation Thesis

Radu Andy Sascău, MD, PhD

Associate Professor

Contents

REZUMATUL TEZEI	1
THESIS SUMMARY	3
SECTION I. SYNOPSIS OF PERSONAL ACADEMIC, PROFESSIONAL, AND SCIENTIFIC ACCOMPLISHMENTS	5
SECTION II. SCIENTIFIC ACCOMPLISHMENTS	10
Introduction	10
Chapter 1. Role of cardiac imaging techniques in diagnosis and risk stratification of patients with cardiovascular disease	15
1.1. Background	15
1.2. LUS and BIS in HF with reduced left ventricular ejection fraction	17
1.2.1. Aim	17
1.2.2. Materials	17
1.2.3. Results	20
1.2.4. Discussion	25
1.2.5. Conclusions	27
1.3. Identification of subgroups of risk in some patients with HF and HFrEF	27
1.3.1. Aim	27
1.3.2. Material and methods	27
1.3.3. Results	29
1.3.4. Discussion	35
1.3.5. Conclusions	37
1.4. The role of New Multimodality Imaging in Patients with Hypertrophic Cardiomyopathy	37
1.4.1. Aim	37
1.4.2. Methods	37
1.4.3. Results and discussion	37
1.4.4. Conclusions	50
1.5. Multimodality Imaging in Patients with Infiltrative Cardiomyopathies	50
1.5.1. Aim	50
1.5.2. Material and methods	50
1.5.3. Results and discussion	50
1.5.4. Conclusions	73
Chapter 2. Predictive power of cardiovascular imaging in CKD patients	74
2.1. Background	74
2.2. Predictors for mortality in HD patients	76
2.2.1. Aim	76
2.2.2. Material and methods	76
2.2.3. Results	77

2.2.4. Discussion	82
2.2.5. Conclusions	84
2.3. Overhydration, Cardiac Function and Survival in HD Patients	84
2.3.1. Aim	84
2.3.2. Material and methods	84
2.3.3. Results	85
2.3.4. Discussion	90
2.2.5. Conclusions	91
2.4. Optimal risk prediction in hemodialysis patients	92
2.4.1. Aim	92
2.4.2. Material and methods	92
2.4.3. Results	93
2.4.4. Discussion	97
2.4.5. Conclusions	98
2.5. Methods of dry weight assessment in low cardiovascular risk hemodialysis patients	99
2.5.1. Aim	99
2.5.2. Material and methods	99
2.5.3. Results	101
2.5.4. Discussion	106
2.5.5. Conclusions	108
2.6. Cardiac imaging in advanced CKD	108
2.6.1. Aim	108
2.6.2. Material and methods	108
2.5.3. Results and discussion	108
2.5.4. Conclusion	116
Chapter 3. Imaging the heart in sleep-related breathing disorder	117
3.1. Background	117
3.2. Review of Echocardiographic Findings in Patients with OSA	118
3.2.1. Aim	118
3.2.2. Materials	118
3.2.3. Results and discussion	118
3.2.4. Conclusion	131
SECTION III. FUTURE DEVELOPMENTS IN THE ACADEMIC, PROFESSIONAL AND RESEARCH FIELD	132
III.1. Developments in the academic area	132
III.2. Future professional improvements	133
III.3. Perspectives for research field	133
III.4. Final remarks	142
Section IV. References	143

ABBREVIATION LIST

ACEI - angiotensin-converting enzyme inhibitors
AFO- absolute fluid overload
AHI – apnea hypopnea index
AIC- akaike information criterion
ARB - angiotensin II receptor blockers.
ATTR - amyloidosis and transthyretin amyloid
BIC- bayesian information criterion
BIS - bioimpedance spectroscopy
BMI- body mass index
CAD – coronary artery disease
CART – Classification and Regression Tree
CD146 – cluster of differentiation 146
CHF-chronic heart failure
CI- confidence interval
CKD - chronic kidney disease
CKD-EPI - Chronic Kidney Disease Epidemiology Collaboration
CMR- cardiac magnetic resonance
CRP – C-reactive protein
CT- computed tomography
CT-1 – cardiotrophin-1
CVD- cardiovascular disease
CVE- cardiovascular events
DBP – diastolic blood pressure
eGFR – estimated glomerular filtration rate
ELW- extravascular lung water
FWLS - free wall longitudinal strain
GLS - global longitudinal strain
HCM - hypertrophic cardiomyopathy
HD- hemodialysis
HDL – high-density lipoprotein
HF- heart failure
HH - hereditary hemochromatosis
HR- hazard ratio
ICD -implantable cardioverter defibrillator
ICMs - infiltrative cardiomyopathies
ICW- intracellular water
IVSD – interventricular septum thickness
LAA – left atrial area
LAVI – left atrial volume index
LAVI – left atrial volume index
LDL – low-density lipoprotein
LTI – lean tissue index
LUS - lung ultrasonography

LV – left ventricle
LV EDD – LV end diastolic diameter
LV EDVi – left ventricular end diastolic volume index
LV ESD – LV end systolic diameter
LV ESVi – left ventricular end systolic volume index
LVEF – left ventricular ejection fraction
LVMI - left ventricular mass index
LVOT- left ventricular outflow tract
LVPWT - left ventricular posterior wall thickness
MPI -myocardial performance index
NT-proBNP - N-Terminal Pro-Brain Natriuretic Peptide
NYHA- New York Heart Association
OSA - obstructive sleep apnea
PAPS – pulmonary artery systolic pressure
PAT – pulmonary artery acceleration time
PWD – posterior wall thickness
RAVI – right atrial volume index
RCM - restrictive cardiomyopathy
RFO – relative fluid overload
RVEDV – right ventricular end diastolic volume
RV-EF – right ventricular ejection fraction
RVESV – right ventricular end systolic volume
RV-MPI – right ventricular myocardial performance index
RWT – relative wall thickness
SBP – systolic blood pressure
SDB - sleep-disordered breathing
ST2 – soluble suppression of tumorigenesis 2
TAFO- time averaged fluid overload
TAPSE – tricuspid annular plane excursion
TBW – total body water
TTE -transthoracic echocardiography
ULC- ultrasound lung comets

REZUMATUL TEZEI

Profesia de cadru didactic reprezintă în primul rând o profesie cu o puternică influență asupra societății, având un rol însemnat în dezvoltarea resurselor umane și modelarea viitoarelor generații. Este o profesie complexă, a cărei reușită are la bază flexibilitatea, dinamismul, receptivitatea la nou și reflecția critică.

Întreaga activitate a cadrului didactic trebuie să fie orientată către dobândirea continuă de cunoștințe, abilități și competențe specifice centrate pe trei direcții esențiale: educație, sănătate, cercetare.

Astfel, chiar dacă satisfacțiile profesionale sunt numeroase, ele impun o pregătire multidisciplinară continuă pentru a putea face față cerințelor, exigențelor sau competiției existente în fiecare din aceste domenii.

Consider elaborarea acestei teze de abilitare un moment de bilanț care îmi permite o analiză a activității profesionale, academice și științifice din perioada postdoctorală. Lucrarea este structurată în conformitate cu recomandările Consiliului Național de Atestare a Titlurilor, Diplomelor și Certificatelor Universitare (CNATDCU) și conține o sinteză a preocupărilor mele anterioare, cât și direcțiile viitoare în plan academic, profesional și nu în ultimul rând al activității de cercetare.

Teza este structurată în 4 secțiuni : I - parcursul profesional; II - activitatea de cercetare din perioada postdoctorală; III - direcții de dezvoltare și proiecte de cercetare viitoare; IV – referințe bibliografice.

Secțiunea întâi a tezei de abilitare se referă pe scurt la rezultatele în plan academic, științific și medical obținute în cei 18 ani de activitate, până la poziția actuală de conferențiar universitar.

Secțiunea a doua este structurată metodic în 3 capitole și reflectă principala arie de interes, și anume importanța imagisticii cardiace, nu doar în patologia cardiovasculară, ci și în alte patologii conexe, renale și respiratorii, cu implicații cardiovasculare majore.

Primul capitol ilustrează beneficiile imagisticii cardiace în diagnosticul și stratificarea riscului la pacienții cu boli cardiovasculare. Tehnicile de imagistică cardiacă sunt adoptate în baza simptomelor individuale, caracteristicilor specifice și disponibilității locale.

În ultimii ani, cu ajutorul imagisticii cardiace multimodale s-au făcut progrese semnificative în diagnosticul și managementul terapeutic al insuficienței cardiace, aceasta reprezentând o problemă majoră de sănătate publică la nivel mondial.

Cu toate acestea, imagistica cardiacă este, de asemenea, utilă pentru identificarea precisă a diferitelor cardiomiopatii sau a bolilor cardiace structurale sau congenitale. Acest capitol sintetizează cele mai importante rezultate în această direcție.

Al doilea capitol evidențiază contribuția semnificativă a imagisticii cardiace multimodale în managementul pacienților cu boală cronică renală. Ilustrează principalele instrumente imagistice, utilizate în prezent pentru monitorizarea bilanțului hidric în boala cronică renală,

supraîncărcarea volemică fiind cel mai comun factor de risc modificabil, asociat cu un risc crescut de mortalitate la acești pacienți.

Deoarece pacienții cu afecțiuni renale cronice pot prezenta dispnee secundară supraîncărcării volemice, chiar și în absența bolilor cardiace structurale sau dimpotrivă pot prezenta o simptomatologie atipică, cantitatea de informații adusă de tehnicile imagistice mai noi este crucială pentru un diagnostic precis și instituirea măsurilor terapeutice într-un interval de timp util.

Interesul meu pentru acest subiect este parțial subliniat de granturile de cercetare și articolele incluse în prezenta teză de abilitare.

Capitolul trei prezintă utilitatea tehnicilor ecocardiografice standard, precum și a celor noi, în identificarea pacienților cu sindrom de apnee în somn de tip obstructiv, cu risc ridicat de a dezvolta insuficiență cardiacă clinic manifestă și alte evenimente adverse cardiace.

Screening-ul prin ecocardiografie transtoracică poate crește gradul de conștientizare cu privire la implicațiile cardiovasculare ale sindromului de apnee în somn de tip obstructiv. Acest lucru ar putea completa tehnicile educaționale, tehnologice și psihosociale actuale care vizează îmbunătățirea aderenței pacienților atât la terapia prin dispozitive, cât și la modificările stilului de viață.

Secțiunea a treia se referă la principalele direcții în activitatea didactică, clinică și de cercetare științifică viitoare.

În mod concret, în activitatea didactică am prezentat direcțiile de evoluție privind interacțiunea cu studenții, medicii rezidenți și colegii mai tineri. În activitatea clinică viitoare voi urmări acumularea de noi cunoștințe, implementarea de noi tehnici imagistice și dezvoltarea de noi competențe. Cercetarea științifică va fi orientată pe următoarele direcții de cercetare :

- *reabilitarea cardiovasculară la pacienți postinfarct miocardic tratați prin angioplastie coronariană percutană* - studiul modificărilor clinice și paraclinice – pornind de la ideea că infarctul miocardic rămâne o patologie de mare interes prin prognosticul nefast, iar optimizarea managementului multimodal este în atenția lumii medicale, cu accent în ultimele decade pe beneficiile recuperării cardiace.

- *disfuncția diastolică ventriculară stângă și strainul atrial stâng* - obiectivul principal al studiului va fi urmărirea puterii predictive a strainului atrial stâng în apariția disfuncției diastolice, a hipertensiunii pulmonare, a fibrilației atriale și a insuficienței cardiace după un infarct miocardic acut.

- *studiul infarctului miocardic cu artere coronare non-obstructive (MINOCA)* – obiectivul principal va fi evaluarea riscului de evenimente aritmice majore și a riscului de moarte subită în populația MINOCA, iar obiectivul secundar determinarea incidenței cumulative a reinfarctizării, examinarea etiologiei acestora și evaluarea valorii prognostice a imagisticii CMR.

În activitatea viitoare voi fi deschis în a aborda și alte teme de cercetare clinică în care să pot implica doctoranzii cu teme de cercetare de cardiologie sau alte specializări conexe.

Secțiunea a patra cuprinde referințele bibliografice care au stat la baza realizării prezentei teze de abilitare.

THESIS SUMMARY

The teaching profession is primarily a profession with a strong influence on society, having a significant role in the development of human resources and in shaping future generations. It is a complex profession whose success is based on flexibility, dynamism, receptivity to the new and critical reflection.

The entire teaching activity must be oriented towards the continuous acquisition of specific knowledge, skills and competencies focused on three essential directions: education, health, research.

Thus, even if the professional satisfaction is enormous, it requires a continuous multidisciplinary training in order to be able to meet the existing demands or competition in each of these fields.

I consider the elaboration of this habilitation thesis a moment of review, that allows me to retrospectively analyze my professional, academic and scientific activity beginning with the post-doctoral period.

The paper is structured in accordance with the recommendations of the The National Council for Attestation of University Degrees, Diplomas and Certificates (*rom. CNATDCU) and comprises a summary of my previous concerns as well as my future directions in academia, in the professional career and last but not least in the field of research.

The thesis is structured in 4 sections: I - professional path; II –research activity from the post-doctoral period; III - development directions and future research projects; IV - bibliography.

Section I briefly nominates the academic, scientific and medical achievements, obtained in 18 years of activity, up to the current position of associate professor.

Section II is methodically structured into 3 chapters and reflects my area of focus, namely the prominence of imaging the heart not only in cardiovascular diseases, but also in other pathologies that ultimately lead to the emergence of cardiac disorders.

Chapter 1 illustrates the benefits of cardiac imaging in the diagnosis and risk stratification of patients with cardiovascular disease. Cardiac imaging techniques are adopted based on individual symptoms, specific features and local availability.

In recent years, based on multimodality imaging techniques significant advances have been made in the diagnosis and therapeutic management of heart failure, which represents a major public health issue worldwide.

Nevertheless, cardiac imaging is also useful in accurately identifying various cardiomyopathies, or structural or congenital heart disease. This chapter synthesizes the most important results within this direction.

Chapter 2 highlights the significant contribution of multimodality cardiac imaging in advanced chronic kidney disease.

It focuses on the main imaging tools, currently used in guiding fluid management in chronic kidney disease, volume overload being the most common modifiable risk factor associated with an increased risk of mortality in these patients.

Since patients with chronic kidney disease may either present with dyspnea secondary to volume overload in the absence of CVD, or on the opposite may not develop classical symptoms, the amount of information brought by newer imaging techniques is crucial for an accurate diagnosis and a timely therapeutic intervention.

My interest on this topic is partially emphasized by the research grants and articles included in this habilitation thesis.

Chapter 3 presents the utility of standard and advanced echocardiographic techniques in the identification of patients with obstructive sleep apnea (OSA), at high risk of developing heart failure and future cardiac adverse events.

Echocardiographic screening might raise awareness with regard to the cardiovascular implication of OSA. This could complete the current educational, technological and psychosocial techniques aimed to improve patient adherence to both device therapy and lifestyle changes.

Section three emphasizes the main directions I have for the future didactic, clinical and scientific research activity.

Specifically, into what concerns the teaching activity I intend to improve interaction with students, resident physicians and younger colleagues.

Regarding, my future clinical activity, I will pursue the acquisition of new knowledge and the development of new skills. Scientific research will be focused on the following directions:

- *rehabilitation in post-myocardial infarction patients treated by percutaneous coronary intervention* - study of clinical and paraclinical changes.

Acute myocardial infarction remains a pathology of great interest due to its poor prognosis and the optimization of its multimodal management is in the attention of the medical world, with emphasis in recent decades on the benefits of cardiac rehabilitation

The optimization of the management of these patients is still a major concern for the health care system, with emphasis in recent decades on the benefits of cardiac rehabilitation.

- *left ventricular diastolic dysfunction and left atrial strain* - the main objective of the study will be to monitor the predictive power of left atrial strain for the onset of diastolic dysfunction, pulmonary hypertension, atrial fibrillation and heart failure following an acute myocardial infarction.

- *the study of myocardial infarction with nonobstructive coronary arteries (MINOCA)* - the main objective will be to assess the risk of major arrhythmic events and the risk of sudden cardiac death in the MINOCA population.

Secondary objectives will be to determine the cumulative incidence of reinfarction, to examine its etiology and to assess the prognostic value of CMR imaging.

In my future activity I will be open to address other topics of clinical research in which I can involve doctoral students with research themes in cardiology or other related specializations.

Section four contains the bibliographic references on which this habilitation thesis was based.

SECTION I. SYNOPSIS OF PERSONAL ACADEMIC, PROFESSIONAL AND SCIENTIFIC ACCOMPLISHMENTS

A teacher must always be open and motivated towards professional development and performance. By carrying out a continuous self-assessment of the performance level, according to the standards of professional competence, he/she is constantly connected to the educational needs, the current trends and the required teaching certification, with the purpose of self-training and of achieving a high quality teaching practice.

The teaching profession is primarily a profession with a strong influence on society, having a significant role in the development of human resources and in shaping future generations. It is a complex profession, whose success is based on flexibility, dynamism, responsiveness to change and critical reflection.

The current requirements formulated for teachers are primordially related to the awareness of the continuous character of their own training, the integration of the new methods and technologies of information and communication within the teaching activity, the promotion of a quality learning and education.

In this context, the teacher should become a good collaborator, contribute to projects that are often institutional and have a flexible thinking. He/she should be innovative and critical, but at the same time open to suggestions from the younger generations.

The whole activity of a teacher must be oriented towards the continuous acquisition of specific knowledge, skills and competence focused on three essential directions: education, health, research.

Thus, even if the professional satisfactions are numerous, they require a continuous multidisciplinary training in order to be able to meet the current requirements.

1.1. Academic development

I started my academic career at the University of Medicine and Pharmacy "Gr.T.Popa" of Iași in March 2002, being admitted as Teaching Assistant by contest at the Cardiology Discipline, Cardiology Center of Iași, under the guidance of Prof. Dr. George I.M. Georgescu and Mrs. Prof. Dr. Cătălina Arsenescu Georgescu.

The high level of teaching activity I have encountered in this clinical discipline as a newcomer, has determined me to adapt my conduct and work style to that of my new colleagues and also to learn from their experience.

At the same time, I have come to believe that the evolution of my performance as an educator mostly depends on the success of my professional debut.

My academic career continued, so that in 2007 I was promoted by contest to Assistant Professor. The complexity of the teaching activity stimulated me to reach a level of performance that gave me comfort and prestige as a young educator in front of a group of students.

In February 2017, I promoted the contest for the position of lecturer and in January 2020 for the position of Associate Professor. By excellence, the teaching profession involves permanent training and development, so that one can offer to the students a comprehensive perspective on the field they teach.

Consequently, during all this period, one of my continuous pursuit was related to the accumulation of quality and updated information in the field of pedagogy and communication, as a means to reach knowledge.

Thus, I participated as a speaker in numerous medical education projects and courses, both locally and nationally, under the auspices of the Romanian Society of Cardiology. Of course, the switch from the learner to the lecturer status involved several aspects: professional behavior, the ability to convey information, to communicate easily, to adjust my vocabulary to that of the audience, the capacity to respond precisely and clearly to questions, to adapt to the challenges launched by the public, but also the sincerity to recognize my own limits and the constant desire to overcome them.

Starting with the 2017 academic year, I have coordinated the courses of internal medicine for the 4th year medical students - teaching directions in English and Romanian. Moreover, as the tutor of the 4th year, I actively got involved into the academic problems faced by the young and counseled them into what concerns their professional careers.

I believe that my ability to guide students, residents and young researchers is highly illustrated by the number of undergraduate thesis that I have coordinated, by my participation as a lecturer or mentor in various cardiology workshops, as well as my expertise in research projects, held under the auspices of University of Medicine and Pharmacy “Grigore T. Popa”, Iași.

Last but not least, I would like to mention my contribution as an author in the elaboration of numerous educational materials with didactic purposes. In addition to the aspects related to the teaching act, the didactic activity requires also organizational skills. In this regard, I was a member of the evaluation committee for the titles of specialist and senior doctor, as well as for academic position promotion.

A few of my future academic goals include being competitive, a very good professional, an educator and at the same time an inspiring model. This is the example I received from my mentors and that I intend to follow.

1.2. Professional evolution

The beginning of my academic career in the Discipline of Cardiology was doubled by the training in the specialty of cardiology according to the curriculum. Starting from the first year of residency, I went to the Echocardiography Laboratory, where I learned the echocardiographic examination techniques, an extremely important aspect for clinical practice, as echocardiography is the mainstay investigation in cardiovascular diseases.

At that point, I developed my passion for cardiac imaging which later proved to be a source of inspiration for both scientific publications and doctoral research. With the entry into the

residency program, I have started to participate in numerous medical conferences both in the country and abroad.

From the very beginning, I asked myself the question of how the speakers managed to transmit the desired information and to be understood even by us, the youngest at that time.

In 2007, I completed the cardiology fellowship program and received integration within the Department of Non-Invasive Functional Exploration Laboratory of the Institute of Cardiovascular Diseases "Prof. Dr. George I.M. Georgescu" of Iași.

In 2008 I attended the postgraduate course in Transesophageal Echocardiography hosted at the "Heart Institute" of Cluj Napoca and obtained the *Certificate of Complementary Studies in Transesophageal Echocardiography*.

Succeeding the exam held at EUROECHO 2010 (Copenhagen) organized by the European Association of Cardiovascular Imaging under the auspices of the European Society of Cardiology, I obtained the *Certification in Adult Transthoracic Echocardiography Written Assessment*.

Since 2011, I am a member of the Scientific and Organising Committee of the National Conference "George Georgescu", a prestigious national event, with international participation.

In 2012 I obtained the title of senior cardiologist, as the crowning achievement of my entire medical career.

In December 2014, I have been entitled the Head of the Non-Invasive Functional Exploration Laboratory of the Institute of Cardiovascular Diseases "Prof. Dr. George I.M. Georgescu".

Between 2015 and 2017, I was the President of the Ethics Committee of the Institute of Cardiovascular Diseases "Prof. Dr. George I.M. Georgescu" and a member of the Ethics Committee of the College of Physicians, Iași.

In January 2018, I received the approval (Ministry of Health & University of Medicine and Pharmacy Iași) for coordinating the echocardiography training program at the completion of which the candidates obtain the *Certificate in General Echocardiography*.

My constant preoccupation for improvement, motivates me to still invest in my professional development opportunities and to carry on the prestige of the institution where I studied.

1.3. Scientific activity

In my opinion, scientific research is a key element of educational development. I have started with my scientific research activity in the early 2000's trained by Prof. Dr. George Georgescu and later by Prof. Dr. Cătălina Arsenescu Georgescu, as Principal Investigators for a series of 18 research grants and phase II or III international clinical trials, the research team of the Institute of Cardiovascular Diseases" Prof George IM Georgescu" having me as a co-investigator. The active involvement in these research projects allowed me to develop teamwork skills and critical thinking, to set up individual goals.

In 2005 I was admitted to PhD studies within the Doctoral School of the University of Medicine and Pharmacy "Gr.T.Popa" of Iași, under the guidance of Prof. Dr. Cătălina Arsenescu Georgescu.

At the end of the PhD program, in October 2006, I shaped my thesis named “*Echocardiographic criteria for predicting postoperative results in aortic valve surgery*” – a turning point for my personal research activity. This chapter of my life was marked by different publications in extenso in indexed journals in international databases and by multiple presentations at national and international events.

By working every day in the Echocardiography Laboratory of the Institute of Cardiovascular Diseases” Prof. Dr. George I.M. Georgescu” of Iași, I have outlined my own doctoral grant, I organized, designed, followed the results, but also compared them with literature data.

The main objective of my study was to assess the optimal timing of surgical procedures in patients with aortic valve disease. During my research, I had presentations both in the country and abroad and I published some of the results. I obtained the title of Doctor of Medical Sciences in 2012.

In the academic year 2005 – 2006, I attended a Master program in Epidemiology and Methodology of Clinical Research, at the University of Medicine and Pharmacy "Gr.T.Popa" of Iași, that further expanded my knowledge about research projects.

My research activity has also been materialized through a series of collaborations for prestigious books, both nationally and internationally.

In 2006, I have joined the research team from the Nephrology Clinic of the Dr. C.I. Parhon Hospital in Iași, coordinated by Prof. Dr. Adrian Covic under the auspices of the University of Medicine and Pharmacy "Grigore T. Popa" of Iași.

I have collaborated with them in numerous research projects - both national and international grants, that have resulted in important data published in journals with major international scientific flow. Within the team, I was the only cardiologist expert, with the role of performing cardiovascular evaluations with echocardiographic examinations:

- the LUST project: the „*LUng water by Ultra - Sound guided Treatment to prevent death and cardiovascular events in high risk end stage renal disease (ESRD) patients with cardiomyopathy*” ongoing since 2013, coordinator EURECA-m / ERA - EDTA, EURECA-m steering committee members: Zoccali Carmine (study coordinator), Covic Adrian, Fliser Danilo, London Gerard Michael, Martinez- Castelao Alberto, Massy Ziad , Ortiz Arduan Alberto, Sulleymanlar Gultekin, Wiecek Andrzej - center “*Dr. C. I. Parhon ”Iași Romania - Principal Investigator Prof.Dr. Adrian COVIC;*
- IDEI project, contract no. 351/2012 entitled: "*Extravascular lung water monitoring by combined ultrasound and bioimpedance as a guide for treatment in cardiomyopathic renal hemodialysis patients*", carried out in the period of 2012 - 2016, under the auspices of the University of Medicine and Pharmacy "GR. T. Popa" of Iași, project manager Prof. Dr. Adrian Constantin COVIC;

- Internal Grant U.M.F. Iasi (University of Medicine and Pharmacy), contract no. 1641/2013 entitled: "*The complex assessment of the fluid status of hemodialysis patients by pulmonary ultrasonography and electrical bioimpedance and correlations with certain echocardiographic parameters*", carried out in 2013-2014, coordinator University of Medicine and Pharmacy "Gr. T. Popa of Iași", project manager Dr. Mugurel Costel Apetrii.

Other research collaboration were with the Cardiovascular Recovery Clinic team within the following projects:

- *Assessment of arterial stiffness and the role of cardiovascular recovery in patients with sleep apnea syndrome*; the staff of the Nephrology Clinic Sp. Dr. CI Parhon;
- *Grant of Ministry of Research and Innovation, CNCS-UEFISCDI, project number PN-III-P1-1.1-PD-2016-0287, within PNCDI III*;
- *Bioimpedance for the evaluation of heart failure - a comparison with clinical assessment, lung ultrasonography, cardiac biomarkers and echocardiography - Project Manager - Dimitrie Siriopol*.

I have also contributed to the foundation of the Romanian Registry of Hypertrophic Cardiomyopathy (Ionila P, Jurcuț R, Ferariu N, Roșca M, Sascău R, et al.).

The recognition for my professional activity is depicted by the distinctions and awards obtained, namely:

- The European Society of Cardiology Gratefully Acknowledges the Contribution of Dr. Radu A. Sascău to the EURO HEART SURVEY PROGRAM (VALVULAR HEART DISEASE, 2002-2003);
- "Certificate of APPRECIATION for professional efficiency and team spirit", offered by the Manager of the Cardiology Center of Iasi, 2006;
- „Diploma of Excellence as Distinguished Lecturer” granted by the Romanian Society of Hypertension, on the occasion of the First International Conference of Hypertension, Central University Library, Iași, 2012;
- "Diploma of Excellence" offered by the University of Medicine and Pharmacy "Carol Davila" of Bucharest, for expertise, participation and contribution to achieving the objectives of the project: "AD-COR "Innovative training program in pediatric cardiology ", POSDRU/179/3.2/ S/152012;
- "Medal of Excellence in Cardiology" offered by the Institute of Cardiovascular Diseases "Prof. Dr. George I. M. Georgescu” of Iași, on the 20th foundation anniversary of the Institute of Cardiovascular Diseases “Prof. Dr. George I. M. Georgescu” of Iași;
- 2nd Prize - at the e-Posters category of the 12th National Congress of the Romanian Society of Cardiovascular Surgery, October 13-16, 2016, for the paper: “Surgical Treatment in Aortic Insufficiency using CoreMatrix after antibiotic management of infective endocarditis”.

SECTION II. SCIENTIFIC ACHIEVEMENTS

Introduction

In the previous decades, there have been substantial refinements in the armamentarium of non-invasive imaging techniques utilized in the diagnosis and treatment monitoring of patients suffering from various cardiovascular diseases, including heart failure.

We have witnessed a switch in focus, from a single imaging technique-based diagnosis to an integrated, comprehensive multi-modality imaging approach with the purpose of acquiring an early and accurate diagnosis and of a timely implementation of a targeted treatment (Di Carli et al.,2016).

Heart failure (HF) represents a major public health issue and a large economic burden, affecting approximately 26 million subjects worldwide, with 1-2% of the total healthcare resources being allocated to its therapeutic management (Kato et al.,2019; Ambrosy et al.,2014).

Cardiac imaging is a powerful tool for screening, risk stratification, and treatment monitoring in subjects with HF. Transthoracic echocardiography has the advantages of being widely available and of providing valuable information regarding cardiac geometry and function as well as hemodynamics, representing the cornerstone of imaging in HF (Wong et al., 2016).

By assessing left ventricular ejection fraction (EF) via two-dimensional transthoracic echocardiography, three categories of HF can be identified: HF with reduced EF (HFrEF) characterized by an $EF \leq 40\%$, HF with preserved EF (HFpEF) defined by an $EF \geq 50\%$, and HF with mid-range EF (HFmrEF) referring to the subjects whose EFs vary from 40% to 49% (Ponikowski et al.,2016).

As congestion epitomizes the dominant cause of hospitalization in subjects with HF, improvements in the imaging detection of both intravascular and tissue congestion have revolutionized the therapeutic management, leading to changes in patient care. In decompensated HF, echocardiography through the measurement of the inferior vena cava diameter helps estimating right atrial pressure and guiding decongestive therapies.

Pulmonary ultrasonography has also become an indispensable imaging technique in the evaluation of acute decompensated HF. The total count of comet-tail reverberation artifacts, known as B-lines estimates the amount of pulmonary water. Less than five B-lines on a complete anterolateral evaluation exclude the presence of pulmonary edema, while more than 30 B-lines strongly support this diagnosis (Boorsma et al., 2020).

Into what concerns the etiology of HF, primary myocardial disorders, comprising hypertrophic, dilated, and restrictive cardiomyopathies constitute leading causes. Nowadays, advances in cardiac imaging have enabled the acquirement of an accurate, timely diagnosis as well as the distinction between these three major types of cardiomyopathies.

Of note, for hypertrophic, dilated, and restrictive cardiomyopathies, transthoracic echocardiography is the first-line imaging, possessing important diagnostic, therapeutic, and prognostic implications.

In hypertrophic cardiomyopathy, the combined use of advanced cardiac imaging modalities helps to identify the patients who would benefit the most from the initiation of novel, revolutionary pharmacotherapies (e.g. mavacamten), from minimally-invasive procedures (e.g. transcatheter mitral valve repair, septal radiofrequency ablation) or gene editing and gene silencing therapy (Tuohy et al., 2020).

In dilated cardiomyopathy, left ventricular ejection fraction evaluated via transthoracic echocardiography stands as the sole criterion in choosing the eligible candidates for primary prevention implantable cardioverter-defibrillators, which represents a life-saving intervention in subjects with $EF \leq 35\%$ (Stolfo et al., 2020). However, the evolving role of cardiac magnetic resonance imaging in the assessment and risk stratification of patients with dilated cardiomyopathy has been repeatedly emphasized by the results of large studies (Halliday et al., 2017).

Finally yet importantly, in cardiac amyloidosis, the paradigm of restrictive cardiomyopathies, multimodality imaging, including echocardiography, cardiac magnetic resonance, and bone scintigraphy, holds a key role in improving outcomes via the timely initiation of appropriate patient care, in monitoring disease progression, and treatment response (Martinez Naharro et al., 2020).

Emerging evidence suggests the existence of a complex relationship between sleep-disordered breathing and cardiovascular disease, and supports the presence of a causal connection between obstructive sleep apnea (OSA) and hypertension, coronary heart disease, arrhythmias, heart failure, and stroke (Javaheri et al., 2017).

The mechanisms linking OSA and HF are complex. The recurrent episodes of collapse of the upper airway that occurs during sleep trigger oxidative stress, sympathetic activation, inflammation, hypercoagulability, endothelial dysfunction, and metabolic dysregulation, which in turn favor the alteration of cardiac structure and function.

Therefore, OSA either initiates or worsens HF, irrespective of blood pressure control (Sanchez-de-la-Torre et al., 2013). Out of 963 subjects, included in a study that aimed to evaluate the prognostic value of sleep-disordered breathing (SDB) in stable HFrEF patients, 58% were found to have concomitant moderate to severe SDB. Additionally, the burden of nocturnal hypoxemia appeared to be an independent predictor of all-cause mortality in this large cohort of HFrEF subjects (Oldenburg et al., 2016).

In the light of the above-mentioned data, it is being emphasized the importance of screening for OSA in HF and HF in OSA, echocardiography being the mainstay imaging method of assessing the long-term consequences of OSA on the heart.

Another well recognized major public health issue worldwide is represented by chronic kidney disease (CKD). Epidemiological data indicate that CKD represents a dominant cause of morbi-mortality, affecting nearly 11–13% of the total worldwide population (Hill et al., 2016; Ali et al., 2020). Its incidence is constantly increasing, holding both economic and social implications and portraying a poor prognosis.

In Romania, the results of the PREDATORR study published in 2015, performed on 2717 individuals, indicated that the prevalence of CKD is 6.74% (95% CI 5.60-7.88%) (Moța, 2015).

From a pathophysiological point of view, CKD is defined as a progressive loss of renal function lasting more than three months, materialized in a glomerular filtration rate (GFR) <60 mL/min/1.73 m² (Inker et al., 2014).

Nevertheless, cardiovascular disease (CVD) is still the leading cause of global deaths, accounting for more than 17.9 million deaths in 2016 (GBDS, 2018). Importantly, patients with CKD have a significantly increased risk of cardiovascular disease (CVD) (Gargiulo et al., 2015). Patients on long-term dialysis have a 10- to 30-fold increased risk for cardiovascular mortality when compared to the general population.

Different epidemiological data proved that more than 80% of the subjects with ESRD have concurrent CVD (Cheung et al., 2004). Also, CVD is the most important cause of death among patients receiving long-term dialysis, accounting for 44% of overall mortality.

Hypertension and diabetes mellitus are the most frequent conditions that lead to end-stage renal disease (ESRD), with recent data suggesting that ESRD is an independent risk factor by itself for the development of CVDs (Cozzolino et al., 2017).

Cozzolino et al. identified that the prevalence of coronary heart disease and left ventricular hypertrophy within the CKD population is ranging from 40% - 70% and that almost 35% of these subjects have a history of an ischaemic event (myocardial infarction or angina) by the time of the presentation to a nephrology department (Cozzolino et al., 2018).

CKD is highly prevalent in the elderly as well as in patients with hypertension, diabetes, and other non-traditional risk factors. Consequently, CKD patients are likely to be confused with patients suffering from cardiovascular disease.

The histophysiology of the cardiovascular system changes with the deterioration of renal function. Primary, excessive sodium and water retention not only increases the cardiac output but also activates the sympathetic nervous system with a boost in peripheral vascular resistance and blood pressure. High blood pressure and fluid overload further affect the heart.

Complications of CKD, including anemia, metabolic acidosis, elevated calcium-phosphate product, hyperparathyroidism, chronic inflammation, and hyperhomocysteinemia cause endothelial dysfunction, left ventricular (LV) hypertrophy, and adverse cardiac remodeling.

These comorbidities can further lead to heart failure (HF) and eventually death. Premature atherosclerotic coronary disease is driven by multiple risk factors, including dyslipidemia and oxidative stress.

Structural abnormalities of the heart in patients with CKD include LV hypertrophy, expansion of the cardiac interstitium with extensive myocardial fibrosis, and myocardial calcification. All these abnormalities promote LV systolic as well as diastolic dysfunction, thus favoring the emergence of overt heart failure and sudden cardiac death (London et al., 2006). The magnitude of the problem has become more evident because of an increase in the lifespan of CKD patients via hemodialysis (Mc Cullough et al., 2004).

A better characterization of the high cardiovascular risk of these individuals can be attained by performing a standard transthoracic echocardiographic evaluation. Echocardiography is a non-

invasive examination, largely used for the assessment of heart structure and function, bringing several ultrasound techniques in a single examination (Oh, 2005).

Concerning *left ventricular hypertrophy*, it is known that LV mass is proportional to body size and, conventionally, the indexation to body surface has been used for this correction. In patients undergoing hemodialysis, this parameter is highly influenced by body weight variations, due to changes in fluid volume and to the nutritional status impairment.

Therefore, the indexation to height raised to the power of 2.7, proposed by deSimone and coworkers, seems to be the most accurate method to estimate LV mass in this group of patients. Also, this convention has a slightly superior value in predicting general and cardiovascular mortality in patients undergoing hemodialysis (Zoccali et al., 2001).

An important issue to acknowledge is that in patients undergoing hemodialysis, LV geometry is related to the moment when the echocardiogram is performed. Shortly after a hemodialysis session, a reduction in the LV end-diastolic diameter along with an increase in the LV wall thickness can be noticed as a consequence of volume depletion.

When the assessment is carried out right before hemodialysis, LV dilatation with eccentric hypertrophy is relatively common. This type of variation can lead to evaluation errors, that one can minimize by performing the echocardiographic examination within the interdialytic interval.

LV systolic dysfunction remains an unfavorable prognostic factor in individuals undergoing hemodialysis, as well as in kidney transplant recipients. The underlying mechanisms for LV systolic impairment are multifactorial, including coronary heart disease, anemia, hyperparathyroidism, uremic toxicity, malnutrition, and chronic hemodynamic overload. The assessment of the LV systolic function via echocardiography should be performed annually, with the evaluation of LV shortening and ejection fractions. (Folley et al., 2000).

LV diastolic dysfunction includes alterations in ventricular relaxation and compliance, with an increase in the LV filling pressures in more advanced phases. The increase in the LV filling pressures is responsible for the emergence of symptomatic HF. In studies based on experimentally induced uremia, the morphological examinations revealed diffuse myocardial interstitial fibrosis. The activation of several humoral factors affiliated with LV hypertrophy (high plasma levels of angiotensin II, parathyroid hormone, endothelin, aldosterone, and catecholamines) and myocardial ischemia are the culprit mechanisms of myocardial fibrosis. The increase in LV chamber stiffness related to fibrosis leads to the exacerbation of the volemic variation effects on LV filling (Hung et al., 2012).

Consequently, even in patients with normal EF, a small increase in the cardiac preload can generate pulmonary congestion, while volemic depletion can induce arterial hypotension and hemodynamic instability.

Accordingly, it is important to adequately assess not only the LV systolic function but also the diastolic function, whose alterations can also trigger episodes of acute pulmonary edema as well as intradialytic hypotension (Hung et al., 2012).

Left atrial (LA) volume is related to the severity as well as the duration of LV diastolic dysfunction. LA is a surrogate of the chronicity of diastolic dysfunction, reflecting the duration of increased filling pressures (Abhayaratna et al., 2006).

Left atrial (LA) volume seems to be a strong predictor of cardiovascular outcomes in the general population as well as in other clinical entities. It is considered to be superior in predicting different cardiovascular events comprising atrial fibrillation, cerebrovascular accident, heart failure, myocardial infarction, and cardiac death (Abhayaratna et al., 2006).

Pulmonary hypertension (PH) is an independent predictor of mortality in CKD patients, mainly in those receiving renal replacement therapy. Significant PH is a relative contraindication for renal transplantation and many patients with CKD visit their physicians because of dyspnea. PH is identified during the echocardiographic examination and is frequently mentioned as the potential etiology of dyspnea, requiring vasodilator therapy (Zlotnick et al., 2010).

Assessments of PH prevalence in patients with CKD are based primarily on echocardiographic parameters, with slight validation by the recommended gold standard - right heart catheterization. It is difficult to appreciate the timing of PH onset and its cumulative incidence in progressive stages of CKD due to the lack of prospective case-control studies. Statistics on PH prevalence among patients with stage 5 CKD prior to the initiation of renal replacement therapy (RRT) are rare (Yigla et al., 2009).

Current research is trying to clarify whether PH plays a causative role for the adverse outcomes in HD patients or it just symbolizes a marker of more severe cardiac dysfunction. In PH, the reduced capacity of the right heart to maintain adequate filling pressures in the face of intermittent dialytic fluid removal can potentially contribute to intradialytic myocardial stunning, ischemia, and myocardial fibrosis. Myocardial remodeling is considered to be a major contributor to sudden cardiac death in the HD population due to its proarrhythmogenic effects. Therefore, by identifying patients with potential reversibility of PH, kidney transplant selection could be improved. There is some evidence that the degree of PH improves post-transplantation. Patients with potential reversibility might benefit from vasodilator treatment prior to the consideration for kidney transplantation (Sharma et al., 2007).

Valvular calcifications are highly prevalent in hemodialysis patients. Valvular calcifications are not only the consequence of the natural aging process and the calcium-phosphorus metabolism disorders, but there are also caused by inflammation, similar to what it has been described for atherosclerosis. Its importance lies in the association that has been reported between valvular calcification and the higher risk of mortality and adverse cardiovascular events in the uremic patient (Wang et al., 2003).

Acute pericarditis can arise in almost 20% of cases, before the initiation of RRT or during chronic dialysis. The most common causes are uremia and/or ineffective dialysis. Subjects with important pericardial effusion usually do not respond adequately to the intensification of the dialysis therapy and need to be referred to early elective pericardial drainage as a means of preventing hemodynamic complications. Constrictive pericarditis is less common in patients undergoing hemodialysis (Banerjee et al., 2006).

Chapter 1. Role of cardiac imaging techniques in diagnosis and risk stratification of patients with cardiovascular disease

1.1. Background

Chronic heart failure (HF) epitomizes a major public health issue. In the United States, approximately 6.2 million adult Americans suffer from chronic HF, with an increase to more than 8 million cases being expected by 2030 (Benjamin et al., 2019). Similar findings were also noticed in European countries (Ohlmeier et al., 2015; Buja et al., 2016).

Despite important advances in diagnosis and management over the past two decades (Michalska-Kasiczak et al., 2018), chronic HF patients still portend a poor prognosis (Benjamin et al., 2019; Arundel et al., 2018; Beiert et al. 2019; Orimoloye et al., 2019; Polikandrioti et al., 2019) with an estimated mortality of about 50% at 5 years (Roger et al., 2004).

Data concerning heart failure (HF) are inconsistent due to the absence of case reports in underdeveloped countries, and secondly to the discrepancy of approaches used for evaluating this condition incidence. Nevertheless, epidemiological studies report the existence of approximately 26 million cases of HF worldwide (Ponikowski et al., 2014).

As the population ages, HF prevalence increases (Dunlay, Roger, 2014), along with its cost-related issues (Lesyuk et al., 2018).

Numerous therapeutic options have become largely available during the past years: β -blockers, mineralocorticoid receptor antagonists, ivabradine, and more recently sacubitril/valsartan and SGLT-2 inhibitors.

Additionally, device therapy, including implantable cardioverter defibrillators were introduced into clinical practice. However, mortality rates in patients with HF are still unacceptably high, of about 50% at 5 years and 70% at 10 years, comparable to those reported in the early 2000's (Taylor et al., 2017; Gerber et al., 2015).

Researchers have always pursued to design some risk prediction models, in order to statistically calculate the risk of HF-related complications, but the use of these models is largely limited, given the difficulty of their individualization for each patient (Howlett, 2013).

Lung congestion represents one of the most frequent manifestations of HF and the leading cause for hospitalization in adults aged 65 years or above from the United States (Heidenreich et al., 2013).

Conventionally, lung congestion has been assessed via clinical examination or thoracic radiography. In recent years lung ultrasonography (LUS) has emerged as a powerful, reliable diagnostic test in HF patients (Martindale et al., 2016).

Furthermore, LUS, through the assessment of the B-lines, is a promising instrument for monitoring lung congestion changes (Platz et al., 2017) and for prognostic stratification (Platz et al., 2017; Miglioranza et al., 2017). The B-lines are discrete laser-like vertical hyperechoic reverberation artifacts that arise from the pleural line, extend to the bottom of the screen without fading, that move in tandem with lung sliding (Volpicelli et al., 2012), and originate most often

from volumetric variations in the relationship between the aerated and tissue/fluid-filled parts of the lung (Spinelli et al., 2012).

Bioimpedance spectroscopy (BIS) is used to objectively evaluate and monitor fluid status. It has been validated against “gold-standard” methods (Wabel et al., 2009; Raimann et al., 2014) and its use in dialysis patients has been linked to improved survival (Onofriescu et al., 2014), rigorous blood pressure control (Covic et al., 2017) and decreased arterial stiffness (Onofriescu et al., 2014).

Cardiomyopathies are a heterogeneous group of primary myocardial disorders and a major cause of heart failure (Seferovic et al., 2020).

Based on the phenotype, three main forms of cardiomyopathy have been reported: hypertrophic, dilated, and restrictive cardiomyopathies (RCMs). RCM is the rarest and is further classified as infiltrative and non infiltrative, storage diseases, and endomyocardial disorders (Pereira et al., 2018).

Over the past decades, significant improvements have been achieved in the diagnosis and therapeutic management of hypertrophic cardiomyopathy (HCM), which has led to an increase in life expectancy and quality.

According to the European Society of Cardiology Guideline HCM is characterized by a wall thickness ≥ 15 mm in one or more left ventricular myocardial segments, hypertrophy that is not caused only by abnormal loading conditions, such as valvulopathies and hypertension (Elliott et al., 2014). In the majority of cases, the hypertrophic process implies the interventricular septum, being severe and asymmetric.

However, this is not a pathognomonic modification and can be found also in subjects with isolated interventricular septal hypertrophy or in those with hypertensive cardiomyopathy (Marian et al., 2014). The coexistence of aortic stenosis or arterial hypertension represents a challenge for the clinician, to differentiate between primary and secondary hypertrophy.

Multimodality imaging techniques help attaining a proper differential diagnosis and also contribute to a precise characterization of the left ventricle wall thickness and chamber size, mitral valve morphology, and myocardial tissue.

Therefore, imaging tests possess a central role in diagnosing, evaluating the regional distribution and severity of the disease, and appreciating the prognosis (Cardim et al., 2015). Moreover, imaging contributes to the implementation of an optimal therapeutic strategy in hypertrophic cardiomyopathy, whether it is pharmaceutical, interventional, or surgical.

However, the information regarding the achievement of a timely diagnosis in HCM subjects is limited, with difficulties in reducing the risk of sudden cardiac death (Anghel et al., 2020).

Infiltrative cardiomyopathies (ICMs) include a large spectrum of inherited and acquired conditions, where the progressive accumulation of abnormal substances within the myocardium leads to left ventricular hypertrophy and manifests as restrictive physiology (Bejar et al., 2015). The most common etiologies are cardiac amyloidosis, sarcoidosis, and hemochromatosis, although

Fabry disease, Dannon disease, and Friedreich's ataxia, are important, but less frequent (Sascau et al., 2021).

Noninvasive multimodality imaging has progressively removed the necessity of endomyocardial biopsy from the diagnostic frame of ICMs. Nevertheless, even with wide availability of imaging techniques, these conditions continue being largely under- or misdiagnosed.

Considering the emergence of new, revolutionary pharmacotherapies for cardiac amyloidosis, the prototypal example of ICM, and a life-threatening disease, a standardized diagnostic approach is highly needed.

The preoccupations related to the role of cardiac imaging techniques in diagnosis and risk stratification of patients with cardiovascular disease were partially synthesized in the following article:

Siriopol D, Siriopol M, Mihaila M, Rusu F, **Sascau R**, Costache I, Vasiliu V, Bucur A, Neamtu A, Popa R, Cianga P, Kanbay M, Covic A. Prognostic value of lung ultrasonography and bioimpedance spectroscopy in patients with heart failure and reduced ejection fraction. *Arch Med Sci* 2020; 1-9. **IF:2.807**

Siriopol D, Popa R, Mihaila M, Rusu F, **Sascau R**, Statescu C, Cătălina Z, Vasiliu V, Bucur A, Neamtu A, Siriopol I, Cianga P, Kanbay M, Covic A. Application of survival classification and regression tree analysis for identification of subgroups of risk in patients with heart failure and reduced left ventricular ejection fraction. *Int J Cardiovasc Imaging* 2021 Jan 16. **IF: 1.969**

Anghel L, Stătescu C, Șerban IL, Mărănducă MA, Butcovan D, Clement A, Bostan M, **Sascău R**. The Advantages of New Multimodality Imaging in Choosing the Optimal Management Strategy for Patients with Hypertrophic Cardiomyopathy. *Diagnostics (Basel)*. 2020; 10(9):719. **IF: 3.110**

Sascău R, Anghel L, Clement A, Bostan M, Radu R, Stătescu C. The Importance of Multimodality Imaging in the Diagnosis and Management of Patients with Infiltrative Cardiomyopathies: An Update. *Diagnostics (Basel)*. 2021; 11(9):1-24. **IF: 3.110**

1.2. Lung ultrasonography and bioimpedance spectroscopy in heart failure with reduced left ventricular ejection fraction

1.2.1. Aim

In our research, we sought to evaluate the link between lung congestion, as assessed via lung ultrasonography (LUS), bioimpedance spectroscopy (BIS) body fluid compartments, and echocardiographic parameters, and to appreciate the effect of these associations on all-cause mortality in HF subjects.

1.2.2. Materials

Patients and study design

We conducted a prospective observational study during 2016 and 2018 on subjects addressed for clinically indicated transthoracic echocardiograms at our hospital. Eligible patients, with a left ventricular ejection fraction (LVEF) below 45% were identified through daily echocardiographic assessments. From a total number of 264 eligible subjects, 127 were excluded because of limb amputation (N=3), metallic joint prostheses (N=10), cardiac pacemakers or stents (N=78), decompensated cirrhosis (N=5), previous diagnosis of pulmonary fibrosis (N=4), pneumectomy (N=1), massive pleural effusion (N=6), end-stage renal disease (N=3), active systemic infections (N=4) and terminal illnesses (N=13).

Additionally, 15 patients refused to participate and were not included. Details of the final study cohort (N=122) are shown in Tables I, II, and III.

The investigation conforms with the principles outlined in the Declaration of Helsinki (Rickham, 1964). The study was approved by the Research Ethics Committee of the “Grigore T. Popa” University of Medicine and Pharmacy Iasi and all included subjects signed informed consent.

Demographic and clinical parameters

At baseline, the following demographic parameters were recorded: age, gender, weight, height, comorbidities (diabetes, coronary artery disease, hypertension, atrial fibrillation, chronic kidney disease (CKD)), and smoking status.

Blood pressure was evaluated in the morning by a physician, after a 15-min resting period, with the mean values for three consecutive measurements calculated for systolic (SBP) and diastolic blood pressure (DBP).

We used an automatic BP measuring device certified by the Association for the Advancement of Medical Instrumentation, European Society of Hypertension, and British Society of Hypertension—model OMRON M6 with an adjustable cuff for arm circumferences from 24 to 42 cm, respecting the current guideline recommendations (Mancia et al., 2013).

Hypertension was defined as a SBP greater than 140 mmHg and/or diastolic BP higher than 90 mmHg or previously diagnosed hypertension under treatment for at least 2 weeks, regardless of BP values.

We considered that a patient had coronary artery disease if in the medical records there was a history of coronary artery/heart disease, angina or angina pectoris, or myocardial infarction. CKD was established according to the Kidney Disease Improving Global Outcomes guidelines (Levin et al., 2013).

We also assessed diuresis, the existence of peripheral edema (slight pitting of at least 2 mm depth with no visible distortion) (Seidel, 1995), the NYHA functional class, and the medication.

Biochemical analysis

All blood samples were obtained early in the morning, after minimum 12 hours of fasting. Serum creatinine, hemoglobin, glucose, total cholesterol, triglycerides (TG), high-density lipoprotein (HDL), low-density lipoprotein (LDL) cholesterol, C-reactive protein (CRP), uric acid,

and sodium levels were measured. Estimated glomerular filtration rate (eGFR) was calculated with the help of the Chronic Kidney Disease Epidemiology Collaboration (CKD-EPI) equation (Levey et al., 2009).

Laboratory tests were performed by standard procedures with certified methods, in the same day with the lung ultrasonography and BIS assessments. We stored serum at -80°C for subsequent analyses. N-Terminal Pro-Brain Natriuretic Peptide (NT-proBNP) was analyzed using the Elabscience® ELISA Kit, an electro-chemiluminescence 'sandwich' immunoassay based on antibodies against Human NT-proBNP.

Echocardiographic assessment

Echocardiographic evaluations were performed on the same day or maximum a day before LUS and BIS assessments by two trained echocardiographers according to the recommendations of the American Society of Echocardiography (Lang et al., 2015).

B-lines assessment

LUS was performed with subjects in the supine position, with a total of 28 sites per complete examination, as previously detailed (Jambrik et al., 2004). At every scanning site, B-lines were counted from 0 (no B-lines) to 10 (complete white screen) (Supplementary Figure 1).

The sum of the B-lines provided a score illustrating the magnitude of extravascular lung water. Two trained physicians blinded to the echocardiographic measurements conducted all B-line assessments.

Bioimpedance analysis

The hydration state and the body composition were evaluated instantly after LUS, by utilizing a portable whole-body BIS device (BCM—Fresenius Medical Care D GmbH (www.fmc-au.com/therapy-systems-and-services/analysis-systems/bcm)). Electrodes were attached to the patient's forearm and ipsilateral ankle and the device measured the impedance spectroscopy at 50 frequencies.

The extracellular water (ECW), intracellular water (ICW) and TBW were determined as previously detailed (Moissl et al., 2006).

Outcome

The main outcome was all-cause mortality. Death was certified via follow-up phone calls, hospital's electronic medical records or the social security death index.

Statistical analysis

Variables were expressed as median with interquartile range (IQR), mean \pm standard deviation (SD), or as percentage of frequency, as appropriate. For the categorical variables, the between-group comparisons were performed using the Chi-square test and for the continuous variables using the Mann-Whitney U test or the independent T-test, as appropriate.

The Shapiro-Wilk test was implemented for evaluating the normality of the distribution and logarithmic conversion was conducted for non-normally distributed variables, including B-lines number, glucose, HDL and LDL-cholesterol, triglycerides, CRP and uric acid levels.

Pearson's correlation coefficient was used to determine correlations between variables. Backward stepwise multivariable regression analysis including all univariate associates ($p < 0.05$) was employed to assess the predictors for B-lines.

Time-to-event analysis of all-cause mortality was performed using Kaplan–Meier cumulative survival plots and Cox proportional hazards model, including adjustment for potential confounding factors.

In model 1, we adjusted for clinical risk factors: age, sex and diabetes. In model 2, we adjusted for biochemical and echocardiographic (LVEF) risk factors: CRP, eGFR, NT-proBNP and LVEF. In model 3, we adjusted for all the variables used in previous two models. We also made an additional model (model 4) in which we adjusted also for ECW (for the B-lines analysis) or B-lines (for the ECW analysis).

To establish the optimal cut-off point for the number of B-lines and ECW as predictors of all-cause mortality the relationship between the number of B-lines and ECW and the outcome was analyzed using the Martingale residuals in Cox's proportional hazard regression analysis (Grambsch et al., 1995).

We discovered that the categorization of the number of B-lines and ECW into two categories (using 15 B-lines and 18.3 L as cut-offs for the number of B-line and ECW, respectively) was the best approach for modeling these relationships.

Analyses were conducted with B-lines and ECW as a categorical (based on the cut-offs mentioned above) and also as a continuous variable. Data is presented in the form of Hazard ratios and 95% confidence intervals.

We tested the proportional hazards assumptions using the Schoenfeld residuals and, when necessary, we performed bootstrapping validation as a means to prevent the issue of overfitting due to the low number of deaths.

All analyses were performed using Stata SE software, version 13 (StatCorp, College Station, TX, USA) and the R (version 3.6.1) package for statistical analysis (Foundation for Statistical Computing, Vienna, Austria). A p value < 0.05 was considered to be statistically significant.

1.2.3. Results

Characteristics of the study population

Our study cohort comprised 122 patients (67.2% males) with a mean age of 67.2 years. The most common cause of HF was dilated cardiomyopathy – 47 (43.1%) patients. Nevertheless, the precise etiology of HF was indeterminate in 25 (20.5%) subjects.

More than half of the study population presented with at least NYHA class III; the median number of B-lines was 16. Other features of the population are presented in Tables I and II and Supplementary Table 1.

Table I. Baseline demographic, clinical and biological characteristics of the study population

Parameter	Total (N=122)	Group 1 (N=57)	Group 2 (N=65)	P value
Age [years]	67.2±11.0	65.1±9.9	68.9±12.1	0.06
BMI [kg/m ²]	29.2±5.3	29.1±4.7	29.3±5.8	0.88
Male, n [%]	82 (67.2)	42 (73.7)	40 (61.5)	0.15
SBP [mmHg]	124.6±18.7	125.1±17.2	124.1±20.1	0.78
DBP [mmHg]	75.0±11.3	76.3±9.5	73.8±12.7	0.22
Smoking, n [%]	34 (27.9)	15 (26.3)	19 (29.2)	0.72
Diuresis [L/day]	1.4±0.5	1.3±0.5	1.4±0.5	0.24
Oedema, n [%]	66 (54.1)	17 (29.8)	49 (75.4)	<0.001
III/IV NYHA class, n [%]	66 (54.1)	13 (22.8)	53 (81.5)	<0.001
B-lines	16.0 (4.0-35.0)	3.0 (1.0-9.0)	34.0 (23.0-51.0)	<0.001
<i>Comorbidities</i>				
Diabetes, n [%]	44 (36.1)	17 (29.8)	27 (41.5)	0.18
Coronary artery disease, n [%]	67 (54.9)	31 (54.4)	36 (55.4)	0.91
Hypertension, n [%]	77 (63.1)	40 (70.2)	37 (56.9)	0.13
Atrial fibrillation, n [%]	71 (58.2)	34 (59.7)	37 (56.9)	0.76
CKD, n [%]	32 (26.2)	11 (19.3)	21 (32.3)	0.10
<i>Biological parameters</i>				
Serum creatinine [mg/dL]				
EGFR [ml/min/1.73m ²]	66.2±24.2	73.3±20.4	59.9±25.6	0.002
Hemoglobin [g/dL]	13.2±2.1	13.9±2.1	12.6±1.9	<0.001
Serum glucose [mg/dL]	106.0 (97.0-131.0)	104.0 (95.0-128.0)	107.0 (99.0-134.0)	0.33
Total Cholesterol [mg/dL]	153.3±44.1	161.4±46.9	146.2±40.4	0.06
LDL Cholesterol [mg/dL]	87.5 (70.0-115.0)	97.0 (76.0-125.0)	85.0 (69.0-101.0)	0.12
HDL Cholesterol [mg/dL]	37.0 (29.0-45.0)	39.0 (32.0-46.0)	35.0 (28.0-45.0)	0.12
Serum Triglycerides [mg/dL]	124.0 (96.0-148.0)	122.0 (96.0-148.0)	125 (97.0-147.0)	0.54
CRP [mg/L]	27.0 (11.2-57.8)	18.2 (6.5-49.5)	35.0 (18.2-108.0)	0.01
Uric acid [mg/dL]	7.4 (6.2-8.8)	7.0 (6.2-7.9)	7.8 (6.2-9.2)	0.03
Serum sodium [mmol/L]	137.4±4.9	138.9±3.2	136.2±4.9	0.001
NT-proBNP [pg/mL]	895.0 (300.0–1600.0)	600.0 (200.0–1300.0)	1080.0 (500.0–1950.0)	0.002

BMI – body mass index; CKD – chronic kidney disease; CRP – C-reactive protein; DBP – diastolic blood pressure; eGFR – estimated glomerular filtration rate; HDL – high-density lipoprotein; LDL – low-density lipoprotein; NT-proBNP – N-Terminal Pro-Brain Natriuretic Peptide; SBP – systolic blood pressure.

As a primary approach, we segregated the study population according to the number of B-lines (*Group 1 B-lines* below 15 and *Group 2 B-lines* with at least 15 B-lines). Predictably, individuals in Group 1 B-lines presented a lower prevalence of edema and less severe NYHA class;

they also exhibited better renal function (as assessed by eGFR) and lower CRP, NT-proBNP and uric acid levels than subjects from Group 2 B-lines (Table I). Additionally, these individuals had lower left atrial and left ventricular volumes, and a better LVEF than patients from Group 2 B-lines (see Table II). BIS fluid status assessment demonstrated that even though there was no significant difference between these two groups in TBW, subjects from Group 1 B-lines had lower ECW and higher ICW volumes (Table II).

Table II. Echocardiographic and bioimpedance characteristics of the study population

	Total (N=122)	Group 1 (N=57)	Group 2 (N=65)	P value
<i>Echocardiography</i>				
LV EDVi [mL/m ²]	85.4 (71.4-107.3)	81.3 (68.8-99.3)	88.8 (76.4-110.9)	0.04
LV ESVi [mL/m ²]	46.1 (30.2-73.3)	37.9 (26.9-58.0)	58.2 (35.1-78.2)	0.004
Septal wall thickness [cm]	1.2 (1.1-1.4)	1.3 (1.2-1.4)	1.2 (1.1-1.3)	0.18
LV mass index [g/m ²]	154.4 (131.6-187.3)	148.3 (131.4-173.4)	164.9 (132.3-192.7)	0.17
LA volume index [mL/m ²]	43.6 (33.6-68.5)	39.4 (32.8-58.5)	54.1 (34.7-74.0)	0.03
LVEF [%]	32.8±9.1	36.8±7.6	29.3±8.9	<0.001
<i>Bioimpedance</i>				
TBW [l]	36.5±5.8	36.4±5.9	36.6±5.8	0.85
ECW[l]	18.3±2.9	17.4±3.0	19.1±2.7	0.001
ICW[l]	18.0±3.4	18.7±3.6	17.4±3.3	0.04

AFO – absolute fluid overload, ECW – extracellular water, ICW – intracellular water, LA – left atrial, LVEF – left ventricular ejection fraction, LV EDD – LV end diastolic diameter, LV EDVi – left ventricular end diastolic volume index, LV ESD – LV end systolic diameter, LV ESVi – left ventricular end systolic volume index, RFO – relative fluid overload, TBW – total body water.

Correlations of lung congestion with demographic, clinical, biological and bioimpedance parameters

In univariable analysis, we recognized eGFR, CRP, serum sodium, NT-proBNP, and different clinical, echocardiographic, and BIS derived characteristics as significant correlates for the number of B-lines. In multivariable linear regression analysis, comprising all the univariable predictors of lung congestion, only NYHA class, ECW, eGFR, and LVEF levels preserved an independent association (R^2 of the model = 0.42) with the number of B-lines (see Table III).

All-cause mortality according to the number of B-lines and ECW volume

During the follow-up (mean 12.5 months, median 11.2 months), 33 patients (27.1%) died. 7 deaths were recorded in the group of patients with a number of B-lines below 15, while in the other group 26 deaths were registered (12 deaths in the group of patients with below 18.3 L of ECW and 21 deaths in the group with at least 18.3 L of ECW). Kaplan–Meier curves demonstrated

significantly higher all-cause mortality in HF patients with at least 15 B-lines (see Figure 1A) or 18.3 L ECW volume (Figure 1B).

Table III. Univariable and multivariable associates of B-lines (log transformed) in the study population

	Univariate ρ	P
Edema (0 – No, 1 – Yes)	0.43	<0.001
NYHA class (0 – II, 1 – III/IV)	0.56	<0.001
Diuretic use (0 – No, 1 – Yes)	0.19	0.03
Log LV ESVi [ml/m ²)	0.19	0.03
Log LA volume index [ml/m ²)	0.23	0.01
Log LVEF [%)	-0.33	<0.001
ECW [l)	0.29	<0.001
ICW [l)	-0.17	0.04
EGFR [ml/min/1.73m ²)	-0.33	<0.001
Log CRP [mg/l)	0.23	0.01
Serum sodium [mmol/l)	-0.32	<0.001
	Multivariate β	P
NYHA class (0 – II, 1 – III/IV)	1.11	<0.001
Log LVEF [%)	-0.61	0.04
ECW [l)	0.08	0.01
EGFR [ml/min/1.73m ²)	-0.01	0.001

CRP – C-reactive protein; ECW – extracellular water; eGFR – estimated glomerular filtration rate; ICW – intracellular water; LA – Left atrial; LVEF – Left ventricular ejection fraction; LV ESVi – left ventricular end systolic volume index; NT-proBNP – N-Terminal Pro-Brain Natriuretic Peptide; TBW – total body water.

In unadjusted Cox regression, patients belonging to *Group 2 B-lines* had a HR of 3.96 (95%CI 1.78-8.79), while those in *Group 2 ECW* had a HR for death of 2.47 (95%CI 1.23-4.98) for the outcome of interest (see Table IV). In multivariable Cox analysis, a number of B-lines greater than 15 continued to be significantly related to all-cause mortality, independently of different clinical, echocardiographic, biological or BIS derived fluid characteristics (Table IV). However, an 18.3 L of ECW volume remained significantly linked to the outcome after adjustments for clinical, echocardiographic or biological risk factors (Table IV, Models 1 and 2), but lost this significance after adjustment for all the above-mentioned risk factors (Table 4, Model 3) or for lung congestion (Table IV, Model 4).

By utilizing the number of B-lines and ECW as continuous variables, we identified in univariate Cox analysis that both variables were associated with an elevated risk of death (HR 2.04, 95% CI 1.36-3.08 and HR 1.16, 95% 1.03-1.29 for each increment of 1 SD in log number of B-lines and 1 L in ECW volume, respectively). After adjustment, the number of B-lines remained significantly associated to the outcome in all the multivariable Cox models, while ECW lost the

significance for this relationship after adjustment for biological characteristics and LVEF (Supplementary Table 2).

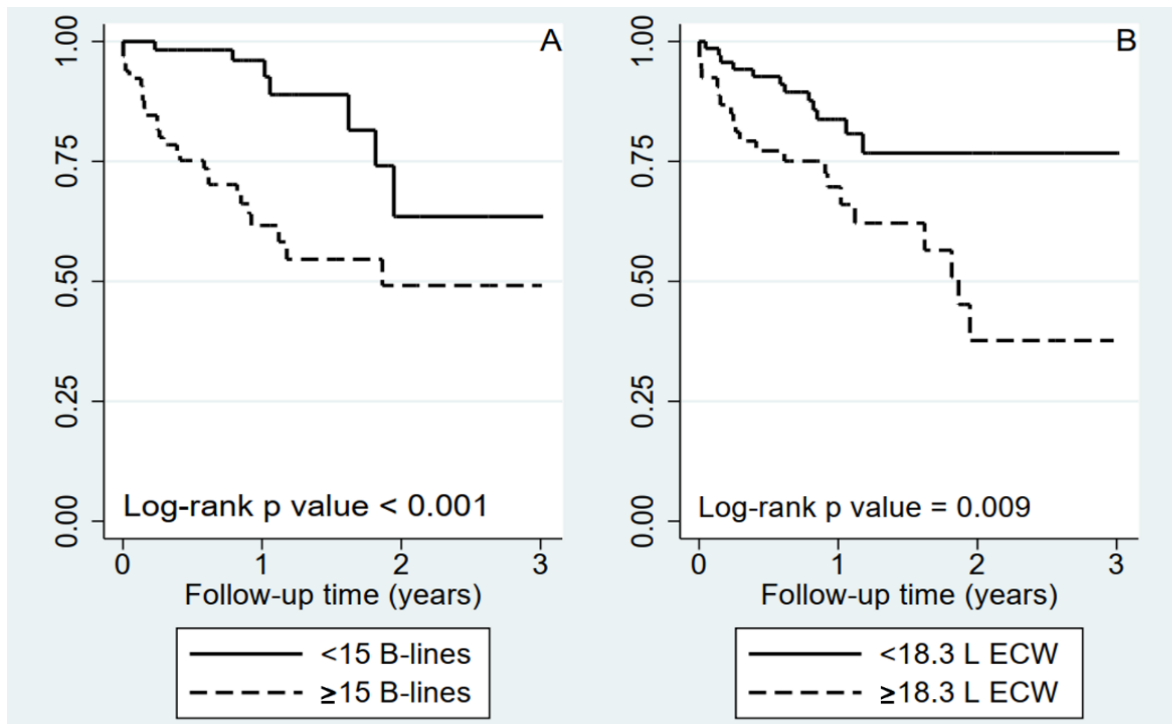
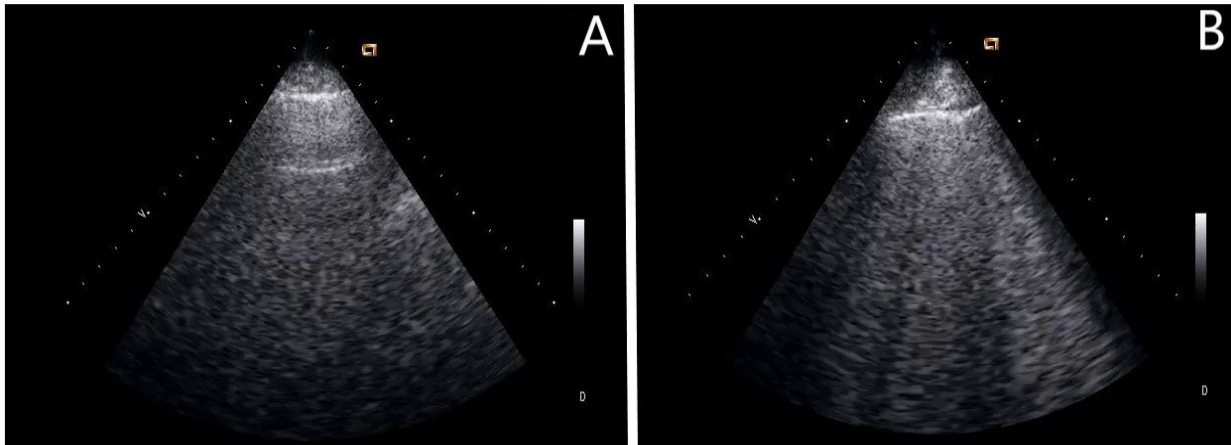


Figure 1. Kaplan–Meier curves for all-cause mortality according to the B-lines (A) and ECW (B) groups.



Supplementary Figure 1. Lung ultrasonography of a normal lung scan (A) and of multiple B-lines (B)

CKD was defined according to the Kidney Disease Improving Global Outcomes guidelines (Levin et al., 2013).

Table IV. Lung congestion and extracellular water as predictors of all-cause mortality (using the B-lines and ECW groups)

	B-lines		ECW	
	HR*	95% CI	HR*	95% CI
Unadjusted	3.96	1.78-8.79	2.47	1.23-4.98
Adjusted				
Model 1	4.88	1.66-14.34	2.19	1.07-4.48
Model 2	3.58	1.55-8.29	2.24	1.09-4.59
Model 3	3.87	1.16-12.91	1.99	0.94-4.18
Model 4	3.84	1.12-13.09	1.62	0.75-3.51

Abbreviations: CI, confidence interval; ECW, extracellular water; HR, hazard ratio.

Model 1: age, sex, diabetes;

Model 2: C-reactive protein, estimated glomerular filtration rate, left ventricular ejection fraction, N-Terminal Pro-Brain Natriuretic Peptide;

Model 3: variables in model 1 + variables in model 2.

Model 4: Model 3 + ECW (for the B-lines groups) or Model 3 + B-lines (for the ECW groups)

*Hazard ratio for Group 2 vs Group 1.

1.2.4. Discussion

This research illustrates for the first time that, in HF subjects, with reduced LVEF, lung congestion is dependent on eGFR, LVEF, and ECW volume, as assessed via BIS. We also certify the increased risk of death related to pulmonary congestion, but we also demonstrate that this association is independent of cardiac and renal function or body fluid compartments.

Congestion is the main characteristic and cause for hospitalization in HF subjects. However, the physiopathological shift from hemodynamic congestion (increased left ventricular filling pressures) to lung congestion (increased extravascular lung water) and ultimately to clinical congestion (signs and symptoms of congestion) is complex and not fully elucidated. Extravascular lung water, a relatively small component of body fluids compartments, is typically correlated to increased left ventricular filling pressures and total body fluids. Some analysis suggest that pulmonary congestion is linked more to fluid redistribution than to total body fluid accumulation. In the IMPACT-HP trial, the authors revealed that the extent of weight loss was not corresponding to a clinical improvement (Gattis et al., 2004). Similarly, in the EVEREST study, the weight reduction derived from using tolvaptan was not linked to improvements in global clinical status (Gheorghiade et al., 2007).

Our study reinforces this hypothesis and adds new data to this puzzling issue. We revealed that even though there is no difference in TBW between the subjects below and those with at least 15 B-lines, ECW volumes are significantly higher in patients from the latter group. Additionally, in the multivariable regression model, ECW is one of the variables that stayed independently associated with lung congestion. Another essential aspect is the relationship between eGFR, as an indicator of renal function, and the extent of pulmonary congestion in HF subjects. We illustrated

an inverse and independent association between eGFR and the number of B-lines. There is an acknowledged bidirectional lung-kidney crosstalk generally present in health and specific pathological states (Domenech et al., 2017). As reflected in acute kidney injury or CKD, the levels of different mediators could alter pulmonary vascular permeability (Domenech et al., 2017) and increase the risk of pulmonary congestion. However, pulmonary congestion with impaired gas exchange could result in decreased renal blood flow and alterations in eGFR through stimulation of adrenergic nerves, and perturbations in nitric oxide homeostasis (Sharkey et al., 2009). Even though in this relationship the primary cause is unknown, our results clinically validate the increased risk of pulmonary congestion connected to worse renal function in HF subjects with reduced LVEF.

It is now well-documented that LUS, via the assessment of B-lines, is a practical diagnostic and prognostic tool in both acute and chronic HF (Platz et al., 2017). Results from studies conducted on chronic HF subjects support that those with pulmonary congestion are at a higher risk of hospitalization or death (Miglioranza et al., 2017; Gustafsson et al., 2015; Platz et al., 2016; Dwyer et al., 2018). With a fourfold increase in the risk for all-cause mortality, our findings are in accordance with these studies; however, by comparison with the above-mentioned studies, although the authors adjusted the results for demographical (Gustafsson et al., 2015; Platz et al., 2016; Dwyer et al., 2018), clinical (Platz et al., 2016; Miglioranza et al., 2017) or cardiac characteristics (Gustafsson et al., 2015; Miglioranza et al., 2017), our analysis is the only one that integrates demographical clinical, cardiac, biological and, most importantly, BIS derived fluid status confounders into the survival analysis. As the number of B-lines is linked to all-cause mortality even after all these adjustments, the crucial role played by pulmonary congestion in predicting adverse outcomes in HF patients is strengthened. Our cut-off of 15 B-lines, derived from statistical analysis, is the same as the clinical cut-off proposed and used in previous studies (Platz et al., 2017; Miglioranza et al., 2017).

BIS has shown promising results, particularly in dialysis subjects (Onofriescu et al., 2014), in HF patients its utility being limited to only two diagnostic studies performed in an acute setting with no follow-up outcomes (Parrinello et al., 2008; Park et al., 2018). Although our research reveals that a greater than 18.3 L of ECW is connected with death in the initial multivariable Cox models, after different adjustments, including pulmonary congestion, this relationship becomes non-significant. We have acquired similar results in a previous study conducted on dialysis patients. In the final model, the number of B-lines, and not the BIS derived fluid status parameter, was linked to all-cause mortality (Siriopol et al., 2013).

This study reinforces previous findings regarding the impact of lung congestion on all-cause mortality in HF patients, but at the same time refines this association. We employed a holistic approach in our analysis, trying to emphasize the intricate relationship between the lung, heart and kidney and its effect on survival in this type of patient.

Our study has some *limitations* that must be addressed. We included a relatively small sample size of selected HF patients from a single-center with a relatively low number of death events, but we used different statistical approaches to overcome these shortcomings. Additionally,

we are not able to entirely eliminate the presence of residual confounding in our regression models. These elements could limit the generalizability of the results achieved in this study. However, our findings are notably promising as they underline the complex pathways that connect lung congestion with cardiac and renal function and body fluid compartments. Preferably, these findings should be validated in other HF populations, including larger cohorts. Besides, we could not specify the reason of death and the data about nonfatal events were not collected.

1.2.5. Conclusions

We illustrated for the first time in HF subjects that pulmonary congestion, as evaluated via LUS, is linked with the severity of NYHA class, LVEF, eGFR, and ECW, and recognizes those at high risk of death.

1.3. Identification of subgroups of risk in some patients with HF and HFrEF

1.3.1. Aim

Within this research, we sought to identify by classification and regression tree (CART) analysis, groups of subjects with different survival patterns in a heart failure with reduced left ventricular ejection fraction (HFrEF) population. In order to reach our objective, we employed standard procedures of heart function assessment and also non-traditional methods for evaluating hydration and nutritional status in HF subjects, namely lung ultrasonography (LUS) and bioimpedance spectroscopy (BIS). Ultimately, we compared the prognostic value of these novel methods with that of conventional Cox survival analysis.

1.3.2. Material and methods

We conducted a prospective observational study of outpatient adults referred for clinically indicated transthoracic echocardiograms in our hospital between 2016 and 2018. Information concerning this study has been previously reported (Siriopol et al., 2020). We enrolled in the analysis subjects with a left ventricular ejection fraction (LVEF) below 45% assessed via transthoracic echocardiography. The total number of eligible subjects was 321. The exclusion criteria were limb amputation, metallic joint prostheses, cardiac pacemakers or stents, decompensated cirrhosis, prior diagnosis of pulmonary fibrosis, pneumectomy, massive pleural effusion, end-stage renal disease, active systemic infections and terminal illnesses. 17 individuals did not sign the informed consent. Accordingly, 151 patients were considered for the final investigation. Within the study, all procedures were done following the principles outlined in the Declaration of Helsinki (Rickham, 1964). The protocol was approved by the Research Ethics Committee of the “Grigore T. Popa” University of Medicine and Pharmacy Iasi.

The demographic variables recorded at baseline were age, gender, weight, height, comorbidities (diabetes, coronary artery disease, hypertension, atrial fibrillation, chronic kidney disease), and smoking status. The arterial blood pressure values were recorded in the morning in all subjects by a trained physician by three consecutive evaluations, after a 15-min resting period, with the mean values calculated for systolic (SBP) and diastolic blood pressure (DBP) (Mancia et

al., 2013). According to current guideline recommendations, hypertension was defined as a SBP greater than 140 mmHg and/or DBP greater than 90 mmHg or previously diagnosed hypertension under treatment for at least 2 weeks, irrespective of BP values. A medical history of coronary artery/heart disease, angina or angina pectoris, or myocardial infarction was considered as coronary artery disease. The diuresis, the presence of peripheral edema (slight pitting of at least 2 mm depth with no visible distortion) (Seidel et al., 1995), the NYHA functional class, and the medication were also recorded. Biochemical analyses of serum creatinine, hemoglobin, glucose, total cholesterol, triglycerides (TG), high-density lipoprotein (HDL), low-density lipoprotein (LDL) cholesterol, C-reactive protein (CRP), uric acid, and sodium levels were performed. We assessed the estimated glomerular filtration rate (eGFR) by using the Chronic Kidney Disease Epidemiology Collaboration (CKD-EPI) equation (Levey et al., 2009).

Echocardiography was performed before LUS and BIS evaluations by two trained echocardiographers according to the recommendations of the American Society of Echocardiography (Lang et al., 2015).

B-lines assessment

As previously stated by Jambrik et al., LUS was performed with subjects in the supine position, for a total of 28 sites per complete examination (Jambrik et al., 2004); the total number of B-lines was recorded for each zone (from a minimum of 0 to a maximum of 10) and the degree of lung congestion was derived by summing the scores from all the 28 zones – as seen in Figure 2 with two images belonging to two different patients from our study.

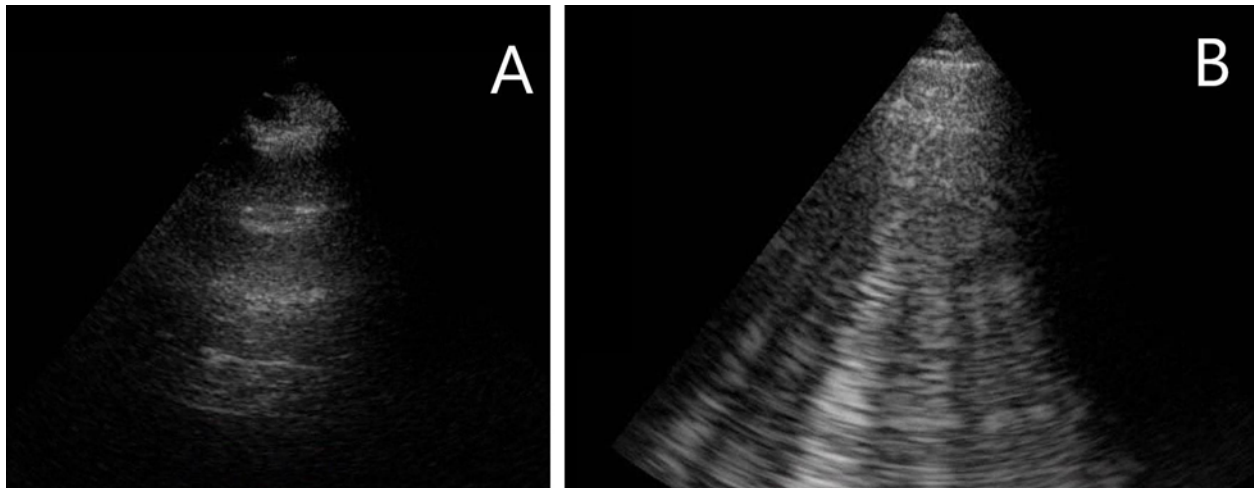


Figure 2. Images from the lung ultrasound from two different sites from patients from our study, showing 0 (A) and 10 B-lines (B).

Bioimpedance analysis

After performing LUS measurements, we evaluated the hydration state and the body composition (<https://www.fmc-au.com/therapy-systems-and-services/analysis-systems/bcm>).

We determined the extracellular water (ECW), intracellular water (ICW) and TBW as previously described (Moissl et al., 2006). The device expresses body composition as a three-compartment

model, being capable of supplying information about overhydration, lean, and tissue mass. Absolute fluid overload (AFO), delimited as the difference between the expected patient's ECW under normal physiological conditions and the actual ECW, and relative fluid overload (RFO), determined as the AFO to ECW ratio, were utilised as a means to characterize the hydration status. The lean tissue index (LTI) and fat tissue index (FTI) were also assessed, where LTI and FTI are the respective tissue masses normalized to height squared. Because in individuals with limb amputation, metallic joint prostheses, cardiac pacemakers or stents, or decompensated cirrhosis, this method could provide unreliable results (Wizemann et al., 2009), this category of subjects was excluded from the study as previously stated.

Outcome

The major outcome was all-cause mortality. Deaths were confirmed through patient follow-up phone calls, hospital's electronic medical records, or the social security death index.

Within the study, the *statistical analysis* was performed by using Stata SE software, version 13 (StatCorp, College Station, TX, USA). A p-value <0.05 was considered to be statistically significant. Variables were expressed as median with interquartile range (IQR), mean \pm standard deviation (SD), or as percentage of frequency, as appropriate. The between-group comparisons were performed using the Chi-square test for categorical variables, and Mann-Whitney U test or the independent T-test, for continuous variables. The Shapiro-Wilk test helped us to assess the normality of the distribution and logarithmic conversion was performed for non-normally distributed variables. CART analysis was valuable to categorize subgroups of risk for all-cause mortality, as well as cut-off values for the factors identified as significant risk predictors (Lofaro et al., 2016). The analysis begins by dividing data into smaller sections to provide a clearer view of interactions among variables.

We further compared the results of two Cox proportional hazard models to assess whether the use of CART analysis offers higher predictive performance over conventional Cox survival analysis: the first one a conventional Cox model and the second one using only the subgroups identified by the CART analysis. For the CART analysis, all the available variables were included in the initial step. All data were offered in the form of Hazard ratios (HR) and 95% confidence intervals (CI). We achieved bootstrapping validation when needed to avoid the problem of overfitting due to the low number of incident outcomes. We compared the two Cox models using the concordance index (c-index), a measure equivalent to the area under the receiver operating characteristic curve in logistic regression. The Bayesian information criterion (BIC) and the Akaike information criterion (AIC) were also calculated for each Cox model; there is no statistical test that compares different BIC or AIC estimations, and a lower value indicates a better-fitted model.

1.3.3. Results

Our 151 patients had a mean age of 67.1 ± 12.1 years. Into what concerns sex distribution, 69.2% were males. Dilated and ischemic cardiomyopathy, with 56 (37.1%) and 47 (31.1%) patients, respectively, were the most common causes of HF. Demographic, biological,

bioimpedance, echocardiographic, and treatment characteristics of the study population are presented in Tables V and VI and Supplementary Table V.

35,1% (53) individuals died all through the follow-up. These subjects had a higher prevalence of peripheral edema and severe baseline NYHA class. When compared to survivors, they also had a significantly higher number of B-lines (median 21 vs. median 7.5, $p<0.001$), urea, CRP, soluble ST2, and galectin-3 levels (see Table V).

Nevertheless, these subjects displayed significantly lower eGFR (61.1 ± 25.3 vs. 69.4 ± 23.7 ml/min/1.73 m², $p=0.04$), hemoglobin (12.6 ± 2.1 vs. 13.8 ± 2.0 g/dL, $p=0.001$), serum sodium (135.5 ± 5.3 vs. 138.2 ± 4.3 , $p<0.001$) and leptin (median 13.5 vs. median 24.8 ng/mL, $p=0.01$) values.

Table V. Baseline demographic, clinical and biological characteristics of the study population

	All (N=151)	All-cause death NO (N=98)	All-cause death YES (N=53)	P value
Age, years	67.1±12.1	65.6±12.1	69.8±11.7	0.03
BMI, kg/m²	28.9±4.7	29.2±4.6	28.4±4.8	0.33
Male, n (%)	105 (69.5)	70 (71.4)	35 (66.0)	0.49
SBP, mmHg	124.6±18.3	124.5±16.9	124.8±20.8	0.90
DBP, mmHg	75.4±11.3	76.1±10.5	74.0±12.6	0.28
Smoking, n (%)	60 (39.7)	37 (37.8)	23 (43.4)	0.49
Diuresis, L/day	1.4±0.5	1.4±0.5	1.5±0.5	0.09
Edema, n (%)	75 (49.7)	36 (36.7)	39 (73.6)	<0.001
III/IV NYHA class, n (%)	73 (48.3)	41 (41.8)	32 (60.4)	0.03
B-lines	12.0 (3.0-32.0)	7.5 (2.0-26.0)	21.0 (10.0-48.0)	<0.001
<i>Comorbidities</i>				
Diabetes, n (%)	53 (35.1)	31 (31.6)	22 (41.5)	0.23
CAD, n (%)	89 (58.9)	63 (64.3)	26 (49.1)	0.07
Hypertension, n (%)	93 (61.6)	57 (58.2)	36 (67.9)	0.24
Atrial fibrillation, n (%)	80 (53.3)	50 (51.6)	30 (56.6)	0.55
<i>Biological parameters</i>				
Serum creatinine, mg/dL	1.1 (0.9-1.4)	1.1 (0.9-1.3)	1.2 (0.9-1.4)	0.12
eGFR, ml/min/1.73m²	66.5±24.5	69.4±23.7	61.1±25.3	0.04
Urea, mg/dL	47.0 (35.0-69.0)	43.5 (33.0-62.0)	58.0 (41.0-80.0)	<0.001
Hemoglobin, g/dL	13.4±2.1	13.8±2.0	12.6±2.1	0.001
Serum glucose, mg/dL	107.0 (96.0-131.0)	107.5 (95.0-131.0)	106.0 (98.0-128.0)	0.52
Total Cholesterol, mg/dL	151.0 (127.0-187.0)	153.0 (132.1-187.0)	144.0 (123.0-184.0)	0.32
LDL Cholesterol, mg/dL	91.0	93.5 (77.0-116.0)	87.0 (74.0-124.0)	0.68

	(75.0-117.4)			
HDL Cholesterol, mg/dL	38.0 (30.0-46.0)	37.0 (31.0-47.0)	40.0 (30.0-45.0)	0.84
Serum Triglycerides, mg/dL	121.0 (96.0-148.0)	121.0 (97.0-148.0)	123.0 (81.0-147.0)	0.35
CRP, mg/L	25.6 (9.0-56.4)	19.9 (7.8-46.9)	35.1 (15.8-89.7)	0.01
Uric acid, mg/dL	7.5 (6.2-8.8)	7.5 (6.1-8.4)	7.8 (6.5-9.1)	0.29
Serum sodium, mmol/L	137.2±4.9	138.2±4.3	135.5±5.3	<0.001
Soluble CD146, ng/mL	236.00 (189.60-329.20)	221.4 (190.2-338.0)	236.8 (188.8-314.0)	0.48
NT-proBNP, pg/mL	800.0 (400.0-1500.0)	795.0 (300.0-1500.0)	910.0 (500.0-1320.0)	0.26
ST2, pg/mL	8.17 (4.61-14.35)	6.47 (3.67-11.93)	10.32 (5.77-14.85)	0.02
Galectin-3, ng/mL	26.40 (18.30-35.80)	24.3 (17.0-35.4)	29.2 (22.4-37.0)	0.04
CT-1, pg/mL	1.40 (0.30-10.20)	2.7 (0.4-10.9)	1.2 (0.3-6.7)	0.26
Acylated ghrelin, pg/mL	10.30 (1.30-41.5)	11.6 (2.0-41.6)	6.1 (1.0-40.9)	0.32
Leptin, ng/mL	21.90 (7.70-49.10)	24.8 (10.8-49.7)	13.5 (6.2-29.7)	0.01

Data are expressed as mean±SD, or median with IR, or percent frequency, as appropriate. Significant values are indicated in bold. Abbreviations: BMI – body mass index; CAD – coronary artery disease; CKD – chronic kidney disease; CRP – C-reactive protein; CD146 – cluster of differentiation 146; CT-1 – cardiotrophin-1; DBP – diastolic blood pressure; eGFR – estimated glomerular filtration rate; HDL – high-density lipoprotein; LDL – low-density lipoprotein; NT-proBNP – N-terminal brain natriuretic peptide; SBP – systolic blood pressure; ST2 – soluble suppression of tumorigenesis 2

Within the research, we noticed that individuals who died had higher values for ECW (19.1±2.7 vs. 17.4±3.4 L, p=0.001), AFO (2.0±2.3 vs. 0.6±2.9 L, p=0.002), and RFO (10.2±11.9 vs. 1.9±13.6%, p<0.001), but lower values for ICW (17.4±3.3 vs. 18.7±3.6 L, p=0.04) and LTI (10.5±2.3 vs. 11.6±2.6 Kg/m², p=0.01) than those who survived. However, no differences between these patients regarding TBW and FTI were noticed (see Table VI).

Survival and prognostic analysis

The follow-up included a mean and median time of 18.8 and 20.4 months, respectively. The severity of NYHA class, the number of B-lines, urea, CRP, NT-proBNP, LVMI, LAVI, AFO, and RFO values were positively linked to all-cause mortality, while hemoglobin, serum sodium, leptin, ICW, and LTI levels were negatively connected with the outcome as seen in Table VII. A vital aspect of our analysis was to determine if CART analysis could provide superior predictive performance over conventional Cox survival analysis.

Table VI. Echocardiographic and bioimpedance characteristics of the study population

	All (N=151)	All-cause death NO(N=98)	All-cause death YES (N=53)	P value
<i>Echocardiography</i>				
LV EDVi, mL/m ²	85.1 (70.3-107.8)	81.3 (68.2-103.8)	97.8 (79.4-111.1)	0.01
LV ESVi, mL/m ²	54.2 (31.3-80.8)	46.6 (29.5-79.9)	61.9 (38.1-82.9)	0.13
Septal wall thickness, mm	12.5±2.2	12.5±2.1	12.5±2.5	0.99
Posterior wall thickness, mm	11.8±1.8	11.7±1.7	11.9±1.9	0.53
LVMI, g/m ²	152.9 (126.9-187.3)	144.7 (121.1-179.3)	168.0 (139.4-200.8)	0.004
LAVI, mL/m ²	40.7 (32.4-62.9)	36.4 (27.6-50.9)	57.3 (41.0-74.0)	<0.001
LVEF, %	32.5±10.2	32.7±10.5	32.0±9.8	0.68
<i>Bioimpedance</i>				
TBW, L	36.5±5.8	36.4±5.9	36.6±5.8	0.85
ECW, L	18.3±2.9	17.4±3.0	19.1±2.7	0.001
ICW, L	18.0±3.4	18.7±3.6	17.4±3.3	0.04
AFO, L	1.1±2.8	0.6±2.9	2.0±2.3	0.002
RFO, %	4.8±13.5	1.9±13.6	10.2±11.9	<0.001
LTI, Kg/m ²	11.2±2.6	11.6±2.6	10.5±2.3	0.01
FTI, Kg/m ²	16.8±5.2	17.0±5.3	16.5±4.9	0.52

Data are expressed as mean±SD, or median with IQR, as appropriate. Significant values are indicated in bold. Abbreviations: AFO – absolute fluid overload; ECW – extracellular water; FTI – fat tissue index; ICW – intracellular water; LAVI – Left atrial volume index; LVEF – Left ventricular ejection fraction; LV EDD – LV end diastolic diameter; LV EDVi – left ventricular end diastolic volume index; LV ESD – LV end systolic diameter; LV ESVi – left ventricular end systolic volume index; LVMI – left ventricular mass index; LTI – lean tissue index; RFO – relative fluid overload; TBW – total body water

Supplementary Table V. Medications

	All (N=151)	All-cause death NO (N=98)	All-cause death YES (N=53)	P value
ACEIs/ARBs, n (%)	68 (45.0)	46 (46.9)	22 (41.5)	0.52
Beta-blockers, n (%)	116 (76.8)	76 (77.6)	40 (75.5)	0.77
Diuretics, n (%)	109 (72.2)	67 (68.4)	42 (79.3)	0.16
Spirolactone, n (%)	90 (59.6)	54 (55.1)	36 (67.9)	0.13
Antiplatelet agents, n (%)	74 (49.0)	46 (46.9)	28 (52.8)	0.49
Anticoagulation, n (%)	105 (69.5)	74 (75.5)	31 (58.5)	0.03
Statins, n (%)	70 (46.4)	52 (53.1)	18 (33.9)	0.03
Nitrate, n (%)	55 (36.4)	39 (39.8)	16 (30.2)	0.24

Digoxin, n (%)	33 (21.9)	16 (16.3)	17 (32.1)	0.03
Amiodarone, n (%)	38 (25.2)	25 (25.5)	13 (24.5)	0.89

Data are expressed as percent frequency. Significant values are indicated in bold.

Abbreviations: ACEI - Angiotensin-converting enzyme inhibitors; ARB - Angiotensin II receptor blockers.

Table VII. Univariable Cox survival analysis

	HR	IC 95%	P value
Age, years	1.03	1.00-1.05	0.03
NYHA Class, (reference Class I-II)	3.27	1.78-6.01	<0.001
Log B-lines	1.50	1.18-1.92	0.001
Hemoglobin, g/dL	0.82	0.72-0.93	0.002
Log Urea, mg/dL	1.84	1.06-3.20	0.03
Log CRP, mg/L	1.27	1.05-1.53	0.01
Serum sodium, mmol/L	0.92	0.88-0.96	<0.001
Log NT-proBNP, pg/mL	1.26	1.01-1.59	0.04
Log Leptin, ng/mL	0.76	0.62-0.94	0.01
Log LVMI, g/m², g/m²	2.58	1.02-6.55	0.04
Log LAVI, mL/m²	2.49	1.29-4.79	0.006
ICW, L	0.92	0.85-0.99	0.04
AFO, L	1.11	1.02-1.19	0.01
RFO, %	1.02	1.01-1.04	0.004
LTI, Kg/m²	0.88	0.78-0.98	0.03

Abbreviations: AFO – absolute fluid overload; CI – confidence interval; CRP – C-reactive protein; HR – hazard ratio; ICW – intracellular water; LAVI – Left atrial volume index; LVMI – left ventricular mass index; LTI – lean tissue index; NT-proBNP – N-terminal brain natriuretic peptide; RFO – relative fluid overload.

By using a backward stepwise Cox survival analysis, and including all the univariable associates of the outcome, we observed that only age, the severity of NYHA class, hemoglobin, serum sodium, and LTI were retained in the final model.

Within the study, we used the CART algorithm, and we included all the available variables in the initial approach.

Subsequently, we designated five groups based on serum sodium, the severity of NYHA class, serum urea, and systolic blood pressure (as seen in Figure 3 and Supplementary VII).

Subjects with serum sodium greater than 136 mmol/L and NYHA class I or II (Group 1 in Figure 3 and Supplementary VII) had the best survival, while a remarkable worse prognosis was seen in patients with serum sodium ≥ 136 mmol/L, NYHA class III or IV, and serum urea ≥ 70 mg/dL (Group 3 in Figure 3 and Supplementary VII), in those with serum sodium < 136 mmol/L and SBP < 120 mmHg (Group 4 in Figure 3 and Supplementary VII) and in those with serum sodium < 136 mmol/L and SBP ≥ 120 mmHg (Group 5 in Figure 3 and Supplementary VII).

A trend towards a worse survival was also noticed in subjects with serum sodium ≥ 136 mmol/L, NYHA class III or IV, and serum urea < 70 mg/dL; (Group 2 in Figure 3 and Supplementary VII), but no statistical significance was recorded.

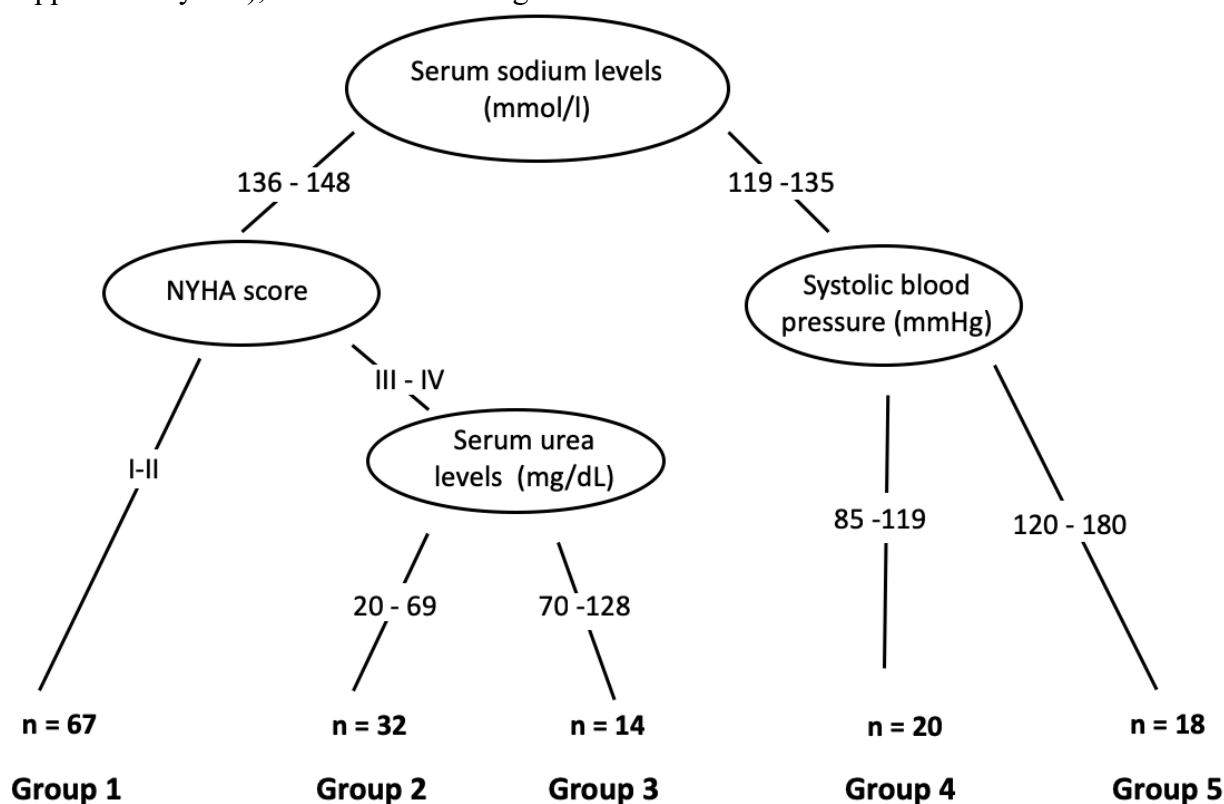


Figure 3. Tree for classification of survival subgroups

Supplementary VII. Cox survival analysis using the categories defined by CART

	Patients	HR	CI 95%	P value
Group 1	67		Reference	
Group 2	32	2.23	0.86-5.81	0.09
Group 3	14	10.59	4.15-27.08	<0.001
Group 4	20	5.48	2.24-13.42	<0.001
Group 5	18	20.93	8.43-51.97	<0.001

Group 1: Serum sodium ≥ 136 mmol/L, NYHA class I/II; **Group 2:** Serum sodium ≥ 136 mmol/L, NYHA class III/IV, Serum urea < 70 mg/dL; **Group 3:** Serum sodium ≥ 136 mmol/L, NYHA class III/IV, Serum urea ≥ 70 mg/dL; **Group 4:** Serum sodium < 136 mmol/L, SBP < 120 mmHg; **Group 5:** Serum sodium < 136 mmol/L, SBP ≥ 120 mmHg. Abbreviations: CI – confidence interval; HR – hazard ratio; SBP – systolic blood pressure.

We further compared the two models. We concluded that the model derived from the CART analysis exhibited better predictive power than the conventional Cox model (c-index 0.790, 95% CI 0.723-0.857 vs. 0.736, 95%CI 0.664-0.807, $p < 0.05$ – see Table VIII).

Table VIII. Performance comparison of Cox models using only patient data and only CART subgroups

	c-index (95% CI)	AIC	BIC
Conventional model^a	0.736 (0.664-0.807)	447.81	462.89
CART model^b	0.790 (0.723-0.857)*	428.59	440.66

^aConventional model includes age, NYHA Class, hemoglobin, serum sodium and LTI.

^bCART model includes the 5 groups identified by CART analysis.

* $P < 0.05$ versus conventional model

Abbreviations: AIC – Akaike Information Criterion; BIC – Bayesian Information Criterion; CART – Classification and Regression Tree; LTI – lean tissue index.

1.3.4. Discussion

In our research, we identified different groups of risk for all-cause mortality in subjects with HFrEF by using CART analysis that displayed enhanced prediction capabilities when compared to more conventional statistical methods. For quite a long time, the prediction of future outcomes in HF was made via prognostic stratification. Nevertheless, it is complicated to introduce them in clinical practice (Howlett, 2013), most likely because of low reliability at a patient level, the multitude of methods to choose from, or the complexity of the used statistical approaches (Canepa et al., 2018).

A systematic review from 2020 found 40 studies with 58 risk prediction models and 105 distinct predictors (Di Tanna et al., 2020), emphasizing the complex physiopathological mechanisms that portray HF as a leading clinical and public health issue. The authors used conventional statistical prognosis analysis and deduced that the most common variables included in the prognostic models were NT-proBNP, age, diabetes, and sex, but also sodium and NYHA class (Di Tanna et al., 2020). By comparison, in our analysis (model from Supplementary Table XLIV), NT-proBNP levels were not included in the final model, but age, the severity of NYHA class, and serum sodium were retained.

According to our conventional Cox analysis, hemoglobin and LTI were also independently connected to all-cause mortality. Previous studies illustrated that hemoglobin levels could be a surrogate of fluid control/a marker of extracellular water (Hung et al., 2015).

Accordingly, the relationship between hemoglobin and outcome was expected. Other studies showed that an increase in BMI is considered a risk factor for the development of HF, and a higher BMI in those with recognized HF is linked to better outcomes (Horwich et al., 2001; Sharma et al., 2015).

Our newly identified negative relationship between LTI and outcome of interest could explain, at least partially, the previous mentioned obesity paradox (e.g. a higher BMI with an

increase in LTI, and not FTI, could be protective). CART analysis has significant advantages, considering its potency to identify predictive cut-off values for continuous, and even related, variables.

Previously published reports have used arbitrary cut-off values based on subjective evaluations, or the data distribution in their sample (Levy et al., 2006; Agostoni et al., 2013). CART algorithm allows an investigative subgrouping of subjects based only on outcome and prognosis.

Besides, another important characteristic of the phenotypes identified via CART analysis is correlated to its straightforwardness and simplicity. Although serum sodium, NYHA class, SBP, and even serum urea levels could be used as indirect indicators of fluid status/overhydration, it is important to notice that these variables were retained in the final model, while other, more affiliated to body fluid compartments (like LUS and BIS related characteristics), were not.

LUS, via B-lines evaluation, is a well-known diagnostical and prognostic method for both acute and chronic HF patients, while BIS is not a validated tool in HF subjects (as opposed to hemodialysis patients) (Wizemann et al., 2009; Onofriescu et al., 2014; Onofriescu et al., 2015; Siroopol et al., 2019)), (Platz et al., 2016; Gustafsson et al., 2015; Platz et al., 2017; Coiro et al., 2020; Buessler et al., 2020).

We observed that in our study group of chronic HF subjects, the number of B-lines was not maintained as a prognostic variable in none of the two prognostic models. This feature could be related to the variances in the included subjects (without pacemakers or stents, all patients with a LVEF below 45%), in the LUS protocol, but also to the differences in the correcting factors as we included both serum sodium and serum urea levels, while in the other studies these variables were not (Gustafsson et al., 2015; Platz et al., 2016).

As a final remark, the use of the tree classification, helped us to identify combined effects of different factors, asserting also the significance of such factors in the context of others.

For example, in our CART analysis, the significance of SBP values is limited only to patients who are hyponatremic and, similarly, serum urea levels only to severe HF. In HF subjects, a lower serum sodium level generally indicates poor water excretion or the use of diuretics.

Therefore, SBP level used in this context of further classification could represent a surrogate of fluid status, renal function, or activation of the renin-angiotensin-aldosterone (RAA) or sympathetic systems. Likewise, in the situation of severe HF, serum urea levels could suggest a poorer renal function or an increase in the activation of the RAA system.

The present study has *limitations and strengths*. First of all, we included a relatively small sample size of selected HF patients from a single-center unit and we weren't capable of identifying the exact cause of death. Yet, we used a special automated survival tree algorithm that has supplied different benefits over the conventional statistical approach.

Our HF cohort was a particular one, as we excluded those patients with conditions that could interfere with volume assessment techniques, and therefore, the generalizability of the results to the entire HF population could be limited. Moreover, since we didn't have a validation cohort, these results should be validated in other HF populations, including larger samples.

1.3.5. Conclusions

CART analysis enabled us to recognize different groups of risk for all-cause mortality in subjects with HFrEF. The use of this type of modeling suggested an improved prediction ability over that of using more conventional statistical approaches.

1.4. The role of New Multimodality Imaging in Patients with Hypertrophic Cardiomyopathy

1.4.1. Aim

The review sought to emphasize the benefits of contemporary cardiac imaging in selecting the optimal management strategies in HCM subjects, considering the advent of novel therapies that are currently applied or studied for this population.

1.4.2. Methods

Limited information is available, regarding how to achieve a timely diagnosis in HCM subjects, as a means to initiate an early treatment and to reduce the risk of sudden cardiac death (SCD). Therefore, we conducted a literature search on several databases, as Medline, PubMed, Embase, CINAHL, PsycInfo, and Ageline. We also reviewed Clinical Evidence, UpToDate, and the websites of major guideline development organisations.

1.4.3. Results and discussion

Hypertrophic cardiomyopathy (HCM) is the most common inherited cardiac condition, typically caused by mutations in genes that encode for sarcomeric proteins (Tuohy et al., 2020). It is characterized by an unexplained left ventricular hypertrophy (LVH), with systolic and diastolic left ventricular dysfunction, malignant ventricular arrhythmias that predispose to sudden cardiac death (SCD), and histopathologic modifications, including myofibrillar disarray and myocardial fibrosis (ESC, 2014; Maron, 2018; Makavos et al., 2019; Spudich et al., 2019). For the adult population, the prevalence of hypertrophic cardiomyopathy is estimated at 0.16% to 0.29%, with higher prevalence in older subjects, due to an age-dependent expression of gene mutations (Maron et al., 1995; Zou et al., 2004; Ramchand et al., 2020; Rowin et al., 2020).

HCM was firstly described in 1958 (Teare, 1958) and was considered as a life-threatening disease, without a curative treatment, and the most frequent cause of SCD in young subjects (Braunwald, 1964).

The clinical presentation, treatment, and prognosis of patients with HCM are largely unpredictable. This heterogeneity has resulted in large controversy regarding the optimal management strategy for these patients. The dominant symptoms in HCM are dyspnea, chest pain, palpitations, a decreased exercise tolerance or syncope.

No linkage between symptoms and signs of HCM and the degree of left ventricular hypertrophy or left ventricular outflow tract (LVOT) obstruction has been established. Besides, a considerable cohort of young subjects with HCM are asymptomatic or minimally symptomatic

(Teekakirikul et al., 2019). Sudden cardiac death, although not frequent (0.31 to 0.39 per HCM person-years), represents the most severe manifestation of hypertrophic cardiomyopathy (Weissler-Snir et al., 2019). Therefore, proper identification of subjects at high risk of SCD is of paramount importance.

Echocardiography

Transthoracic echocardiography represents the mainstay of imaging in hypertrophic cardiomyopathy. It provides crucial data regarding the presence, severity, and distribution of LVH, the abnormalities of the mitral valve and subvalvular apparatus, left atrial dimensions, the systolic and diastolic left ventricular function. It also evaluates the existence of left ventricular outflow tract obstruction (Geske et al., 2018; Maron et al., 2017).

2.1. Left Ventricular Wall Thickness

Left ventricular wall thickness should be measured during end-diastole, perpendicular to the left ventricular cavity. The echocardiographer should avoid the inclusion of left or right ventricular trabeculations (Bois et al., 2017; Tower-Rader et al., 2020). The measurements are more precise when using bidimensional echocardiography, in the short-axis view, at the apical, papillary muscles, and mitral valve levels (Cardim et al., 2015).

The most frequent segment affected by hypertrophy is the basal interventricular septum. However, taking into account the aspect that frequently there are non-contiguous patterns of myocardial hypertrophy, all left ventricular segments should be measured, from base to apex (Maron et al., 1986; Maron et al., 2009).

Several morphologies have been described for the interventricular septum, as follows: sigmoid, reverse curve, apical or neutral. These morphologies are important for guiding the septal reduction therapy. Increased wall thickness (massive hypertrophy of ≥ 30 mm), is connected with a high risk of SCD (Maron et al., 2015).

It is important to also assess right ventricular wall thickness, during end-diastole, in either the subcostal or parasternal long-axis views, at the level of the tricuspid chordae. Its normal value is below 5 mm (Gersh et al., 2011). When the bidimensional echocardiography images are suboptimal and the severity of ventricular hypertrophy or the septal morphology can not be clearly established, one could use contrast imaging (Klarich et al., 2013; Rowin et al., 2017). Contrast echocardiography also helps identifying apical aneurysms in subjects with apical HCM. Strain imaging provides information regarding myocardial mechanics and distinguishes HCM from amyloidosis. In cardiac amyloidosis, the apical strain is preserved, while in the basal segments is significantly affected (Bois et al., 2017).

2.2. Mitral Valve and Subvalvular Apparatus Morphology and Mitral Hemodynamics

Mitral valve abnormalities are frequent in subjects with HCM, including an increased length of the mitral valve leaflets, an important elongation of either posterior (≥ 17 mm in length) or anterior (≥ 30 mm in length) leaflet (Olivotto et al., 2016). The enhanced length of the mitral

valve leaflets may be the underlying mechanism of LVOT obstruction, if one of them extends across from the coaptation point, in systole moving into the LVOT, to contact the interventricular septum (Nishimura et al., 2017).

The duration of mitral valve-interventricular septum contact during systole will influence the severity of LVOT gradient. Subvalvular apparatus abnormalities, such as a hypertrophied anterolateral papillary muscle that is inserted directly on the anterior mitral leaflet, without chordae tendineae, can also result in a mid-cavity muscular obstruction, independent of systolic anterior motion (SAM). The presence of accessory papillary muscles or left ventricular muscle bundles can also produce outflow obstruction, by misplacing the mitral valve coaptation plane anteriorly, towards the interventricular septum (Agarwal et al., 2010; Nishimura et al., 2017). As a consequence of SAM, patients will present a mitral regurgitation, which is often difficult to distinguish from LV outflow jet.

Therefore, it is essential to examine the Doppler systolic flow pattern, as in mitral regurgitation it starts abruptly in systole and has increased velocities that persist in all systole, while the velocity from LVOT rises gradually in mid systole. The severity of mitral regurgitation differs with the gravity of LVOT obstruction and is commonly inferolateral directed (Wigle et al., 2001; Sherrid et al., 2009; Agarwal et al., 2010).

When the mitral regurgitation jet is centrally directed, it is typically due to an intrinsic mitral valve abnormality. Therefore, transesophageal echocardiography may be necessary for differential diagnosis (Marian et al., 2017; Veselka et al., 2017).

2.3. Left Ventricular Outflow Obstruction

Left ventricular outflow tract obstruction is the result of various complex mechanisms, including a reduced area of the left ventricular outflow tract, elongation of the anterior and/or posterior mitral leaflet, with an extension across from the coaptation point toward the interventricular septum and also the basal anteroseptal hypertrophy which bulges into LVOT (Olivotto et al., 2016; Maron, 2018; Spudich et al., 2019). Even though the definition of HCM is founded on the existence of LV hypertrophy, the LVOT obstruction produces heart failure symptoms and thus has become a specific feature of HCM (Maron et al., 2006; Kramer et al., 2015; Marian et al., 2017). Dynamic LVOT obstruction may also occur in subjects with hypertension, hypovolemia, calcification of the posterior mitral annulus, or hypercontractile states. LVOT obstruction is identified as a Doppler outflow tract pressure gradient exceeding 30 mmHg at rest or during provocation (Valsalva maneuver, standing, or exercise) (Elliott et al., 2014). Some data suggest that post-prandial LVOT gradients are higher than those from the fasting state (Nistri et al., 2012).

Certifying LVOT obstruction is extremely important. It helps to choose the right management of symptoms and also to prevent sudden cardiac death (Elliott et al., 2014). The optimal method of generating LVOT obstruction, in symptomatic subjects without resting LVOT obstruction, is exercise (stress) echocardiography. Since only 50% of individuals with provokable LVOT obstruction at stress echocardiography also have a positive response to the Valsalva

maneuver, a normal response will not preclude LVOT obstruction (Maron et al., 2006; Veselka et al., 2017). It is highly recommended to avoid dobutamine for stress testing, as it may generate LVOT obstruction in healthy subjects as well. A gradient in LVOT greater than 50 mmHg is usually considered the threshold at which LVOT obstruction is hemodynamically significant and it demands for septal reduction (Marian et al., 2017; Gersh et al., 2011) (Figure 4).

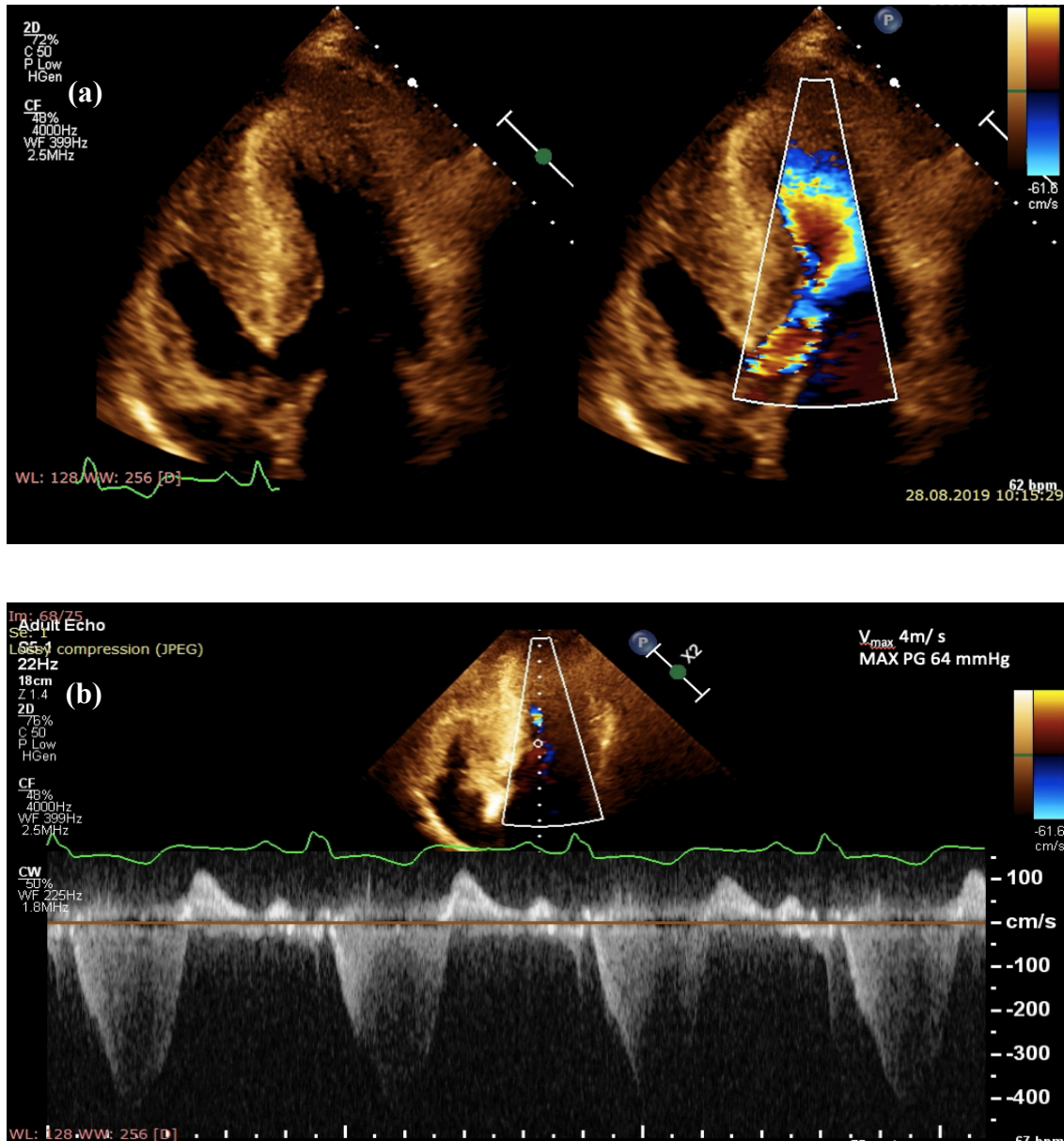


Figure 4. Echocardiography assessment at rest, in a 20-year-old male with obstructive hypertrophic cardiomyopathy: (a) apical five-chamber view with and without color Doppler demonstrating left ventricular mid-cavity and outflow tract obstruction, with turbulent flow; (b) continuous wave Doppler through the left ventricular outflow tract demonstrating the obstruction, with a peak gradient of gradient of 64

The connection between the existence of LVOT obstruction, especially at rest, and the increased risk of sudden cardiac death has been already demonstrated by previous studies (Maron et al., 2003; Gimeno et al., 2009). In a recent analysis, it has been emphasized that subjects without resting LVOT obstruction, but with an increased provoked LVOT gradient of ≥ 90 mmHg, have worse outcomes when compared to those with a low LVOT gradient < 89 mmHg (Lu et al., 2017). According to the recommendations for the identification and treatment of LVOT obstruction, included in the European Society of Cardiology Guideline (Elliott et al., 2014), 2D and Doppler echocardiography at rest and during a Valsalva maneuver, in the sitting or standing position (if no gradient is induced), is necessary in all subjects with HCM (Maron et al., 2006; Dimitrow et al., 2009).

If the maximum provoked LVOT gradient is lower than 50 mmHg and the individual is asymptomatic, it is suggested to annually repeat echocardiography. Exercise stress echocardiography should be deemed when LVOT gradient is important for lifestyle counseling or for selecting the optimal medical treatment. For subjects with a maximum provoked peak LVOT gradient ≥ 50 mmHg, treatment of LVOT obstruction is highly recommended. It is also strongly advisable for subjects with a maximum provoked LVOT gradient < 50 mmHg who are symptomatic, and if during exercise stress echocardiography, maximum provoked peak LVOT gradient increases to ≥ 50 mmHg (Elliott et al., 2014).

2.4. Left Atrial Enlargement

The majority of HCM subjects have a left atrial enlargement and its dimensions deliver important data regarding the prognostic (Spirito et al., 2009; Guttmann et al., 2014; O'Mahony et al., 2014). There are only a few studies that have assessed the relationship between left atrial volume and the risk of SCD (Yang et al., 2009; Debonnaire et al., 2014). However, the information about whether left atrial enlargement as an independent predictor of SCD is still controversial. It might be the result of LVH, LVOT obstruction, mitral regurgitation, diastolic dysfunction or atrial arrhythmia (Tower-Rader et al., 2020). The most common causes for left atrial enlargement are mitral regurgitation, as a consequence of SAM, and enhanced left ventricular filling pressures (Elliott et al., 2014).

2.5. Left Ventricular Ejection Fraction

Left ventricular ejection fraction (LVEF) should be evaluated by using the biplane method of discs. When there is a poor echocardiographic window or when it is difficult to delineate the endocardial border, we might use cardiac magnetic resonance (CMR) (Tower-Rader et al., 2020).

Approximately 10% of subjects with nonobstructive HCM will gradually develop end-stage heart failure, becoming eligible for heart transplantation (Tower-Rader et al., 2020). Additionally, half of them may develop left ventricular enlargement and remodeling, with regression of ventricular hypertrophy due to the enhanced interstitial myocardial fibrosis (Penicka et al., 2009; Toepfer et al., 2019). Subjects with a left ventricular ejection fraction below 50% commonly present an abrupt clinical deterioration due to microvascular dysfunction, which results in

myocardial ischemia and subsequently in fibrosis. Therefore, for subjects with HCM and decreased left ventricular ejection fraction ($\leq 50\%$), American College of Cardiology/ American Heart Association (ACC/AHA) guidelines advocate for the usage of implantable cardioverter defibrillators (ICDs), considering their increased risk of adverse cardiac events (Gersh et al., 2011). Conversely, the European Society of Cardiology did not include this statement in the current guidelines (Marian et al., 2017).

2.6. Diastolic Function

Diastolic dysfunction is highly prevalent in HCM patients. Almost half of HCM subjects with preserved left ventricular ejection fraction present symptoms of end-stage heart failure because of diastolic dysfunction (Toepfer et al., 2019). As the echocardiographic measurements used for assessing left ventricular diastolic function, respectively, mitral inflow (E/A ratio) or tissue Doppler imaging-derived parameters, do not correlate with the results obtained via cardiac catheterization, they should not be used as independent predictors of risk of end-stage heart failure or exercise duration (Araujo et al., 2005). Individuals with HCM and a restrictive mitral inflow pattern, portend a poor prognosis (Biagini et al., 2009).

The most reliable diastolic echocardiographic parameter, with a good correlation to left ventricular filling pressures, is the mitral early diastolic inflow to early diastolic tissue velocity (E/e'). It has recently been documented that E/e' ratio could be used for risk stratification in HCM, a higher value of E/e' being associated with worse event-free survival rate in nonobstructive HCM as well as in those with residual obstruction following myectomy (Lu et al., 2018).

2.7. Apical Aneurysm

Left ventricular apical aneurysm is identified as thin-walled, scarred akinetic, or dyskinetic wall segments, connected with both, midventricular and apical hypertrophy (Maron et al., 2008). Apical hypertrophy is defined as an apical wall thickness greater than 5 mm measured in end-diastole, or as a maximal apical to basal wall thickness ratio greater than 1.3 (Suzuki et al., 1999). Left ventricular apical aneurysms may be small-sized (transversal dimension ranging from 1 to 2 cm) or large-sized (>6 cm) and extremely rare change in size over time.

Apical aneurysm may be the consequence of increased apical pressure, myocardial wall stress, and ischemia. Sometimes, the extension of the transmural scarring of the aneurysm into the distal interventricular septum and/or left ventricular free wall may generate ventricular tachyarrhythmias (Nijenkamp et al., 2018).

The prevalence of apical aneurysms varies between 1.3% and 4.8% (Rowin et al., 2017; Xiao et al., 2016), and, in the majority of cases, its presence may be documented through the help of echocardiography. However, in almost 40% of cases, the existence of an apical aneurysm may be missed by echocardiography (Maron et al., 2008; Lee et al., 2013).

Accordingly, the use of contrast enhancement, which will better outline the endocardium, can help to identify the presence of an apical thrombus, myocardial fibrosis, or scar (To et al., 2011).

Recent studies emphasized that subjects with apical aneurysm possess an enhanced risk of serious adverse events (Maron et al., 2008; Ichida et al., 2014; Rowin et al., 2017) and, thus, the 2011 ACC/AHA guidelines added apical aneurysm as a risk modifier in HCM (Gersh et al., 2011). These subjects present an increased risk of sudden cardiac death and have to be considered for primary prevention implantable cardioverter-defibrillator and radiofrequency ablation (Nijenkamp et al., 2018).

On top of these, these subjects are at high risk of thromboembolic stroke (Maron et al., 2008; Rowin et al., 2017), but there is still not enough information as to initiate anticoagulant therapy in subjects with apical aneurysm without an apical thrombus (Gersh et al., 2011; Marian et al., 2017).

Echocardiography is the mainstay imaging investigation for screening. During puberty, it is recommended to be performed every 12 to 18 months and thereafter, to at least midlife, at every 3 to 5 years (Maron, 2018; Spudich et al., 2019).

Myocardial Strain

In left ventricular hypertrophy, left ventricular ejection fraction is not a reliable measure of systolic function, considering that in HCM it may be increased as a result of an increase in radial forces. Additionally, due to left ventricular hypertrophy, the left ventricular cavity size will be reduced causing a reduction in the stroke volume.

On this basis, a new and suitable method to evaluate myocardial deformation and subsequently left ventricular systolic function in patients with hypertrophic cardiomyopathy is the two-dimensional strain. It derives from speckle tracking imaging and is a non-invasive and sensitive method, proposed as an additional test to differentiate physiological from pathological left ventricular hypertrophy (Serri et al., 2006; Kansal et al., 2011). Myocardial deformation comprises three major components - longitudinal, radial, and circumferential deformation.

Global longitudinal strain (GLS) is a valuable measure in clinical practice, being used in patients with preserved ejection fraction for identifying subclinical left ventricular dysfunction (Collier et al., 2017). In subjects with left ventricular hypertrophy, myocardial fiber disarray and fibrosis compromise longitudinal function.

Therefore, in the early stages of the disease, subjects may present with a reduced GLS, despite a normal left ventricular ejection fraction (Figure 5).

Moreover, relatives of HCM subjects may have an impaired global longitudinal strain before the development of left ventricular hypertrophy (Yang et al., 2010; Urbano-Moral et al., 2014). In the past years, GLS has emerged as a powerful tool for evaluating left ventricular function and some studies support its role as a clinical predictor of adverse cardiovascular events (Paraskevaïdis et al., 2009; Tower-Rader et al., 2019).

Thus, in a large prospective study, the authors documented that a reduced GLS value (GLS > -16%) was independently linked with an increased risk of ventricular tachycardia/ventricular fibrillation, heart failure, cardiac transplantation, and all-cause death. Further, a GLS > -10% had significantly higher event rates, and four times higher risk of events compared with GLS ≤ -16% ($p = 0.006$) (Liu et al., 2017).

The relationship between abnormal global longitudinal strain and adverse cardiac outcomes and ventricular arrhythmia was also documented in a systematic review that analyzed more than 3000 patients with HCM from a total of 14 observational studies.

The authors have noticed that mean GLS was reduced, from -10% to -16% , in HCM patients and that the lower the GLS values (less negative), the higher the risk of adverse cardiovascular events (Weng et al., 2016).

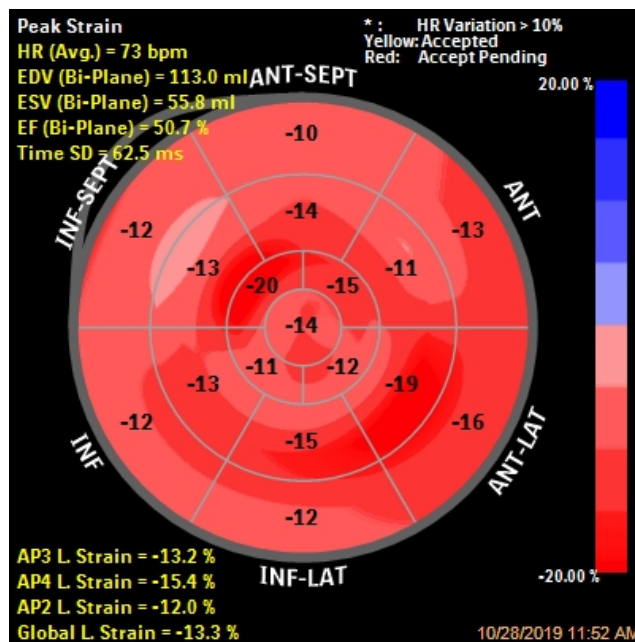


Figure 5. Longitudinal strain bull's-eye plot in the same 20-year-old patient with obstructive hypertrophic cardiomyopathy. This patient has a reduced global longitudinal strain (GLS = -13.3%), in the presence of a normal left ventricular ejection fraction.

Another study has assessed the effects of myocardial hypertrophy and cardiac afterload on myocardial deformation, at rest, and during standardized exercise, in asymptomatic subjects with moderate to severe aortic stenosis and individuals with hypertrophic cardiomyopathy.

The authors documented that during submaximal exercise, longitudinal and circumferential LV deformations were lower in aortic stenosis subjects than in those with HCM. These differences were not present at rest, and this can be explicated by the higher afterload noticed in these patients, which reduces the contractile reserve.

Thus, it has been underlined that moderate exercise echocardiography displays impaired myocardial contractility, which is not found at rest, in subjects with resembling types of left ventricular hypertrophy, respectively, individuals with hypertrophic cardiomyopathy and aortic stenosis (Schnell et al., 2013).

There are only a limited number of studies that assessed left ventricular segmental strain in subjects with HCM and concluded that regional LVH and myocardial fibrosis are independently and significantly linked to worse strain values (Popović et al., 2008; Collier et al., 2017).

However, considering the shortage of prospective clinical studies; GLS cannot be employed as a powerful clinical predictor of adverse cardiovascular events (Weng et al., 2016). Additionally, there are some problems concerning the potency of GLS to recognize asymptomatic obstructive HCM subjects or nonobstructive HCM subjects at risk of end-stage heart failure, as a means to commence adequate therapeutic strategies.

Exercise Testing

Exercise testing is an important noninvasive technique for evaluating and guiding treatment strategies in HCM. Different exercise testing methods were previously underutilized in patients with HCM but now have become increasingly employed.

Exercise (stress) echocardiography is typically used with the purpose of evaluating left ventricular kinetic disorders in subjects with suspicion of atherosclerotic coronary artery disease. More recently, this imaging modality has come to light as an important test in HCM (Desai et al., 2014; Rowin et al., 2017).

It predicts heart failure progression and also guides treatment strategies in HCM. It has been demonstrated that subjects with no or mild baseline symptoms but with provokable obstruction during exercise testing, are at higher risk of developing severe heart failure symptoms than those with nonobstructive HCM (3.2% per year vs. 1.6% per year, $p = 0.002$).

Additionally, subjects with New York Heart Association functional class III/IV symptoms and provokable obstruction during exercise, are candidates for myectomy or alcohol septal ablation, while those without obstruction are heart transplant candidates (Coats et al. 2015).

Thus, stress echocardiography predicts heart failure progression and is capable of differentiating between obstructive and nonobstructive HCM, guiding individual management strategies such as heart transplant for patients without obstruction, respectively, myectomy or alcohol septal ablation for those with (Rowin et al., 2017).

For measuring oxygen capacity and evaluating the functional capacity, cardiopulmonary (metabolic) exercise testing is particularly useful. The peak myocardial oxygen consumption with maximal exercise (Vo_2) helps to identify high-risk patients, potential heart transplant candidates (Sorajja et al., 2012; Finocchiaro et al., 2015; Masri et al., 2015; Magri et al., 2016).

Thus, exercise testing plays a pivotal role in appreciating long-term prognosis and selecting an optimized treatment in subjects with HCM (Rowin et al., 2017).

Computed Tomography Angiography

At least 25% of subjects with hypertrophic cardiomyopathy may experience angina, either on exertion or at rest (Gersh et al., 2011; Maron et al., 2014; Marian et al., 2017). There are different causes of chest pain in subjects with HCM: microvascular ischemia caused by abnormal intramural coronary arterioles, loss of normal vasodilation reaction, which results in a significant

reduction of the coronary flow reserve, an increased oxygen demand because of the hypertrophied myocardium, and impaired left ventricular relaxation, affecting the coronary blood flow (Gersh et al., 2011; Maron et al., 2014; Raphael et al., 2016; Marian et al., 2017).

As only 50% of subjects with HCM and coronary artery disease may present with obvious left ventricular kinetic disorders at exercise echocardiography, computed tomography angiography represents a noninvasive alternative for subjects at lower risk (Gersh et al., 2011). For symptomatic individuals with moderate-to-high risk of coronary artery disease, coronary angiography is still the gold standard test (Raphael et al., 2016).

It has recently been suggested that preprocedural computed tomography imaging has significant power on localizing the appropriate target septal artery for alcohol septal ablation and limiting the area of myocardial necrosis (Yanagiuchi et al., 2019).

Cardiac Nuclear Imaging

Although it is not commonly employed in clinical practice for evaluating patients with hypertrophic cardiomyopathy, positron emission tomography allows the appraisal of myocardial blood flow.

In subjects with no evidence of epicardial coronary artery disease, positron emission tomography may be used as a surrogate of microvascular dysfunction. Studies emphasized that subjects with a significant impairment of myocardial blood flow have an increased risk of end-stage heart failure and cardiovascular mortality (Olivotto et al. 2006).

Cardiac Magnetic Resonance

Cardiac magnetic resonance plays a vital role in diagnosis, risk stratification, and treatment of HCM subjects, considering its high spatial resolution, better contrast between blood and myocardium, accurate volumetric evaluation of cardiac chambers, and the fact that it is not influenced by the chest anatomy and associated pulmonary parenchymal pathologies when compared to echocardiography.

It is deemed as the gold standard for the assessment of left ventricular wall thickness and chamber size, allowing a precise characterization of heart volumes and functions, tissue morphology, and burden of myocardial hypertrophy (Conte et al., 2011; Freitas et al., 2019).

It possesses an excellent imaging capability of identifying apical aneurysms, clots, or papillary muscles. In compliance with the European Society of Cardiology guidelines (Cardim et al., 2015), CMR should be done, at least, as part of the initial evaluation, in all HCM subjects, when local resources and expertise allow.

Cardiac magnetic resonance imaging also evaluate the extension of left ventricular hypertrophy, which can be focal (1–2 hypertrophic segments, the rarest), intermediate (3–7 hypertrophic segments), and diffuse (8–16 hypertrophic segment, the most frequent) (Elliott et al., 2014).

CMR sequences used for the assessment of primary myocardial disorders can be segregated into tissue characterization sequences and functional assessment. Therefore, late gadolinium

enhancement (LGE) technique can identify the presence and pattern of LGE; cine sequences are utilized for the evaluation of systolic function (ejection fraction), ventricular volumes and wall morphology; T2* imaging identifies iron deposition; T1 mapping is used for the evaluation of diffuse myocardial fibrosis and T2 mapping for the assessment of tissue edema (Elliott et al., 2014; Freitas et al., 2019).

From all CMR sequences, LGE images have the most crucial role in tissue characterization in HCM. Through the help of gadolinium-based contrast agents, the late gadolinium enhancement method offers a high spatial resolution (less or equal to 1 mm in plane).

It can identify with great accuracy small areas of myocardial fibrosis, myocardial disarray, and scarring. LGE is encountered in about two-thirds of HCM subjects, commonly in areas of hypertrophy or right ventricular insertion points (Conte et al., 2011) (Figure 6).

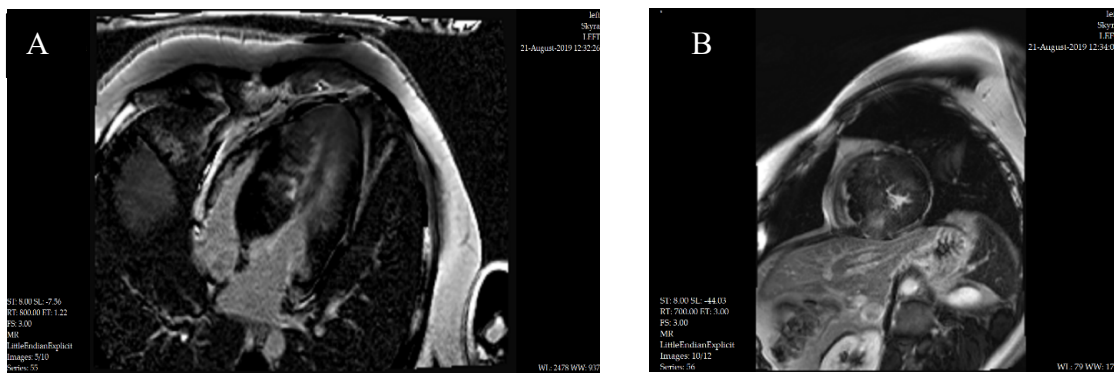


Figure 6. Late gadolinium enhancement images: (A) four-chamber view and (B) short-axis view, with diffuse nonischemic fibrotic lesions in the left ventricular myocardium and intramural nodular fibrotic lesions in the interventricular septum, in the same 20-year-old patient.

Lately, there has been an increased acknowledgment that the existence and degree of LGE on CMR is an important risk factor for sudden cardiac death in HCM patients. Numerous studies and meta-analyses documented a higher risk of cardiovascular mortality, heart failure, and all-cause death in the coexistence of LGE on CMR imaging in HCM subjects (Bruder et al., 2010; Green et al., 2012; Weng et al., 2016; Marian et al., 2017).

Green et al. conducted a meta-analysis on almost 1100 HCM subjects from four different studies, over an average follow-up of 3.1 years. They sought to appreciate the risk of adverse events in connection with the presence of LGE. In their study, the presence of LGE was statistically significantly associated with cardiac death, heart failure, and all-cause mortality, but they had no information concerning the extent of LGE (Green et al., 2012).

Another meta-analysis that has evaluated the predictive value of LGE-CMR for adverse events and death in HCM patients was published by Weng and coworkers. This meta-analysis comprised almost 3000 subjects, followed-up for a median of 3.1 years. The authors documented that the extent of LGE is significantly linked to a higher risk of SCD, even after adjusting for baseline characteristics (Hazard Ratio (HR) adjusted: 1.36/10% LGE; 95% CI: 1.10 to 1.69; $p = 0.005$).

The existence of LGE was also connected to a high risk of all-cause mortality, cardiovascular mortality, and a trend towards heart failure death (Weng et al., 2016). Mentias et al. sought to evaluate the prognostic utility of LGE in individuals with HCM, with low to intermediate sudden cardiac death risk and preserved left ventricular ejection fraction. They have emphasized that in subjects with HCM (obstructive, myectomy and nonobstructive) with preserved LVEF and low to intermediate risk of SCD, the extent of LGE was statistically significantly connected with a higher rate of composite endpoints, giving incremental prognostic utility (Mentias et al., 2018).

The importance of LGE-CMR in improving risk stratification strategies in HCM subjects was also evaluated by Freitas et al. During a median follow-up of 3.4 years, their results indicated that the amount of LGE has an important prognostic utility and that employing LGE for sudden cardiac death risk stratification would properly requalify a considerable proportion of subjects (Freitas et al., 2019).

All these studies emphasized that LGE is an independent predictor of sudden cardiac death in HCM and useful in identifying patients who will benefit the most from implantation of a cardioverter-defibrillator (ICD) for the primary prevention of sudden cardiac death (Marian et al., 2017; Weng et al., 2016; Bruder et al., 2010; Green et al., 2012; Mentias et al., 2018). T1 mapping is a novel CMR technique used to appreciate the extracellular volume fraction and for further detecting diffuse interstitial fibrosis.

Although there is limited information concerning the relationship between increased native T1 times and extracellular volume with adverse outcomes, most research supports its clinical utility in differentiating HCM from Fabry disease, cardiac amyloidosis, or hypertensive heart disease (Sado et al., 2013; Hinojar et al. 2015; Avanesov et al., 2017). T2* mapping can identify ischemic segments, and HCM subjects, potentially triggered via relative ischemia, have had reduced T2* values (Gastl et al., 2019). A recent retrospective study aimed to assess the risk of arrhythmia and heart failure in HCM subjects, in relation to myocardial T2* mapping.

In non-obstructive HCM individuals, it was particularly noticed that low T2* values are minimally related to arrhythmic events. There was no relationship between T2* and heart failure. Therefore, myocardial fibrosis assessed via LGE continues to be the strongest CMR predictor, while T2* mapping can be used only in particular clinical contexts (Gastl et al., 2020).

In Table IX, we synthesized the indications and therapeutic implications of multimodality imaging in subjects with hypertrophic cardiomyopathy. There are other newer techniques, such as CMR diffusion tensor imaging, but these were not yet included in clinical practice usage.

Table IX. Indications and therapeutic implications of multimodality imaging in choosing the optimal treatment in hypertrophic cardiomyopathy

Multimodality Imaging	Indications	Therapeutic Implications
Echocardiography	<ul style="list-style-type: none"> - first line technique in all HCM patients; - should be performed every 1–2 years, in clinically stable patients; 	<ul style="list-style-type: none"> - patients with massive hypertrophy (wall thickness ≥ 30 mm) have an increased risk of arrhythmic SCD and primary prevention ICDs are

Multimodality Imaging	Indications	Therapeutic Implications
	<ul style="list-style-type: none"> - evaluates the <i>left ventricle</i> (wall thickness, cavity size, systolic and diastolic function, left ventricular outflow tract obstruction), <i>mitral valve</i> (systolic anterior motion of the mitral valve, leaflets, chordae and papillary muscles abnormalities, severity of mitral regurgitation) and <i>aortic valve</i> (leaflet sclerosis, mid-systolic partial valve closure). 	<ul style="list-style-type: none"> - effective. They may also develop progressive drug-refractory HF, but this is reversible in most cases, after surgical myectomy. - GLS identifies patients with subclinical left ventricular dysfunction in the presence of preserved ejection fraction.
Cardiac magnetic resonance	<ul style="list-style-type: none"> - should be performed at the initial evaluation, if it is possible; - used for LGE/fibrosis assessment; anatomical assessment before invasive gradient reduction therapy; differential diagnosis or in case of suboptimal echo images. 	<ul style="list-style-type: none"> - extensive LGE identifies patients at risk of SCD (they deserve consideration for primary prevention ICDs) and patients at risk of end-stage HF (require close clinical surveillance); - in 40% of cases, the apical aneurysm may be missed by echocardiography and we may use contrast enhancement. These patients have an increased risk of serious adverse events and need to be considered for primary prevention ICDs and radiofrequency ablation for those with recurrent ventricular tachyarrhythmia.
Computed tomography angiography	<ul style="list-style-type: none"> - used for anatomical assessment of the epicardial coronary arteries (bridging, epicardial CAD) or in case of suboptimal echo images and contraindications for cardiac magnetic resonance. 	<ul style="list-style-type: none"> - is important in localization of the appropriate target septal artery for alcohol septal ablation and to limit the area of myocardial necrosis.
Cardiac nuclear imaging	<ul style="list-style-type: none"> - to assess the myocardial perfusion; metabolism, receptors and innervation; differential diagnosis or in case of suboptimal echo images and contraindications for cardiac magnetic resonance. 	<ul style="list-style-type: none"> - patients with the most significant impairment of the myocardial blood flow have an increased risk of end-stage HF and cardiovascular mortality.
Cardiopulmonary exercise testing	<ul style="list-style-type: none"> - used to assess functional capacity by evaluating O₂ capacity. 	<ul style="list-style-type: none"> - is relevant for nonobstructive HCM patients with end-stage HF that are

Multimodality Imaging	Indications	Therapeutic Implications
CAD, coronary artery disease; GLS, global longitudinal strain; HCM, hypertrophic cardiomyopathy; HF, heart failure; ICDs, implantable cardioverter-defibrillator; LGE, late gadolinium enhancement; SCD, sudden cardiac death.		candidates for a heart transplant and for patients with obstructive HCM that require invasive septal reduction therapy.

1.4.4. Conclusion

Multimodality imaging is useful in evaluating the morphology of hypertrophic cardiomyopathy. It possesses a significant role in choosing the optimal treatment and in appreciating long-term prognosis. Considering that patients with HCM that are at low risk, according to the current risk stratification framework, might still experience adverse events, it is necessary to detect additional surrogates of adverse outcomes and select the proper treatment option. We believe that all recent advances in multimodality imaging techniques will significantly transform the HCM treatment in the coming years, considering the advent of gene-based therapies and minimally invasive procedural techniques. The implementation of multimodality imaging methods, including cardiac magnetic resonance, myocardial strain, computed tomography angiography, or positron emission tomography, enables an improvement in the therapeutic strategies, which will improve the prognosis and life quality in HCM.

1.5. Multimodality Imaging in Patients with Infiltrative Cardiomyopathies

1.5.1. Aim

This review intends to highlight the significance of contemporary cardiac imaging in diagnosing specific ICM and improving outcomes through the early initiation of a targeted treatment.

1.5.2. Materials and methods

We performed literature research regarding the significance of multimodality imaging in the diagnosis and management of patients with infiltrative cardiomyopathies, focusing primarily on cardiac amyloidosis, sarcoidosis, and hemochromatosis.

1.5.3 Results and discussion

Cardiac amyloidosis, the prototype of RCM, results as a consequence of amyloid accumulation in the heart, which typically occurs in immunoglobulin-light chain amyloid (AL) amyloidosis and transthyretin amyloid (ATTR) amyloidosis (either hereditary or wild-type) (Martinez-Naharro et al., 2020). In AL amyloidosis, the most common type of systemic

amyloidosis, disproportionate monoclonal light chain production, due to plasma cell dyscrasia, favors amyloid fibrillogenesis. In ATTR amyloidosis, transthyretin, a homotetrameric transport protein produced by the liver, dissociates into monomers that consequently misfold and self-assemble in amyloid fibrils (Nienhuis et al., 2016; Vergaro et al., 2020).

Sarcoidosis is a multisystem, inflammatory, noncaseating granulomatous condition of undetermined etiology that dominantly impacts the lungs and lymphatic nodes. This pathology presents three sequential histological phases: edema, granulomatous infiltration, and fibrosis, the latter being not only the most devastating but also an independent prognostic factor (Rammos et al., 2017; Greulich et al., 2013). Cardiac sarcoidosis is responsible for considerable morbidity, with recorded mortality rates greater than 60% (Pierre-Louis et al., 2009; Perry et al., 2019). Additionally, as stated by a recent CMR imaging study conducted on 205 subjects with sarcoidosis, the prevalence of cardiac involvement appears to exceed 25%, and therefore, the necessity for awareness and expertise in identifying ICMs (Murtagh et al., 2016; Pereira et al., 2018).

Hemochromatosis might develop either from a gene mutation (hereditary hemochromatosis) or from a secondary cause (hemosiderosis) (Seward et al., 2010; Rammos et al., 2017). Hereditary hemochromatosis (HH) is characterized by iron overload because of an increased gastrointestinal absorption. Cardiac involvement emerges later when compared to other organs caught in the pathogenic process (e.g., liver, pancreas, skin) and is less frequent, happening only in 15-20% of cases (Mughtar et al., 2017). Impairment in iron deposition within the heart causes, in the early stage, altered left ventricular (LV) diastolic function, with a restrictive filling pattern that, without the implementation of iron chelation treatment, habitually leads to LV dilatation and impaired systolic function (Habib et al., 2017).

➤ **Conventional Transthoracic Echocardiography (TTE)**

Transthoracic echocardiography (TTE) is an important, largely-available diagnostic instrument and a pivotal initial step in evaluating subjects with ICMs. It supplies precious data concerning LV wall thickness, LV cavity size, LV systolic and diastolic function, the coexistence of pericardial effusion or right heart involvement. Echocardiographic findings help diagnosing ICMs, but they only arouse suspicion about the etiology. TTE is neither specific nor sensitive in diagnosing cardiac amyloidosis (Falk, 2005).

However, as reported by a large multicentric study conducted by Boldrin M et al., echocardiography's diagnostic performance in subjects with proven systemic AL amyloidosis can be increased via the usage of highly sensitive and specific cutoffs (Boldrini et al., 2020). Similarly, a normal echocardiogram cannot exclude cardiac involvement in a patient with systemic sarcoidosis (Kim et al., 2009).

Additionally, TTE represent a second-line imaging method, after cardiac magnetic resonance, for the assessment of cardiac involvement in hemochromatosis, being more helpful in regular clinical follow-up and screening than in measuring biventricular systolic function (Giakoumis et al., 2007; Pennell et al., 2013; Habib et al., 2017).

- **Left Ventricular Wall Thickness and Cavity Size**

Left Ventricular Wall Thickness and Cavity Size in Amyloidosis

As the infiltrative process primarily affects the left ventricular walls, the ordinary echocardiographic findings in cardiac amyloidosis are represented of a concentric LV pseudohypertrophy with a reduced LV cavity size, features that can be seen in more than 90% of cases (Vergaro et al., 2020).

The main characteristic of cardiac amyloidosis is represented by the discrepancy between low QRS voltage on the electrocardiogram and enhanced LV wall thickness on the echocardiogram (Martinez-Naharro et al., 2020).

Nevertheless, up to 20% of subjects with cardiac amyloidosis can present electrocardiographic evidence of LV hypertrophy, particularly those with ATTR wild-type amyloidosis (Maurer et al., 2017).

ATTR wild-type amyloidosis is characterized by greater LV wall thickness and mass when compared to hereditary ATTR amyloidosis and AL amyloidosis, suggesting a longer period of amyloid accumulation (Dorbala et al., 2020). The sparkling or granular aspect of the myocardium initially deemed a unique trait of cardiac amyloidosis, is not a pathognomonic sign as it lacks sensitivity (Perry et al., 2019).

However, in the initial phases, asymmetrical septal hypertrophy, with LV outflow tract obstruction may be observed (Habib et al., 2017).

The tendency toward symmetrical hypertrophy is more obvious in AL amyloidosis, while in ATTR amyloidosis, there is a predisposition to an asymmetrical increase in LV wall thickness (Chacko et al., 2019).

Left Ventricular Wall thickness and Cavity Size in Sarcoidosis

The echocardiographic recordings in cardiac sarcoidosis are of high variability. A slight increase in left ventricular wall thickness, mimicking hypertrophic cardiomyopathy, can be noticed during edema and granulomatous infiltration (Kurmann et al., 2018).

On the contrary, basal septal thinning, which is highly common and a specific trait of cardiac sarcoidosis, is the result of myocardial fibrosis (Ayyala et al., 2008; Rammos et al., 2017). LV cavity size is often normal or increased (Ramos et al., 2017).

Left Ventricular Wall Thickness and Cavity Size in Hemochromatosis

Myocardial concentric or asymmetric nonextreme hypertrophy with progressive left ventricular remodeling and dysfunction is the most frequent phenotype in cardiac hemochromatosis (Díez-López et al., 2018).

Rozwadowska et al. conducted a study on 39 individuals with early diagnosed HH and 19 with long-lasting and long-treated HH and demonstrated that both early and old HH are connected to LV hypertrophy, irrespective of other conditions such as arterial hypertension and diabetes (Rozwadowska et al., 2019).

- **Diastolic Dysfunction**

Diastolic Dysfunction in Amyloidosis

Diastolic function is severely impaired in cardiac amyloidosis, the extent of impairment being connected to the burden of amyloid accumulation and an independent surrogate of poor outcomes, and mortality (Klein et al., 1991). As the disease advances, LV wall stiffness increases, resulting in impaired relaxation and, finally in increased filling pressures.

Restrictive filling pattern, the paradigm of ICMs, is defined by increased peak E wave velocity with short E wave deceleration time, reduced atrial filling velocity (A wave) with increased E/A ratio.

The impairment of diastolic function, along with amyloid atrial infiltration, promotes biatrial enlargement and increases the thromboembolic risk (Chacko et al., 2019). Intra-atrial thrombosis is frequent even within-subjects with cardiac amyloidosis and sinus rhythm, as stated by a large autopsy study (Feng et al., 2007).

In advanced cardiac amyloidosis, the pulmonary vein flow pattern is abnormal, characterized by decreased systolic flow velocity and increased diastolic flow velocity (Di Nunzio et al., 2019).

Tissue Doppler imaging (TDI) is a relatively new echocardiographic method that helps to differentiate between cardiac amyloidosis and constrictive pericarditis or hypertrophic cardiomyopathy. Early diastolic mitral annulus velocity (e') as evaluated via TDI incrementally decreases during the progression of cardiac amyloidosis, while in constrictive pericarditis and hypertrophic cardiomyopathy is normal or only slightly reduced (figure 7) (Kyriakou et al., 2018). Besides, E/e' ratio values seem to be higher in cardiac amyloidosis than in hypertensive LV hypertrophy and improve echocardiography's discrimination power when mixed with LV basal longitudinal strain assessment (Schiano-Lomoriello et al., 2016).

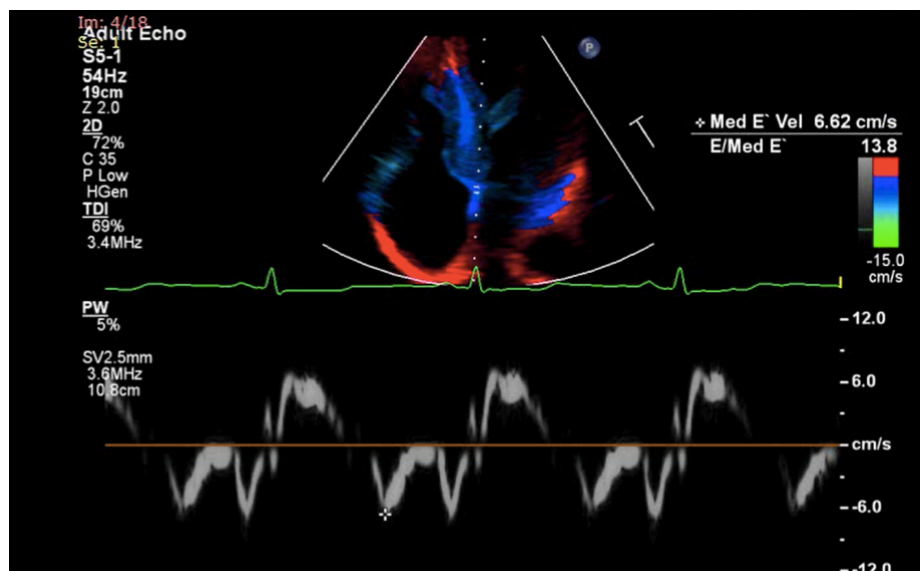


Figure 7. Tissue Doppler imaging demonstrating decreased septal e' velocity and increased E/e' ratio in a female with cardiac amyloidosis.

Diastolic Dysfunction in Sarcoidosis and Hemochromatosis

Analogously, diastolic dysfunction (DD) is invariably present in hemochromatosis and sarcoidosis. It begins with grade 1 DD or impaired relaxation and it ends with grade 3 DD or D or restrictive pattern with high LV filling pressures (Habib et al., 2017; Kurmann et al., 2018).

In hemochromatosis, a pseudonormal filling pattern, known as grade 2 DD, can be found as well and can be better evaluated via tissue Doppler imaging, which typically identifies decreased diastolic early filling mitral annular tissue velocity, starting with the early phases of the disease. An increase in the duration of the pulmonary venous atrial reversal flow provides further help. Concerning the relationship between DD and outcomes in myocardial iron overload cardiomyopathies, very few information is accessible.

Restrictive DD can promote the development of right-sided heart failure with preserved LV ejection fraction (Habib et al., 2017; Pereira et al., 2018). In cardiac sarcoidosis, the degree of LV and/or RV DD seems to accurately connect with the degree of myocardial involvement assessed through the help of cardiac magnetic resonance imaging (Habib et al., 2017; Pereira et al., 2018). Remarkably, DD does not embody a specific sign of cardiac involvement in sarcoidosis, although it is constantly present (Perry et al., 2019).

➤ **Systolic Function**

Systolic Function in Amyloidosis

In cardiac amyloidosis, longitudinal ventricular contraction is affected before radial contraction. Thus, LV ejection fraction (LVEF) as assessed with 2D conventional TTE, is preserved until advanced stages of the disease, and it is not a suitable indicator of LV systolic performance. The mitral annulus's systolic excursion in M-mode echocardiography (MAPSE) is frequently reduced, despite normal LVEF (Chacko et al., 2019).

Myocardial performance index (MPI) or Tei index, defined as the sum of isovolumetric contraction time and isovolumetric relaxation time divided by ejection time, increases in cardiac amyloidosis.

This pattern was firstly described by Tei et al., who demonstrated that in cardiac amyloidosis, the isovolumetric relaxation time is lengthened in all phases. Subsequently, the pre-ejection time is prolonged, and the ejection time is shortened, resulting in an increase in MPI (Tei et al., 1996; Di Nunzio et al., 2019).

Systolic Function in Sarcoidosis

Because of regional wall motion abnormalities that do not respect a coronary distribution, systolic dysfunction is frequent in cardiac sarcoidosis (Birnie et al., 2016; Habib et al., 2017). Subjects with cardiac sarcoidosis and LVEF < 50% appear to have inferior survival rates than those with preserved ejection fraction. They are also less responsive to corticosteroids (Yazaki et al., 2001).

Systolic Function in Hemochromatosis

In cardiac hemochromatosis, if the cause of iron excessive accumulation is not eliminated, the majority of the patients will develop LV remodeling with dilation and reduced LVEF (Kremastinos et al., 2011).

Echocardiography aids in identifying LV systolic dysfunction, but this occurrence does not specifically support the diagnosis of cardiac hemochromatosis. There is limited information concerning the timeline of progressing to a dilated phenotype from a restrictive one, as well as the factors that favor this evolution.

Nonetheless, advanced echocardiographic techniques, including strain rate imaging, provides a more precise image of LV systolic performance in cardiac hemochromatosis (Pereira et al., 2018).

➤ **Right Heart Involvement**

Right Heart Involvement in Amyloidosis

Concurrent right ventricular (RV) free wall hypertrophy highly supports the diagnosis of cardiac amyloidosis or another ICM (Khor et al., 2020). When the right ventricle is affected by the amyloidotic fibrils' pathological accumulation, the anterior wall is firstly involved (Figure 8). RV hypertrophy emerges after LV amyloid infiltration, and it portends a worse prognosis (Khor et al., 2020).

Longitudinal RV systolic function impairment is depicted by a reduction in the tricuspid annular plane systolic excursion (TAPSE) in M mode echocardiography (Dorbala et al., 2020).

A cutoff <14 mm of TAPSE independently predicted the risk of major adverse cardiac events including death, heart transplantation, and acute heart failure in 82 subjects with confirmed cardiac amyloidosis (Bodez et al., 2016).

The predictive value of RV involvement in cardiac amyloidosis was also assessed via a retrospective study, published by Cicco et coworkers. They retrospectively evaluated 135 subjects with systemic amyloidosis, 54 of them having signs of cardiac amyloidosis (CA) at enrolment. In the control group, they have included 81 patients with non-cardiac amyloidosis (nCA).

A significant increase in the right atrium, right ventricular basal diameter, and the diameter of the inferior cava vein at rest, in CA patients, was recorded. The authors have also documented statistically significant differences in right ventricular wall thickness, which was increased in CA patients (CA 9.87 ± 1.73 vs. nCA 7.00 ± 1.05 mm; $p = 0.0001$).

Into what concerns the RV systolic function, evaluated via M-mode echocardiography they have encountered a decreased value of TAPSE in CA compared to nCA patients (CA 18.73 ± 8.32 vs. nCA 26.58 ± 1.73 mm; $p = 0.0317$). Although increased values of estimated pulmonary arterial pressure have been recorded in CA subjects (CA 38.27 ± 10.67 vs. nCA 28.38 ± 3.75 mmHg; $p = 0.0053$), there were no differences regarding the tricuspid regurgitation velocity between these two groups.

A reduced TAPSE suggested a worse prognosis and exhibited a significant positive correlation with lymphocyte count, gamma globulins, monoclonal components, and

immunoglobulin G values, while the inferior vena cava diameter, the right atrium area, and the estimated pulmonary arterial pressure, correlated only to diastolic function, evaluated as E/e' ratio (Cicco et al., 2020).

To compare the right ventricular involvement in transthyretin amyloidosis and hypertrophic cardiomyopathy, Arvidsson et al. assessed the echocardiographic conventional parameters and the RV global and segmental strain on 42 patients with ATTR amyloidosis and echocardiographic evidence of left ventricular hypertrophy (cardiac ATTR), 19 ATTR individuals with normal LV wall thickness (non-cardiac ATTR), 25 subjects with biopsy proven or genetically diagnosed HCM, and 30 healthy volunteers.

They highlighted that, into what concerns RV structure and function, only RV segmental strain may help to differentiate between these two pathologies. In the cardiac ATTR amyloidosis subgroup, an apex-to-base RV strain gradient was documented, with relative apical sparing, similarly to what has been previously described for the LV. Segmental RV strain was lower in the apical region of HCM patients, this reverse pattern demanding more research (Arvidsson et al., 2018).

Regarding RV diastolic function, equivalent modifications in the tricuspid inflow pattern are generally detected. RV dilatation reflects advanced disease and indicates a worse prognosis (Bodez et al., 2016).

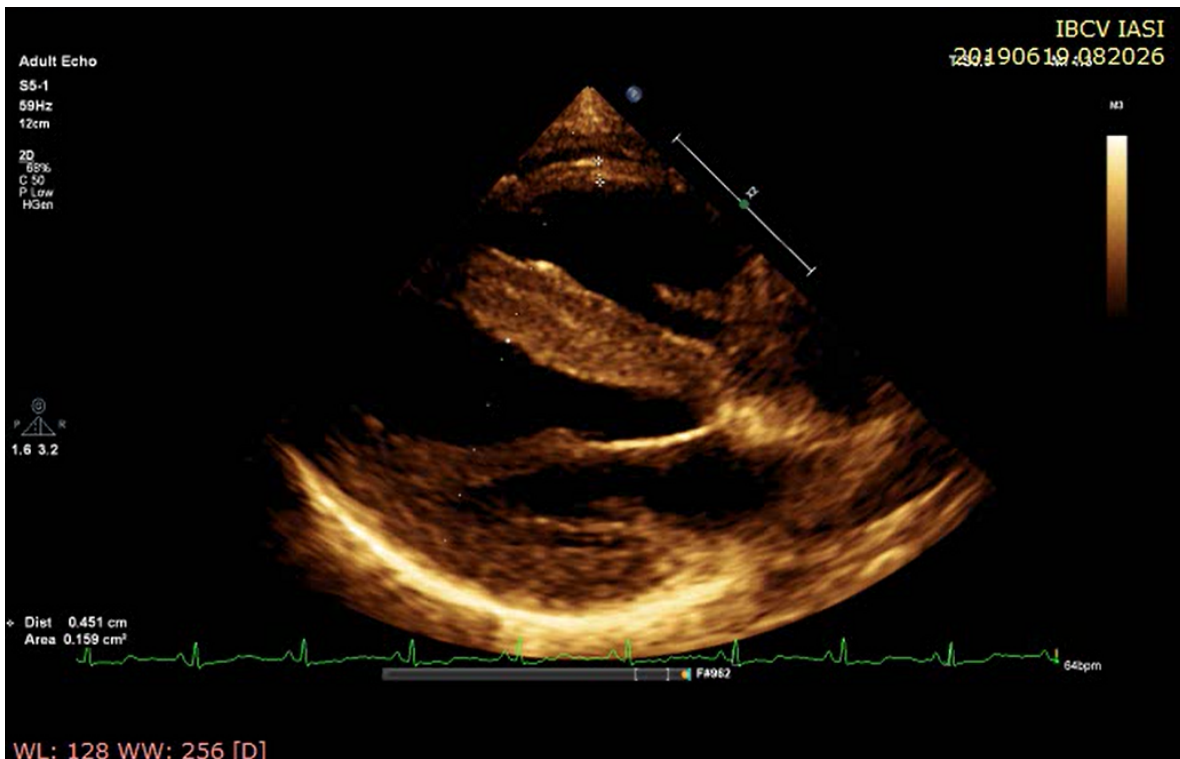


Figure 8. Echocardiographic assessment at rest, in a young female with ATTR amyloidosis: parasternal long-axis view demonstrating concentric left ventricular pseudohypertrophy with concomitant right ventricular free wall hypertrophy.

Right Heart Involvement in Sarcoidosis

Although the greatest predisposition to granulomatous infiltration is within the basal interventricular septum and LV lateral free wall, it is important to understand that cardiac sarcoidosis can directly affect the RV (Kurmann et al., 2018).

Half of the subjects with cardiac sarcoidosis present RV wall motion abnormalities and systolic dysfunction (Smedema et al., 2017). LV and lung sarcoid infiltration can cause pulmonary hypertension and subsequently RV dilatation (Patel et al., 2016).

The real prevalence of pulmonary hypertension in sarcoidosis is unknown, varying from 5-20% to more than 50% in patients with constant or unexplained dyspnea (Huitema et al., 2016).

Cardiac sarcoidosis and arrhythmogenic right ventricular cardiomyopathy (ARVC) can present overlapping phenotypes.

In a study conducted by Philips et al., 15 subjects from the Johns Hopkins ARVC registry were in the end regrouped as having cardiac sarcoidosis (Philips et al., 2014). RV abnormalities can be better assessed via cardiac magnetic resonance (CMR) imaging, RV involvement in cardiac sarcoidosis representing a vital prognostic factor, and an important risk stratification instrument (Velangi et al., 2020; Kagioka et al., 2020).

Right Heart Involvement in Hemochromatosis

As hemochromatosis progresses, RV dilation and systolic dysfunction can appear evident (Mughtar et al., 2017).

➤ **Other Echocardiographic Findings**

Other Echocardiographic Findings in Amyloidosis

Even though most of the echocardiographic signs of cardiac amyloidosis are nonspecific, it is important to acknowledge that these can become highly suggestive if incorporated into the context.

Biatrial enlargement, small pericardial and pleural effusions, thickening of the atrioventricular valve, and of the interatrial septum represent other common echocardiographic characteristics of cardiac amyloidosis (Mughtar et al., 2017) (Figure 9).

Zhao et al. assessed the prognostic value of left atrial (LA) size on 104 patients with cardiac amyloidosis. As illustrated by the results of their study, LA enlargement, characterized by a LA diameter indexed to body surface area higher than 23 mm/m², is highly connected to all cause-mortality and severe heart failure (Zhao et al., 2016).

The analysis performed by Falk et al. was among the earliest echocardiographic studies and demonstrated that increased atrial septal thickening was present in 60% of the patients with cardiac amyloidosis and had 60% sensitivity and 100% specificity for cardiac amyloidosis diagnosis when coupled with increased myocardial echogenicity (Falk et al., 1987; Jurcuț et al., 2020).

Left heart valve thickening is common in AL amyloidosis and connected to worse outcomes and increased mortality (Mohty et al., 2017). Damy T et al. performed an observational

study on 266 subjects with cardiac amyloidosis and highlighted that pericardial effusion, if present, even in small quantities, is a powerful death predictor (Damy et al., 2016).

Notably, no discrepancies in subtype-specific reasons of death were recorded between AL and ATTRwt cardiac amyloidosis subjects (Escher et al., 2020).

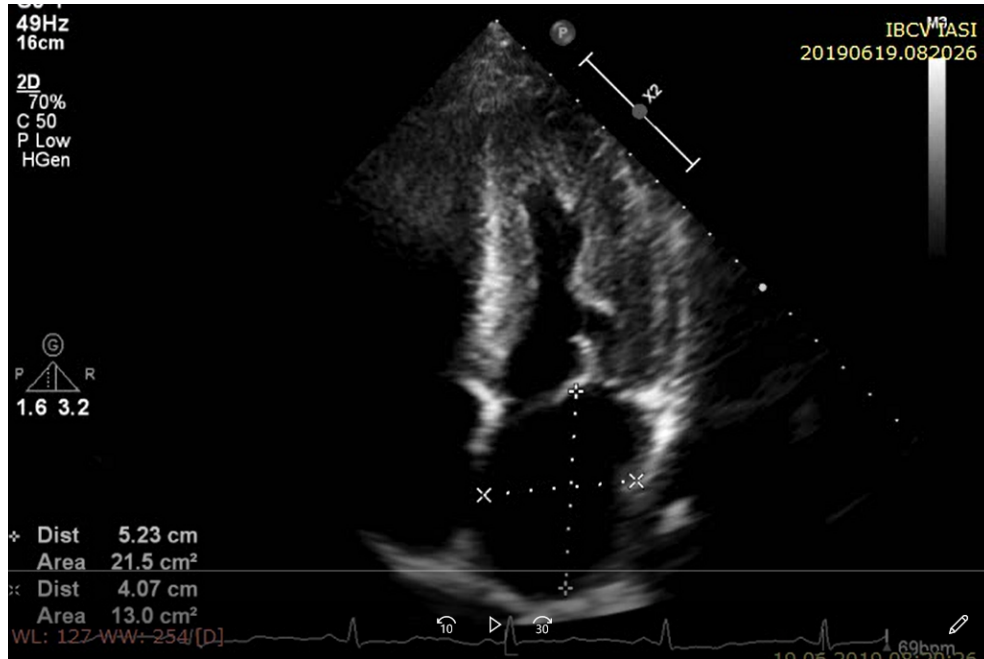


Figure 9. Transthoracic echocardiogram, apical four-chamber view in a patient with cardiac amyloidosis showing: increased thickness of left ventricle wall with “granular sparkling” appearance, increased biatrial dimensions in contrast with a small left ventricle cavity, and pericardial effusion.

Other Echocardiographic Findings in Sarcoidosis

In cardiac sarcoidosis, granulomatous infiltration can involve any cardiac structure, including the endocardium, myocardium, pericardium, conduction system, coronary arteries, and vena cava (Perry et al., 2019). Myocardial granulomatous infiltration can lead to LV aneurysm formation. Mitral regurgitation is the consequence of either papillary muscle malfunction or direct infiltration of the valve (Pereira et al., 2018).

Pericardial effusion is a less common manifestation of cardiac sarcoidosis. However, it has been reported by various case reports (Peña-García et al., 2019). On top of these, cardiac sarcoidosis might imitate coronary artery disease, Takotsubo cardiomyopathy, right ventricular cardiomyopathy, hypertrophic cardiomyopathy, and valvular dysfunction (Arvidsson et al., 2018). The bright echogenicity of the interventricular septum and the free wall suggests scars and inflammation (Kurmann et al., 2018).

Other Echocardiographic Findings in Hemochromatosis

In cardiac hemochromatosis, echocardiography identifies the consequence of iron overload, which ranges from a restrictive pattern with biatrial enlargement to biventricular

dilatation with systolic dysfunction. A myocardial phenotype of left ventricular noncompaction may occur in cardiac hemochromatosis (Díez-López et al., 2018).

➤ **Advanced Echocardiographic Techniques**

Advanced Echocardiographic Techniques in Amyloidosis

In cardiac amyloidosis, TDI allows differentiating between cardiac amyloidotic pseudohypertrophy and true hypertrophy. Myocardial velocities registered by placing the sample volume in the septal or lateral ventricular myocardium, next to the mitral annulus, are significantly decreased. This is mostly due to the fact that the amyloidotic infiltration of the heart compromises myocytes' longitudinal contraction. If TDI presents some limitations, such as the interference with translational and tethering movements of the heart, speckle tracking echocardiography (STE) portrays great spatial and temporal resolution (Di Nunzio et al., 2019).

STE is a powerful diagnostic instrument, capable of distinguishing between cardiac amyloidosis and hypertensive heart disease or hypertrophic cardiomyopathy.

A simple diagnostic algorithm, based on T troponin blood levels and two echo-derived strain parameters, namely global longitudinal strain and apical to basal longitudinal strain gradient, has recently been proposed as an alternative for diagnosing cardiac involvement in AL amyloidosis, possessing great accuracy when compared to consensus criteria (Di Nunzio et al., 2019).

Quarta et al. conducted a comprehensive echocardiographic study on 172 patients with amyloidosis and emphasized that global longitudinal strain values are considerably decreased even in subjects with preserved ejection fraction (Quarta et al., 2014). The abnormal global longitudinal strain possesses an incremental prognostic value, being linked to poor survival in both types of cardiac amyloidosis (Dorbala et al., 2020).

Nevertheless, longitudinal myocardial deformation is dominantly decreased at the level of the mid and basal segments, the apical sparing of the longitudinal strain generating a distinctive “bullseye pattern” described as the “cherry-on-the-top” sign. This particular preservation of the apex's contractile function generally symbolizes a reduced degree of amyloid accumulation at the ventricular apex when compared to the base (Martinez-Naharro et al., 2020) (Figure 10).

Pagourelis et al. indicated that a cut off value of 4.1 of LVEF strain ratio (LVEF/ absolute value of global longitudinal strain) helps the diagnosis of cardiac amyloidosis out of the cluster of thickened myocardium pathologies, being extremely useful in the subgroup of subjects with mild hypertrophy and preserved ejection fraction (Pagourelis et al., 2016). Remarkably, not only longitudinal strain is impaired in cardiac amyloidosis, but also circumferential and radial deformations (Vergaro et al., 2020).

Despite the extensive research on LV longitudinal strain as evaluated via speckle tracking echocardiography and tissue Doppler imaging, it is important to acknowledge that RV free wall longitudinal strain (FWLS) is also a powerful prognostic instrument in cardiac amyloidosis. As illustrated by a retrospective analysis on 36 patients with AL amyloidosis and 57 with ATTR amyloidosis, baseline RV FWLS was independently related to all-cause mortality and cardiovascular hospitalizations at 1-year follow-up, while other echocardiographic parameters of

right heart performance were not. RV FWLS decreased considerably during follow-up evaluations, in both types of amyloidosis, while other RV measurements did not, naming RV FWLS as a sensitive indicator of the degree of RV involvement in cardiac amyloidosis (Fine et al., 2020). A decrease in RV free wall systolic velocity via tissue Doppler echocardiography can be noticed as well (Perry et al., 2019).

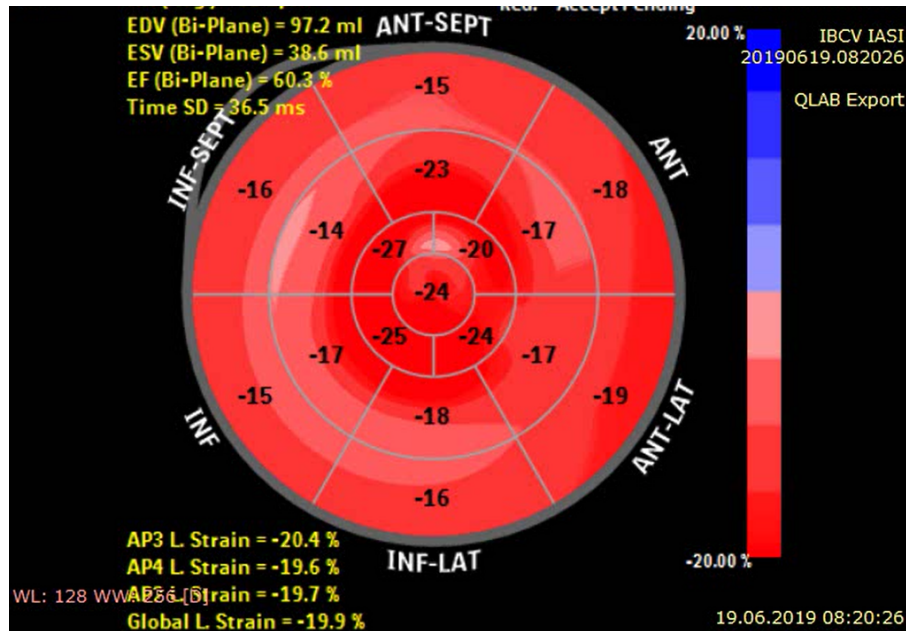


Figure 10. Distinctive bull's-eye plot in cardiac amyloidosis, with slight impairment of the GLS in the basal and mid-ventricular segments and relative apical-sparing.

Left atrial strain, as evaluated through the help of 2D-STE, emerged as a new useful surrogate of cardiac amyloidosis. All left atrial strain, and strain rate parameters appear to be considerably decreased in cardiac amyloidosis patients, to a higher degree than in the hypertensive population.

A LA reservoir strain cut-off value of 20% had a sensitivity of 86.4% and a specificity of 88.6% in identifying cardiac amyloidosis in an analysis that has comprised 44 subjects with cardiac amyloidosis and 25 with hypertensive heart disease and increased LV wall thickness (Rausch et al., 2020).

Additionally, in cardiac amyloidosis, 2D-STE-derived LA phasic functions strongly connect with LV global longitudinal strain. Nochioka et al. illustrated that worse LA strain in cardiac amyloidosis is related to a more important impairment of LV systolic and diastolic functions (Nochioka et al., 2017).

The study conducted by Mohty et al. was the first to evaluate the link between LA strain parameters derived by three-dimensional STE, NT-proBNP, and cardiac troponin T levels and Mayo Clinic staging on a cohort including 77 patients with confirmed AL amyloidosis and 39 healthy volunteers. Reduced 3D-LA total emptying fraction and 3D peak atrial longitudinal strain were linked with a reduced two-year survival rate, independently of LA volume (Mohty et al., 2018).

Advanced Echocardiographic Techniques in Sarcoidosis

As previously stated, TTE possesses reduced sensitivity in identifying cardiac sarcoidosis, the appearance of newer imaging techniques resulting in an improvement in the diagnostic performance (Mughtar et al., 2017). Myocardial deformation strain imaging helps to identify subclinical cardiac sarcoidosis in the context of reduced GLS with preserved LVEF (Kurmann et al., 2018).

A single-center retrospective analysis, comprising 83 subjects with extracardiac, biopsy-proven sarcoidosis, and definite/ probable cardiac involvement, assessed the diagnostic and prognostic powers of 2D-STE in cardiac sarcoidosis. Abnormal LV GLS, inferoseptal and inferior wall strain, and RV GLS are surrogates of cardiac sarcoidosis, even when LVEF and RV systolic parameters are normal. Regarding STE's predictive value in cardiac sarcoidosis, in this study, a LV GLS more positive than -14% was connected to an increased rate of hospitalizations and heart failure (Di Stefano et al., 2020).

Kusunose K et al. prospectively assessed with 2D-STE 139 subjects with systemic sarcoidosis without preexisting structural heart disease and 52 age- and gender-matched control subjects. They documented that basal longitudinal strain and RV free wall longitudinal strain offer incremental value over standard evaluation, being considerably altered in subjects with cardiac sarcoidosis than in those without. Individuals with biventricular strain impairment also had reduced event-free survival (Kusunose et al., 2020).

A meta-analysis conducted by Barssoum K. et al., including 9 studies and 967 subjects, demonstrated that both LV GLS and global circumferential strain are remarkably lower in extracardiac sarcoidosis subjects with no clinical signs of cardiac involvement and that the extent of LV GLS alteration is connected with the occurrence of major cardiac events (Barssoum et al., 2020). Moreover, the circumferential strain has demonstrated to accurately appreciate fibrosis burden in patients with extracardiac sarcoidosis. Decreased circumferential strain assessed with 2D-STE relates to large delayed enhancement in cardiac magnetic resonance imaging, as highlighted by Orii et al.'s study (Orii et al., 2015).

Advanced Echocardiographic Techniques in Hemochromatosis

In hereditary hemochromatosis cardiomyopathy, TDI helps illustrate a reduction in early diastolic velocity of the lateral and medial mitral annulus (Palka et al., 2004). As emphasized by Shizukuda et al., myocardial strain imaging seems to connect better with the effect of oxidative stress on LV diastolic function than with iron overload (Shizukuda et al., 2009).

2D-STE emerged as a more sensitive measure of cardiac involvement in HH when compared to conventional transthoracic echocardiography. Rozwadowska K et al. prospectively enrolled 24 patients with newly diagnosed HH and with no evidence of structural heart disease along with 23 age- and sex-matched healthy volunteers. All standard echocardiographic measurements were within normal ranges in all study participants. However, 2D-STE illustrated notably worse basal and apical rotation, twist, and torsion values in the HH subgroup, with reduced peak systolic longitudinal strain (Rozwadowska et al., 2018).

Byrne D et al. documented that in 25 subjects with newly diagnosed HH and without heart failure, radial strain evaluated through STE, left atrial force calculated by the Manning method, and isovolumic relaxation time considerably enhanced after one year of treatment with venesection. These results suggested that radial strain, isovolumic relaxation time, and left atrial force are useful in monitoring cardiac function, guiding treatment, and identifying subclinical cardiac involvement (Byrne et al., 2020).

➤ **Computed Tomography Imaging**

Computed tomography (CT) imaging is useful in describing the main structural features of RCM and, therefore, of ICM, including biatrial enlargement, dilatation of inferior vena cava and coronary sinus, pericardial effusion, pulmonary congestion, and pleural effusion. It is a powerful tool for quantifying LV mass and wall thickness when other imaging methods are not accessible or are contraindicated and also aids in noticing extracardiac involvement in ICM (e.g., pulmonary nodules and fibrosis with lymphadenopathy in sarcoidosis). Its main disadvantage is represented by high radiation exposure (Habib et al., 2017).

Computed Tomography Imaging in Amyloidosis

Advances in CT imaging techniques have expanded the recommendations on cardiac CT, initially designed to evaluate the coronary arteries. Currently, it enables myocardial characterization through the help of late iodine enhancement (LIE) imaging as well as extracellular volume (ECV) quantification (Oda et al., 2019). Treibel T et al. indicated that CT imaging can be employed to quantify the cardiac amyloid extent and that the ECV evaluated via CT correlates well with the myocardial ECV assessed via CMR imaging. These authors have conducted a 5 minute contrast-enhanced gated cardiac CT analysis on 26 subjects with a biopsy-proven systemic amyloidosis and 26 subjects with severe aortic stenosis and documented higher ECV values within the CA subgroup (Treibel et al., 2015).

Importantly, the affiliation of aortic stenosis with cardiac amyloidosis is frequent, especially among the elderly. Distinguishing between these two pathologies is challenging as aortic stenosis and cardiac amyloidosis present some common characteristics. Aortic valve calcium score evaluated by non-contrast CT helps to grade aortic stenosis severity (Ternacle et al., 2019). Additionally, the evaluation of myocardial ECV during transcatheter aortic valve replacement (TAVR) planning CT can identify occult, concomitant cardiac amyloidosis in individuals with severe aortic stenosis (Oda et al., 2020). In systemic amyloidosis, CT imaging can recognize lung and respiratory tract involvement (e.g. nodular pulmonary amyloidosis, diffuse alveolar-septal amyloidosis, tracheobronchial amyloidosis, or amyloidosis of the pleura) (Milani et al., 2017).

Computed Tomography Imaging in Sarcoidosis

In systemic sarcoidosis, CT imaging is helpful in detecting both cardiac and lung involvement. Commonly, pulmonary CT findings in sarcoidosis include mediastinal and symmetric hilar lymphadenopathy and upper lobe predominant perilymphatic pulmonary nodules

(Sanchez et al., 2020). The ability of contrast-enhanced CT imaging to characterize myocardial tissue was further emphasized by Raimondi et al. who have reported a case of cardiac sarcoidosis in which marked myocardial hypoattenuation on CT imaging was in concordance with CMR, PET, and SPECT imaging findings (Raimondi et al., 2020).

In cardiac sarcoidosis, large myocardial scarring increases the risk of malignant ventricular arrhythmia and sudden cardiac death and, thus, the need for noninvasive evaluation. Late gadolinium enhancement imaging via CMR allows the identification of myocardial fibrosis. As previously mentioned, a new functional CT technique has been developed and enables the quantitative assessment of myocardial perfusion and ECV. In this context, So A et al. have suggested that this CT imaging may possess an additive value to CMR or PET for detecting cardiac sarcoidosis, being extremely helpful in subjects with metallic prostheses and cases where CMR or PET are not accessible or are contraindicated (So et al., 2020).

Computed Tomography Imaging in Hemochromatosis

There is limited literature information concerning cardiac computed tomography's advantages in diagnosing cardiac hemochromatosis, especially in evaluating cardiac iron levels. CMR imaging is the gold-standard technique for the assessment of cardiac hemochromatosis, but cardiac CT may help appreciate cardiac function (Pennell et al., 2013).

➤ **Cardiac Magnetic Resonance Imaging**

CMR presents high accuracy for evaluating the cardiac interstitium and, subsequently, ICM. The most employed IRM evaluating methods are static images, cine, and contrast-enhanced imaging, as well as parametric mapping. The static images have the function of differentiating according to the tissue characteristics, the pericardial myocardium, and the vascular structures, and T1 and T2 provide complementary data. T1 weighted images exhibit a high signal from fat, and T2 weighted short tau inversion recovery (STIR) images can detect myocardial edema as in the acute phase of sarcoidosis. It is feasible to use averaged heartbeats typical cine CMR images as a means of achieving better temporal resolution.

Nevertheless, real-time images present additive value, as in the case of displaying the typical septal shift in the course of respiratory maneuvers to identify a restrictive pattern at the level of the atrioventricular valves (Cosyns et al., 2015).

Late gadolinium enhancement (LGE) is a key characteristic of CMR and can distinguish fibrosis, scarring, and myocardial infiltration, thus supporting the distinction between different types of ICM. The roles of LGE can be further classified into diagnostic and prognostic ones (Fontana et al., 2015). Parametric mapping techniques support quantitative measurements, but also tissue characterization.

Researchers have employed T1 mapping for quantifying inflammation and myocardial fibrosis, as well as measuring native T1 relaxation times, parameters that are correlated with the severity of amyloidosis (Karamitsos et al., 2013). The combined utilization of native and post-

contrast T1 mapping enables the assessment of myocardial extracellular volume fraction, an element of differentiation between different amyloidosis types.

In ICM, although ventricular walls often exhibit increased thickness via steady-state free precession sequences, the major benefit of CMR lies in its capability to define myocardial tissue in terms of intrinsic magnetic characteristics and distribution pattern of the gadolinium-based contrast agents (Pereira et al., 2018).

Myocardial edema and inflammation appear as hyperintense areas in fast spin-echo T2-weighted sequences or quantitative T2 mapping, while decreased T2-weighted signal intensities are frequently associated with iron overload myocardial disorders (Rapezzi et al., 2013). Approximately one-third of restrictive cardiomyopathy cases present with delayed myocardial enhancement due to inflammation and associated fibrosis (Cheng et al., 2011).

Additionally, contrast-enhanced T1 mapping might be utilized as a means to better quantify myocardial fibrosis, while delayed enhanced inversion recovery imaging helps to identify different types of infiltrative cardiomyopathies (Muehlberg et al., 2016).

In AL amyloidosis, delayed gadolinium enhancement may possess prognostic value, on top of serum biomarkers, while T1 has shown higher sensitivity in the early detection of amyloid deposits when compared to gadolinium (Boynton et al., 2016).

Cardiac Magnetic Resonance Imaging in Amyloidosis

In amyloidosis, CMR has both diagnostic and prognostic benefits. Compared to echocardiography, CMR presents a higher spatial resolution, permitting a better measurement of the longitudinal and radial systolic function. These are strong arguments for considering CMR the gold standard in amyloidosis.

Cine imaging provides major diagnostic criteria, including ventricular wall thickness, measurements of ejection fraction, and diastolic function, which enables distinguishing between types of amyloidosis (Martinez-Naharro et al., 2017). Additionally, CMR can provide data about strain patterns, tricuspid and mitral annular plane systolic excursion, and the presence of pericardial or pleural effusion (Knight et al., 2019).

LGE is a powerful diagnostic instrument in amyloidosis. Nevertheless, the information concerning its prognostic value is controversial due to heterogeneous cardiac amyloidosis patterns, which generates differences in coding when using Magnitude only Inversion Recovery (MAG-IR). Additionally, for the early phases of the disease, a patchy pattern has been described. The existence of effusions generates artifacts, and arrhythmias' occurrence, making the image acquisition more complicated (Di Bella et al., 2010).

Transmural LGE seems to correlate with higher mortality rates than the subendocardial pattern (Raina et al., 2016). Its prognostic value has been validated for both types of amyloidosis, while a differential diagnosis between ATTR and AL amyloidosis is difficult to be made based only on the LGE pattern (Dungu et al., 2014). Future research addresses right ventricle LGE as a prognostic marker (Figure 11).

As amyloidosis is characterized by extensive interstitial infiltration, T1 is usually increased. Moreover, the extracellular volume (ECV) is also increased, and it appears to strongly

connect to cardiac involvement and mortality when compared to native myocardial T1 (Banypersad et al., 2015).

The concomitant analysis of T1 and ECV enables differentiating amyloidosis from other diseases characterized by ventricular hypertrophy. Studies advocate for the evaluation of ECV as a means for a timely diagnosis of amyloidosis, being extremely helpful in follow-up and evaluation of myocardial amyloid regression (Martinez-Naharro et al., 2018).

Recent studies have documented the utility of ECV in distinguishing between AL and ATTR amyloidosis. By performing $1-(ECV \times LV \text{ mass})$ and calculating the mean cell volume, an increase has been illustrated only in ATTR amyloidosis.

The histopathological explanation of this finding relies on myocardial cell hypertrophy, in addition to the interstitial expansion, which can be encountered in ATTR amyloidosis and is connected to better survival rates (Fontana et al., 2015).

T2 mapping is related to myocardial edema and has limited advantages in amyloidosis. Nevertheless, recent studies have suggested that T2 might increase in amyloidosis and is linked with a worse systolic function (Kotecha et al., 2018).

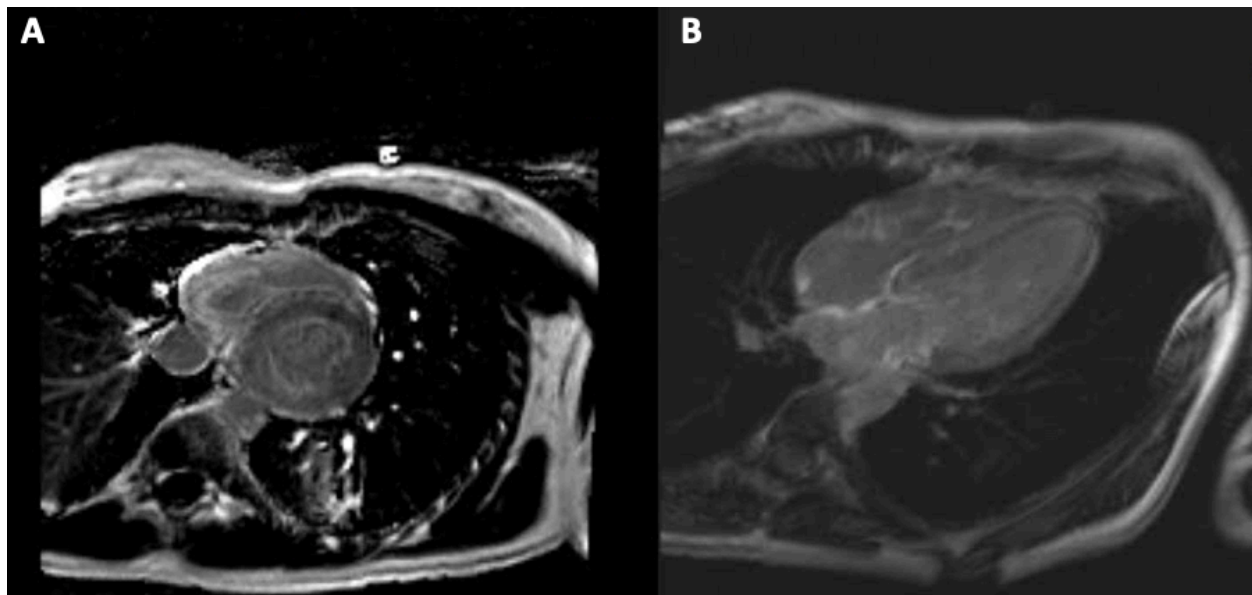


Figure 1 1. Biventricular subendocardial late gadolinium enhancement (A) and atrial late gadolinium enhancement (B) in a young patient with cardiac amyloidosis.

Cardiac Magnetic Resonance Imaging in Sarcoidosis

CMR possessed a 75–100% sensitivity and 76–78% specificity in identifying cardiac sarcoidosis, and it is considered to be more than twice as sensitive compared to the Japanese Ministry of Health and Welfare (JMHW) criteria in diagnosing cardiac involvement in systemic sarcoidosis (Patel et al., 2009). This is mostly due to its capability of identifying myocardial edema, perfusion abnormalities, and scarring. Concerning inflammation, CMR, through its T2 weighted imaging and T2 mapping, has significant power of detection, although the latter did not

demonstrate being superior to PET (Ramirez et al., 2019). T1 and T2 mapping were recently documented as helpful for timely identification of sarcoidosis. These techniques help to identify myocardial inflammation by directly reporting the altered magnetization properties (Puntmann et al., 2017). LGE is the method of choice for scarring assessment.

Sarcoidosis dominantly affects the septal, basal, and lateral segments of the left ventricle and papillary muscles with relative sparing of the subendocardium. LGE in sarcoidosis was linked in different studies with patients' prognosis and the emergence of major cardiovascular events. Therefore, it has been suggested that CMR imaging should be part of the decision of cardioverter-defibrillator implantation (Birnie et al., 2014).

Other studies identified LGE as an independent and strong predictor of all-cause mortality, sustained ventricular tachycardia episodes, or heart failure development (Kouranos et al., 2017). LGE can also be employed for observing treatment response.

The main disadvantage of LGE is that it cannot distinguish between active and chronic inflammation. In the early stages, edema and inflammation increase ventricular wall thickness and leads to motion abnormalities on cine images. Supplementary, it increases T2 signal intensity (Perez et al., 2017).

In the chronic stage, the walls become thin and dysfunctional. T1 and T2 could be effectively employed for early identification of cardiac involvement when LGE and left ventricle function are normal, T2 weighted imaging being more specific for active inflammation and edema, and T1 being a better surrogate of the onset of the disease.

Compared to FDG-PET, CMR has some benefits, including lack of ionizing radiation exposure with low risk from gadolinium contrast in subjects with an estimated GFR >30 mL/min, higher spatial resolution, and better detection of small areas of fibrosis.

Importantly, these two methods detect different characteristics of cardiac sarcoidosis: active inflammation via FDG PET and scarring via CMR. This is why some studies advocate for the usage of combined techniques to better evaluate patients in terms of myocardial function, injury pattern, and disease activity (Ahmadian et al., 2017).

Cardiac Magnetic Resonance Imaging in Hemochromatosis

In hemochromatosis, CMR is helpful for tissue characterization and myocardial iron overload (MIO) quantification. Due to myocardial iron deposition, both T1 and T2 sequences are modified. However, the validated method for MIO assessment is T2 mapping. Higher values of T2 are powerfully related to both hepatic and myocardial involvement, while lower ones may be connected to increased risks of arrhythmias and heart failure.

Because of an immediate identification ability, CMR can guide therapy and follow-up, having a pivotal role in decreasing mortality and morbidity (Habib et al., 2017).

➤ **Nuclear Imaging**

Nuclear imaging is useful in diagnosing infiltrative cardiomyopathies, particularly amyloidosis and sarcoidosis, having the benefit of specific targeted molecular imaging. Positron emission

tomography (PET) and single-photon emission computed tomography (SPECT) are the most important nuclear imaging techniques, both presenting benefits and limitations (Habib et al., 2017). A major issue regarding nuclear imaging is represented by the fact that both PET and SPECT are functional imaging techniques, while other imaging modalities, including radiography or computed tomography, are anatomical techniques.

On top of these, SPECT has the value of a robust, cheaper, and well-validated camera system, while PET possesses a great spatial resolution, robust built-in attenuation correction, quantitative analysis, and low-patient radiation exposure (Habib et al., 2017; Maurer et al., 2019). The two of them shape three-dimensional images, while scintigraphy forms two-dimensional images (Maurer et al., 2019).

Nuclear Imaging in Amyloidosis

Emerging evidence indicates the importance of nuclear imaging techniques in a timely detection and differential diagnosis of cardiac amyloidosis, particularly of transthyretin-related amyloidosis (ATTR). Radiolabelled SPECT phosphate derivatives, initially utilized as bone-seeking tracers, were recently designated as a suitable method for identifying amyloid deposits.

Several radiotracers have been approved for the diagnosis of cardiac amyloidosis, targeting different altered components of the heart: perfusion, metabolism, sympathetic innervation, or amyloid-deposits (Aljaroudi et al., 2014; Longhi et al., 2014; Sperry et al., 2018; Mohamed-Salem et al., 2018). The most commonly exploited SPECT tracer in Europe and Asia is ^{99m}Tc -diphosphonate (^{99m}Tc -DPD), while in the USA it is technetium pyrophosphate (^{99m}Tc -PYP) (Habib et al., 2017; Maurer et al., 2019). Of note, not all radiotracers are suitable for diagnosing cardiac amyloidosis. A reliable explanation for this might be the coexistence of microcalcifications. Microcalcifications are more frequent in subjects with ATTR amyloidosis than in those with AL amyloidosis causing different myocardial detention of radiotracers (Aljaroudi et al., 2014). A paramount advantage is an avid uptake in ATTR and only a minimal uptake in the light-chain (AL) amyloidosis subtype.

Therefore, this imaging technique is one of the best non-invasive methods of distinguishing between these two subtypes (Aljaroudi et al., 2014). By grading myocardial uptake in relation to ribs on SPECT and by quantifying radiotracer uptake by using heart-to-contralateral lung ratio (H/CL), it can be quantified the intensity of radiotracer uptake in the heart (Bokhari et al., 2014).

The current diagnostic criteria for subjects with ATTR cardiac amyloidosis are represented by a visual myocardial uptake greater than that of the ribs or a H/CL ratio of ≥ 1.5 . A H/CL ratio of ≥ 1.6 indicates a poor survival (Castano et al., 2016).

Perugini and coworkers ranked cardiac amyloid uptake in four grades, in reliance to a simple visual scoring system of the delayed (3 h) planar image: grade 0 (no cardiac uptake); grade 1 (mild cardiac uptake—less than in bone); grade 2 (cardiac uptake higher than that noticed in bone, but uptake in bone remains clearly visible); and grade 3 (considerable cardiac uptake with a poor or no signal visible in bone) (Figure 12) (Castano et al., 2016; Habib et al., 2017).

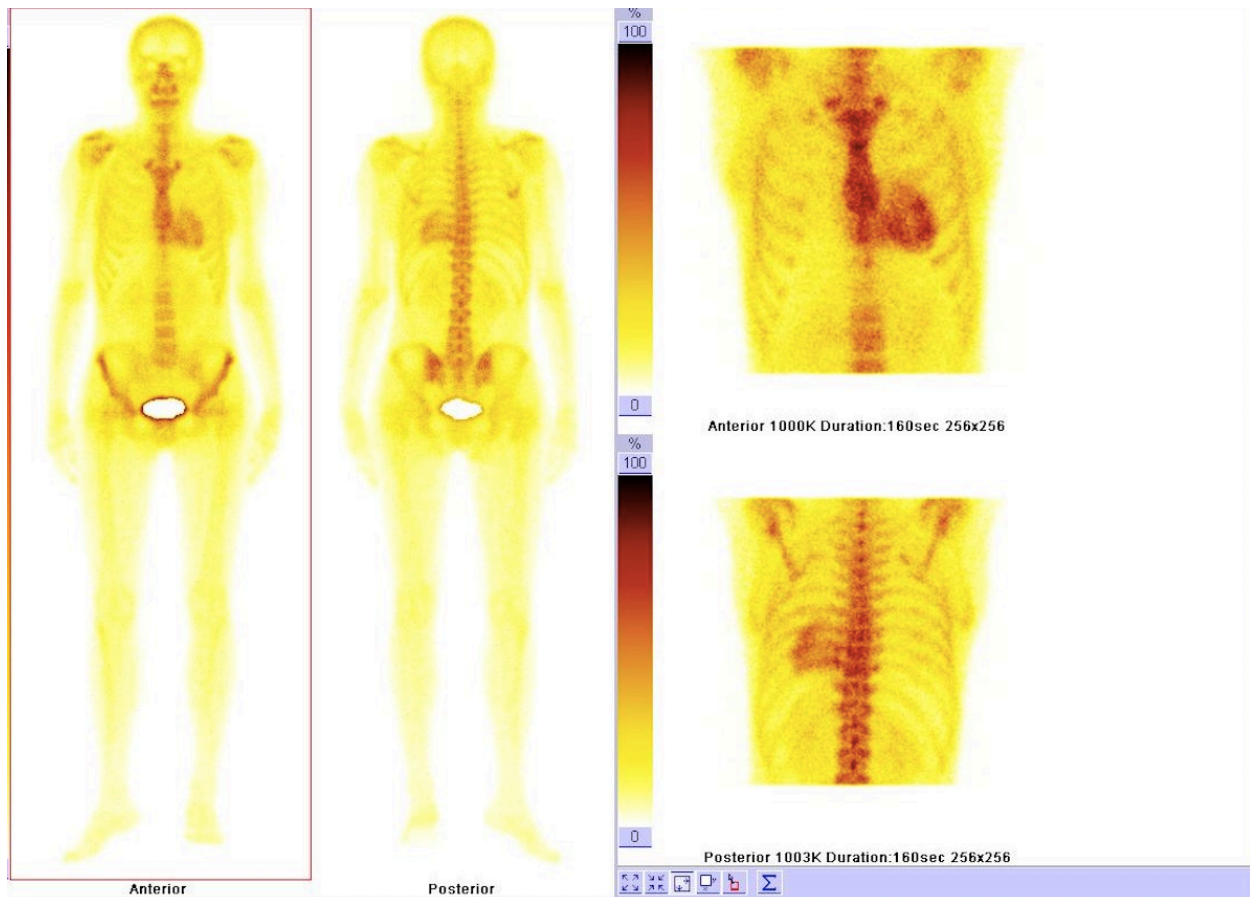


Figure 12. Bone scintigraphy with Technetium-99m hydroxymethylene diphosphonate illustrating abnormal myocardial uptake (Perugini grade 3) in a young woman with transthyretin amyloid cardiomyopathy

A multicenter study reported that bone-avid tracers possess a 100% specificity and positive predictive value for identifying ATTR cardiac amyloidosis, when monoclonal proteins are absent (Castano et al., 2016).

Additionally, through the help of nuclear imaging, ATTR cardiomyopathy can be identified beginning with asymptomatic stages before the increase in left ventricular wall thickness or decreased electrocardiographic voltage become visible (Gillmore et al., 2016; Maurer et al., 2019).

Moreover, subjects with ATTR cardiac amyloidosis and enhanced myocardial uptake of ^{99m}Tc -PYP portend a poor prognosis, with an increased risk of major adverse cardiac events, acute heart failure, and mortality (Castano et al., 2016; Yamamoto et al., 2019).

For the diagnosis of cardiac amyloidosis, positron emission tomography is another helpful nuclear imaging technique. Several tracers have been effectively used as PET tracers, favoring the detection of amyloid deposits regardless of the precursor protein.

These techniques are quantitative methods, enabling the measurement of amyloid burden. Only a few, small-sized studies have reported a higher myocardial retention index of ¹⁸F-florbetapir in subjects with AL cardiac amyloidosis compared to those with ATTR cardiac amyloidosis, and no significant retention in healthy volunteers (Dorbala et al. 2014; Osborne et al., 2015).

Law et al. conducted a small study and sought to evaluate the myocardial retention of ¹⁸F-florbetaben in subjects with cardiac amyloidosis compared with control patients with hypertension. The authors have reported greater myocardial retention in subjects with AL or ATTR cardiac amyloidosis than in controls, this uptake being inversely correlated with left ventricular global and right ventricular free-wall longitudinal strain (Law et al., 2016).

Taking into consideration the above-mentioned data, the diagnosis of ATTR cardiac amyloidosis can be confidently made in subjects presenting with a typical clinical phenotype, with echocardiographic or cardiac magnetic resonance findings consistent with amyloidosis, grade 2 or 3 tracer uptake in the heart on radionuclide bone scintigraphy, and the absence of detectable monoclonal immunoglobulin in the blood and urine (Habib et al., 2017).

Consequently, only a few subjects with ATTR cardiomyopathy will demand endomyocardial biopsy, particularly those in whom a monoclonal immunoglobulin is detected, for the differential diagnosis with AL amyloidosis (Gillmore et al., 2016).

In conclusion, nuclear imaging modalities are fundamental for timely diagnosis, severity grading, and treatment initiation in subjects with cardiac amyloidosis. The most important benefits of nuclear imaging are large accessibility, simplicity of imaging, low cost, and high specificity for cardiac ATTR amyloid deposits (Maurer et al., 2019).

Nuclear Imaging in Sarcoidosis

Multimodality imaging plays a pivotal role in diagnosing sarcoidosis and guiding the biopsy. It can appreciate the extent of the disease and help to monitor treatment response. In systemic sarcoidosis, cardiac involvement is a prognostic factor, increasing the morbi-mortality.

Nuclear imaging is an important part of the evaluation of cardiac sarcoidosis (Keijsers et al., 2011). Although (⁶⁷Ga)-citrate scintigraphy is employed as a major diagnostic criterion for cardiac sarcoidosis, it has a considerably lower sensitivity when compared to [18 fluorine] fluoro-deoxy-glucose—positron emission tomography/computed tomography ([¹⁸F]FDG-PET/CT). This is why [¹⁸F]FDG-PET/CT has become the most utilized imaging tool in identifying myocardial inflammation.

Considering the inflammatory nature of cardiac sarcoidosis, PET is undoubtedly useful for diagnosis and follow-up. An increased [¹⁸F]FDG accumulation on PET/CT imaging can be noticed as inflammatory cells of the active sarcoid lesions utilize glucose as the main energy source (Youssef et al., 2012). For this reason, before [¹⁸F]FDG-PET/CT is performed, it is recommended that subjects adhere to a high-fat–low-carbohydrate diet followed by prolonged fasting as a means of suppressing physiological myocardial glucose uptake (Tang et al., 2016).

PET is more sensitive, but less specific than cardiac magnetic resonance (CMR), being commonly recommended in subjects with contraindications to CMR, in those with indeterminate findings on CMR, and when CMR is not accessible for monitoring treatment response (Habib et al., 2017).

Nevertheless, these two imaging methods provide different insights into cardiac sarcoidosis. An increased [18F]FDG uptake symbolizes active inflammation, while increased late gadolinium enhancement on CMR imaging, suggests interstitial fibrosis and scarring (Youssef et al., 2012). The most significant advantage of FDG PET/CMR is the possibility to evaluate left ventricular function, the pattern of myocardial injury, and disease activity by a single scan (Tang et al., 2016).

Serial [18F]FDG-PET/CT imaging help assess treatment response and the persistence of inflammatory activity and metabolic response. Studies documented a decreased [18F]FDG uptake in patients with cardiac sarcoidosis following corticosteroid or immunosuppressive therapies (Osborne et al., 2014; Ohira et al., 2016).

Nuclear Imaging in Hemochromatosis

In the past decades, the importance of [18F]FDG-PET imaging in diagnosis and treatment monitoring of inflammatory and infectious diseases has been repeatedly demonstrated by large epidemiological studies.

Conversely, only a few clinical cases documented the role of [18F]FDG-PET imaging in the management of subjects with hemochromatosis. To our knowledge, there are no studies about FDG PET/CT uptake of the heart in subjects diagnosed with hemochromatosis, and only two studies documented a liver uptake within this pathology (Ito et al., 2011; Infante et al., 2015).

A recent study reported a high liver uptake of [18F]FDG in a 64-year-old man with a history of non-Hodgkin diffuse B-cell lymphoma treated with chemotherapy, radiotherapy, and stem cell transplant. Following treatment completion, [18F]FDG-PET/CT evaluation exhibited normal distribution.

One month later, the subject was addressed with a clinical and biological profile suggestive of hereditary hemochromatosis, and the PET/CT images conducted as a follow-up for his malignancy, in the absence of tumor recurrence, showed high glucose metabolism in the liver with a homogeneous pattern.

After another 5 months, the subject was free of lymphoma, and the authors emphasized that the enhanced FDA uptake was subsequent to the liver injury triggered by overload iron deposits secondary to intense hematological therapy (Infante et al., 2015). Conclusively, to our knowledge, there is no evidence about the utility of [18F]FDGPET imaging in the diagnosis and treatment monitoring of patients with cardiac hemochromatosis. CMR remains the mainstay imaging, enabling the quantification of myocardial iron overload and the assessment of RV and LV dimensions and functions.

In Table X, we summarize the strength and the weakness of each imaging modality in the diagnosis and management of subjects with infiltrative cardiomyopathies.

Table X. Strength and weakness of each imaging modality in the diagnosis and management of subjects with infiltrative cardiomyopathies.

Multimodality imaging	Cardiac amyloidosis	Sarcoidosis	Hemochromatosis
Echocardiography	<p>Strength: widely available, LVH with bull’s eye pattern on strain imaging is a well-known red flag for CA.</p> <p>Weakness: lack of sensitivity and specificity.</p>	<p>Strength: first imaging screening method for CS.</p> <p>Weakness: lack of sensitivity in identifying early cardiac involvement and high variability of echocardiographic findings.</p>	<p>Strength: useful in screening and regular follow-up.</p> <p>Weakness: second-line imaging method, after CMR for the evaluation of cardiac hemochromatosis.</p>
Cardiac magnetic resonance	<p>Strength: able to establish the diagnosis of CA.</p> <p>Weakness: not capable of distinguishing between ATTR and AL amyloidosis.</p>	<p>Strength: allows an early identification of active inflammation and myocardial scarring.</p> <p>Weakness: there is no distinctive feature of CS on CMR.</p>	<p>Strength: CMR imaging (particularly T2 relaxation times) is the method of choice for assessing cardiac hemochromatosis, evaluating myocardial fibrosis and edema.</p> <p>Weakness: risk of gadolinium toxicity.</p>
Computed tomography	<p>Strength: enables myocardial characterization via LIE imaging as well as cardiac amyloid burden assessment via ECV quantification.</p> <p>Weakness: use of ionizing radiation and iodinated contrast.</p>	<p>Strength: useful in recognizing both cardiac and lung involvement, especially in subjects with metallic implants.</p> <p>Weakness: radiation-related risk and complications.</p>	<p>Strength: limited literature information available; might help evaluate cardiac function.</p> <p>Weakness: radiation exposure.</p>
Nuclear imaging	<p>Strength: useful in diagnosing ATTR cardiomyopathy beginning with early stages, eliminating the need of histological confirmation.</p> <p>Weakness: its diagnostic accuracy highly depends on the used radiotracers.</p>	<p>Strength: useful in monitoring disease activity and response to immunosuppressive therapy as well as in guiding biopsy.</p> <p>Weakness: less specific than CMR imaging, being recommended in subjects with contraindications to CMR.</p>	<p>No evidence available regarding the role of nuclear imaging in diagnosing, guiding therapy or monitoring disease evolution in cardiac hemochromatosis.</p>

ATTR, transthyretin amyloid amyloidosis; CA, cardiac amyloidosis; CMR, cardiac magnetic resonance; CS, cardiac sarcoidosis; ECV, extracellular volume; LIE, late iodine enhancement; LVH, left ventricular hypertrophy

➤ **Implications of Multimodality Imaging in Monitoring Disease Progression and Treatment Response in Infiltrative Cardiomyopathies**

Implications of Multimodality Imaging in Amyloidosis

The delay in diagnosing cardiac amyloidosis is still the main hindrance for the early implementation of a specific therapy. Observational studies have illustrated that if left untreated, patients with systemic AL amyloidosis die within one year when cardiac involvement is present, while those with ATTR cardiac amyloidosis die within three years (Pinney et al., 2013). Considering the advent of new, powerful disease-modifying therapies for both types of amyloidosis, the importance of multimodality imaging in diagnosing and distinguishing cardiac amyloidosis is higher than before.

Echocardiography only raises suspicion of the existence of cardiac amyloidosis but is neither sensitive nor specific. As illustrated by Brownrigg et al. in a systematic review and meta-analysis, CMR imaging is able of detecting cardiac amyloidosis with high accuracy, but it demands nuclear imaging for further grouping the disease in ATTR or AL amyloidosis (Brownrigg et al., 2019). For this reason, including diphosphonate scintigraphy into the diagnostic framework of cardiac amyloidosis is essential, as AL and ATTR amyloidosis demand different therapeutic strategies.

In AL amyloidosis, chemotherapy regimens, comprising melphalan, dexamethasone, and bortezomib, with or without autologous stem cell transplantation, are effective (Brownrigg et al., 2019; Gertz et al., 2020), while in subjects with amyloidotic cardiomyopathy due to ATTR amyloidosis (either hereditary or wild-type), tafamidis is recommended in those with NYHA class I to III symptoms (Kittleson et al., 2020). Patisiran and inotersen should be considered only in subjects with hereditary ATTR amyloidosis and polyneuropathy, none of these two transthyretin gene silencers being advised in hereditary ATTR cardiomyopathy without polyneuropathy or in wild-type ATTR cardiomyopathy (Dasgupta et al., 2020).

Up to now, the potency of multimodality imaging to monitor treatment response in cardiac amyloidosis has not been documented, and no uniform definition of progression or response to therapy has been introduced for clinical use. Survival, hospitalizations, functional capacity, quality of life, cardiac biomarkers, and different imaging techniques (including echocardiography, cardiac magnetic resonance imaging, and positron emission tomography) are presently employed, but future research addressing this aspect is necessary (Kittleson et al., 2020).

Implications of Multimodality Imaging in Sarcoidosis

A recent Danish nationwide cohort study, including 11,834 subjects with sarcoidosis and 47,336 control subjects emphasized that sarcoidosis is linked to a higher long-term risk of incident heart failure, higher mortality among the subjects who develop heart failure, and higher long-term risk of adverse cardiac outcomes when compared to the background population.

Therefore, awareness and increased diagnostic performance are needed (Yafasova et al., 2020). Multimodality imaging has led to enhanced identification of cardiac involvement in systemic sarcoidosis, which commonly manifests with atrioventricular conduction disturbances, ventricular arrhythmias, sudden cardiac death, and heart failure. There is insufficient data concerning the best screening method for cardiac involvement in systemic sarcoidosis. Echocardiographic findings are non-specific and highly variable. Nevertheless, according to Mehta et al., when combining transthoracic echocardiography with Holter monitoring, electrocardiogram, and clinical history, the diagnosis of cardiac sarcoidosis can be attained in 100% of cases (Mehta et al., 2008).

There are no pathognomonic findings of cardiac sarcoidosis in cardiac magnetic resonance imaging. However, the degree of late gadolinium enhancement, commonly positioned in the basal segments of the interventricular septum and lateral wall, ordinarily in the epicardium and mid myocardium, has proved to be an essential prognostic factor (Birnie et al., 2017; Kawai et al., 2020; Ribeiro et al., 2020).

Immunosuppressive drugs are the cornerstone of treatment in systemic sarcoidosis, but the impact of immunosuppression has not been methodically assessed for cardiac sarcoidosis. Cacoub et al. documented that intravenous cyclophosphamide correlate with a lower relapse rate in cardiac sarcoidosis (Cacoub et al., 2020). Fluorodeoxyglucose positron emission tomography helps detect active disease and guides immunosuppressive therapy (Mehta et al., 2008).

In conclusion, patients with cardiac sarcoidosis and LV dysfunction need to be treated according to the current heart failure guidelines, with standard medication, device therapies or even heart transplantation (Mehta et al., 2008).

Implications of Multimodality Imaging in Hemochromatosis

Long-term survival in hereditary hemochromatosis largely depends on the existence of liver involvement, but cardiovascular death can emerge in about 20% of situations (Niederau et al., 1996). Cardiac magnetic resonance is the most important diagnostic and follow-up imaging tool in cardiac hemochromatosis. However, transthoracic echocardiography has the benefits of being more accessible (Díez-López et al., 2018). Phlebotomy, chelation therapy with either parenteral deferoxamine or oral deferiprone and deferasirox, and dietary are recommended in cardiac hemochromatosis (Pereira et al., 2018).

Conclusions

Regardless of the contradictory classification within the current guidelines, ICMs are the archetypal example of RCM. Cardiac amyloidosis, sarcoidosis, and hemochromatosis are common causes of ICM. All three diseases require a high level of knowledge and competence in order to be identified. By combining multimodality imaging methods, an early diagnosis can be acquired, and precious diagnostic and prognostic data can be attained.

In ICM, the use of multimodality imaging plays a pivotal role in guiding therapy and follow-up and results in better outcomes through timely disease-modifying strategies.

Chapter 2. Predictive power of cardiovascular imaging in CKD patients

2.1. Background

Patients with end stage disease on chronic dialysis have a worryingly high mortality (Sarnak et al., 2003). For standard treatment (three HD sessions per week) of patients with HD, the major goal is to maintain a normal extracellular volume status and to avoid chronic fluid overload. Volume overload in dialysis patients is associated with hypertension, increased arterial stiffness, left ventricular hypertrophy, heart failure and ultimately higher mortality and morbidity, thus the importance of its avoidance (KDOQI, 2006; Tonelli et al., 2006). Surrogate clinical as pedal oedema, interdialytic weight gain, ultrafiltration rate or blood pressure (Jaeger, and Mehta, 1999; Levin et al., 2001) and paraclinical parameters as inferior vena cava diameter and its collapsibility index, relative plasma volume monitoring (Cherix et al., 1989; Sinha et al. 2010) are largely used in order to determine the hydration status.

For objectifying the individual (over)hydration status, which is an important and independent predictor of mortality in chronic HD patients secondary only to the presence of diabetes (Wizemann et al., 2009), but stronger than blood pressure (Chazot et al., 2012), multifrequency bioimpedance spectroscopy seems to be an encouraging technique. The method is validated by isotope dilution techniques, by accepted reference body composition techniques and by techniques that measure relative changes in fluid volumes (Moissl et al., 2007).

Previous data proved that extravascular lung water (ELW), a small but yet fundamental component of body fluid volumes, representing the water content of the lung interstitium (Crandall et al., 1983) is strictly related to the filling pressure of the left ventricle - a well-known haemodynamic parameter for risk stratification and monitoring of fluid therapy in critical care (McGee et al., 2006). In the past decades, clinical research focused on the utility of lung ultrasonography, to identify ELW, in patients with heart failure (Picano et al., 2010), intensive care (Jambrick et al., 2004) and chronic kidney disease submitted to HD (Noble et al., 2009; Mallamaci et al., 2010). Even more, this method can predict the all-cause mortality and cardiac events in HD patients (Zoccali et al., 2013).

In clinical practice, trial and error clinical methods (Charra et al., 1996) were used to achieve the “dry weight” in HD patients. But, this approach rarely deciphers the problems of hypertension, intradialytic hypotension and subclinical overhydration. Bioimpedance devices have lately become available for routine practice, showing comparable abilities in predicting an adequate “dry weight” (Chazot et al., 2012). It was proved that a strict bioimpedance guided fluid management has a valuable influence on blood pressure, arterial stiffness, LVH and survival (Machek et al., 2010; Moissl et al., 2013; Hur et al., 2013; Onofriescu et al., 2014). Nevertheless, the best cut-off point for defining overhydration has yet to be verified. Additionally, different bioimpedance derived parameters have been used - absolute fluid overload (AFO), relative fluid overload (RFO), time averaged fluid overload (TAFO) - with different cut-off points being proposed to define overhydration (Wabel et al., 2008; Wizemann et al., 2009).

Within numerous studies it was shown that echocardiographic abnormalities in ESDR are almost universal (Foley et al., 1995), a report on 315 patients with ESRD showing that only 11.5% and 3.4% of all patients had normal left ventricular (LV) geometry and normal LV filling pattern, respectively (Matsuo et al., 2018). Still, the field of cardiovascular imaging has fundamentally developed in the last years, with progresses in echocardiography methods and optimizations in fresher imaging modalities, as cardiac computed tomography (CT) and magnetic resonance (CMR). Because of the fact that patients with CKD may either present with dyspnea secondary to volume overload in the absence of CVD, or on the opposite may not develop classical symptoms, the amount of information brought by newer imaging techniques is crucial for an accurate diagnosis and management (Henry et al., 2002).

Within this direction, I was a team member of a research international project.

LUST: the „Lung water by Ultra – Sound guided Treatment to prevent death and cardiovascular events in high risk end stage renal disease (ESRD) patients with cardiomyopathy”, from 2013; coordinator EURECA-m / ERA – EDTA; EURECA-m steering committee members: Zoccali Carmine (study coordinator), Covic Adrian, Fliser Danilo, London Gerard Michael, Martinez- Castelao Alberto, Massy Ziad, Ortiz Arduan Alberto, Sulleymanlar Gultekin, Wiecek Andrzej; Sascau R - the cardiologist of the research team, “Dr. C. I. Parhon” Hospital, Iași Romania.

The preoccupations related to predictive power of cardiovascular imaging in CKD patients were partially synthesized in the following articles:

Siriopol D, Hogas S, Voroneanu L, Onofriescu M, Apetrii M, Oleniuc M, Moscalu M, **Sascau R**, Covic A. Predicting mortality in haemodialysis patients: a comparison between lung ultrasonography, bioimpedance data and echocardiography parameters. *Nephrol Dial Transplant*. 2013; 28(11):2851-2859. doi:10.1093/ndt/gft260. **IF: 3.488.**

Onofriescu M, Siriopol D, Voroneanu L, Hogas S, Nistor I, Apetrii M, Florea L, Veisa G, Mititiuc I, Kanbay M, **Sascau R**, Covic A. Overhydration, Cardiac Function and Survival in Hemodialysis Patients. *PLoS One*. 2015;10(8): e0135691. doi:10.1371/journal.pone.0135691. **IF: 3.057.**

Siriopol D, Voroneanu L, Hogas S, Apetrii M, Gramaticu A, Dumea R, Burlacu A, **Sascau R**, Kanbay M, Covic A. Bioimpedance analysis versus lung ultrasonography for optimal risk prediction in hemodialysis patients. *Int J Cardiovasc Imaging*. 2016;32(2):263-270. doi:10.1007/s10554-015-0768-x. **IF: 1.896**

Siriopol D, Onofriescu M, Voroneanu L, Apetrii M, Nistor I, Hogas S, Kanbay M, **Sascau R**, Scripcariu D, Covic A. Dry weight assessment by combined ultrasound and bioimpedance

monitoring in low cardiovascular risk hemodialysis patients: a randomized controlled trial. *Int Urol Nephrol*. 2017; 49(1):143-153. doi:10.1007/s11255-016-1471-0. **IF: 1.692.**

Ureche C, **Sascău R**, Țăpoi L, Covic A, Moroșanu C, Voroneanu L, Burlacu A, Stătescu C, Covic A. Multi-modality cardiac imaging in advanced chronic kidney disease. *Echocardiogr-J Card* 2019; 36 (7): 1372– 1380. doi.org/10.1111/echo.14413. **IF: 1.393.**

2.2. Predictors for mortality in HD patients

2.2.1. Aim

Lung congestion represents the result of both overall overhydration and/or cardiac dysfunction, but the precise role of different tests to mortality is not fully elucidated. Within our study we aimed to investigate the value of ultrasound lung comets (ULC) combined with bioimpedance-derived data and some echocardiographic parameters in predicting mortality in haemodialysed patients.

2.2.2. Material and methods

Patients undergoing chronic HD treatment for at least 3 months in a single unit during 26 May 2011 and 3 July 2012 were included in the study. The exclusion criteria were age under 18 years; systemic infections and terminal neoplasia; metallic joint prostheses, cardiac pacemakers or stents; decompensated cirrhosis and limb amputations. The protocol was approved by the Ethics Committee of University Hospital ‘Dr C.I.Parhon’ (Iasi, Romania). The final study population consisted of 96 subjects, the main features being presented in table XI. Biochemical parameters were monthly assessed, pre-dialysis, after the long interval of dialysis.

We performed echocardiographic examinations after a short dialysis period, 15–20 min before dialysis, and 35 min after dialysis. Ultrasound scanning of the anterior and lateral chest was obtained on the right and left haemithorax, for a total of 28 positions per examination, as was previously described (Jambrik et al., 2004). We defined comet-tail sign as an echogenic, coherent, wedge-shaped signal with a narrow origin in the near field of the image. In each intercostal space, the number of comet-tail signs was recorded at the parasternal, midclavicular, anterior axillary and midaxillary sites. At every scanning site, ultrasound lung comets (ULC) could be counted from 0 to 10. The sum of the comet-tail signs generated a score representing the extent of extravascular fluid in the lung (Picano et al., 2006). Based on this score values (Moissl et al., 2006), we grouped the patients into three categories of progressively severe pulmonary congestion (none or mild < 16 comets).

The hydration state and the body composition were assessed using a bioimpedance spectroscopy device (BCM—Fresenius Medical Care D GmbH). Measurements were performed before the start and 30 min after the end of the HD treatment. The extracellular water (ECW), intracellular water (ICW) and TBW were determined as previously described (Moissl et al., 2006).

To simplify the comparison between patients, the hydration state was normalized to the ECW ($\Delta\text{HS} = \text{HS}/\text{ECW}$). The study population was divided into a hyperhydrated, normohydrated and hypohydrated groups using a cut-off of 15% for the relative hydration status. Based on the work described by Wabel et al. and Wizemann et al., we defined hyperhydration as a $\Delta\text{HS} > 15\%$ (Wabel et al., 2008) (Wizemann et al., 2009).

Echocardiographic assessments were made in each patient and they were carried out according to the recommendations of the American Society of Echocardiography (Lang et al., 2005) by a blind observer.

Statistical analysis: All the results were analyzed by SPSS for Windows, version 19.0.1, Chicago, IL and expressed as mean \pm SD, median and inter-quartile range or as percent frequency, as appropriate. Comparisons among groups and patients were made by P-value t-test (normally distributed data) or by the Wilcoxon signed-rank test (non-normally distributed data). Correlations between the variables were investigated by the Pearson correlation coefficient or by the Spearman rank correlation coefficient, as appropriate. Kaplan–Meier and Cox regression analysis were used to investigate the prognostic value of the lung comets score for predicting mortality. The contribution of covariates explaining the dependent variable was assessed by the Wald test, with a P-value of < 0.05 considered as significant.

2.2.3. Results

The demographic and clinical characteristics of the 96 patients enrolled in the study group are summarized in Table XI. Patients with lung disease had a higher ULC score (median: 30, inter-quartile range 15.6–101.5) than those without (median: 9, inter-quartile range 3–17, $P = 0.003$). Thirty-one (32.3%) patients had NYHA score of at least 3. All patients had residual diuresis of < 500 mL per day (median 200 mL per day).

Our measurements revealed a mean pre-dialysis arterial pressure and heart rate of $147.6 \pm 24.6/74.9 \pm 15.3$ mmHg and 76.6 ± 16 beats/min, respectively. The median number of pre-dialysis ULC was 11 (inter-quartile range 4–19). Lung congestion was classified as absent to mild (≤ 15 lung comets) in 67 patients (67.7%), moderate (16–30 lung comets) in 19 patients (19.8%) and severe (> 30 lung comets) in the remaining 12 patients (12.5%). We noticed no difference between these three groups in gender distribution, diabetes prevalence, systolic and diastolic blood pressure and different biochemical parameters.

We observed a significant difference between these groups when we analyzed the distribution of the NYHA functional class: patients with moderate or severe lung congestion had a higher NYHA functional class (Table XI, Figure 13).

On the basis of ΔHS , 77 (80.2%) patients were classified as being normohydrated and 19 (19.8%) as hyperhydrated. The statistical analysis showed that hyperhydrated patients were younger (49.4 ± 16.9 versus 61.5 ± 12.5 years, $P < 0.01$) and had significantly more ULC (a median of 12, inter-quartile ranges 8–22 versus a median of 9, interquartile range 3–16.5, $P = 0.048$) than the normohydrated ones. There was no difference in regard to gender distribution, diabetes

prevalence, systolic and diastolic blood pressure and NYHA class between the normohydrated and hyperhydrated patients.

The data proved that 14 hyperhydrated patients (73.7%) were asymptomatic (NYHA Class I and II) (Figure 13). Moreover, no differences were found when we compared the echocardiographic parameters between the normohydrated and hyperhydrated patients (as defined by Δ HS).

Table XI. Main demographic, clinical, somatometric and pre-dialysis haemodynamic data of the study population

	All	<16 (N = 65)	16–30 (N = 19)	>30 (N = 12)	P for trend	r (P)
Age, years	59.1 ± 14.2	58.7 ± 14.0	58.5 ± 15.8	62.2 ± 14.0	0.72	0.05 (0.60)
Dialysis vintage, months	64.3 ± 59.2	59.6 ± 54.7	73.6 ± 66.8	75.1 ± 71.5	0.53	0.05 (0.61)
BMI, kg/m ²	25.9 ± 6.1	26.8 ± 6.1	23.2 ± 4.8	25.6 ± 7.4	0.08	-0.24 (0.018)
Male sex, %	51	52.3	36.8	66.7	0.96	
Diabetes, %	24	26.2	15.8	25.0	0.54	
Systolic pressure, mmHg	147.6 ± 24.6	145.6 ± 22.8	150.4 ± 27.4	153.8 ± 30.2	0.50	0.18 (0.08)
Diastolic pressure, mmHg	74.9 ± 15.3	75.3 ± 14.6	70.8 ± 17	79.5 ± 15.7	0.29	0.06 (0.54)
Heart rate, beats/min	76.6 ± 16.0	75.0 ± 12.8	78.2 ± 24.2	82.3 ± 15.6	0.32	0.04 (0.67)
Haemoglobin, g/dL	11.2 ± 1.5	11.4 ± 1.5	10.9 ± 1.5)	10.9 ± 1.5	0.34	-0.16 (0.12)
Albumin, g/dL	3.9 ± 0.3	3.9 ± 0.3	3.9 ± 0.4	3.7 ± 0.4	0.14	-0.03 (0.76)
Calcium, mg/dL	8.4 ± 0.7	8.5 ± 0.7	8.0 ± 0.8	8.7 ± 0.7	0.01	0.002 (0.99)
Phosphate, mg/dL	5.6 ± 2	5.7 ± 2.1	5.4 ± 1.8	5.5 ± 1.9	0.88	0.04 (0.70)
<i>eKt/V</i>	1.5 ± 0.3	1.4 ± 0.2	1.6 ± 0.3	1.5 ± 0.4	0.15	0.16 (0.12)
Cholesterol, mg/dL	171.9 ± 42.2	173.5 ± 40.2	163.8 ± 34	175.9 ± 62.7	0.64	0.08 (0.43)
Lung disease, %	6.3	1.5	15.8	25.0	0.034	
CRP	12.0 ± 22.8	11.7 ± 23.3	8.2 ± 9.6	14.8 ± 17.5	0.38	0.21 (0.04)
NYHA class, %	I (34.4)	I (40.0)	I (36.8)	I (0)	0.014	
	II	II (33.3)	II (32.3)	II (42.1)	II (25.0)	
	III	III (30.2)	III (27.7)	III (21.1)	III (58.3)	
	IV	IV (2.1)	IV (0)	IV (0)	IV (16.7)	

Data are expressed as mean ± SD or percent frequency, as appropriate. Bold values are statistically significant. r, Spearman rank correlation coefficient between lung comets score and variables; BMI, body mass index; NYHA, New York Heart Association.

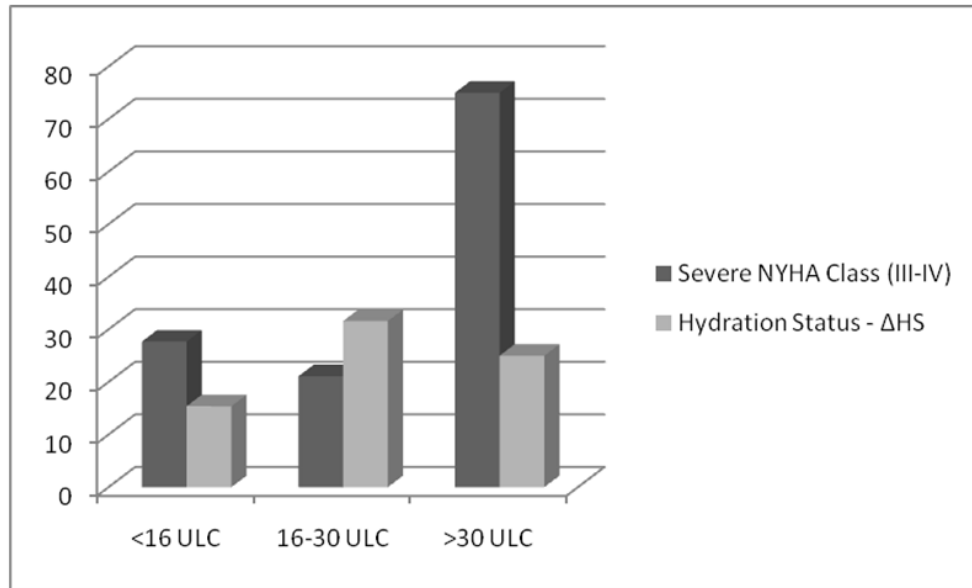


Figure 13. NYHA class and hydration status across the groups of lung congestion

Tables XII and XIII summarize the bioimpedance (BCM derived) data (Δ HS, TBW, ECW and ICW) and echocardiographic parameters, respectively, as well as their distribution across the three ULC-derived categories of lung congestion. There was a significant difference in the Δ HS and left atrial diameter among the three groups of lung congestion ($P < 0.05$ for both). The pre-dialysis ULC score significantly correlated with all the BCM-derived parameters (Δ HS, TBW, ECW and ICW), but this was not related to any of the anatomical and functional echocardiographic parameters evaluated in the study.

Table XII. Bioimpedance spectroscopy data of the study population

	All	<16 (N = 65)	16–30 (N = 19)	>30 (N = 12)	P for trend	r (P)
TBW, l	31.7 ± 6.3	32.6 ± 6.4	28.7 ± 5.1	31.7 ± 6.1	0.06	-0.22 (0.034)
ECW, l	15.6 ± 3.7	16.1 ± 3.8	14 ± 2.7	15.8 ± 3.7	0.08	-0.21 (0.042)
ICW, l	16.2 ± 3.4	16.7 ± 3.5	14.7 ± 2.7	15.9 ± 2.9	0.07	-0.24 (0.021)
Δ HS, %	7.9 ± 7.5	6.5 ± 7.2	10.1 ± 8.1	11.6 ± 6.6	0.03	0.29 (0.004)

Data are expressed as mean ± SD. Bold values are statistically significant. r, Spearman rank correlation coefficient between lung comets score and variables.

The mean post-dialysis arterial pressure and heart rate were $134.0 \pm 20.2/70.0 \pm 11.7$ mmHg and 77.0 ± 11.7 beats/min, respectively. The median number of post-dialysis ULC was 4.5 (inter-quartile range 2–9). After dialysis, there were 87 (90.6%) patients with absent or mild lung congestion, 4 (4.2%) with moderate and 5 (5.2%) with severe lung congestion. Using the post-

dialysis Δ HHS, 11 (11.5%) patients were hypohydrated, 84 (87.5%) were normohydrated and only 1 (1%) remained hyperhydrated.

Table XIII. Echocardiographic Parameters of the Study Population

	All	<16 (N = 65)	16–30 (N = 19)	>30 (N = 12)	P for trend	r (P)
LVMI, g/m ²	153.0 ± 44.8	150.0 ± 42.7	150.8 ± 28.8	172.2 ± 70.5	0.35	0.18 (0.12)
Left atrial diameter, mm	46.3 ± 7.6	45.6 ± 7.4	45.1 ± 6.6	51.8 ± 8.5	0.04	0.20 (0.08)
Interventricular septum, mm	12.4 ± 2.4	12.3 ± 2.6	12.7 ± 2.1	12.7 ± 2.1	0.78	0.10 (0.40)
LVPWT, mm	12.0 ± 2.3	11.9 ± 2.4	12.5 ± 2.0	12.1 ± 1.9	0.68	0.13 (0.25)
End-diastolic left ventricular diameter, mm	48.4 ± 7.5	49 ± 7.4	45 ± 6.5	50.8 ± 8.3	0.10	-0.07 (0.53)
End-systolic left ventricular diameter, mm	32.2 ± 6.8	32.2 ± 6.9	30.3 ± 4.7	34.9 ± 8.5	0.25	0.13 (0.91)
LVEF, %	61.5 ± 7.7	61.8 ± 7.7	62.6 ± 4.5	58.2 ± 10.7	0.69	-0.75 (0.51)

Data are expressed as mean ± SD. Bold values are statistically significant. r, Spearman rank correlation coefficient between lung comets score and variables; LVMI, left ventricular mass index; LVPWT, left ventricular posterior wall thickness; LVEF, left ventricular ejection fraction.

Within the study, 7 patients with >30 lung comets before dialysis changed their class of lung congestion post-dialysis (four moved to the absent or mild, while three to the moderate lung congestion class). There were no significant (demographic, clinical, biochemical, bioimpedance and echocardiographic parameters) differences between the three ULC groups of lung congestion. The observed difference in NYHA functional class prevalence between the ULC categories was also maintained after dialysis ($r = 0.548$, $P < 0.001$). Similar to the pre-dialysis results, a weak correlation between the ULC score and some of the BCM parameters was observed (Δ HHS: $r = 0.30$, $P = 0.003$; TBW: $r = -0.24$, $P = 0.018$; ICW: $r = -0.27$, $P = 0.009$). The ULC score after dialysis correlated weakly with the left atrial diameter and the left ventricular ejection fraction (LVEF; $r = 0.28$, $P = 0.013$ and $r = -0.28$, $P = 0.013$, respectively).

According to our data, the body weight decreased from 70.2 ± 17.3 pre-dialysis to 68.4 ± 17.1 kg post-dialysis ($P < 0.001$). The mean arterial pressure and the ULC score were also significantly lower compared with the start of dialysis ($P \leq 0.001$ for all). The proportion of patients who were hyperhydrated fell significantly after dialysis ($P < 0.001$). The decrease in the ULC score was correlated with the pre-dialysis ULC score ($r = 0.83$, $P < 0.001$), but not with the ultrafiltration volume or any of the BCM or echocardiographic parameters.

With regard to survival, the median time of observation was 405.5 (interquartile range 234.8–518.0) days. During the follow-up, 13 (13.5%) patients died: 6 (9.2%) in the group with

absent or mild lung congestion and 2 (10.5%) and 5 (41.7%) in the group with moderate and severe lung congestion, respectively. In the survival analysis (Table XIV, Figure 14), the hazard ratio (HR) for mortality was higher in the group with pre-dialysis severe lung congestion (ULC >30 comets) compared with the other two groups (HR = 5.03, 95% CI = 1.5–16.5).

Table XIV. Survival of the study population

	Hazard ratio (95% CI and P-value)	Adjusted hazard ratio (95% CI and P-value)
Lung comets score		
<16	1	1
16–30	1.11 (0.22–5.48), P = 0.90	1.21 (0.24–6.12), P = 0.82
>30	5.03 (1.53–16.53), P < 0.01	3.63 (1.03–12.74), P < 0.05
NYHA class (0 = I–II, 1 = III–IV)		2.59 (0.77–8.70), P = 0.12
Hydration status (0 = normohydrated, 1 = hyperhydrated)		1.22 (0.26–5.74), P = 0.80

Bold values are statistically significant. CI, confidence interval; NYHA, New York Heart Association

Considering that the ULC score can be theoretically influenced by either the left ventricular function and/or the body water content, we evaluated the real impact of lung water on survival in a multivariate Cox model that included demographic, echocardiographic and bioimpedance parameters (Table XV).

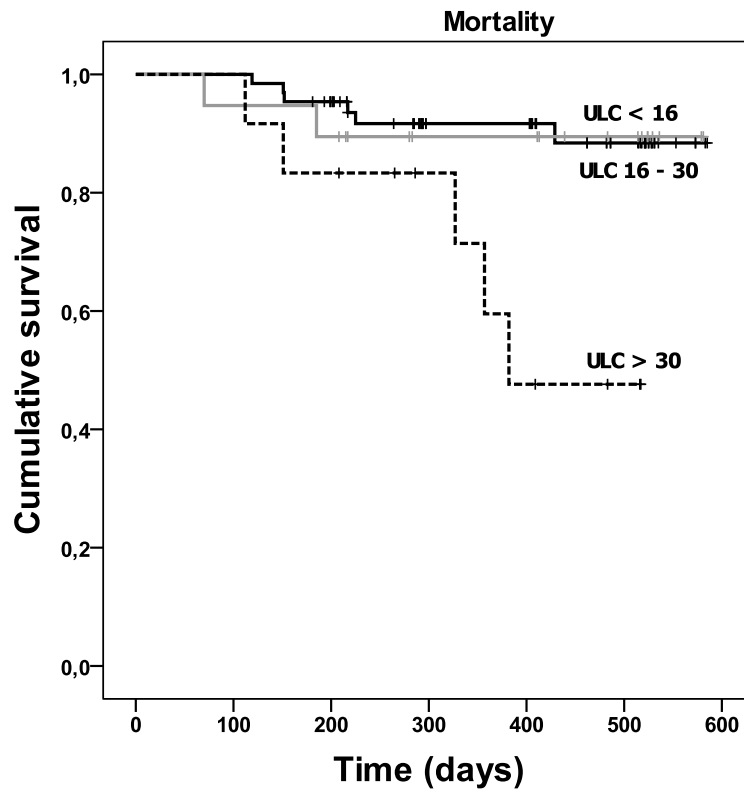


Figure 14. Kaplan-Meier survival analysis according to the ULC score

Based on our results, the pre-dialysis ULC score and the left ventricular mass index (LVMI) remained significantly associated with survival time. These predictors (LVMI and pre-dialysis ULC) maintained their statistical significance after bootstrapping analysis. The post-dialysis ULC score also had a significant (albeit low) impact on survival in the crude Cox analysis ($P = 0.003$, $HR = 1.021$, $95\% CI = 1.007-1.036$). Nevertheless, after adjusting for different confounders (LVMI, ejection fraction, post-dialysis hydration status, albumin, age and dialysis vintage), the score lost its statistical significance. As a final point, we compared the discriminative power for predicting survival (the area under the curve—AUC) for: pre-dialysis ULC (AUC – ULC = 0.791, $P = 0.008$), NYHA class (AUC – NYHA = 0.785, $P = 0.014$) and LVMI (AUC – LVMI = 0.762, $P = 0.004$). The hydration status had no discriminatory abilities in terms of survival (AUC – $\Delta HS = 0.612$, $P = 0.197$).

Table XV. Adjusted Cox regression for mortality

Pre-dialysis variables	β	SE	Wald	Significant P-value	Exp (β) HR	95% CI for Exp (β)	
						Lower	Upper
ULC score, pre-dialysis	0.975	0.049	4.939	0.026	2.651	1.122	6.262
LVMI, g/m ²	0.020	0.008	5.889	0.015	1.320	1.004	1.437
Age, years	0.048	0.035	1.949	0.163	1.049	0.981	1.123
CRP, mg/L	0.018	0.019	0.897	0.344	1.018	0.981	1.058
Hydration status—pre ΔHS	0.051	0.059	0.739	0.390	1.052	0.937	1.182
Albumin, g/dL	-1.047	0.091	0.630	0.427	0.351	0.026	4.657
LVEF, %	-0.017	0.046	0.135	0.713	0.983	0.899	1.076
Dialysis vintage, months	0.002	0.007	0.099	0.754	1.002	0.989	1.015

Bold values are statistically significant. CI, confidence interval; HR, hazard ratio; SE, standard error; ULC, ultrasound lung comets; LVMI, left ventricular mass index; CRP, C-reactive protein; LVEF, left ventricular ejection fraction.

2.2.4. Discussion

Within our study, the ELW evaluated by lung ultrasonography proved to be a valuable instrument for evaluating and predicting the harmful effect of occult overhydration in HD patients. By associating pre-/post-dialysis lung ultrasound and total body impedance, with modern echocardiographic imaging, in a survival analysis, our study was the first that holistically explored the hydration status and its cardiovascular effects. The ULC score proved to be the best predictor for the relationship hydration status - mortality, independently of bioimpedance-derived parameters. These results offered encouraging opportunities for upcoming interventional trials. Even though, bioimpedance analysis proved its usefulness in clinical studies for decades, only recently helped revealing the influence of hyperhydration on survival (Wizemann et al., 2009; Chazot, et al., 2011). Wizemann et al. measured baseline overhydration in 269 HD patients in a prospective study. The authors followed the patients for a period of 3.5 years (Wizemann et al.,

2009) and the $\Delta\text{HS} >15\%$ as a marker of overhydration, was found to be an independent predictor of mortality (HR for all-cause mortality = 2.1). A study performed in 2011 on 158 patients selected from Giessen (Germany) with 50 patients selected from Tassin (France) considered as a reference population (Chazot, et al., 2012), used the relative expansion of the extracellular compartment ($\Delta\text{HS} >15\%$) as a cut-off to stratify all patients into non-hyperhydrated and hyperhydrated. The follow-up period was 6.5 years; at the end, there was no difference in mortality between the Tassin group and the non-hyperhydrated group from Giessen, although the multivariate adjusted all-cause mortality was considerably increased in the hyperhydrated Giessen patient group (HR = 3.41). Even though our study population included fewer patients and the follow-up period was shorter, the percentage of patients who were hyperhydrated was similar. Within our study, there was a significant difference in age between the normohydrated and hyperhydrated patients, the hyperhydrated patients being younger. However, including age into the Cox regression model did not alter the outcomes of the survival analysis. The lack of echocardiographic measurements represented a serious limitation of the two previous studies. Though these are associated with the high intra- and interobserver variability (Pinedo et al., 2010), the prognostic value of different echocardiographic parameters in haemodialysed patients has been obviously proved (Zoccali et al., 2000; Zoccali et al., 2004).

The usefulness of lung ultrasound examination has been established in HD patients. Mallamaci et al. used this method in a population of 75 HD patients to cross-sectionally estimate the prevalence of pulmonary congestion and its reversibility after dialysis (Mallamaci et al., 2010). The results of the study showed that the high prevalence of pulmonary congestion in both symptomatic and asymptomatic patients was unrelated to the hydration status, but was strongly associated with the LVEF.

Zoccali et al. tested in 2010 the prognostic value of ELW measured by lung ultrasound in a multicentric study that enrolled 392 HD patients. Within the study, patients with very severe pulmonary congestion (>60 ULC) had an HR = 4.2 for death and HR = 3.2 for cardiac events, compared with those having mild or no pulmonary congestion, even after multiple adjustments for NYHA functional class and other risk factors. Nevertheless, it is obvious that lung congestion is a direct result of either overall overhydration and/or cardiac dysfunction. Additionally, there is a direct pathophysiological connection between overall hydration and LV structure and function. The nutritional and inflammatory status involved in cardiovascular outcomes and hydration mechanics, through the malnutrition-inflammation-atherosclerosis syndrome are also important. Consequently, it was undefined which of these three interrelated aspects is most appropriate for diagnostic and therapeutic purposes.

The Cox model that included demographic parameters, ULC score, bioimpedance-determined ECW and ICW, as well as LV mass/LV systolic function showed that the ULC score remains the best overall independent predictor for mortality. The differences between our results, regarding the relation between ULC, bioimpedance parameters and LVEF, and that of Mallamaci et al. are most probably the result of differences in study populations. Our patients were younger and probably with less comorbidities and therefore had improved volaemic control and a preserved

left ventricular systolic function. But we considered such differences as being a strength, as they independently confirmed and complemented the findings from previous reports, in a different dialysis setting. Our findings supported the impact of the ULC score on survival and brought new players into this relationship. The prospective observational study performed by Zoccali et al. was a path breaker, but its main limitation was the lack of information concerning the overall hydration status and cardiac function. By assessing survival in a more complex pattern, our results clearly showed that the estimation of lung water is most likely the best predictor of mortality, outstanding the overall hydration status and cardiac parameters.

Limitations of the study: We included in our study group a relatively small number of patients from a single dialysis center and the follow-up period was relatively short. We could not specify the cause of death and the information about nonfatal events were not collected.

2.2.5. Conclusions

The lung comet score emerged as the best predictor for the relationship hydration status - mortality independently of bioimpedance-derived parameters in our population, opening the path for large multicentric interventional trials.

2.3. Overhydration, Cardiac Function and Survival in HD Patients

2.3.1. Aim

It is known that chronic subclinical volume overload take place commonly and may be universal in hemodialysis (HD) patients who follow the standard thrice-weekly treatment. In addition, it is directly linked to hypertension, increased arterial stiffness, left ventricular hypertrophy, heart failure, and eventually, higher mortality and morbidity. Starting from this data, we evaluated for the first time the relationship between bioimpedance assessed overhydration and survival taking into consideration different cardiac parameters assessed by echocardiography.

2.3.2. Material and methods

Our study group included a final number of 221 subjects undergoing chronic HD treatment for at least 3 months in the “Dr. C. I. Parhon” hemodialysis unit between May 2008 and December 2010. The protocol was approved by the Ethics Committee of University Hospital ‘Dr C. I.Parhon’ (Iasi, Romania). The exclusion criteria were patients with metallic joint prostheses, cardiac pacemakers, decompensated cirrhosis and limb amputations, refusal to take part in the study, age <18 years old, active systemic infections and terminal illnesses.

The body composition was determined before dialysis using a bioimpedance analysis device (BCM). The extracellular water (ECW), the intracellular water (ICW) and the total body water (TBW) were calculated in order to determine the amount of fluid overload. We calculated AFO as the difference between the expected patient’s ECW under normal physiological conditions and the actual ECW, and RFO as the absolute fluid overload to extracellular water ratio (AFO/ECW). Patients were considered overhydrated using a cut-off of >15% for the relative

hydration status. This definition of overhydration was based on the work described by Wabel and Wizemann (Wabel et al., 2008; Wizemann et al., 2009). We determined another cut-off for defining overhydration (RFO>17.4%) using a different statistical approach. From the BCM data, we also obtained lean tissue index (LTI–lean mass normalized to body surface area) and fat tissue index (FTI–fat mass normalized to body surface area).

Echocardiographic evaluations were achieved after a short dialysis period being carried out according to the recommendations of the American Society of Echocardiography (Lang et al., 2005) by a cardiologist blinded to the bioimpedance results. From the total number of subjects, we were able to perform an echocardiography assessment in only 157 patients (the echocardiographic subgroup). We defined predialysis BP as an average BP measurement from the previous three consecutive HD sessions. We considered hypertension a predialysis BP >140/90 mmHg or the use of antihypertensive medications.

The major outcomes were all-cause mortality and CVE. Secondary outcomes were hospitalizations for any reason and hospitalizations for decompensated heart failure. Patients were censored at the last follow-up (31 May 2014) or if they moved to another dialysis unit, switched to peritoneal dialysis or received a kidney transplant. Information on fatal and nonfatal CVE including death, stroke, and myocardial infarction were obtained from the Dialysis Unit registries. *Statistical analysis:* All statistical analyses were performed using the SPSS software, version 19.0.1 (SPSS Inc., Chicago, IL, USA). Continuous variables were expressed as mean \pm SD or median and inter-quartile range (IR) according to normal or non-normal distribution. The association between RFO and all-cause mortality was investigated by Kaplan–Meier analysis and Cox regression analysis. To determine the optimal cut-off point for the RFO as a predictor of all-cause mortality the relationship between RFO and outcome was analyzed using the Martingale residuals in Cox’s proportional hazard regression analysis (Grambsch et al., 1995). In the multivariate Cox models, we included all the available variables that are known to influence all-cause mortality in HD patients. For the Cox regression analysis performed in the echocardiographic subgroup, due to the low number of incident outcomes, we determined the CIs for estimating β by bootstrapping. Proportional hazards assumptions were tested using log minus log survival plots and Schoenfeld residuals. The Bayesian information criterion (BIC) and the Akaike information criterion (AIC) were calculated for each Cox model; there is no statistical test to compares different BIC or AIC estimations, and a lower value indicates a better fitted model. We also performed a post-hoc power analysis (Rosner, 2011). The level of significance was set to $P = 0.05$.

2.3.3. Results

The study population included 221 patients: 52.5% males, mean age 53.8 ± 13.9 years, median dialysis vintage of 83.0 (IR = 49.0–130.5) months. Analyzing the features of the study group, we noticed that the most frequent cause of ESRD was chronic glomerulonephritis (38.9%). 59 (26.7%) patients were considered overhydrated when judged by the RFO = 15% cut-off.

We identified no significant differences in age, systolic and diastolic BP, or incidence of diabetes and cardiovascular comorbidities between patients with RFO >15% and patients with RFO ≤15%. Though, there were significant differences between the two groups regarding dialysis vintage and, as expected, other bioimpedance parameters (Table XVI).

Throughout a median follow-up period of 66.2 (IR = 42.4–70.2) months, 66 deaths and 78 CVE were recorded. Patients in the overhydrated group (RFO>15%) had a 2.12 and 2.46 fold increased risk for all-cause mortality and CVE, respectively (Table XVII, Figures 15 and 16).

In the multivariable Cox analysis, after adjustment for age, gender, dialysis vintage, diabetes, cardiovascular comorbidities and hypertension, a RFO>15% remained independently associated with both outcomes (Table XVII).

Within the study, patients considered overhydrated (RFO>17.4%) had an increased risk for both outcomes as compared to patients considered normohydrated, both in the univariate and in the multivariate survival analysis after adjustment for age, gender, dialysis vintage, diabetes, cardiovascular comorbidities, and hypertension (Table XVIII).

Table XVI. Demographic characteristics and bioimpedance assessment of the entire study population and of the overhydrated and normohydrated patients (using the RFO = 15% cut-off).

	All patients (N = 221)	RFO≤15% (N = 162)	RFO > 15% (N = 59)	P#
Age, years	53.8±13.9	53.5±13.7	54.6±14.4	0.59
Male, N (%)	116 (52.5)	78 (48.1)	38 (64.4)	0.03
Dialysis vintage, months	83.0 (49.0–130.5)	70.8 (45.8–121.9)	107.9 (74.5–150.3)	<0.001
Diabetes, N (%)	23 (10.4)	14 (8.6)	9 (15.3)	0.15
BMI, kg/m ²	25.5±5.0	25.9±5.3	24.2±3.9	0.01
Hypertensive, N (%)	145 (65.6)	104 (64.2)	41 (69.5)	0.46
SBP, mmHg	143.1±15.7	142.4±15.7	145.0±15.9	0.27
DBP, mmHg	80.5±10.3	80.5±10.6	80.3±9.7	0.90
CV comorbidities, N (%)	112 (50.7)	82 (50.6)	30 (50.8)	0.98
CAD, N (%)	50 (22.6)	41 (25.3)	9 (15.3)	0.11
PVD, N (%)	28 (12.7)	21 (13.0)	7 (11.9)	0.83
Heart failure, N (%)	71 (32.1)	52 (32.1)	19 (32.2)	0.99
Stroke, N (%)	13 (5.9)	8 (4.9)	5 (8.5)	0.34
AFO, L	1.7±1.4	1.0±0.9	3.4±0.8	<0.001
RFO, L	9.7±8.1	6.0±5.8	19.7±3.6	<0.001
TBW, L	33.9±6.1	33.8±6.0	34.5±6.1	0.40
ECW, L	16.4±2.9	15.9±2.9	17.5±2.9	0.001
ICW, L	17.6±3.4	17.8±3.4	17.1±3.5	0.18
LTI, Kg/m ²	12.6±2.5	12.7±2.6	12.2±2.5	0.22
FTI, Kg/m ²	11.2 (7.6–15.4)	12.3 (8.4–16.0)	10.0 (6.9–13.4)	0.01
Deaths, N (%)	66 (29.9)	39 (24.1)	27 (45.8)	0.002
CVE, N (%)	78 (35.3)	46 (28.4)	32 (54.2)	<0.001

Data are expressed as mean ± SD, median with IR, or total number with percentages, as appropriate. Bold values are statistically significant. # —comparison between groups.

Table XVII. Survival analysis using the predefined cut-off of RFO (15%)

	All-cause mortality		Cardiovascular events	
	HR ^a	95% CI	HR ^a	95% CI
Unadjusted	2.12	1.30–3.47	2.46	1.56–3.87
Adjusted ^b	1.87	1.12–3.13	2.31	1.42–3.77

a. The group of patients with a RFO ≤ 15% was used as reference.

b. Adjusted for: age, gender, dialysis vintage, diabetes, cardiovascular comorbidities, and hypertension.

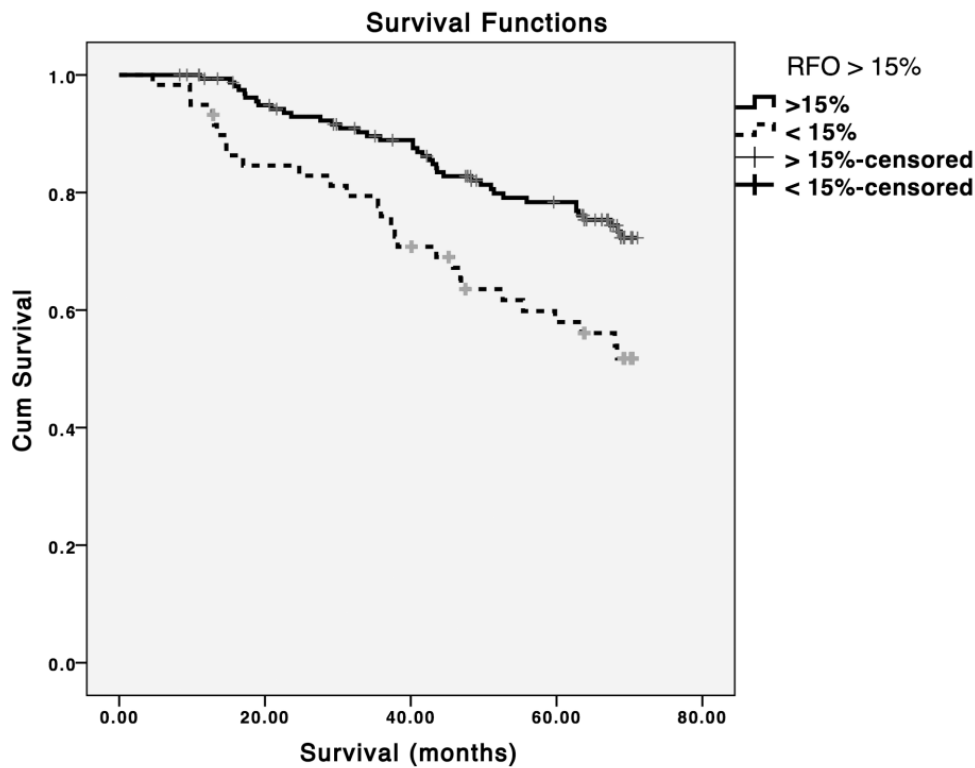


Figure 15. Kaplan Meier survival analysis for a RFO > 15% cut-off point (Log rank p = 0.002).

However, the Cox models obtained using the RFO = 17.4% cut-off showed a better goodness of fit than the models that were obtained using the RFO = 15% cut-off (all-cause mortality—for the univariate analysis: AIC = 663.26, BIC = 664.82 vs. AIC = 668.78, BIC = 670.34; for the multivariate analysis: AIC = 652.06, BIC = 662.98 vs. AIC = 658.81, BIC = 669.73; CVE—for the univariate analysis: AIC = 762.87, BIC = 764.43 vs. AIC = 773.56, BIC = 775.12; for the multivariate analysis: AIC = 748.84, BIC = 759.77 vs. AIC = 763.87, BIC = 774.79).

Studying the all-cause hospital admissions, only the patients found overhydrated by the new cut-off showed a significant increase in the incidence rate for this outcome.

Nevertheless, the hydration status (considered by either of the two cut-offs) was not associated with an increase in the incident rate for decompensated heart failure hospitalizations.

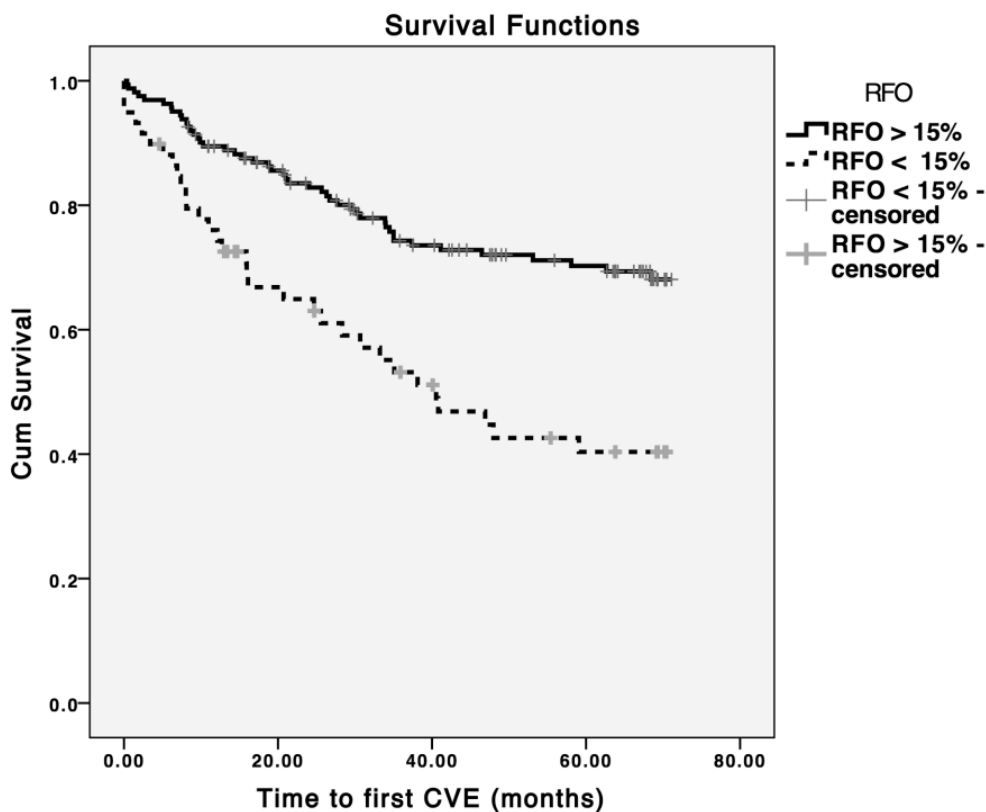


Figure 16. Time to first CVE analysis for a RFO > 15% cut-off point (Log rank $p < 0.001$)

Table XVIII. Survival analysis using the new cut-off of RFO (17.4%)

	All-cause mortality		Cardiovascular events	
	HR ^a	95% CI	HR ^a	95% CI
Unadjusted	2.86	1.72–4.78	3.67	2.29–5.89
Adjusted ^b	2.72	1.60–4.63	4.17	2.48–7.02

a. The group of patients with a RFO ≤ 17.4% was used as reference.

b. Adjusted for: age, gender, dialysis vintage, diabetes, cardiovascular comorbidities, and hypertension.

Baseline echocardiography was performed in 157 patients. Demographic characteristics, bioimpedance-derived and echocardiographic parameters of this cohort are described in Table XIX. Most significantly, there were no significant differences between the entire group and the echocardiographic subgroup in regard to any of the parameters evaluated in the study (Table XIX).

All through the follow-up period (median 68.4 months, IR = 47.8–70.3 months) 39 deaths and 60 CVE were recorded. In the univariate Cox survival analysis, a RFO > 15% was associated with an increased risk for all-cause mortality and CVE (HR = 1.91, 95%CI = 1.00–3.64 and HR = 1.83, 95%CI = 1.07–3.12).

Notably, after adjustment for age, gender, dialysis vintage, diabetes, cardiovascular comorbidities, hypertension, and echocardiographic parameters (LVMI or LVEF as continuous variables) these associations were lost. Still, performing the same analysis with the 17.4% RFO

cut-off, showed that patients in the overhydrated group (RFO>17.4%) had an increased risk for both outcomes, in the univariate and also in the fully adjusted Cox models (Table XX). Using LVEF as a categorical variable didn't influence the final results of the Cox analysis.

Table XIX. Demographic features, bioimpedance and echocardiography assessment of the echocardiographic subgroup and of the overhydrated and normohydrated patients (using the RFO = 17.4% cut-off).

	All patients (N = 157)	P*	RFO<17.4% (N = 135)	RFO > 17.4% (N = 22)	P#
Age, years	53.1±12.9	0.64	53.6±12.7	50.1±14.5	0.25
Male, N (%)	81 (51.6)	0.86	64 (47.4)	17 (77.3)	0.01
Dialysis vintage, months	85.2 (55.9–134.9)	0.39	82.0 (51.8–131.5)	117.6 (73.4–149.3)	0.02
Diabetes, N (%)	13 (8.3)	0.49	13 (9.6)	0 (0.0)	0.22
BMI, kg/m ²	24.9±4.3	0.52	25.2±4.4	23.1±2.4	0.002
Hypertensive, N (%)	108 (68.8)	0.52	92 (68.1)	16 (72.7)	0.67
SBP, mmHg	142.9±15.4	0.87	142.9±15.6	143.6±14.2	0.89
DBP, mmHg	81.4±9.9	0.45	81.4±9.9	81.1±9.3	0.76
CV comorb, N (%)	80 (51.0)	0.96	69 (51.1)	11 (50.0)	0.92
CAD, N (%)	37 (23.6)	0.83	34 (25.2)	3 (13.6)	0.24
PVD, N (%)	19 (12.1)	0.87	17 (12.6)	2 (9.1)	0.64
Heart failure, N (%)	58 (36.9)	0.33	50 (37.0)	8 (36.4)	0.95
Stroke, N (%)	7 (4.5)	0.54	6 (4.4)	1 (4.5)	0.98
AFO, L	1.6±1.3	0.81	1.3±1.1	3.6±0.8	<0.001
RFO, %	9.5±7.4	0.80	7.7±6.4	20.1±3.1	<0.001
TBW, L	34.1±5.9	0.86	33.8±5.9	35.6±5.4	0.16
ECW, L	16.3±2.9	0.75	16.1±2.9	17.8±2.4	0.01
ICW, L	17.8±3.3	0.56	17.8±3.3	17.9±3.2	0.84
LTI, %	12.9±2.5	0.27	12.9±2.4	12.7±2.7	0.70
FTI, %	10.6 (7.4–14.9)	0.28	11.0 (7.6–15.4)	8.9 (6.7–10.9)	0.02
LVMi (g/m ^{2.7})	147.1 (120.5–177.7)	-	147.1 (120.9–78.1)	151.8 (119.7–184.2)	0.79
Interventricular septum, mm	11.5±1.7	-	11.6±1.7	11.3±1.8	0.43
LVPWT, mm	10.7±1.8	-	10.8±1.9	10.6±1.6	0.88
End-diastolic left ventricular diameter, mm	52.0±6.2	-	51.7±5.9	54.1±6.7	0.09
End-systolic left ventricular diameter, mm	32.8±5.3	-	32.6±4.9	34.3±7.1	0.33
LVEF, %	60.3 (57.1–64.5)	-	60.4 (57.3–64.5)	60.0 (56.8–64.5)	0.68
Deaths, N (%)	39 (24.8)	0.28	29 (21.5)	10 (45.5)	0.02

Data are expressed as mean ± SD, median with IR, or total number with percentages, as appropriate. Bold values are statistically significant; *—comparison between the entire and the echocardiographic cohort #—comparison between groups.

Table XX. Survival analysis using the new cut-off of RFO (17.4%) in the echocardiographic subgroup

	All-cause mortality		Cardiovascular events	
	HR ^a	95% CI	HR ^a	95% CI
Unadjusted	2.27	1.11–4.66	3.26	1.85–5.75
Model 1	2.19	1.02–4.69	3.99	2.13–7.46
Model 2	2.29	1.08–4.89	4.32	2.32–8.05

a. The group of patients with a RFO \leq 17.4% was used as reference.

Model 1: adjusted for age, gender, dialysis vintage, diabetes, cardiovascular comorbidities, hypertension, and left ventricular mass index

Model 2: adjusted for age, gender, dialysis vintage, diabetes, cardiovascular comorbidities, hypertension, and left ventricular ejection fraction.

2.3.4. Discussion

Within our study, we investigated the impact of overhydration on all-cause mortality and CVE, by using a previously reported cut-off value for overhydration (a RFO of 15%) and by defining a new RFO cut-off value. Additionally, we intended to assess for the first time if the relationship between bioimpedance measured overhydration and these outcomes is present even after adjustments for echocardiographic parameters.

Our data show that hydration status estimated by bioimpedance spectroscopy is associated, independently of clinical and echocardiographic parameters, with all-cause mortality and CVE in a HD population. Moreover, we proved that overhydration is associated with an increased incidence rate for all-cause hospitalizations; we identified a better cut-off to optimally outline the increased risk for these outcomes associated with overhydration. At the moment, this was the first study assessing mortality, CVE and hospitalization risk associated with overhydration, taking into consideration different cardiac parameters.

It is known that overhydration represents an independent predictor for death in dialysis populations. The bioimpedance analysis seems to be useful in this respect (Davies et al., 2014) Previous prospective observational studies emphasizing its utility in evaluating and optimizing the correct hydration status. A normohydration status leads to a better control of hypertension (Machek et al., 2010; Moissl et al., 2013), less intradialytic adverse events and improved cardiac function (Machek et al., 2010; Ferrario et al., 2014).

Bioimpedance is routinely used in a growing number of dialysis centers. The operational threshold for (a RFO > 15%) relative overhydration is based on the prospective observational study performed by Wissemann et al. on 269 prevalent HD patient cohort (Wizemann et al., 2009). Even though our study population included patients with a mean age 53.8 vs. 65 years, with a longer dialysis vintage and a lower prevalence of diabetes (10.4% vs. 28%), the bioimpedance assessment of fluid compartments was similar and generated a similar prognostic significance.

Within our study, we defined a new cut-off for RFO – 17.4% and showed that this value performed better than the previous one in survival analyses. The new threshold remained

independently associated with mortality, even after adjustment for different baseline echocardiographic parameters (Foley et al., 1995; Silberberg et al., 1989; London et al., 2001; Zoccali et al., 2001; Covic et al., 2013). Our findings confirmed the results from a single previous cohort, and proved that bioimpedance parameters are significant predictors for outcomes, even when adjustments are made for cardiovascular comorbidities or for well-recognized predictors such as LVMI or cardiac function.

In the literature, there are only few randomized controlled trials that compared this bedside method with usual clinical methods of fluid assessment. A trial published by Hur et al. displayed that over 12 months, the exclusive use of bioimpedance for determining the dry weight leads to a significant decrease in BP values, arterial stiffness and ultimately LVMI (Hur et al., 2013). Other randomized trial established that strict bioimpedance guided fluid management leads to a better BP control, a decrease in arterial stiffness and most importantly, an improved survival (Onofriescu et al., 2014). Still, these trials do not appropriately define the intimate relationship between overhydration, cardiac function and survival. It is known that there is a direct link between hydration status and cardiac function, but whether the increased mortality associated with overhydration is mediated through changes in cardiac performance is currently unknown. The present study is the first one that addressed this endeavor, proposing that overhydration is linked to mortality independently of cardiac function.

Limitations of the study: Primary, echocardiography was not performed in all patients that had the bioimpedance assessment, but this is frequently encountered in similar studies due to objective reason. Moreover, transthoracic echocardiography is less performant for evaluating cardiac function and structure when compared to other imagistic methods. Another limitation is represented by the fact that we did not evaluated residual renal function and this parameter could have influenced body fluid composition, but the high dialysis vintage observed in our study implies that most of the patients were anuric. Besides, the number of patients and outcome events were relatively low, but we used different statistical approaches to strongly overcome these shortcomings. Our patients came from a country with one of the best survival rates in the world (Kramer et al., 2012) and, as such, our results may not be inferred to other populations. Finally, even though LVMI is associated with diastolic dysfunction, and also that both LVMI and LVEF are independent and important prognostic factors in HD populations (Yu et al., 2012, Liu et al., 2012), our results cannot be generalized to HD patients with only diastolic dysfunction.

2.3.5. Conclusion

Even though there are numerous data regarding the usefulness of bioimpedance for routine dialysis management, in fact limited randomized controlled trials compared this bedside technique with common clinical methods of fluid assessment. Moreover, this data does not appropriately explain the link between overhydration, cardiac function and survival. Within our study we proved that the hydration status is associated with mortality, cardiovascular events and hospitalization risk in a HD population, independently of cardiac morphology and function. We

suggest a new cut-off for RFO, in order to better define the relationship between overhydration and worse outcomes.

2.4. Optimal risk prediction in hemodialysis patients

2.4.1. Aim

Fluid overload is associated with adverse outcomes in hemodialysis (HD) patients. In this regard, bioimpedance and lung ultrasonography are used to objectively evaluate fluid status, but their prognostic implication is still under study. In our research we intended to precisely analyze the prognostic significance of bioimpedance versus lung ultrasonography in optimal evaluation of fluid status in HD patients.

2.4.2. Material and methods

From an overall eligible 215 HD patients, we included in the study only 173 patients undergoing chronic HD treatment for at least 3 months in a single dialysis unit between 26 May 2011 and 26 October 2012. The exclusion criteria were: patients under 18 years old, systemic infections and terminal neoplasia, subjects with metallic joint prostheses, cardiac pacemakers or stents, decompensated cirrhosis and limb amputations. Our subjects were on 4 h HD session x three times per week. Biochemical parameters were determined pre-dialysis, at the beginning of each month. The study protocol was approved by the Ethics Committee of University Hospital “Dr CI Parhon” (Iasi, Romania).

Lung ultrasonography examinations were performed before dialysis, with patients in the near-to-supine or supine positions. Ultrasound scanning was performed for a total of 28 positions per complete examination, as previously described (Jambrik et al., 2004; Picano et al., 2006). At every scanning site, *B-lines* could be counted from 0 to 10. Zero was defined as a complete absence of B-lines in the investigated area, while the full white screen is considered, when using a cardiac probe, as corresponding to 10 lung comets. The sum of the B-lines yielded a score denoting the extent of extravascular fluid in the lung (Picano et al., 2006).

We evaluated the hydration status and the body composition using a portable whole body bioimpedance spectroscopy device (BCM-Fresenius Medical Care D GmbH) which generally measures the impedance spectroscopy at 50 frequencies. Measurements were performed before dialysis. As previously stated, we determined the extracellular water (ECW), intracellular water (ICW) and TBW (Moissl et al., 2006) along with absolute fluid overload (AFO) and relative fluid overload (RFO).

Echocardiographic measurements were made according to the recommendations of the American Society of Echocardiography (Lang et al., 2005), on an interdialytic day by two blind echocardiographers.

Statistical analysis: Data were analyzed using SPSS for Windows, version 19.0.1, Chicago, IL and R and expressed as mean \pm SD, median and interquartile range or as percent frequency, as appropriate. In order to define the optimal cut-off points for the RFO or BLS as predictors of all-cause mortality, the method described by Contal and O’Quigley was used (Contal et al., 1999).

Kaplan–Meier and Cox models evaluated time-to-event analysis of death. From Cox proportional hazards models including conventional predictors with and without continuous RFO or BLS, we evaluated the C statistic difference, continuous NRIs, and IDI using methods accounting for censoring (Pencina et al., 2004; Pencina et al., 2011). We used the Hosmer and Lemeshow test to evaluate the calibration of the models. Additionally, we calculated the Bayesian information criterion (BIC) and the Akaike information criterion (AIC) for each Cox model. We also performed bootstrapping validation, in order to determine the confidence intervals for estimating β in the Cox proportional hazard regression.

2.4.3. Results

The study included 173 patients whose demographic, biological, bioimpedance, and echocardiographic parameters are accessible in Tables XXI, XXII, XXIII and XXIV. Chronic glomerulonephritis (33.4 %) was the most common cause of ESRD. 31 patients (17.9 %) with a higher prevalence of diabetes and a more severe baseline NYHA class, significantly lower diastolic blood pressure, higher hs-CRP levels, and increased left atrium volume and fluid overload died during follow up. There was no difference related to BLS between the two groups ($p = 0.12$).

Table XXI. Demographic and clinical parameters of the study population

	All (N = 173)	Survivors (N = 142)	Deceased (N = 31)	p*
Age (years)	57.9 ± 14.0	57.1 ± 13.8	61.8 ± 14.9	0.05
Dialysis vintage (months)	48.9 (17.5–96.1)	50.6 (20.2–95.1)	44.5 (14.3–97.9)	0.46
Weight (Kg)	69.5 (58.5–81.9)	69.7 (58.5–81.9)	66.6 (58.6–78.6)	0.70
Anuric [N (%)]	74 (42.8)	62 (43.7)	12 (38.7)	0.61
Male [N (%)]	85 (49.1)	69 (48.6)	16 (51.6)	0.76
Smoking [N (%)]	56 (32.4)	43 (30.3)	13 (41.9)	0.21
Diabetes [N (%)]	36 (20.8)	25 (17.6)	11 (35.5)	0.03
Hypertension [N (%)]	134 (77.5)	112 (78.9)	22 (71.0)	0.35
SBP (mmHg)	143.3 ± 22.9	144.0 ± 23.2	139.9 ± 21.9	0.37
DBP (mmHg)	74.8 ± 15.0	76.2 ± 15.1	68.5 ± 13.3	0.01
Heart rate (beats/min)	74.0 (67.0–82.0)	74.0 (67.0–81.0)	76.0 (69.0–85.0)	0.27
NYHA class [N (%)]	1–2: 133 (76.9)	1–2: 116 (81.7)	1–2: 17 (54.8)	0.001
	3–4: 40 (23.1)	3–4: 26 (18.3)	3–4: 14 (45.2)	
HCV [N (%)]	43 (24.9)	36 (25.4)	7 (22.6)	0.75
HBV [N (%)]	14 (8.1)	10 (7.0)	4 (12.9)	0.28
BLS	9.0 (3.0–14.0)	8.0 (3.0–13.0)	11.0 (3.0–29.0)	0.12

Significant values are indicated in bold

* Comparison between survivors and deceased

Table XXII. Biological parameters of the entire study population

	All (N = 173)	Survivors (N = 142)	Deceased (N = 31)	p*
Hemoglobin (g/dl)	11.5 ± 1.6	11.5 ± 1.5	11.6 ± 1.9	0.76
WBC (x10 ³ /mme)	6.2 (5.2–7.7)	6.2 (5.1–7.7)	6.9 (5.5–7.9)	0.30
Albumin (g/dl)	3.9 (3.7–4.1)	3.9 (3.7–4.1)	3.8 (3.5–3.9)	0.06
hsCRP (mg/l)	0.4 (0.2–1.0)	0.4 (0.2–1.0)	0.8 (0.3–1.2)	0.02
Calcium (mg/dl)	8.5 (8.1–8.8)	8.5 (8.2–8.8)	8.5 (8.1–8.9)	0.86
Phosphorus (mg/dl)	5.2 (4.2–6.6)	5.2 (4.3–6.7)	5.1 (3.7–5.9)	0.15
iPTH (ng/l)	306.2 (163.1–482.8)	319.4 (184.2–473.6)	197.0 (93.9–632.9)	0.13
Cholesterol (mg/dl)	171.0 (146.5–212.0)	170.5 (147.0–210.5)	173.0 (141.0–217.0)	0.86
Triglycerides (mg/dl)	131.6 (93.9–189.5)	132.1 (91.7–195.4)	130.8 (96.3–158.1)	0.60
eKt/V	1.5 (1.3–1.7)	1.5 (1.4–1.7)	1.5 (1.2–1.7)	0.46

Significant values are indicated in bold

* Comparison between survivors and deceased

Table XXIII. Bioimpedance analysis of the entire study population

	All (N = 173)	Survivors (N = 142)	Deceased (N = 31)	p*
TBW (L)	32.0 (27.8–36.6)	32.1 (27.9–36.8)	30.6 (26.8–33.8)	0.14
ECW (l)	15.2 (13.5–17.9)	15.2 (13.5–18.0)	15.0 (13.0–17.0)	0.63
ICW (l)	16.4(14.3–18.8)	16.6 (14.6–19.1)	15.7 (13.0–17.0)	0.03
AFO (l)	1.2 ± 1.3	1.1 ± 1.4	1.7 ± 1.1	0.03
RFO (%)	7.4 ± 7.9	6.7 ± 8.1	10.7 ± 6.1	0.01

Significant values are indicated in bold

* Comparison between survivors and deceased

Table XXIV. Echocardiographic parameters of the entire study population

	All (N = 173)	Survivors (N = 142)	Deceased (N = 31)	p*
LVMI (g/m ²)	155.4 ± 39.6	152.7 ± 36.6	167.9 ± 42.2	0.05
LAVI (ml/m ²)	38.2 ± 6.6	37.5 ± 5.9	40.9 ± 8.8	0.05
E/E'	15.6 ± 6.3	15.4 ± 6.3	16.8 ± 6.3	0.35
IVST (mm)	12.0 (10.6–13.0)	12.0 (10.6–13.0)	12.4 (11.0–14.5)	0.22
LVPWT (mm)	11.6 (10.3–13.0)	11.6 (10.3–12.9)	11.9 (10.9–14.0)	0.09
LVEF (%)	60.0 (57.0–65.0)	60.0 (56.8–65.0)	60.0 (57.0–65.0)	0.72

* Comparison between survivors and deceased

Within the study, the median time of observation was 21.3 (interquartile range 19.9–30.3) months. The RFO cut-off had better sensitivity, but lower specificity for the outcome than the BLS cut-off (74.2 %, 95 % CI 55.4–88.1 % vs. 32.3 %, 95 % CI 16.7–51.4 % and 52.1 %, 95 % CI 43.6–60.6 % vs. 87.3 % 95 % CI 80.7–92.3 %, respectively).

Using these cut-offs, patients who had more than 22 BLS or a RFO greater than 6.88 % had an increased risk for death in the univariate Cox survival analysis (Table XXV, Fig. 17, Fig. 18).

Table XXV. Lung congestion and relative fluid overload association with all-cause mortality

	ULC		RFO	
	HR ^a	95 % CI	HR ^b	95 % CI
Unadjusted	3.08	1.45–6.54	2.68	1.20–6.03
Adjusted	2.72	1.19–6.16	2.93	1.30–6.58

Adjusted for: severity of NYHA class (0—NYHA class 1, 2; 1— NYHA class 3, 4), diabetes, hs-CRP, and left ventricular mass index

^a The group with B ≤ 22 ULC was used as reference

^b The group with B ≤ 6.88 RFO was used as reference

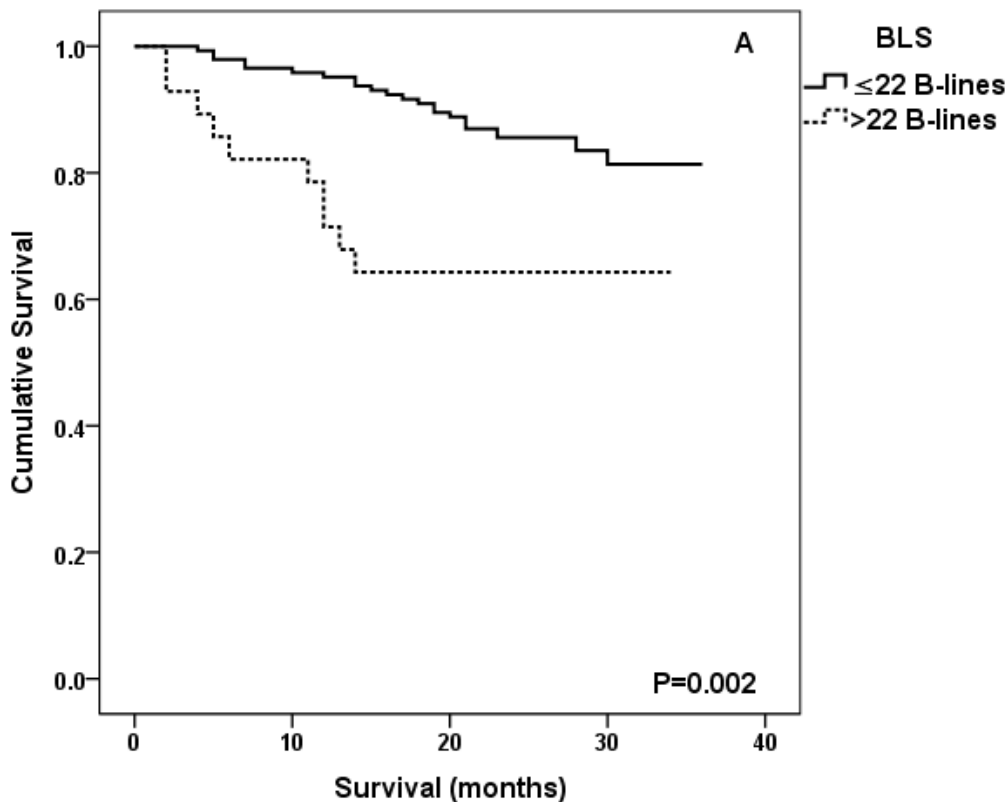


Figure 17. Kaplan-Meier analysis for all-cause mortality according to B-lines score cut-offs

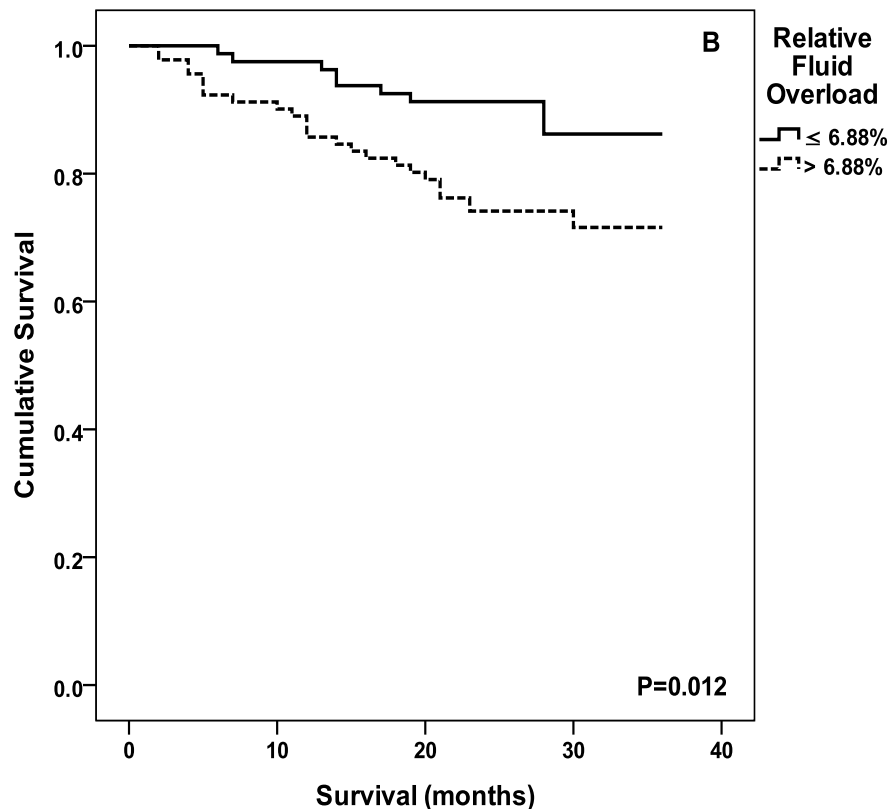


Figure 18. Kaplan-Meier analysis for all-cause mortality according to relative fluid overload cut-offs

We also aimed to determine if LUS (the BLS) or bioimpedance (the RFO value) are able to improve the risk prediction for death, apart from that of clinical, biological and echocardiographic parameters.

In this regard, we tested the potential incremental prognostic value of individually adding BLS or RFO value to commonly used risk factors as the severity of NYHA class, diabetes, hs-CRP levels or LVMI, by using three measurements of performance: calibration, discrimination and reclassification.

The models used in the prognostic analysis showed good calibration ($p > 0.05$) for the Hosmer–Lemeshow test for all three models (Table XXVI).

The model that included RFO had the lowest AIC and BIC, showing better global goodness-of-fit than the other two models (Table XXVI).

After analyzing the discrimination abilities of the models, the C statistic for the all-cause mortality prediction increased significantly when the RFO was included into the baseline model (DC statistics 0.058 95 % CI = 0.003–0.114), but not when the BLS was included into the same model.

In the same way, only the model that incorporated RFO showed significantly better risk reclassification abilities than the baseline model (IDI = 3.6 % and continuous NRI = 24.8 %)(Table XXVI).

Table XXVI. Performance of the models

	Model 1	Model 2	Model 3
<i>Discrimination^a</i>			
ΔC statistics, 95 % CI	Reference	0.017 (-0.060–0.094)	0.058 (0.003–0.114)
<i>Calibration</i>			
AIC	299.69	299.53	293.88
BIC	305.42	306.71	301.05
H–L	$\chi^2 = 8.25$	$\chi^2 = 13.91$	$\chi^2 = 13.61$
	p = 0.41	p = 0.08	p = 0.09
<i>Reclassification^a</i>			
IDI, 95 % CI	Reference	0.036 (-0.005–0.141)	0.036 (0.000–0.096)
NRI, 95 % CI	Reference	0.125 (-0.188–0.350)	0.248 (0.021–0.112)

C statistic with only conventional predictors was 0.728

Model 1—severity of NYHA class, diabetes, hs-CRP, and left ventricular mass index;

Model 2—Model 1 + LogULC score;

Model 3—Model 1 + RFO;

^a Comparison with model 1

2.4.4. Discussion

Our results support the fact that BLS and RFO are independently associated with all-cause mortality in a HD population. This was the first research showing that overhydration, evaluated by bioimpedance, and not by lung ultrasonography, improves risk prediction for death, compared to classical and echocardiographic-based risk prediction scores/parameters. Methods like inferior vena cava diameter, blood volume monitoring, or different plasma volume markers were previously used to appropriately assess and manage fluid overload. At present, only two have been prospectively associated with mortality risk in dialysis populations: bioimpedance analysis and lung ultrasonography.

Prospective observational studies have revealed that using bioimpedance analysis for measuring and correcting fluid overload improves cardiac function (Machek et al., 2010; Ferrario et al., 2014) as well as the control of blood pressure (Machek et al., 2010; Moissl et al., 2013), with less intradialytic adverse events (Machek et al., 2010). Wizemann et al. demonstrated that overhydration is associated with mortality in a prevalent HD population (Wizemann et al., 2009). In this regard, our research group confirmed these results in a comparable HD population, and additionally demonstrated that the bioimpedance assessed overhydration is associated with survival independently of echocardiographic parameters (Onofriescu et al., 2015), which are recognized as determinants of worse outcomes in these patients (Liu et al., 2012; Wald et al., 2014). Other randomized controlled trials proved that using bioimpedance analysis for dry weight estimation led to a significant reduction in arterial stiffness, blood pressure (Hur et al., 2013; Onofriescu et al., 2014), LVMI (Hur et al., 2013) and to a better survival (Onofriescu et al., 2014).

LUS can identify pulmonary congestion at a pre-clinical stage in HD patients (Mallamaci et al., 2010), being related with cardiac function (Mallamaci et al., 2010) and bioimpedance parameters (Siriopol et al., 2013) or NT-proBNP (Paudel et al., 2015). Previous studies (Zoccali et al., 2013) revealed that patients with very severe congestion (BLS>60) had a 4.2-fold risk of death and a 3.2-fold risk of CVE (adjusted for NYHA class and other risk factors), when compared with patients having mild or no congestion. Moreover, we consequently reported that BLS is associated with survival, even after adjustments for echocardiographic or bioimpedance-derived parameters (Siriopol et al., 2013).

Zoccali et al. have shown that lung ultrasonography can improve risk prediction for CVE and mortality in HD patients, but this was confirmed only against clinical and biological parameters (Zoccali et al., 2013). Our results proved that including the BLS into a baseline model along with LVMI does not significantly improve the predictive abilities of the model. Moreover, including RFO into the same model determined the improvement of both discrimination and reclassification abilities for prediction of all-cause mortality. The subjects included in these two studies were similar into what concerns the age, nutrition parameters, and observational period; still, our group had a lower dialysis vintage, diabetes prevalence and a less severe cardiac failure explaining the lower mortality incidence observed in our study. Moreover, we emphasized the independent associations between fluid overload indices, as assessed by bioimpedance and pulmonary ultrasonography, and mortality. With regard to relationship between cardiac function, fluid overload and mortality, pulmonary ultrasonography provides comparable information to echocardiography. This method could be implemented in the clinical practice as it is easier to be performed, cheaper and more available than echocardiography (Gargani, 2011).

In our study we noted two cut-offs for defining fluid overload association with mortality in HD patients, as evaluated by pulmonary ultrasonography and bioimpedance, the 22 BLS cut-off for defining pulmonary congestion's risk for mortality and the 6.88 % cut-off for RFO, very similar to the previously described upper-limit of normohydration status (-7 %) (Wizemann et al., 2009; Wabel et al., 2008). In our analysis, the RFO cut-off showed better sensitivity, but a lower specificity for mortality than the BLS cut-off. Therefore, this feature could be used as an instrument for improving screening and identifying high-risk patients.

Limitations of the study: Our population came from a single dialysis center from a country with one of the best survival rates in the world (Kramer et al., 2012) and our cohort may not represent the typical US HD patient; therefore, all data should be certified in other HD cohorts. Moreover, our sample size and number of outcome events are relatively unassertive; in this regard, we used different statistical methods to overcome these limitations. Not least, we weren't able to exactly find the specific cause of death.

2.4.5. Conclusion

This study is the first one that compares the prognostic abilities of the two most important methods for fluid status assessment in HD patients. According to our results, overhydration

assessed by bioimpedance and not by lung ultrasonography, improves risk prediction for death beyond classical and echocardiographic-based risk prediction scores/ parameters.

2.5. Methods of dry weight assessment in low cardiovascular risk hemodialysis patients

2.5.1. Aim

Taking into account that the precise assessment of hydration status in HD patients remains a major challenge for nephrologists, our objective was to explore whether combining LUS with BIS may provide valid information to guide treatment in patients with less severe cardiovascular involvement in HD population.

2.5.2. Material and methods

We performed a prospective, randomized, open-label clinical trial in patients on HD in Iasi, Romania in two HD centers - the BUST Study (Extravascular Lung Water Monitoring by Combined Bioimpedance and Ultrasonography as a Guide for Treatment in Hemodialysis Patients). (Clinical Trials ID – NCT 01,815,762), which was complementary to LUST. The protocol was approved by the ethics committee and all participating patients signed a written informed consent.

The following inclusion criteria were used: patients aged >18 years receiving thrice-weekly HD for more than 3 months. As main exclusion criteria we considered: severe cardiac failure (NYHA class III–IV), past myocardial infarction, stable or unstable angina, and acute coronary syndrome, patients with metallic joint prostheses, cardiac stent or pacemakers, decompensated cirrhosis, pregnancy, and limb amputations, malignancy, active infections, temporary or permanent catheter as a vascular access, mental incompetence, and unwillingness to participate in the study. We also excluded patients with known persistent pleurisy, pulmonary fibrosis or pneumectomy, due to LUS measurement limitation.

All individuals were randomized 1:1 to have a dry weight assessment based on clinical (control) or LUS–bioimpedance (active)-guided protocol, the intervention in the BUST being basically different from that of the LUST study. Within the control group, post-dialysis dry weight was adjusted based on clinical criteria only (blood pressure, presence of edema, intradialytic hypotension, cramps, etc.) while in the active group the target weight was assessed using LUS and bioimpedance (Fig. 19).

LUS measurements were performed once a week until the treatment goal was achieved (< 15 BLS pre-dialysis) and once a month after that in subjects with moderate to severe lung congestion (≥ 15 BLS pre-dialysis) as well as in patients without evidence of lung congestion at baseline who developed pulmonary congestion (≥ 15 BLS). The treatment goal was achieved by ultrafiltration intensification within the same HD schedule or, by extra-dialyses, according to individual tolerance and feasibility. Supplemental dry weight adjustments were performed according to the bioimpedance measurement in case of clinical hypovolemia. Patients in the control arm of the study were managed strictly with standard criteria according to current recommendations; the use of LUS/bioimpedance assistance was not allowed in these patients. The

distribution of the patients in each study groups was achieved through the aid of a computerized method. The recruitment period was one month, and the study was finalized when all surviving patients had a follow-up of 24 months.

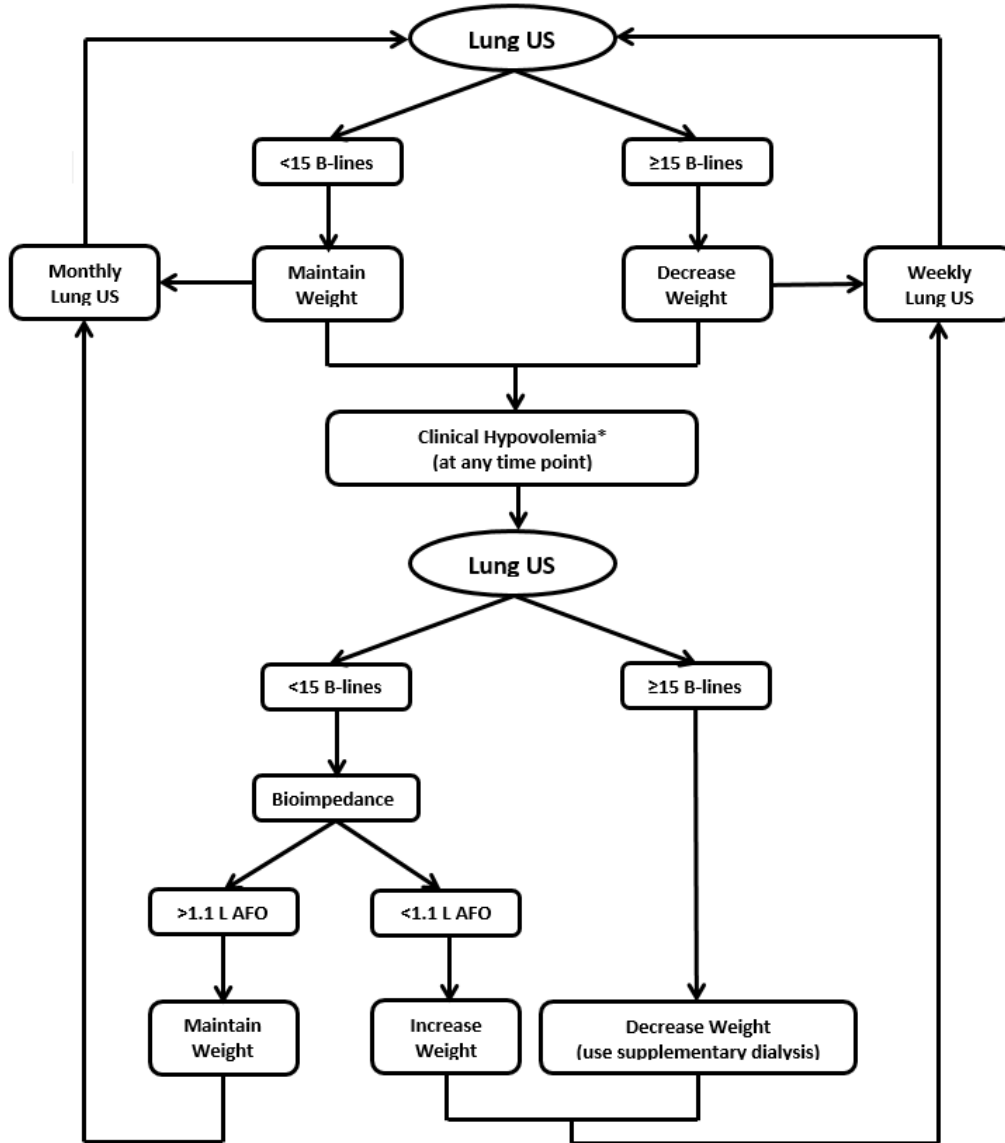


Figure 19. BUST operating protocol. AFO absolute fluid overload, US ultrasound.

*Persistent cramps, post-dialysis hypotension

There were differences between LUST and BUST regarding primary outcome. BUST aimed to assess the effect of a LUS–bioimpedance-guided dry weight adjustment protocol on a composite of all-cause mortality and first cardiovascular events.

The secondary objectives were all-cause mortality, CVE, all-cause hospitalization, dialysis-related adverse events, alterations in NT-proBNP and hs-cTnT levels, hemoglobin, C-

reactive protein (CRP), calcium, phosphorus, and impact on arterial stiffness (PWV), and on fluid compartments, as assessed by bioimpedance, during the study follow-up. Study population underwent serial bioimpedance measurements. We did not perform echocardiographic measurements and did not apply health-related quality of life questionnaires.

We obtained all information on vascular access and comorbidities at baseline using the electronic database of the dialysis supplier and from the patients' charts.

We calculated also the Charlson Comorbidity Index and then categorized it into 2 groups: 2 (severe renal disease only) or more (Rattanasompattikul et al., 2012). Laboratory data and fluid status estimations were recorded at baseline and every 3 months.

The extracellular water (ECW), intracellular water (ICW) and TBW were assessed using previously described methods (Moissl et al., 2006), along with absolute fluid overload (AFO) and relative fluid overload (RFO). The PWV was calculated from carotid and femoral artery waveforms recorded consecutively. Serum NT-proBNP and hs-cTnT levels were evaluated at baseline, at 12 months and at the study end, before a midweek dialysis session.

Within the sample size calculation, the consequent assumptions were followed: 2-year patient incidence in the primary outcome of 20%, and a two-sided type I error of 5%, an 80% power to detect a decrease of 40% in the annual rate of the primary endpoint in the patients with the dry weight assessment on the basis of the BLS protocol.

The assumption for the 40% risk reduction was based on previous studies (Zoccali et al., 2013; Chertow et al., 2010). We estimated the 20% rate for the primary endpoint on the basis of a 14% annual combined mortality and CVE rate reported in the units included in the study. Therefore, we estimated that the required sample size would be of 480 patients.

Taking into account previously research of Onofriescu et al. (Onofriescu et al., 2005), the final study population achieved initial power calculations for detecting a significant difference between groups in PWV of 2 m/s. Such a change in PWV was computed in regard to mean baseline values of 9.7 m/s (Onofriescu et al., 2005) and would require 80 patients in each group for 95% power at a 2-tailed alpha of 0.05.

Statistical analyses: Data were analyzed using the SPSS for Windows, version 19.0.1 (SPSS Inc., Chicago, IL, USA), and MedCalc, version 16.4.3 and were presented as mean \pm standard deviation, median with interquartile range or number and percent frequency, as appropriate. We considered a P value < 0.05 to be significant.

2.5.3. Results

Based on the results of the CLIMB trial (Reddan et al., 2005), we assumed that simultaneous measurement of lung congestion (by LUS) and fluid overload (by bioimpedance) might be useful to manage less severe degrees of lung congestion, while at the same time avoiding the risk of hypovolemia and clinically imperceptible underperfusion for sensitive vascular beds (Reddan et al., 2005).

We analyzed 284 patients that were performing HD in our dialysis units. 34 individuals did not meet the inclusion criteria or refused to participate, the final number of subjects being 250,

with 123 patients included in the active group and 127 patients in the control group. Baseline demographic, clinical, biological and vascular characteristics of the entire population and in both groups are presented in Tables XXV, XXVI and XXVII.

At baseline, in the active group the median BLS was 7 [interquartile range (IQR) 3–12] and only 19 (15.4%) patients had a BLS higher than 15.

Table XXV. Demographic and clinical characteristics of the study population

	All (N = 250)	All (N = 250)	Control (N = 127)	P*
Age (years)	59.2 ± 14.1	59.0 ± 14.9	59.4 ± 13.3	0.73
Male, N (%)	116 (46.4)	58 (47.2)	58 (45.7)	0.89
Weight (kg)	71.9 ± 15.4	72.1 ± 14.7	71.6 ± 16.1	0.74
Dialysis vintage (months)	43.4 (15.3–87.1)	47.8 (15.7–87.5)	41.1 (14.7–86.0)	0.33
Diabetes, N (%)	48 (19.2)	27 (22.0)	21 (16.5)	0.34
Hypertensive, N (%)	190 (76.0)	92 (74.8)	98 (77.2)	0.77
CAD, N (%)	39 (15.6)	24 (19.5)	15 (11.8)	0.12
PAD, N (%)	39 (15.6)	18 (14.6)	21 (16.5)	0.73
Stroke, N (%)	23 (9.2)	14 (11.4)	9 (7.1)	0.28
CCI > 2, N (%)	96 (38.4)	54 (43.9)	42 (33.1)	0.08
AVF, N (%)	243 (97.2)	118 (95.9)	125 (98.4)	0.28
Anuric, N (%)	141 (53.6)	76 (61.8)	65 (51.2)	0.09

Data are expressed as mean ± SD, median with IQR or number and percent frequency

* Comparison between groups

Table XXVI. Biological and arterial stiffness characteristics of the study population

	All (N = 250)	Active (N = 123)	Control (N = 127)	P*
NT-proBNP (pg/ml)	4396.0 (1615.0–10,744.8)	4505 (1897–11,487)	4166 (1486.6–10,118)	0.41
hs-cTnT (ng/l)	36.9 (24.9–51.7)	38.1 (23.7–55.7)	35.9 (25.5–48.4)	0.74
PWV (m/s)	9.9 (7.8–11.4)	9.4 (6.7–12.0)	10.2 (9.0–11.1)	
Hemoglobin (g/dl)	11.4 ± 1.4	11.6 ± 1.5	11.3 ± 1.4	0.23
Albumin (g/dl)	3.9 ± 0.3	3.8 ± 0.4	3.9 ± 0.3	0.24
Calcium (mg/dl)	8.3 ± 0.6	8.3 ± 0.6	8.4 ± 0.7	0.13
Phosphorus (mg/dl)	5.2 (3.9–6.2)	5.1 (3.5–6.1)	5. (4.3–6.3)	0.10

Data are expressed as mean ± SD

* Comparison between groups

Throughout a mean follow-up period of 21.3 ± 5.6 months, there were 54 (21.6%) composite events (all-cause mortality and CVE) in the entire population, with a 2-year rate of 22.8 and 20.5% in the active and control groups, respectively.

These results are translated into a nonsignificant 9% increase in the risk of this outcome in the active arm (HR = 1.09, 95% CI 0.64–1.86, $p = 0.75$) (Fig. 20a). Additionally, in the active group, baseline BLS was not significantly associated with the primary outcome in the survival analysis.

Table XVII. Bioimpedance characteristics of the study population

	All (N = 250)	Active (N = 123)	Control (N = 127)	P*
AFO, L	1.2 ± 2.2	1.2 ± 1.3	1.3 ± 2.9	0.32
RFO, %	7.1 ± 10.8	7.0 ± 7.2	7.2 ± 13.4	0.30
TBW, L	33.9 ± 6.4	33.9 ± 6.2	33.8 ± 6.5	0.96
ECW, L	16.1 ± 2.9	16.2 ± 2.9	16.1 ± 3.0	0.94
ICW, L	17.7 ± 3.7	17.7 ± 3.7	17.7 ± 3.8	0.97

Data are expressed as mean ± SD

* Comparison between groups

Within the study, we separately analyzed the all-cause mortality outcome. During 22.2 ± 4.7 months, there were registered 36 (14.4%) deaths. The 2 year all-cause mortality rates in the active and control group were 14.6 and 14.2%, respectively, implying a nonsignificant 2% increase in the risk of this outcome (HR = 1.02, 95% CI 0.53–1.96, $p = 0.96$) (Fig. 20b).

Concerning CVE outcome, the mean follow-up period was 21.4 ± 5.5 months. There were 45 (18%) events in the entire study population, with 2 year CVE rates of 17.1 and 18.9% in the active and control group, respectively.

Also, these results are translated into a nonsignificant 11% reduction in the risk of CVE (HR = 0.89, 95% CI 0.49–1.59, $p = 0.69$) (Fig. 20c). Comparable to the primary outcome, in the active group, the baseline BLS was not associated with any of these secondary outcomes in the Cox survival analysis.

There were 193.3 (95% CI 175.8– 212.0) episodes per 100 patient-years of dry weight adjustment according to BLS in the active group. There were only 20 (16.3%) patients in the active arm that had a BLS ≤ 15 during the entire follow-up.

Into what concerns the bioimpedance post-dialysis weight adjustment, there were 620.7 (95% CI 588.9–653.9) episodes per 100 patient-years of increase in the dry weight, as guided by bioimpedance-derived ideal dry weight and BLS < 15.

The rate of intradialytic hypotension, all-cause hospital admissions, and vascular access thrombosis was nonsignificantly different between the two arms (Table XXVIII).

Nevertheless, patients in the active arm had a 19% lower relative risk of pre-dialytic dyspnea (rate ratio—0.81, 95% CI 0.68–0.96), but a 26% higher relative risk of intradialytic cramps (rate ratio—1.26, 95% CI 1.16–1.37) (Table XXVIII).

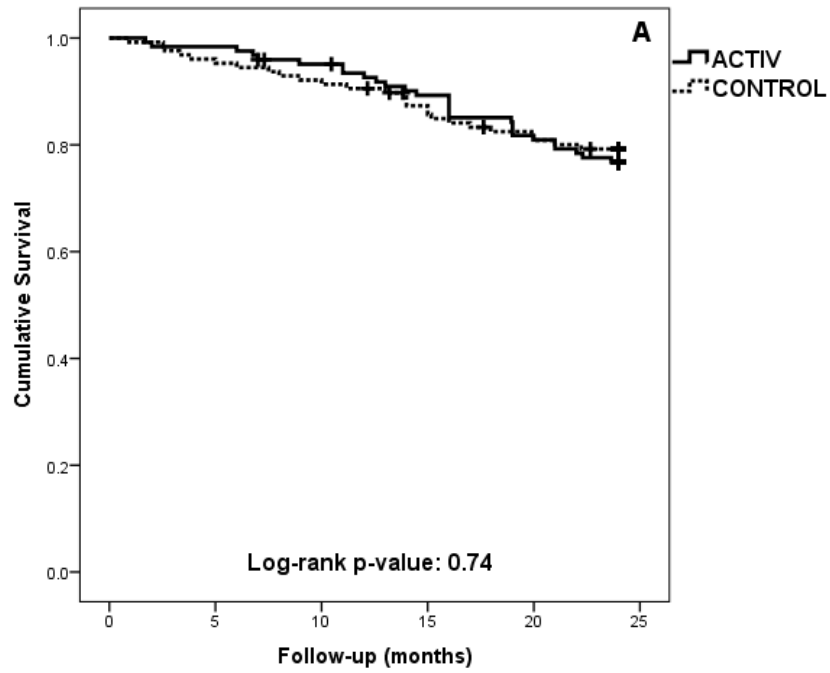


Figure 20.a. Kaplan–Meier curves comparing the two groups for the time to the first primary composite outcome

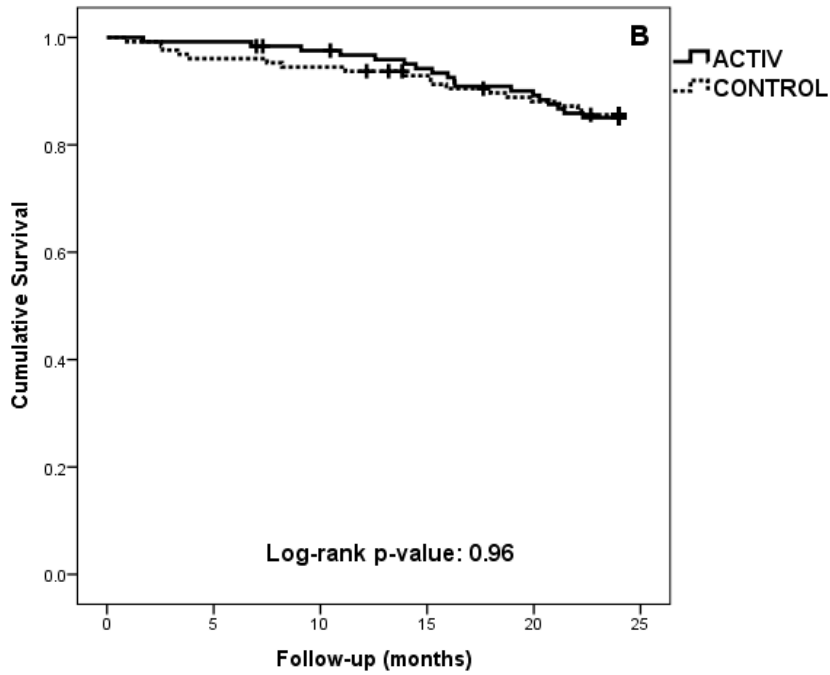


Figure 20.b. Kaplan–Meier curves comparing the two groups for all-cause mortality

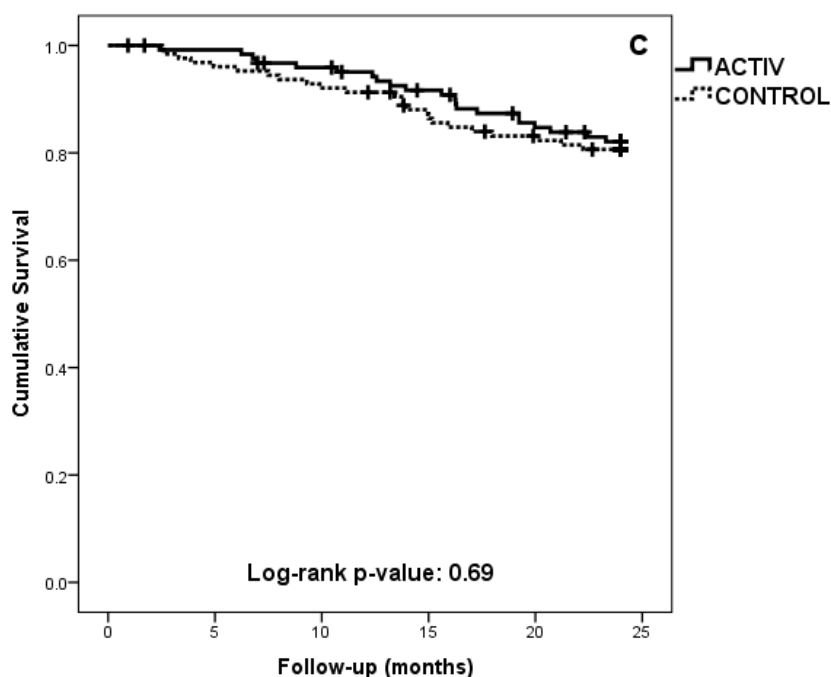


Figure 20.c. Kaplan–Meier curves comparing the two groups for cardiovascular events

We did not observe significantly change during the follow-up regarding serum NT-proBNP and hs-cTnT levels. The values did not differ between the study arms. Though, pulse wave velocity (PWV) significantly increased during the study period, irrespective of treatment group allocation (Table XXIX).

There were no significant changes in regard to hemoglobin, CRP, calcium or phosphorus levels during the 2 years of follow-up.

Table XXVIII. Secondary outcome data for the entire cohort

	Control group (N = 127) (236.3 Patient-years at risk)		Active group (N = 123) (232.3 Patient-years at risk)		Rate ratio (95% CI)
	No. of events	No. of events/100 patient-years	No. of events	No. of events/100 patient-years	
Intradialytic hypotension	1035	438.1	1104	475.3	1.08 (0.99–1.18)
Intradialytic cramps	1056	446.9	1313	565.2	1.26 (1.16–1.37)
Pre-dialytic dyspnea	302	127.8	240	103.3	0.81 (0.68–0.96)
Hospitalizations	89	37.7	103	44.3	1.18 (0.88–1.58)
Vascular access thrombosis	13	5.5	20	8.6	1.56 (0.74–3.42)

Table XXIX. Biomarker levels and arterial stiffness outcomes

	Length of follow-up			p*	p†
	Baseline	12 months	24 months		
NT-proBNP (pg/ml)					
Control	8722.2 (6478.5–10,965.8)	9123.6 (6387.6–11,859.6)	12,186.4 (9256.6–15,115.6)	0.09	0.72
Active	8896.3 (6944.8–10,847.8)	9428.4 (6642.8–12,213.9)	10,728.6 (7775.4–13,680.7)		
p‡	-	0.88	0.49		
Hs-cTnT (ng/l)					
Control	42.9 (37.9–47.8)	45.4 (40.1–50.7)	44.6 (38.9–50.2)	0.14	0.65
Active	44.0 (38.7–49.3)	49.4 (43.9–54.7)	45.0 (39.4–50.7)		
p‡	-	0.30	0.91		
PWV (m/s)					
Control	10.3 (9.8–10.9)	11.0 (10.0–12.1)	12.3 (11.1–13.6)	<0.001	0.32
Active	9.7 (9.1–10.4)	11.5 (10.8–12.3)	12.6 (11.7–13.5)		
p‡	-	0.45	0.77		

Data are presented as mean (95% CI) at baseline, and least-squares mean (95% CI) at 12 months and 24 months. Analysis was conducted using a mixed model for repeated measures

* p value for time effect—trend over time in both arms

† p value for treatment × time interaction—evaluates if changes in one arm are different from the changes in the other arm

‡ p value for comparison between arms at each moment

During the study, dry body weight did not change, but, when analyzing the hydration status, ICW decreased from month 0 to month 24 in both arms, while AFO and RFO increased during the same period. TBW also increased in both groups, but to a lesser extent in the control group. While analyzing only the patients from the active arm, we observed that those patients that did not require a change in the dry weight during the study (N = 45), according to the BLS, had lower RFO values than those patients in which dry weight was reduced (N = 73), both at baseline, but also during the follow-up (p = 0.003). As shown above, RFO increased in the active group, irrespective of the dry weight adjustments.

2.5.4. Discussion

Within the study, we found that a combined LUS–bioimpedance-guided dry weight adjustment protocol did not reduce all-cause mortality and/or CVE compared to the standard clinical approach. As far as we know, this was also the first randomized trial that assessed LUS use for volume control in the HD population. BLS has been shown to correlate to cardiac function

or NTproBNP in patients with acute dyspnea (Frassi et al., 2007) or heart failure (Miglioranza et al., 2013) and helps discriminating between cardiogenic versus noncardiogenic dyspnea (Lichtenstein et al., 1998; Gargani et al., 2008; Sekiguchi et al., 2015).

Previous studies showed that in patients with heart failure and coronary artery disease, the use of LUS predicted death and CVE (Frassi et al., 2007; Bedetti et al., 2010), being more efficient when compared to standard echocardiographic parameters, diabetes or NYHA score (Frassi et al., 2007). Additionally, BLS is hallmarked by good interobserver and interprobe agreement (Mallamaci et al., 2010) and has been correlated with physical performance (Enia et al., 2013), left ventricular ejection fraction (Mallamaci et al., 2010) or bioimpedance-derived parameters (Siriopol et al., 2013;).

In ESRD patients, BLS was associated with all-cause mortality and CVE (Siriopol et al., 2013; 14), independently of clinical and biological parameters (Zoccali et al., 2013) or echocardiographic and bioimpedance-derived features (Siriopol et al., 2013). The addition of BLS to traditional and CKD-related risk factors improved the reclassification abilities of the baseline model for death and CVE (Zoccali et al., 2013), suggesting that this method may offer important information for risk quantification in ESRD patients.

In our study, a primarily BLS-guided protocol did not result in a lower all-cause mortality or CVE. An explanation for this result is that our patients were younger (59 vs. 65 years), with a lower dialysis vintage and prevalence of diabetes (19.2 vs. 29%) and without any severe heart failure (our study included only patients with NYHA classes I and II) when compared to the studies of Zoccali et al. (Zoccali et al., 2013). Even though we did not assess cardiac function directly, it is conceivable that our patients had better cardiac function, with a subsequent lower risk of volume-dependent clinical outcomes. Additionally, baseline NT-proBNP and hs-cTnT levels were similar to other HD populations without significant cardiac disease (Helal et al., 2010). It is known that in HD patients, NT-proBNP and hs-cTnT are associated with echocardiographic parameters (Helal et al., 2010; Yamazaki et al., 2011; Kamano et al., 2012; Artunc et al., 2012) and may accurately identify patients at an increased risk of adverse events (McGill et al., 2010; Hassan et al., 2014; Voroneanu et al., 2014). Also, the baseline BLS score was low, most of the patients having less than 15 B-lines.

The insufficient impact of this strategy on total body water/ body water components could be explained by the neutral results of BLS-derived adjustments in dry weight on study outcomes. We observed a comparable increase between the two study arms in AFO or RFO during follow-up. Onofriescu et al. (Onofriescu et al., 2014) previously revealed that a bioimpedance-derived dry weight adjustment, with a significant subsequent decrease in fluid overload in the active arm, was linked to a decrease in arterial stiffness and even death. All these data propose that in the lack of an adequate control for overall fluid overload as assessed by bioimpedance, there are no beneficial effects of preserving a normal BLS in HD patients. Moreover, in the study performed by Onofriescu et al. (Onofriescu et al., 2014), an increase in PWV in both groups has been noticed after the end of the intervention period and a comparable pattern was observed during the 2 years of follow-up in our study, irrespective of treatment allocation. Besides, we showed that LUS has

lower sensitivity regardless of better specificity for all-cause mortality compared to bioimpedance spectroscopy (Siriopol et al., 2016). Therefore, BIS could be used as a superior routine screening method, identifying high-risk patients in which supplementary studies as LUS should be done.

Limitations of the study: We included in our study only patients from two dialysis units. Still, the results undoubtedly showed that using this protocol did not change the risk of any of the outcomes under investigation. In addition, the selected patients came from only one part of Romania as such our results cannot be inferred to other HD populations. Also, the baseline BLS was low, with a minority of patients having an increased baseline score, implying that following modest amounts of water accumulation in the lung could be irrelevant to clinical outcomes.

At the same time, an echocardiographic evaluation useful to define the relationship between fluid status-cardiac function was not accomplished. However, we did investigate the effect on NT-proBNP levels, a known biomarker strongly associated with cardiac structure and function in HD patients (David et al., 2008; Yamazaki et al., 2011). Lastly, we did not evaluate the precise number of dry weight modifications in the control group.

2.5.5. Conclusion

The BUST study proves that a dry weight adjustment protocol using LUS, as compared with clinical evaluation, does not reduce all-cause mortality and/or CVE in HD patients. Furthermore, this method does not have any positive impact on bioimpedance-assessed fluid status, PWV, or NT-proBNP and cTnT levels.

2.6. Cardiac imaging in advanced CKD

2.6.1. Aim

We propose to review the specific applications of conventional cardiac imaging techniques in patients with ESRD and to offer better insights into the novel imaging methods in order to identify the most important imaging predictors of clinical outcomes in this group of patients.

2.6.2. Material and methods

This literature revision highlighted particular utilizations of standard cardiac imaging techniques in patients with ESRD and offered knowledge into the novel imaging modalities, underlining the newest research in this field. By doing so, we aimed to identify the most significant imaging indicators of clinical outcomes in this population.

2.6.3. Results and discussion

The most useful diagnostic tool in cardiovascular disease is transthoracic echocardiography (TTE) and given its various clinical applications, it has remained the first-line investigation for suspected cardiac disease. In patients with ESRD and particularly in case of dialysis, distinguishing between heart failure and volume overload secondary to renal impairment is very important. As a means to encourage an accurate diagnosis, the Acute Dialysis Quality Initiative (ADQI) XI

Workgroup planned a framework that incorporates eight fundamental parameters reflecting structural abnormalities: LV hypertrophy, increased LV volume index, LV ejection fraction of 45% or less, regional wall-motion abnormalities, diastolic dysfunction, left atrial enlargement, mitral or aortic valvular disease, right ventricular systolic dysfunction. This system characterizes cardiac failure in dialysis by the presence of at least one echocardiographic criterion, dyspnea and the remission of it by dialysis or ultrafiltration (Chawla et al., 2014).

TTE is also useful in stratifying risk and in evaluating the impact of certain interventions, such as dialysis or renal transplantation (RTx)(Pecoits-Filho et al., 2010). Table XXX summarizes the best validated TTE parameters in ESRD.

Table XXX. Validated TTE parameters in ESRD

TTE parameter	Correlation
LVH LV mass	MACE (Park et al., 2012) Renal deaths (Park et al., 2012) eGFR (Paoletti et al., 2016)
LV ejection fraction	All-cause and CV mortality (Zoccali et al., 2004; Wang et al., 2018) Worsening renal function (Verdiani et al., 2010)
Diastolic dysfunction (E/e', LAVi)	All-cause and CV mortality (Tripepi et al., 2007; Tripepi et al., 2009; Choi et al., 2013; Farshid et al., 2013; Valocikova et al., 2016; Matsuo et al., 2018; Abudiab et al., 2017)
RV dysfunction	All-cause mortality (Hickson et al., 2016)
Pulmonary hypertension	CV mortality and events HF hospitalization (Selvaraj et al., 2017; Tang et al., 2018)
Valvular calcifications	Coronary artery disease (Kim et al., 2015)
Global longitudinal strain	All-cause and CV mortality MACE HF hospitalization (Krishnasamy et al., 2014; Hensen et al., 2017; Lofman et al., 2017; Hensen et al., 2018)

The Chronic Renal Insufficiency Cohort (CRIC) study group indicated that *LVH* is the primary myocardial alteration in CKD, with a multifactorial etiology, including the recently described major role of FGF23, alongside with volume overload and increased afterload from higher BP and/or arterial stiffness. Patients with an eGFR < 30 mL/min have a twofold higher risk of LVH, and LV mass correlates directly to eGFR, independently of brain natriuretic peptide (BNP)—as a biomarker of volume overload (Park et al., 2012). In ESRD, uremia-related cardiomyopathy is distinguished by myocardial fibrosis and LVH. Moreover, the prevalence of concentric or eccentric LVH touches a great extent of up to 74% and is related, particularly the eccentric subtype, with a much higher medium-term CV and renal risk (Paoletti et al., 2016). RTx can lead to the regression of concentric LVH (Parfrey et al., 1995; Tayebi-Khosroshahi et al., 2013; Deng et al., 2013; Omrani et al., 2017).

The 2D conventional TTE help us to determine the left ventricular ejection fraction (LVEF) which is one of the most impressive predictors of death and CV morbidity and is conventionally used to assess LV *systolic function*. Studies have demonstrated its independent correlation with all-cause and cardiovascular mortality in ESRD/dialysis patients (Zoccali et al., 2004; Wang et al., 2018). The issue of using LVEF in ESRD emerges basically from its dependency on loading conditions which can influence its accuracy, particularly in dialysis patients, imitating the typical clinical presentation of heart failure. Likewise, if the prognostic value of a low LVEF is well established, an LVEF > 45% can't assess risk (Curtis et al., 2003). RTx can alleviate systolic dysfunction, improve LV contractility and functional status of congestive heart failure (Parfrey et al., 1995; Omrani et al., 2017).

Previous studies reported that diastolic dysfunction (DD) is present in 85%–100% of dialysis patients and that at least 35% have grade 2 or higher dysfunction. Additionally, DD is an autonomous predictor of mortality for these patients (Farshid et al., 2013; Matsuo et al., 2018). Worsening eGFR relates with the severity of DD as evaluated by the E/e' ratio (Jain et al., 2017). E/e' ratio together with LV global longitudinal strain (LV GLS) are the most powerful echocardiographic predictors of CV events and mortality in dialysis patients (Valocikova et al., 2016). An E/e' ratio > 15 indicates high LV filling pressures. Peak E wave velocity correlates with the degree of volume overload and fluctuates with dialysis and ultrafiltration. In contrast, e' velocity reflects LV stiffness and is independent of the patient's volume status (Kim et al., 2017). This is particularly significant since heart failure with preserved EF is the most prevalent form in ESRD, and diagnosing diastolic dysfunction by accurately measuring E/e' ratio may facilitate early therapeutic intervention. Also, given the high prevalence of valvular calcification in ESRD, it is essential to remember that moderate-to-severe mitral annular calcification can influence the precision of e' measurement, when assessing DD. For such specific circumstances the E/A ratio and isovolumic relaxation time can be useful predictors (Abudiab et al., 2017).

Left atrial volume index (LAVi) is a well-validated indicator of DD in the general population. In ESRD, it is related to plasma BNP and ANP levels and can help identify the patients at risk for myocardial ischemia (Tripepi et al., 2009; Choi et al., 2013). LAVi is an independent predictor of death, and monitoring it by echocardiography can predict the risk of CV events in dialysis patients (Tripepi et al., 2007). The effect of RTx on DD is not completely perceived, as previous studies have reported conflicting results. Most data point toward the persistence of DD after RTx, despite the alleviation of LVH, attributing this unexpected finding to immunosuppressant drugs, hypertension, and pre-RTx myocardial fibrosis (Debska-Slizien et al., 2000; Zolty et al., 2008; Souza et al., 2012; Hamidi et al., 2018).

RV systolic and diastolic dysfunction, estimated by TAPSE, S', and fractional area change, are common in ESRD patients on hemodialysis (HD) and are important indicators of mortality (Hickson et al., 2016; Tamulenaite et al., 2018). The pathophysiology of the right ventricular (RV) involvement in ESRD is influenced by various factors, for example, chronic volume overload, anemia, hyperparathyroidism, and especially the presence of a brachial arteriovenous fistula (AVF). The AVF causes chronic RV overload, shifting the interventricular septum to the left and impairing LV filling and systolic function. This right-to-left ventricular interdependence is

important in dialysis, as mortality is twofold higher in patients with biventricular dysfunction (Paneni et al., 2010; Paneni et al., 2013).

Various investigations have demonstrated a link between ESRD and PH and showed that pulmonary artery systolic pressure (PASP) is associated with mortality and CV events, independently of BNP and EF (Yigla et al., 2003; Pabst et al., 2012; Selvaraj et al., 2017; Tang et al., 2018). It is suggested that almost 40% of the dialysis patients have PH (Yigla et al., 2003). Several mechanisms have been hypothesized: PH may be a consequence of left-sided heart failure, of volume overload, or of the AVF which can influence PASP by affecting pulmonary vascular resistance and cardiac output (Pabst et al., 2012). A meta-analysis of 16 studies has found that in ESRD, there is a twofold higher risk of HF admission and mortality compared to non-ESRD patients, both in HD and peritoneal dialysis, partially explained by a higher burden of PH in this population (Tang et al., 2018).

Patients with HD, frequently present both vascular and valvular calcification probably due to CKD-MBD derangements, inflammation, and cardiac overload (Haydar et al., 2004; Maher et al., 1987; Ribeiro et al., 1998; Rattazzi et al., 2013; Matsuo et al., 2018). Valvular calcification in stable HD patients correlates with the presence and severity of coronary artery disease, as shown by Kim YI et al., suggesting that assessment of cardiac calcification by TTE could be a valuable risk stratification tool for CAD in these patients (Kim et al., 2015). Regarding the stable patients with HD, valvular calcifications are associated with worse systolic and diastolic function, more severe LVH, and poorer prognostic (Li et al., 2019). In the general population, left ventricular global longitudinal strain (GLS) is a marker of systolic function that was shown to be superior to LVEF with regard to the prediction of major adverse cardiac events (Kalam et al., 2014). GLS is reported to be a powerful prognostic tool because it is able to detect patients with overt systolic dysfunction in the presence of preserved LVEF (DeVore et al., 2017).

Regarding uremic patients, impaired GLS could be due to microvascular ischemia, interstitial fibrosis, and myocyte hypertrophy caused by hypertension, uremic toxins, and HD-related myocardial stunning that affects the function of subendocardial longitudinal fibers (Sun et al., 2016; Ma et al., 2018). Also in patients with renal impairment, global longitudinal strain was shown to have superior prognostic significance over LVEF. Additionally, both classical Framingham risk factors and renal-specific disturbances, such as hyperphosphatemia, are significant determinants of GLS (Krishnasamy et al., 2014). In a study by Hensen et al, patients in predialysis and dialysis were divided into four groups according to quartiles of LV GLS (Hensen et al., 2017). The lowest quartile of GLS showed the worst prognosis and had a twofold increased risk of all-cause mortality after correcting for RTx. Heart failure with preserved EF is the most frequent form of heart failure among ESRD patients (Lofman et al., 2017). As mentioned above, cardiac remodeling in ESRD can lead to subclinical myocardial impairment despite maintaining EF in a (supra-) normal range. For this population, LV GLS is able to reveal the underlying myocardial damage and perhaps allow early therapeutic intervention since a reduced GLS < 15.2% is associated with increased HF hospitalizations and all-cause mortality (Hensen et al., 2017; Hensen et al., 2018).

No study has evaluated so far the impact of early implementation of HF treatment on CV outcomes based on LV GLS. Reduced GLS peri-RTx is associated with the rate of hospitalization for CVD and all-cause mortality (Fujikura et al., 2018). Additional studies are needed, as GLS could possibly be a useful tool for CV risk stratification pre-RTx. Concerning the effect of RTx on GLS, the study of Hamidi et al recently showed a favorable impact, with both subtle and gross changes in myocardial function improving after surgery (Hamidi et al., 2018).

Another role of speckle-tracking echocardiography (STE) in advanced CKD has recently been postulated. Apparently, LV GLS and LV mechanical dispersion could identify the patients at risk for sudden cardiac death (SCD) due to mixture of scar and fibrous tissue within layers of viable myocardium, despite of relatively preserved LVEF (Hensen et al., 2018).

In autopsy and CMR studies it has been proved that LV GLS correlated with increased myocardial fibrosis (Cameli et al., 2016; Roes et al., 2009). LV mechanical dispersion, as an indicator for the temporal heterogeneity of the mechanical LV contraction as a consequence of myocardial fibrosis, is a good predictor of SCD in several populations (Haugaa et al., 2010). Myocardial fibrosis, which can meddle with the intracellular coupling, delay conduction, and increase the propensity to develop ventricular arrhythmias, is promoted in ESRD by ischemia, uremic toxins, and CKD-MBD derangements (Borioni et al., 2015). Aside from LV GLS, RV GLS has recently proven specific enough to select the asymptomatic HD patients with subclinical dysfunction and normal RV fractional area change (Tamulenaite et al., 2018).

When compared to conventional TTE, *real time 3D echocardiography* (RT3DE) has emerged as a technique capable of superior evaluation of ventricular volumes and function, with results as accurate as the “gold standard” method, CMR (Jenkins et al., 2004). Apart from the indications validated for the general population, data regarding the specific use of RT3DE in ESRD are mostly confined to data obtained during dialysis sessions. Intra-dialytic hypotension (IDH), although common, is yet not totally comprehended, and assessing cardiac dynamics during HD seems a promising option. Traditional TTE can be performed, but geometric assumptions and volume miscalculations are frequent. CMR can defeat these limitations but cannot be performed during HD. Along these lines, two studies addressed the issue of IDH by assessing LV function through RT3DE.

In a pilot study on 12 patients, Krenning et al demonstrated the usefulness of a precise estimation of LV function through RT3DE, by assessing LV volumes and geometry during HD (Krenning et al., 2007). Yang et al performed RT3DE in 29 dialysis patients with IDH and 34 controls and showed that patients with IDH had greater decrease in 3DLVEF, stroke volume, and cardiac index at mid-dialysis, with 3DLVEF being the strongest predictor independently associated with IDH (Yang et al., 2010).

The role of the RV in the development of IDH was recently assessed by Sun et al. who showed that RVEF as assessed by 3DSTE is associated with an increased risk of IDH and may serve for risk stratification in HD patients, whereas lower ultrafiltration rates could be protective for the RV (Sun et al., 2018). Another small study used 3DSTE to evaluate the impact of HD on LV mechanics and proved that HD sessions immediately improve all strain directions and pointed

toward FGF23 as playing a role in the deterioration of LV mechanics in patients with ESRD (Kovacs et al., 2014). Precisely measuring LV volumes in response to blood volume changes is another promising application of RT3DE, as it was shown that in HD patients with DD, colloid infusion determines a decrease in stroke volume variability (SVV), but no change in LV EDV. This finding indicates that HD patients are receptive to fluid infusion and SVV can represent a tool in intra-operative guiding of fluid therapy (Kanda et al., 2015).

In CKD, coronary artery disease (CAD) is associated with a threefold higher risk of death. In dialysis, both atheromatous plaques and coronary artery *calcifications* (CAC) can lead to significant coronary artery stenosis (Haydar et al., 2004). The risk factors involved in the development of CAD in ESRD are age, hypertension, diabetes mellitus, dyslipidemia, and specific CKD-related factors such as hyperparathyroidism, hyperphosphatemia, endothelial dysfunction, chronic inflammation, and the presence of epicardial adipose tissue (Afsar et al., 2014).

Coronary atherosclerosis encompasses the vast majority of the CAD spectrum for the general population. In CKD, CAC are more frequent, severe, rapidly progressive and associated with mortality, a poorer CV outcome, and worse CKD-MBD derangements. In the general population, CAC reflect subintimal atherosclerosis, whereas in CKD, CAC correlate with calcium and phosphorus deposits in the media layer of the arterial wall (Raggi et al., 2017). RTx significantly reduces CAC score in dialysis patients by interference with the calcium-phosphorus homeostasis (Abedi et al., 2009).

Big efforts have been made toward developing noninvasive techniques for assessing CAD in this population, given its high ubiquity. *Single photon emission computed tomography* (SPECT) and *electron beam computed tomography* (EBCT) showed promising results, but failed to enter clinical practice for individuals with ESRD due to low sensitivity, spatial resolution, and high pricing (Lee et al., 2013). Regarding the noninvasive way, *multi-detector computed tomography* (MDCT) is currently available in many units and allows physicians to screen for coronary lesions. In order to gain high-quality information, the patient's heart rate must be below 65 bpm. As indicated by the American Heart Association model, every artery has to be analyzed by segment and diameter and the degree of coronary stenosis has to be assessed - a significant lesion is defined as a luminal narrowing of 50% or more (Lee et al., 2013). Iio et al were the first group to report good sensitivity, specificity, positive and negative predictive value for MDCT in detecting significant coronary artery stenosis when compared to coronary angiography (Iio et al., 2008).

In asymptomatic ESRD patients, coronary artery stenosis is highly prevalent, and therefore early diagnosis through MDCT could help select those who would benefit from a more invasive approach. Likewise, the Agatston score from MDCT can be quantified by an automatic CAC scoring software; this score can serve as a marker of CAD, as it correlates well with significant coronary artery stenosis as assessed by invasive coronary angiography (Mitsutake et al., 2006). MDCT plays an important role in diagnosing calcification and atherosclerotic plaques, patients with these entities having a higher risk for CV events (Lee et al., 2013).

MESA risk score calculator was developed by the investigators of the MESA study by adding CAC score to traditional risk factors for CVD. The modified variant including CAC proved

to be superior as far as risk prediction (C-statistic 0.80 vs 0.75, $P < 0.0001$), providing an accurate estimate of 10-year CAD risk (McClelland et al., 2015). In spite of CKD and ESRD patients having a higher burden of vascular calcification, none of the risk score calculators take into account renal function as a variable and there are no studies validating their use in advanced CKD.

There are sure restrictions of MDCT usage in ESRD. First of all, because of the difficulty to differentiate high-contrast calcium from contrast-enhanced vessel lumen, the presence of high-degree vascular calcifications can lead to misinterpretation. Secondly, MDCT cannot separate medial from intimal (atherosclerotic) calcifications. Moreover, the necessity of iodinated contrast agents can alter the residual renal function (RRF) in patients on RRT. RRF reduces inflammation, improves fluid management, and provides continuous clearance of protein-bound solutes and middle molecules. RRF is related with improved survival and quality of life in dialysis patients and preserving it is imperative. Therefore, using iodinated contrast agents in patients on dialysis is not risk-free and careful monitoring of fluid status and serum potassium are required. Immediate or supplementary HD is not usually necessary (Mathew et al., 2016). Despite of these constraints, the net clinical benefit of noninvasively assessing CAD in ESRD by MDCT is significant as conventional angiography is an invasive method which requires hospitalization, raising concern issues regarding a higher risk of arrhythmias, stroke, cholesterol embolism, coronary artery dissection, or even death (Iio et al., 2008).

A comprehensive assessment of coronary plaques, yielding information beyond routine coronary angiography, can be provided by the *intra-vascular ultrasonography* (IVUS), which has been validated with histological findings (Kawasaki et al., 2002; Shigemoto et al., 2019). An independent predictor of CV events in CAD patients is a high lipid content in the coronary plaques (Sano et al., 2006). Limited data are available regarding the use of IVUS in ESRD. Miyagi et al compared plaque composition assessed by IVUS between two groups of patients and proved that impaired renal function is associated with higher lipid and lower fibrous volume (Munnur et al., 2016). The same influence of low GFR was observed in hypertensive and diabetic patients (Shigemoto et al., 2019). Furthermore, progressively declining GFR is an independent predictor of plaque burden, length, and risk for rupture (Hong et al., 2010). In CKD and ESRD patients, studies proved that IVUS-guided PCI reduced the contrast volume, incidence of contrast-induced acute kidney injury, and induction of renal replacement therapy at 1 year, when compared to angiography-guided PCI. Despite these positive results, IVUS-guided PCI did not reduce 1-year mortality in this population (Mariani et al., 2014; Sakai et al., 2018).

A pilot study conducted by Ali et al presented the concept of low contrast volume PCI in ESRD (Ali et al., 2016). The group performed zero contrast PCI 1 week after performing IVUS, with pre- and post-measurements of fractional and coronary flow reserve, confirming good results without serious complications.

Another intra-coronary diagnostic technique with a better spatial resolution than IVUS named *optical coherence tomography* (OCT). It has become extremely useful in cardiac catheterization laboratories in approaching high-risk lesions. OCT provides important information about coronary morphology, plaque distribution and composition, and neointimal and thrombus

assessment. Furthermore, it can help for PCI guiding and stent sizing. OCT-guided PCI seems to be similar to IVUS-guided PCI and both are superior to angiography-guided PCI, lowering the need for revascularization and the risk of cardiac death at 1 year (Prati et al., 2012; Kume et al., 2018).

By using OCT in patients with ESRD a decrease in the contrast volume as well as in the risk of acute kidney injury can be achieved. Case studies have reported promising results for novel methods such as zero contrast OCT-guided PCI. Karimi et al used a mixture of saline and colloid to displace blood in order to perform OCT and guide PCI in a 67-year-old patient with an eGFR of 13 mL/min (Karimi et al., 2016). Azzalini et al performed PCI using dextran-based OCT guidance, with promising results (Azzalini et al., 2018).

Also, given that OCT is the only intra-vascular method capable of accurately imaging calcium thickening without artifacts, it could represent a reasonable alternative for ESRD patients, taking into account the limitations of MDCT (Kume et al., 2018). Chin et al investigated 62 HD patients by OCT and observed that in comparison with controls, HD- dependent patients had a higher calcium burden with extensively calcified coronary arteries and higher prevalence of nonatherosclerotic intimal calcium (Chin et al., 2017).

In ESRD, myocardial fibrosis is an arrhythmogenic substrate causing ventricular reentering arrhythmias; this may clarify the high prevalence of SCD in this population (Graham-Brown et al., 2016). Increased amounts of uremic toxins and an imbalance in the activity of parathyroid hormone promote different forms of cardiac fibrosis. Fibrosis is compromising the contractile performance, but is also hampering intercellular coupling, is slowing conduction, and thereby in increasing the propensity to develop ventricular arrhythmias.

Cardiac magnetic resonance has emerged as a promising imaging modality for detecting myocardial fibrosis and is currently used for the diagnosis of certain cardiomyopathies. For the general population, the best described technique is based on the delayed washin and washout of the contrast agent from the tissues with increased extracellular space—late gadolinium enhancement. In advanced CKD, the usage of gadolinium based contrast agents (GBCA) should be considered individually as it is limited by the risk of developing a potentially lethal condition, nephrogenic systemic fibrosis (NSF)(Kis et al., 2018; Schieda et al., 2018).

In the previous years, it was demonstrated that persons with normal renal function can also develop NSF when exposed to GBCA, but until the exact pathophysiology of GBCA-induced disease is better understood, alternative gadolinium-free methods should be used whenever possible in advanced CKD (Schieda et al., 2018; Leyba et al., 2019).

Native T1 is a novel non-contrast CMR technique based on the longitudinal recovery time of hydrogen atoms following their excitation. In any given magnetic field strength, every tissue will produce a specific range of values. Prolongation of myocardial relaxation time can appear secondary to fibrosis, amyloid, or edema (Kis et al., 2018).

Several studies have investigated its possible applications in ESRD as a surrogate for myocardial fibrosis. Graham-Brown MPM et al compared native T1, systolic strain, and cardiac function of 35 HD patients and 22 controls, showing that in HD patients, native T1 is significantly

prolonged and associated with reduced systolic, global longitudinal and circumferential strain, especially in the interventricular septum (IVS). The same authors report the method is reproducible and unaffected by fluid variability between dialysis sessions (Graham-Brown et al., 2017).

A study from Rutherford et al studied a very similar cohort consisting of 33 HD patients and 28 controls and showed that global, septal, and mid-septal native T1 is significantly higher in HD patients.

Also, native T1 correlates with LV mass, suggesting that as LVH progresses in severity, the underlying tissue abnormalities simultaneously develop. Interestingly, there was an association between higher septal T1 time and longer QT interval, a risk factor for ventricular arrhythmias and SCD.

Additionally, the authors proved that GLS correlates with galectin-3, a novel marker of myocardial fibrosis (Rutherford et al., 2016). There are certain limitations of using native T1 in HD patients. First of all, there is no histological study demonstrating its correlation with myocardial fibrosis in this population. Moreover, inflammation, iron, and water content can influence native T1, which is extremely important given the chronic inflammation status and fluid variability between patients in ESRD.

Another non-contrast CMR method, T1rho, also referred to as the spin-lattice relaxation time in the rotating frame, was proposed by Wang et al. T1rho has been already used to study intra-articular cartilage, brain, and liver and has the ability to characterize the interaction between tissue components, such as water and macromolecular compositions - collagen and proteoglycans. In ischemic heart disease, it was shown to be able to distinguish normal from infarcted myocardium and detect myocardial fibrosis.

Based on this assumption, the team conducted a study on 32 asymptomatic HD patients and 35 healthy volunteers and showed that T1rho values are significantly higher in ESRD patients with no history of cardiac disease, despite of having similar native T1 time with controls.

Also, they detected higher T1rho values in patients with systolic and DD (Wang et al., 2016). Dobutamine stress CMR was shown to be useful for identifying significant CAD prior to potential RTx in high-risk patients -sensitivity 100%, specificity 89% (Dundon et al., 2015).

Since imaging the right ventricle can be challenging with ETT, CMR has been shown to be able to better assess it. Subclinical RV dysfunction can be detected early by CMR, and it is associated with a worse prognosis. Also, the duration of dialysis is an independent predictor of RV dysfunction (Peng et al., 2018).

2.6.4. Conclusion

Multi-modality cardiac imaging offers data regarding cardiac involvement in ESRD useful for early diagnosis and risk stratification. TTE seems to be the first-line investigation to evaluate cardiac function in CKD; however, including in our daily practice the newer approaches such as speckle-tracking imaging or CMR can offer an ample understanding of CVD in ESRD, leading to the development of new therapeutic approaches capable of refining CV outcomes in ESRD patients.

Chapter 3. Imaging the heart in sleep-related breathing disorder

3.1. Background

Sleep-disordered breathing (SDB) or sleep-related breathing disorders concomitantly affect more than one-third of patients with HF (McKelvie et al., 2011), the most frequent types being represented by central sleep apnea (CSA), obstructive sleep apnea (OSA), and a combined pattern of the two. These conditions are more common in subjects with AHF (Khayat et al., 2015). Additionally, sleep disturbance may be affiliated with depression and anxiety. Thus, an evaluation of the sleep history should be an integrative part of the therapeutic management of HF patients. Epidemiological studies emphasized that CSA and OSA significantly worsen the prognosis in HF (Khayat et al., 2015; Nakamura et al., 2015). Also, OSA accounts for higher risk of incident HF in men (Gottlieb et al., 2010).

Obstructive sleep apnea (OSA) is distinguished by recurrent episodes of collapse of the upper respiratory airways, leading to repetitive apneas or hypopneas, intermittent oxygen desaturations, and nocturnal micro awakenings. The current pandemic of obesity partially explains the increase in OSA prevalence within the general population. Epidemiological data suggested that 4% of middle-aged males and 2% of females suffer from OSA (Young et al., 1993), a disease that increases the overall cardiovascular risk by promoting the emergence of refractory hypertension, oxidative stress, endothelial dysfunction, and increased sympathetic tone (Korcarz et al., 2016). Of note, obesity, diabetes, and metabolic syndrome are frequently linked to OSA (Korcarz et al., 2016a; Korcarz et al., 2016). The mainstay diagnostic test in OSA is represented by an overnight sleep study or polysomnography which records the total number of apneic and hypopneic events. It also enables the quantification of the apnea-hypopnea index (AHI) and therefore the grading of OSA severity into mild, moderate, and severe forms (AHI 5-14, 15-30, and >30 events/hour, respectively) (Lee et al., 2017). Previous studies documented higher rates of cardiac structural or functional abnormalities in subjects with OSA.

Obstructive sleep apnea has negative effects on the cardiovascular system via mechanical, neurohumoral, chemical, and inflammatory mechanisms (Mann et al., 2011). The major occurrences in OSA are represented by an overstated drop in the intrathoracic pressure, hypoxia, and arousal. These lead to a reduced LV filling, pronounced and recurrent increases in systemic blood pressure (BP), and increased sympathetic nervous system activity. The major consequences of the above-mentioned events are represented by myocardial oxygen supply/demand mismatch, enhanced predisposition to acute cardiac ischemia and arrhythmias, and chronically LV hypertrophy, LV enlargement, and ultimately HF (Khattak et al., 2018).

Former studies have estimated that the prevalence of OSA within the HFrEF population ranges from 12% to 53% (Kasai and Bradley, 2011), older age, male sex, increased BMI, and habitual snoring representing major risk factors for OSA (Javaheri, 2006; Yumino et al., 2009; Khattak et al., 2018). Subjects with concomitant HFrEF and OSA declare less daytime sleepiness regardless of shorter sleep duration. In these subjects, Epworth Sleepiness Scale (ESS) does not offer satisfactory results in diagnosing OSA.

In the past decades, several echocardiographic studies sought to assess the prevalence of diastolic dysfunction in OSA subjects with no clinical evidence of HF. However, there is a paucity of information regarding this issue.

Furthermore, no study has evaluated the impact of CPAP therapy on the mortality rates of subjects with OSA and HFpEF, previous data targeting only OSA and HFrEF. Negligible advance has been brought in treating OSA in HFpEF, despite considerable improvements in managing OSA in HFrEF subjects. Subsequently, further research is warranted to assess the impact of CPAP therapy on HF progression as well as survival rates in HFpEF patients with OSA.

Continuous positive airway therapy (CPAP) is deemed the gold standard therapeutic choice in moderate to severe OSA. The major limitations of this device therapy mainly consist of inappropriate subject adherence to and acceptance. As emphasized by Lee et al., only 57% of the subjects diagnosed with moderate to severe OSA initiate CPAP therapy, and only half of them continue to use the device after 1 year (Lee et al., 2017). Optimal CPAP therapy demands more than 4 hours of nightly use. However, up to 83% of subjects on CPAP therapy do not accomplish the advised threshold of 4 hours of nightly use (Weaver and Grunstein, 2008).

The preoccupations related to heart imaging in sleep-related breathing disorder were partially synthesized in the following article:

Sascău R, Zota IM, Stătescu C, Boișteanu D, Roca M, Maștaleru A, Leon Constantin MM, Vasilcu TF, Gavril RS, Mitu F. Review of Echocardiographic Findings in Patients with Obstructive Sleep Apnea. *Can Respir J* 2018; 2018:1206217. **IF:1.803**

<https://www.ncbi.nlm.nih.gov/pmc/articles/PMC6276396/pdf/CRJ2018-1206217.pdf>

3.2. Review of Echocardiographic Findings in OSA

3.2.1. Aim

Moderate and severe OSA is linked to atrial enlargement and affects left ventricular diastolic and systolic functions. This review aimed to emphasize the utility of standard and advanced echocardiographic techniques in the detection of OSA patients at high risk of heart failure and future adverse events.

3.2.2. Materials

We revised the existing literature regarding the importance of echocardiography in OSA subjects evaluation. Echocardiographic screening might increase awareness about the cardiovascular implications of OSA. Additionally, this could complete the current educational, technological, and psychosocial techniques aimed to increase patient compliance to both device therapy and lifestyle changes (Sawyer et al., 2011).

3.2.3. Results and discussion

Left chamber dimensions

Within our analysis, left atrial enlargement was more frequent among subjects with moderate-severe OSA (52,1%) than in those with an apnea-hypopnea index (AHI) <15 (31%, $p < 0.001$) (Holtstrand et al., 2018) and was recorded in 18% of newly diagnosed OSA patients (Baguet et al., 2010). Left atrial diameter appears to be higher in individuals with severe OSA than in those with mild sleep apnea (36.1 ± 5.7 mm versus 32.8 ± 2.3 mm, $p < 0.01$) (Dursunoglu et al., 2005). Previous studies reported that both indexed left atrial volume (LAVI) (Romero-Corral et al., 2007; Altekin et al., 2012; Imai et al., 2015; Varghese et al., 2017) and left atrial area (LAA) (Holtstrand et al., 2018) increase with OSA severity (table XXXI).

Table XXXI. Left atrial volume and area in relationship with OSA severity

Echocardiographic variables		AHI <5 events·h ⁻¹	Mild OSA	Moderate OSA	Severe OSA	p
LAVI (ml/m ²)	Altekin et al., 2012	21.6±4.7	22.2±4.8	27.44±6.9 [†]	32.3±5.1 ^{†‡}	<0.03
	Varghese et al., 2017	28.3±4.1	ND	ND	30.6±3.5	0.02
	Romero-Corral et al., 2007	26.8±11	32.5±15 [†]	30.4±11 [†]		<0.05
	Imai et al., 2015	ND	20.3±4.9		23.3±5.2	<0.0001
LAA (cm ²)	Holtstrand et al., 2018	21.6±4.5		23.7±5.5		<0.001

Abbreviations: LAVI – left atrial volume index. LAA – left atrial area. AHI – apnea hypopnea index. OSA – obstructive sleep apnea. AHI – apnea hypopnea index. OSA – obstructive sleep apnea; † - significantly different from AHI < 5 events·h⁻¹; ‡ - significantly different from mild OSA; ND – not done

Moreover, OSA can lead to the appearance of left ventricular hypertrophy, even in the absence of hypertension, obesity, and diabetes (Dursunoglu et al., 2005; Altekin et al., 2012) (table XXXII). Left ventricular posterior wall (LVPW) thickness, interventricular septum (IVS) thickness, and left ventricular mass (LVM) have higher values in subjects with severe OSA than in patients with moderate and mild OSA (Dursunoglu et al., 2005; Wachter et al., 2013). A study performed in 2016 by Zhou et al. reported a significant difference concerning IVS thickness in subjects with severe and moderate OSA versus controls ($p=0.001$, $p=0.002$ respectively) (Zhou et al., 2016). LVM index significantly increases in patients with severe OSA when compared to controls (Dursunoglu et al., 2005; Baguet et al., 2015), but no statistically significant differences in LV end-systolic and end-diastolic diameters were reported (Dursunoglu et al., 2005; Holtstrand et al., 2018). LVH seems to be associated to mean nocturnal oxygen saturation, which is an independent predictor of left ventricular mass and wall thickness (for every 1% decrease in saturation the authors reported a mass gain of 4.38 g and an increase in wall thickness of 0.14 cm) (Akyol et al., 2016).

Table XXXII. Left ventricular bidimensional parameters in relationship with OSA severity

Echocardiographic variables		AHI <5 events·h ⁻¹	Mild OSA	Moderate OSA	Severe OSA	P
IVSD (cm)	Altekin et al., 2012	0.89±0.09	1.03±0.1	1.03±0.13 †	1.13±0.13 †	<0.05
	Zhou et al., 2016	0.92±0.11	0.97±0.17	1.12±0.16 †	1.14±0.19 †	<0.005
	Dursunoglu et al., 2005	ND	0.99±0.09	1.09±0.13 ‡	1.12±0.11 ‡	≤0.01
	Wachter et al., 2013	1.17±0.16	1.22±0.19 †	1.24±0.18 †		<0.05
	Holtstrand et al., 2018	1.04±0.14		1.07±0.14		0.028
Varghese et al., 2017	1.12±0.12	ND	ND	1.18±0.13	0.05	
Vural et al., 2017	0.95±0.11	0.95±0.11	1.00±0.12	1.01±0.11 †	<0.05	
PWD (cm)	Altekin et al., 2012	0.88±0.07	1.03±0.09 †	1.04±0.12 †	1.11±0.13 †	<0.05
	Dursunoglu et al., 2005	ND	0.98±0.08	1.08±0.09 ‡	1.14±0.09 ‡	≤0.01
	Wachter et al., 2013	1.08±0.14	1.12±0.14 †	1.13±0.14 †		<0.05
	Varghese et al., 2017	1.07±0.11	ND	ND	1.14±0.13	0.05
	Altekin et al., 2012	86.5±18.7	93.2±16.6	94.5±22.9	103.5±22.9 †	<0.05
LVMI (g/m ²)	Varghese et al., 2017	92.4±9.8	ND	ND	98.5±13.5	0.04
	Dursunoglu et al., 2005	ND	100.5±42.3	126.5±41.2 ‡	144.7±39.8 ‡	≤0.002
	Wachter et al., 2013	113±26	119±26	125±29		<0.001
	Imai et al., 2015	ND	107.2±18.5	117.4±19.9		<0.0001
	RWT (cm)	Imai et al., 2015	ND	0.4±0.05	0.4±0.04	

Abbreviations: IVSD – interventricular septum thickness. PWD – posterior wall thickness. LVMI – left ventricular mass index. RWT – relative wall thickness. AHI – apnea hypopnea index. † - significantly different from AHI < 5 events·h⁻¹; ‡ - significantly different from mild OSA; ND – not done

Left ventricular systolic function

Previous information concerning LV ejection fraction (EF) and LV fractional shortening in OSA subjects is controversial and a matter of debate. Several publications reported a normal LVEF (59±10%) among subjects with OSA (Dursunoglu et al., 2005; Wachter et al., 2013), while

other studies stated that there are no significant differences between OSA severity and left ventricular EF or fractional shortening (Dursunoglu et al., 2005; Altekin et al., 2012; Varghese et al., 2017). A study of 411 men, with an average age of 71-years-old, illustrated that LVEF is mildly decreased in subjects with moderate-severe OSA ($61.0\pm 8.9\%$) than in those with an AHI <15 ($62.7\pm 6.3\%$, $p=0.028$) (Holtstrand et al., 2018), while another recent report found that OSA severity is significantly related to a reduction in LVEF ($p=0.005$) (Hammerstingl et al., 2013) (table XXXIII). This observation was further certified by another study of 119 OSA subjects monitored over 18 years, which illustrated that for every tenfold increase in AHI, the left ventricular ejection fraction suffers of a 1.3% independent decrease (Akyol et al., 2016).

Table XXXIII. Left ventricular ejection fraction and OSA severity

Echocardiographic variables		AHI <5 events·h ⁻¹	Mild OSA	Moderate OSA	Severe OSA	p
LV-EF (%)	Hammerstingl et al., 2013	ND	65.0±6.9	59.5±6.9	57.5±5.6	<0.0001
	Holstrand et al., 2018	62.7±6.3	61.0±8.9	ND	ND	0.028

Abbreviations: LV-EF – left ventricular ejection fraction. AHI – apnea hypopnea index. OSA – obstructive sleep apnea; ND – not done;

Left ventricular diastolic dysfunction

Experimental studies based on artificially induced OSA in a canine model (Brooks et al., 1997) have demonstrated that each hypoxic event alters LV diastolic function by increasing left ventricular afterload and that LV systolic dysfunction emerges within 3 months. OSA-induced systolic and diastolic dysfunction appears to follow an analogous model in humans, although it typically develops in a much longer period. It commonly starts by affecting the diastolic function, and it ends with LV systolic impairment after prolonged exposure (>10 years) (Parker et al., 1999; Yang et al., 2012). Yang et al. suggested that nocturnal minimum oxygen saturation $<70\%$ is an independent surrogate of diastolic dysfunction (OR=4,34, $p=0.02$) (Yang et al., 2012).

A study from 2016 indicated that almost 44% of OSA subjects with normal biventricular systolic function present with various degrees of diastolic dysfunction (Korcarz et al., 2016). Wachter et al. showed that diastolic dysfunction prevalence ranges from 56.8% among subjects with mild OSA to 69.7% in the moderate-to-severe OSA group ($p=0.002$) (Wachter et al., 2013). Baguet et al. found that 22.7% of the newly diagnosed OSA patients had an impaired LV relaxation pattern at the Doppler echocardiographic assessment of the mitral inflow (Baguet et al., 2010). It appears that an increased AHI is linked to a decreased mitral E wave (Dursunoglu et al., 2005) and an increased mitral A wave velocities (Dursunoglu et al., 2005; Holtstrand et al., 2018) (table XXXIV).

Varghese et al. did not report any significant difference concerning mitral E/A ratio in subjects with severe OSA (1.1 ± 0.2) when compared to controls (1.2 ± 0.2 , $p=0.09$) (Varghese et al., 2017). Other studies illustrated that the E/A ratio directly decreases with OSA severity (Dursunoglu et al., 2005; Imai et al., 2015; Vural et al., 2017). Conversely, other authors stated that a significantly lower E/A ratio can be noticed in subjects with mild OSA ($p=0.0009$), but not in those with moderate or severe forms of disease (Altekin et al., 2012).

According to the results of Altekin et al., E wave deceleration time (E-DecT) has higher values in subjects with OSA than in healthy volunteers, but no significant differences concerning E-DecT were reported among subjects with different degrees of OSA severity (Altekin et al., 2012). A similar pattern was illustrated for LV isovolumic relaxation time (IVRT) (Altekin et al., 2012) and it appears that both E-DecT and IVRT positively correlate with AHI (Dursunoglu et al., 2005). Other studies have identified significant differences regarding E-Dec and IVRT among OSA patients (table XXXIV).

Left ventricular Tei-index (LV-MPI), as an indicator of both systolic and diastolic function, is higher in subjects with severe sleep apnea (0.64 ± 0.14) than in those with mild OSA (0.50 ± 0.09 ; $p<0.01$) (Dursunoglu et al., 2005) or to controls (Altekin et al., 2012), being a valuable surrogate of LV dysfunction (Fung et al., 2002; Dursunoglu et al., 2005). Only two studies supported the existence of a positive correlation between LV-MPI and AHI ($p<0.001$, $r = 0.825$) (Dursunoglu et al., 2005) and ($p=0.02$, $r=0.27$) (Romero-Corral et al., 2007), while others reported no significant difference regarding LV-MPI between subjects with severe OSA and controls ($p=0.12$) (Varghese et al., 2017) (table XXXV).

Therefore, conventional Doppler echocardiography yields conflicting results concerning OSA consequences on left ventricular diastolic function. Several Doppler parameters are not suitable for use in subjects with atrial fibrillation, while others are influenced by heart rate and blood pressure, or present age-dependency. The need for a more comprehensive echocardiographic analysis has been acknowledged by current international imaging guidelines, which have incorporated tissue Doppler imaging (TDI) in the diagnostic workup of LV diastolic dysfunction (Nagueh et al., 2016).

Table XXXIV. Left ventricular diastolic function in relationship with OSA severity

Echocardiographic variables		AHI <5 events·h ⁻¹	Mild OSA	Moderate OSA	Severe OSA	p
E velocity (cm/s)	Dursunoglu et al., 2005	ND	92±12	77±24	61±13	0.01
A velocity (cm/s)	Dursunoglu et al., 2005	ND	67±25	105±90	87±14	0.01
	Vural et al., 2017	75.1±20.9	78.3±21.5	76.9±13.8	86.2±17.8 [†]	<0.05
E/A ratio	Dursunoglu et al., 2005	ND	1.37±0.02 [†]	0.73±0.01 [‡]	0.70±0.01 [‡]	0.01
	Imai et al., 2015	ND	1.38±0.45		1.03±0.39	<0.0001

	Vural et al., 2017	1.0±0.3	1.0±0.3	1.0±0.3	0.8±0.2 †	<0.05
	Altekin et al., 2012	1.19±0.24	0.96±0.16†	1.01±0.3	1.11±0.28	0.009
DecT (ms)	Altekin et al., 2012	163±26.2	227.4±31.1 †	216.4±60.4†	199.4±39.5 †	<0.001
	Dursunoglu et al., 2005	ND	170.1±20.9	210.0±47.7	240.1±57.7	0.01
	Imai et al., 2015	ND	187.1±33.7		198.4±36.6	0.003
	Vitarelli et al., 2013	143±14	175±17	ND	229±15 †	0.004
	Oliveira et al., 2009	ND	189.2±34.5	231.8±45.2	247.6±48.2 ‡	<0.05
IVRT (ms)	Altekin et al., 2012	88.3±12.5	106.3±12.8†	108.8±12.9	113.2±10.4 †	<0.001
	Vitarelli et al., 2013	74±11	103±9	ND	125±10 †	0.004
	Fung et al., 2002	92.7±16.6			106.4±19.1	0.005
	Dursunoglu et al., 2005	ND	72.0±12.6	100.2±13.7 ‡	125.5±13.1 ‡	0.01

Abbreviations: DecT – deceleration time. IVRT – isovolumic relaxation time. AHI – apnea hypopnea index. OSA – obstructive sleep apnea; † - significantly different from AHI < 5 events·h⁻¹; ‡ - significantly different from mild OSA; ND – not done

Table XXXV. Left ventricular myocardial performance index in relationship with OSA severity

Echocardiographic variables		AHI <5 events·h ⁻¹	Mild OSA	Moderate OSA	Severe OSA	p
LV MPI	Dursunoglu et al., 2005	ND	0.50±0.09	0.60±0.10 ‡	0.64±0.14 ‡	0.01
	Altekin et al., 2012	0.46±0.08	0.48±0.08	0.55±0.06†	0.6±0.13†‡	<0.05
	Vitarelli et al., 2013	0.39±0.08	0.43±0.07	ND	0.58±0.09 †	0.039

Abbreviations: LV-MPI – left ventricular myocardial performance index. AHI – apnea hypopnea index. OSA – obstructive sleep apnea; † - significantly different from AHI < 5 events·h⁻¹; ‡ - significantly different from mild OSA; ND – not done

TDI appears to identify slight alterations in systolo-diastolic ventricular function, even in subjects with an EF within normal ranges. However, it is limited by its angle-dependence, by the necessity of acquiring high frame rate imaging, and by the effect of myocardial translation and tethering forces. LV-S' wave velocity is an indirect surrogate of systolic function. Previous reports

emphasized no significant difference in what concerns LV-S' wave velocity among patients with OSA and controls (Altekin et al., 2012; Zhou et al., 2016), similar to the studies focused on evaluating LV-EF in OSA.

Wachter et al. stated that only tissue Doppler-derived parameters (and not mitral inflow pattern) are significantly different in sleep apnea and that lateral e' is considerably lower in patients with $AHI \geq 15$ (7.4 ± 2.1) than in controls (8.3 ± 2.6) (Wachter et al., 2013). Varghese et al. found that patients with severe forms of obstructive sleep apnea ($AHI > 40$) display lower e' velocities than controls (Varghese et al., 2010), analogous findings being stated by several other authors (table XXXVI).

Multiple studies emphasized that E/e' mean ratio, an indicator of LV end-diastolic pressures, has higher values in patients with moderate-severe OSA than in controls (Oliveira et al., 2009; Varghese et al., 2010; Oliveira et al., 2012; Altekin et al., 2012; Wachter et al., 2013;) and positively corresponds to AHI ($r=0.202$, $p=0.014$) (Vural et al., 2017). As E/E' is also related to the amount of myocardial fibrosis, Altekin et al. stated that fibrosis, together with increased LV filling pressures favor subclinical LV systolic dysfunction in OSA patients (Altekin et al., 2012). Average A' wave velocity and LA volumes (precontraction, maximum and minimum volumes measured in 3D echocardiography) have higher values in subjects with severe OSA, contrary to E'/A' ratio, which decreases with OSA severity (Oliveira et al., 2009).

OSA impact on right chambers

Sanner et al. emphasized that right ventricular failure is more prevalent in subjects with OSA irrespective of the presence of any other respiratory conditions (Sanner et al., 1997). Previous studies demonstrated that right atrial volume index (RAVI) is increased in subjects with severe OSA than in those with mild OSA or controls (Altekin et al., 2012).

The Framingham Study did not identify any difference concerning right ventricular (RV) volumes, end-diastolic dimensions, and systolic function between subjects with sleep-disordered breathing and controls (Guidry et al., 2001). The systolic and diastolic volumes of RV cannot be accurately evaluated via 2D echocardiography because of its complex anatomical shape. RV fractional area change and MPI are indicators of RV global function, while other echocardiographic parameters such as TAPSE and S' have the major disadvantage of providing only a partial description of RV systolic performance (Venkatachalam et al., 2017).

Table XXXVI. Left ventricular tissue Doppler parameters in patients with OSA

Echocardiographic variables		AHI <5 events·h ⁻¹	Mild OSA	Moderate OSA	Severe OSA	p
E' (cm/s)	Imai et al., 2015	ND	10.7±3.0		8.7±1.9	<0.0001
	Varghese et al., 2017	10.6±1.1	ND	ND	9.2±2.1	0.01

	Vural et al., 2017	11.6±1.5	9.6±1.7	6.3±1.1 †‡	6.1±1.4 †‡	<0.05
	Oliveira et al., 2009	ND	7.7±1.5	7.3±2.0	6.2±1.8 ‡*	<0.05
	Vitarelli et al., 2013	12.1±2.2	11.4±2.1	ND	7.7±2.8 †	0.016
E/E'	Altekin et al., 2012	6.88±1.7	6.91±1.9	8.56±2.37	10.29±1.48 †,‡,*	<0.001
	Wachter et al., 2013	11.0±3.6	11.7±3.5	12.7±5.3 †		<0.05
	Imai et al., 2015	ND	7.6±2.2		7.8±2.3	0.04
	Varghese et al., 2017	8.44±1.6	ND	ND	9.69±2.6	0.03
	Altekin et al., 2012	8.13±2.22	8.62±2.68	11.31±2.87 †‡	13.89±2.32 †,‡,*	<0.05
	Vural et al., 2017	6.5±1.2	8.4±2.4 †	11.9±2.2 †‡	12.0±2.8 †‡	<0.05
	Vitarelli et al., 2013	5.6±1.6	5.5±1.8	ND	8.8±2.5 †	0.025
	Oliveira et al., 2009	ND	9.7±1.9	10.4±3.1	11.6±3.6 ‡*	<0.05
	Oliveira et al., 2012	9.4±2.9	10.6±3.0			0.02
A' (cm/s)	Oliveira et al., 2009	ND	6.1±1.4	6.8±1.7	8.2±1.9 ‡*	<0.05
E'/A'	Oliveira et al., 2009	ND	1.3±0.4	1.1±0.3	0.8±0.3 ‡*	<0.05

Abbreviations: AHI – apnea hypopnea index. OSA – obstructive sleep apnea; † - significantly different from AHI < 5 events·h⁻¹; ‡ - significantly different from mild OSA; * - significantly different from moderate OSA; ND - not done

It was stated that satisfactory RV volume estimations can be attained only via 3D technique. Studies assessing RV volume through the help of 3D echocardiography concluded that subjects with moderate-severe OSA have higher indexed RV end-diastolic and end-systolic volumes compared to controls (p<0.05) (Oliveira et al., 2012; Güvenç et al., 2016). While some analyses indicated that RV-EF is similar between patients with and without OSA (Buonauro et al., 2017), others have described a minor, but statistically significant difference in RV-EF (table XXXVII) (Oliveira et al., 2012).

Table XXXVII. Right atrial and ventricular parameters in relationship with OSA

Echocardiographic variables		AHI <5 events·h ⁻¹	Mild OSA	Moderate OSA	Severe OSA	p
AVI (ml/m ²)	Altekin et al., 2012	15.56±4.94	17.31±6.24	21.89±7.91	28.85±7.97 †‡	<0.05
RVESV index (ml/m ²)	Güvenç et al., 2016	22.15±3.85	ND	26.50±8.11		0.01
	Oliveira et al., 2012	15.4±3.6	18.7±4.3			<0.05

RVEDV index (ml/m ²)	Güvenç et al., 2016	41.48±6.45	ND	48.15±11.48		0.009
	Oliveira et al., 2012	49.9±6.0		52.2±7.3		0.02
RV-EF (%)	Oliveira et al., 2012	68.4±5.9		64.3±6.8		<0.01
TAPSE (mm)	Altekin et al., 2012	24.76±1.55	22.30±2.39	21.11±1.56 †	19.42±1.64 †‡*	<0.05
	Zakhama et al., 2016	ND	ND	26.1±3	22.7±4	0.012
RV MPI	Romero-Corral et al., 2007	0.23±0.10	0.26±0.16 †	0.37±0.11 †		<0.05
	Altekin et al., 2012	0.43±0.09	0.46±0.09	0.53±0.08 †	0.56±0.11 †‡	<0.05
	Shivalkar et al., 2006	0.25 ± 0.03		0.29 ± 0.05		0.008
	Zakhama et al., 2016	0.46±0.14		0.55±0.12		0.024
S'RV (cm/s)	Shivalkar et al., 2006	13.5±1.8		11.4±2.3		<0.001
	Zakhama et al., 2016	14.5±3		12.2±2		<0.001
RV E/E'	Güvenç et al., 2016	3.83±1.16	ND	5.23±2.58		0.008
	Altekin et al., 2012	4.19±1.22	4.37±1.22	5.77±1.27 †‡	7.12±2.29 †‡	<0.05

Abbreviations: RAVI – right atrial volume index. RVESV – right ventricular end systolic volume. RVEDV – right ventricular end diastolic volume. RV-EF – right ventricular ejection fraction. TAPSE – tricuspid annular plane excursion. RV-MPI – right ventricular myocardial performance index. AHI – apnea hypopnea index. OSA – obstructive sleep apnea: † - significantly different from AHI < 5 events·h⁻¹; ‡ - significantly different from mild OSA; * - significantly different from moderate OSA; # - significantly different in OSA compared to controls; ND - not done

A strong association between AHI, RV diameter ($r=0.482$, $p=0.0009$) (Shivalkar et al., 2006) and RV-EF ($r=-0.362$, $p=0.02$) (Güvenç et al., 2016) was also reported. RV wall thickness is greater in patients with more severe types of OSA (0.78 ± 0.02 versus 0.68 ± 0.02 , $p=0.005$) (Guidry et al., 2001) and it appears to be related to AHI ($r=0.356$, $p=0.026$) (Güvenç et al., 2016).

While Wachter et al. did not identify a significant reduction in the right ventricular Tei index (RV-MPI) values in individuals with severe sleep apnea (Wachter et al., 2013), another study demonstrated a significant difference in RV-MPI between controls and persons with moderate and severe OSA (Romero-Corral et al., 2007) and also emphasized a positive correlation between RV-MPI and AHI ($r=0.40$, $p=0.002$) (Romero-Corral et al., 2007).

These results are supported by the results of other studies, highlighting that RV-MPI is significantly higher in OSA subjects than in controls (but not between those with mild-moderate versus severe OSA) (Altekin et al., 2012; Zakhama et al., 2016).

It appears that an increase in AHI has a greater impact on RV global function than on the LV one (Altekin et al., 2012). The authors concluded that OSA-induced RV dysfunction may promote the subsequent development of LV dysfunction via ventricular interdependence (Altekin et al., 2012).

As stated above, 2D echocardiographic parameters used for evaluating global RV function are represented by tricuspid annular plane systolic excursion (TAPSE), myocardial performance index, and RV fractional area change (RV-FAC) (Altekin et al., 2012). Of note, tissue Doppler imaging is more sensitive in identifying subclinical RV dysfunction when compared to 2D echocardiography (Altekin et al., 2012).

While the RV E/A ratio does not significantly vary in individuals with moderate-severe OSA living at high altitudes compared to healthy controls, RV E/E' ratio appears to have significantly higher values in the OSA group (Güvenç et al., 2016).

A study performed in 2012 by Altekin et al., did not reveal any differences regarding RV A wave velocity or PAP, but reported that E wave deceleration time, A' velocity, and E/E' ratio were higher in individuals with severe OSA compared to controls and patients with mild OSA (Altekin et al., 2012). TAPSE, E' wave velocity and RV E/A ratio had lower values in patients with moderate-severe OSA than in the control and mild OSA groups (Altekin et al., 2012).

Data regarding the consequences of OSA on RV S' are debatable, with some authors stating that there are no significant differences between individuals with and without OSA (Dobrowolski et al., 2016), and others reporting contrary results (Zakhama et al., 2016), highlighting a significant correlation between AHI and RV S' (Shivalkar et al., 2006). While two recent studies did not reveal a significant difference of TAPSE between subjects with and without OSA (Dobrowolski et al., 2016; Ozkececi et al., 2016), a recent report documented the presence of a correlation between TAPSE and AHI ($r=-0.285$, $p=0.079$) (Güvenç et al., 2016).

Pulmonary hypertension

Epidemiological studies emphasized that the prevalence of pulmonary hypertension (PH) among patients with OSA varies between 12% and 70%. PH prevalence mostly relates to OSA severity, pulmonary artery pressure (PAP) assessment method, the moment of evaluation, and other possible confounding factors.

It is usually assessed via the modified Bernoulli equation which estimates pulmonary artery systolic pressure (PASP) (Ozkececi et al., 2016). Of note, other formulas have been suggested for estimating mean PAP in subjects without tricuspid insufficiency (Dabestani et al., 1987).

While Altekin et al. (Altekin et al., 2012) reported no significant differences between PASP or mean PAP among subjects with different grades of OSA severity and controls, other studies displayed that subjects with moderate and severe OSA have higher PASP than healthy volunteers (Shivalkar et al., 2006; Zhou et al., 2016) (table XXXVIII). Additionally, PASP was significantly higher in subjects with moderate-severe OSA living at high altitudes than in controls ($p=0.002$) (Güvenç et al., 2016). Pulmonary acceleration time appears to be significantly reduced in patients

with moderate-severe OSA living at high altitudes versus controls ($p=0.001$) and to be directly related to AHI ($r=-0.282$, $p=0.077$) (Güvenç et al., 2016).

Table XXXVIII. Pulmonary hypertension parameters in relationship with OSA severity

Echocardiographic variables		AHI <5 events·h ⁻¹	Mild OSA	Moderate OSA	Severe OSA	p
PAPS (mmHg)	Güvenç et al., 2016	30.94±6.47	ND	38.35±8.6		0.002
	Zhou et al., 2016	16.7±6.2	18.2±6.6	31.2±5.6 †	32.8±6.7 †	<0.05
	Shivalkar et al., 2006	22±8	32±10			0.004
PAT (ms)	Güvenç et al., 2016	118.36±16.36	ND	103.13±18.42		0.001

Abbreviations: PAPS – pulmonary artery systolic pressure. PAT – pulmonary artery acceleration time. AHI – apnea hypopnea index. OSA – obstructive sleep apnea.; † - significantly different from AHI < 5 events·h⁻¹; ND - not done

Pulmonary artery (PA) stiffness is linked to both AHI and mean oxygen saturation and is defined as the ratio between pulmonary artery maximal frequency shift and pulmonary acceleration time (Ozkececi et al., 2016).

A previous study emphasized that patients with OSA exhibit increased PA stiffness even in the absence of pulmonary hypertension.

Additionally, the authors of this study suggested that PA stiffness is a more reliable measure when compared to PAP in subjects with OSA (Ozkececi et al., 2016).

Other parameters

Epicardial fat thickness, as an indirect surrogate of visceral adiposity, has considerably higher values in subjects with moderate or severe OSA (AHI>15).

Previous research demonstrated that 24 weeks of CPAP therapy produces a significant decrease of epicardial fat thickness, irrespective of any changes in BMI or waist circumference (Dabestani et al., 1987).

Another study from 2018 performed on subjects with heart failure (LVEF <45%) demonstrated that epicardial fat thickness was significantly higher in subjects with sleep disordered breathing when compared to subjects without sleep apnea ($10.7±2.8$ vs. $8.13±1.8$; $p = 0.001$) (Parisi et al., 2018).

According to the results of a study conducted by Kohler et al., OSA is more frequent among patients with Marfan syndrome and the aortic root diameter is about 0.8 cm higher in OSA subjects ($p<0.0001$), indicating therefore that OSA might promote aortic root enlargement in these patients (Kohler et al., 2009).

Speckle tracking echocardiography

As opposite to tissue Doppler imaging, two-dimensional speckle tracking echocardiography is not angle-dependent. Moreover, both global and segmental systolic functions are more accurately evaluated via speckle tracking imaging. Patients with severe forms of OSA exhibit significantly decreased global longitudinal strain values when compared to the other groups of patients (Altekin et al., 2012). Additionally, significant differences regarding basal, mid, and apical strain values have been emphasized between patients with severe forms of OSA and all other groups (Altekin et al., 2012). Other studies supported that global left ventricular longitudinal strain is decreased in patients with very severe OSA (Varghese et al., 2017). In 2017, Varghese et al. indicated that apical and middle LV segments display more severe longitudinal strain impairment (table XXXIX), while circumferential strain does not significantly vary between patients with very severe OSA and controls (Varghese et al., 2017). An epicardial-to-endocardial strain gradient at each myocardial level has been reported by Zhou et al (Zhou et al., 2015). In their study, only longitudinal (and not circumferential) strain was directly related to AHI. Additionally, subjects with severe forms of OSA exhibited decreased three-layer longitudinal LV strain, despite normal ejection fraction (Zhou et al., 2015).

Table XXXIX. Left and right ventricular strain parameters in subjects with OSA

Echocardiographic variables		AHI <5 events·h ⁻¹	Mild OSA	Moderate OSA	Severe OSA	p
LV GLS (%)	Varghese et al. 2017	-19±1.6	ND	ND	-15±1.8	<0.01
	Vural et al., 2017	-22.3±4.0	-20.0±2.3	-17.2±2.0 †	-15.6±5.6 †‡	<0.05
	Vitarelli et al. 2013	-21.9±2.8	-21.2±2.5	ND	-18.4±2.7 †	0.011
	Altekin et al. 2012	-25.6±2.2	-23.9±3.9	-21.3±2.6 †‡	-16.9±2.7 †‡*	<0.03
LS basal strain (%)	Varghese et al. 2017	-17±1.7	ND	ND	-15±1.9	0.02
	Altekin et al. 2012	-21.4±1.9	-19.9±2.4	-18.4±2.6 †	-15.3±2.9 †‡*	<0.03
LS mid strain (%)	Varghese et al. 2017	-18±1.8	ND	ND	-15±2.3	<0.01
	Altekin et al. 2012	-23.3±2.1	-21.5±2.4	-19.7±2.6 †	-16.9±2.9 †‡*	<0.03
LS apical strain (%)	Varghese et al. 2017	-20±1.7	ND	ND	-16±2.5	<0.01

	Altekin et al. 2012	-27.4±3.7	-24.6±2.9	-23.5±3.9 [†]	-19.2±3.9 ^{†,‡,*}	<0.03
LV radial strain (%)	Vural et al., 2017	45.7±6.1	44.4±7.7	39.8±7.8 [†]	39.8±8.9 [†]	<0.05
LV circumferential strain (%)	Vural et al. 2017	-21.6±3.5	-21.2±1.8	-19.3±2.8 [†]	-18.8±2.7 [†]	<0.05
LV apical rotation °	Vural et al. 2017	8.6±1.0	8.7±1.7	9.1±1.1	7.4±1.3 ^{†,‡,*}	<0.05
LV torsion °	Vural et al. 2017	15.6±1.5	16.1±1.9	16.5±1.6	14.8±1.6 ^{‡,*}	<0.05
2D global RV SI	Hammerstingl et al., 2013	ND	-21.5±6.3	-14.3±5.3	-14.5±8.2	<0.0001
	Buonauro et al. 2017	22.8±3.3	20.9±4.9			<0.05
2D apical RV SI	Hammerstingl et al., 2013	ND	-17.3±8.7	-9.8±6.0	-6.3±5.7	<0.0001
2D basal RV SI	Hammerstingl et al., 2013	ND	-27.4±13.6	-18.2±8.7	-21.6±14.9	0.03
RV strain (%)	Altekin et al. 2012	-34.05±4.29	-31.4±5.37	-22.75±4.89 ^{†,‡}	-20.89±5.59 ^{†,‡}	<0.05
RV systolic strain rate	Altekin et al. 2012	-2.93±0.64	-2.85±0.73	-2.06±0.43 ^{†,‡}	-1.43±0.33 ^{†,‡,*}	<0.05
RV early diastolic strain rate	Altekin et al. 2012	2.38±0.63	2.32±0.84	1.66±0.55 [†]	1±0.54 ^{†,‡}	<0.05
RV late diastolic strain rate	Altekin et al. 2012	2.25±0.33	2.32±0.54	2.79±0.66 [†]	3.29±0.54 ^{†,‡}	<0.05

Abbreviations: LV GLS – left ventricular global longitudinal strain. LS basal – left ventricular basal longitudinal strain. LS mid - left ventricular longitudinal strain in medium segments. LS apical - left ventricular apical longitudinal strain. LV – left ventricular. 2D global RV SI – bidimensional global right ventricular strain index. 2D apical RV SI - bidimensional apical right ventricular strain index. 2D basal RV SI - bidimensional basal right ventricular strain index. RV – right ventricular. AHI – apnea hypopnea index. OSA – obstructive sleep apnea; † - significantly different from AHI < 5 events·h⁻¹; ‡ - significantly different from mild OSA; * - significantly different from moderate OSA; ND – not done

Diastolic dysfunction is commonly connected to abnormal GLS even in the presence of normal LVEF and LV volumes (Park et al., 2008). Longitudinal myocardial fibers, mainly situated in the subendocardium, are susceptible to fibrosis, this process leading to decreased longitudinal shortening, with a compensatory increase in circumferential shortening and torsion (Wang et al., 2008). LV torsion is defined as the twist of the ventricle around its long axis, given by the antagonistic rotation of the basal and apical segments (Vural et al., 2017). Increased LV torsion is

an early marker of left ventricular dysfunction in patients with normal LVEF. There is a literature disagreement regarding LV torsion in OSA patients. Vural et al. indicated that LV torsion is reduced in subjects with $AHI > 30$ and in controls when compared to patients with mild or moderate sleep apnea (Vural et al., 2017). Vitarelli et al. documented a significant increase in LV torsion in severe sleep apnea versus controls (Vitarelli et al., 2013).

According to Vural et al., left atrial strain rate values are significantly higher in subjects with severe OSA and a positive relationship exists between AHI and LA contractile strain, which can be partially improved following 12 weeks of CPAP therapy (Vural et al., 2017). While standard tissue Doppler imaging is influenced by tethering forces and myocardial translational motion, 2D speckle tracking imaging (2D-STE) is not affected by Doppler beam angling or load dependency and delivers a more precise evaluation of RV function.

RV radial function study is prone to major errors because of the anterior position of the RV in the parasternal views and frequent artifacts. For these reasons, RV longitudinal strain and strain rate values are preferred (Altekin et al., 2012). Of note, strain and strain rate assessment of the RV should only focus on the RV free wall as the interventricular septum motion is under the greater influence of the left ventricle (Jurcut et al., 2010; Leung, 2010).

To conclude, the effect of OSA on RV function is controversial. Hammerstingl et al. illustrated that RV global, apical, and basal longitudinal strains are linked to the degree of OSA severity (Hammerstingl et al., 2013). However, following multivariate regression analysis, it appears that only apical RV longitudinal strain is independently connected with severe sleep apnea (Hammerstingl et al., 2013). The results of this study indicate that apical RV longitudinal strain is a sensitive indicator of subclinical RV dysfunction (Wachter et al., 2013). On the other hand, additional studies failed to identify any significant difference regarding segmental RV strain and strain rate between patients with moderate-severe OSA and controls (Güvenç et al., 2016). Individuals with moderate-severe OSA exhibit lower RV strain and RV systolic strain values than controls or subjects with $AHI < 15$ (Altekin et al., 2012). RV early diastolic strain rate decreases with disease severity, while RV late diastolic strain rate increases with AHI (Altekin et al., 2012). Additionally, 2D speckle tracking parameters correlate better with AHI than any other echocardiographic parameter and should be employed in detecting early, subclinical RV dysfunction (Altekin et al., 2012). This characteristic is consistent with the results of Buonauro et al. who have illustrated that subclinical RV dysfunction can be identified through the help of speckle tracking echocardiography (Buonauro et al., 2017).

3.2.4. Conclusions

Moderate and severe forms of OSA are correlated with impaired biventricular function and atrial enlargement and thus with a high incidence of chronic heart failure and atrial fibrillation. 2D-STE has the advantage of not being influenced by Doppler beam angling or load dependency. Abnormal strain values, a surrogate of subclinical systolo-diastolic dysfunction, can be recorded even in subjects with normal EF and chamber volumes. Nevertheless, the role of 2D-STE in OSA patients should be addressed by further studies, as current information yields contradictory results.

SECTION III. FUTURE DEVELOPMENTS IN THE ACADEMIC, PROFESSIONAL AND RESEARCH FIELD

III.1. DEVELOPMENTS IN THE ACADEMIC AREA

Although XXIth century is defined by major changes in science, technologies, education and medicine, the teaching act has become a problem of modern European society, epitomized in specific strategies and objectives.

The responsibility to perpetually redefine the role of the educator and his training according to the new requirements is more than justified. The decrease in the number of young people attracted to the teaching career, doubled by a visible decline in the quality of the pedagogical act are only few of the countless dysfunctions.

The general objectives of my future activity are represented by the acquisition of new skills, knowledge and competences, through a permanent training. I intend to develop a solid expertise in the field of cardiology, as well as in adjacent areas (internal medicine, neurology, nephrology, nutrition diseases, epidemiology, health management) for a better interdisciplinarity.

As a natural consequence, I will follow the applicability and the consolidation of all my skills and acquired knowledge. I also intend to further build a successful academic career, through motivation and hard-work.

My real development approaches in the teaching career can be summarized as follows:

- Improving the teaching act through a permanent training in accordance with the newest developments in the field;
- Development of medical education in cardiology;
- Elaboration of new course materials in Cardiology and Methodology of Documentation and Scientific Research, in accordance with the latest achievements in the field;
- New approaches of the student-teacher relationship in order to make the teaching process more efficient, to promote values and to motivate students to study internal medicine and to understand its practical importance and applicability for their future medical career;
- Orientation of teaching and learning activities toward each student, focusing on their developmental stage;
- Use of strategies based on active participation;
- Implementation of innovative techniques in order to ensure a high-quality medical education;
- Organizing and participating in students' research activity;
- Coordination of undergraduate work.

I will constantly ensure that the evaluation of students' professional activity is accurate, reflecting their real level of professional development.

Therefore, implementing new and more attractive educational approaches will inspire students for knowledge. In this context, I attempt to constantly update the courses designed for students and ensure that they are periodically evaluated by various assessment methods.

I also intend to organize series of workshops for both students and residents based on my previous experience.

Practice is a major component in successfully teaching cardiology and medical simulation plays an increasingly significant role in the education of medical students and residents, as it certifies a comprehensive and standardized training experience for all learners.

The use of simulation in cardiology will provide medical students and residents the opportunity to acquire self-confidence, knowledge, skills, and workplace behaviors.

In my academic position, I will manage the didactic process as best as I can by developing suitable undergraduate, graduate and postgraduate curricula for students, residents and specialists. I plan to collaborate with my younger colleagues, to train them and therefore to improve my teaching skills and keep on learning.

I will also continue to improve my research competences by applying for funding and writing articles for peer-reviewed journals. I will periodically organize sessions of case presentations, allowing the interns to develop the ability to speak in public and to present clinical cases in a comprehensible manner.

III.2. FUTURE PROFESSIONAL IMPROVEMENT

In my specialty, the teaching activity cannot be separated from the medical one, therefore it is essential for me to constantly develop my clinical abilities. Being a cardiologist is a challenge, the fast evolution of technology and knowledge requiring a continuously training in this environment.

I intend to be present at national and international conferences and stay informed with regard to the latest findings in cardiology field. Workshop events, training courses, experience changes, partnerships with disciplines from other departments of our university, universities from our country and from abroad will provide the basis for my continuous individual training in the field of cardiology.

III.3. PERSPECTIVES FOR RESEARCH FIELD

The main objectives of my future scientific activity are to pursue and to expand the research carried out during my doctoral studies, to continue with the research projects I have already initiated, as well as to begin new ones. The results of these studies will be materialized in scientific papers.

Additional objectives are represented by obtaining financing for new research projects through UEFISCDI grants, by active participation through oral presentations and posters at national and international conferences in the field, by publication of specialized books in recognized publishing houses.

Currently, I intend to extend my clinical research preoccupations into three major research directions:

Cardiovascular rehabilitation in post-myocardial infarction patients treated by percutaneous coronary intervention - the study of clinical and paraclinical changes.

Myocardial infarction remains a pathology of great interest due to its poor prognosis, the optimization of the multimodal management being in the attention of the medical world, with emphasis in recent decades on the benefits of cardiac rehabilitation (Heran et al., 2015).

Cardiovascular rehabilitation involves a multidisciplinary program that includes components such as: clinical evaluation, optimization of drug treatment, physical training, psychological and nutritional support, reduction of risk factors for coronary heart disease, lifestyle change and patient education, each of them with a distinct role in attaining benefits (Ryszard, and Jadwiga, 2008).

The cardiovascular rehabilitation program offers cardioprotection through anti-inflammatory, antithrombotic, antiatherogenic, antiarrhythmic, and antiischemic action and also by increasing the success rate on the control of risk factors (Byrkjeland et al., 2015; Bush et al., 2020). The favorable impact on left ventricular remodelling has also been shown, with many published data reporting that in patients with left ventricular dysfunction, physical training prevents the evolution of post-ischemic remodelling (Zhang et al., 2016; Kirolos et al., 2019).

Initial studies focused on cardiovascular rehabilitation in patients with chronic heart failure, but recently, the interest has been directed to its role in ischemic heart disease. There are only few studies in the literature that have specifically evaluated the role of cardiovascular recovery in patients with acute myocardial infarction treated by percutaneous coronary angioplasty (Malfatto et al., 2017). There is clear evidence that cardiovascular rehabilitation leads to a decrease in the number of major cardiovascular events and of hospitalizations and an increase in the quality of life (Bush et al., 2020; de Bakker et al., 2020).

Physical exercise is a crucial component, recommended by both American College of Cardiology and European Society of Cardiology for secondary prevention in post-myocardial infarction (class I, level of evidence A). Cardiac rehabilitation has proven a favorable cost-effectiveness ratio, being considered as a standard post-myocardial infarction therapy along with thrombolytic and lipid-lowering medication (Lawler et al., 2011; Beauchamp et al., 2020).

Despite guidelines recommendation, reference and participation rates in cardiovascular rehabilitation programs are significantly low. Current evidences indicate that only 13.9% of all hospitalized patients with acute myocardial infarction were included in recovery programs. The low accessibility to specialized units and the costs are considered major shortcomings (Pothineni et al., 2011).

Precisely, our study will aim an optimization of the multimodal management of the patient with uncomplicated myocardial infarction. The purpose will be to highlight the benefit of complete cardiovascular rehabilitation programs. Consequently, we intend to catch the attention of cardiologists, so that all patients that have experienced an acute coronary event will be directed to specialized cardiac recovery centers in order to maximize therapeutic intervention.

The echocardiographic evaluation of the patients will be performed using multiple techniques. Conventional 2D and Doppler ultrasound will assess the size, volumes and contents of

the heart cavities, the thickness of the myocardial walls and left ventricular mass, the morphology of the heart valves, motility of the cusps and transvalvular blood flow. Biventricular systolic function will be assessed by 2D echocardiography (left ventricular ejection fraction, tricuspid annular plane systolic excursion), tissue Doppler (longitudinal systolic myocardial velocities), 2D Speckle-Tracking ultrasound (global longitudinal strain).

The diastolic function of the left ventricle will be investigated with the help of the following indices: mitral peak E wave velocity, E/A ratio, E velocity DT, E/e' ratio, systolic-to-diastolic pulmonary venous flow velocity ratio, peak velocity of tricuspid regurgitation, left atrial volume index. Left ventricle torsion will be evaluated using 2D Speckle-Tracking ultrasound (maximum apical rotation, maximum basal rotation and time intervals until they are obtained, maximum LV torsion and time interval until it is reached, corrected LV torsion, rate / peak velocity LV torsion, LV detorsion rate / LV diastolic torsion velocity and time intervals until they are reached). LV deformation analysis will be performed using 2D Speckle-Tracking ultrasound techniques (global longitudinal strain, global radial strain, global circumferential strain, segmental strain, global strain area and strain rate).

The cardiovascular examination will include anamnesis, clinical examination, electrocardiogram, ABPM monitoring and 24-hour Holter ECG. The quality of life will be assessed quantitatively using the validated romanian version of the specific Mac New Heart Disease questionnaire. Exercise tolerance and functional status will be evaluated with the cardiopulmonary exercise testing or using the 6-minute walk test.

Laboratory investigations will include: complete blood count, ionogram, blood glucose, glycosylated hemoglobin, assessment of renal function (urea, creatinine), assessment of liver function (TGO, TGP, GGT), lipid balance (cholesterol, HDL, LDL, TG) and inflammatory status (ESR, CRP, IL-6, TNF α , IL-1 β). Starting from the evidences that such multidisciplinary programs require a complete evaluation, we intend to realize a detailed study in order to highlight the clinical and paraclinical benefits cardiac rehabilitation offers to patients. The quality of cardiac rehabilitation can be evaluated through practical performance measurements. It is known that worldwide a series of clinical and biological indices are validated (Grace et al., 2016; Moghei et al., 2019).

We intend to propose an echocardiographic quality indicator of cardiovascular rehabilitation guided by the current recommendations of the European Association of Cardiovascular Imaging (EACVI). As previously stated, it is highly recommended to include the patients who have experienced an acute myocardial infarction in rehabilitation programs (Beauchamp et al., 2020). The rate of addressability is unfortunately very low (Pothineni et al., 2018), which is why this study aims to raise awareness of the importance of directing patients to cardiovascular recovery centers.

Therefore, our goal is to encourage inter- and intradisciplinary communication and collaboration, with the main objective of gaining the maximum benefit for the patient.

Left ventricular diastolic dysfunction and left atrial strain

Left ventricular diastolic dysfunction contributes greatly to the progress of heart failure with preserved ejection fraction through an alteration of relaxation, an increase in parietal stiffness or a combination of the two (Obokata ET AL., 2020). Feasible information on both relaxation and ventricular compliance can be obtained through two-dimensional and Doppler echocardiography (Silbiger, 2019).

Likewise, because cardiac catheterization is not always available, echocardiographic assessment of left ventricular filling pressures is the preferred alternative. Echocardiographic estimation of left ventricular filling pressures has shown to be particularly useful in patients with exertional dyspnoea of unspecified etiology and has an accuracy of 87%, according to a recent multicenter analysis (Andersen ET AL., 2017).

The American Society of Echocardiography (ASE)/ European Association of Cardiovascular Imaging (EACVI) working group on diastolic function released the latest guideline in 2016. The guideline advise on using four different parameters for the initial assesment of diastolic function: early diastolic mitral annulus velocity (e'), ratio between early diastolic mitral inflow velocity (E) and e' (E/e'), left atrial volume index (LAVi) and tricuspid regurgitation velocity (TR) (Oh ET AL., 2020).It also provides two different algorithms: one for diagnosing diastolic dysfunction in patients with preserved ejection fraction and the other for estimating left ventricular filling pressures in patients with systolic or diastolic dysfunction (Cho and Hwang, 2020).Although this guideline simplified the evaluation of diastolic function, the persistence of a “gray zone”, where echocardiographic findings are inconclusive, led the focus on newer echocardiographic techniques such as left atrial deformation analysis by speckle tracking echocardiography (Mandoli et al., 2020).

The left atrium (LA) is in a close interconnection with the left ventricle during diastole and governs ventricular filling and thus, the overall cardiac performance. On this ground, the size of the LA is considered the “glycated hemoglobin” of diastolic dysfunction. Since the anteroposterior diameter underestimates its real dimensions, LA volume index is the favorite indicator (Tsang et al., 2002; Mandoli et al., 2020).Compared to the Doppler-derived diastolic echocardiographic variables, LAVi reflects the chronicity or the cumulative effect of elevated filling pressures (Smiseth, 2018).In two-dimensional echocardiography, LA volume can be determined with either the modified Simpson’s method of disk summation or the area-length method (Thomas et al., 2020). Under normal circumstances, body size is the main determining factor of LA dimensions. Thereby, indexing LA volume to body surface area is of extreme importance, with 34 mL/m² being the upper threshold value (Mandoli et al., 2020).

Through three-dimensional echocardiography (3DE) more precise information over left atrial volumes can be obtained, which further amplifies the diagnostic accuracy of diastolic dysfunction algorithms. Because 3DE LA volumes link better than the 2DE-derived ones with the metrics acquired with cardiac magnetic resonance, three-dimensional echocardiography is preferred, when available (Mor-Avi et al., 2012; Badano et al., 2020).

Nonetheless, the measurement of left atrial dimensions provides important but not sufficient data with regard to diastolic function (Obokata et al., 2020). Even a normal-sized left

atrium can be malfunctional and therefore LAVi has low sensitivity in the early identification of diastolic dysfunction (Frydas et al., 2020). Furthermore, because LAVi describes a slow and commonly not complete reverse remodeling with the amelioration of diastolic function, the need for a more instantaneous LA pressure parameter has emerged (Cho and Hwang, 2020).

Left atrial strain, assessed by speckle tracking echocardiography, came to light as a novel marker, useful in various clinical scenarios, including heart failure, myocardial infarction diastolic dysfunction and atrial fibrillation (Voigt et al., 2020) (Figure 21). Park et al. suggested that peak atrial longitudinal strain (PALS) could be used as an indicator of a new-onset atrial fibrillation in patients with heart failure and sinus rhythm based on an analysis they have performed among 4312 patients with acute heart failure from 3 tertiary hospitals (Park et al.,).

By substituting left atrial volume index with left atrial reservoir strain (LARS) when assessing diastolic function in 758 asymptomatic subjects, Potter et al. achieved a reduction of 75% in the number of cases with indeterminate diastolic function. Apart from that, a left atrial reservoir strain (LARS) $\leq 24\%$ anticipated the occurrence of heart failure in the elderly, regardless of LAVi (Potter et al., 2020). On top of these, this innovative marker appears to analogize better with the invasively measured filling pressures than the E/e' ratio (Fan et al., 2020). Left atrial filling index, defined as the ratio between early diastolic mitral inflow velocity (E) and left atrial reservoir strain seems therefore to be another valuable tool for predicting left ventricular filling pressures in patients with preserved ejection fraction (Braunauer et al., 2020).

The diagnostic value of left atrial strain has been investigated also in patients with stable coronary artery disease (CAD) and preserved ejection fraction. Left atrial strain was evaluated during the reservoir, the conduit and the booster-pump phases, in 64 patients with stable CAD and LVEF $\geq 50\%$ and 30 healthy volunteers. Left atrial reservoir strain had a good accuracy in estimating left ventricular filling pressures when compared to the values collected during cardiac catheterization. Accordingly, left atrial reservoir strain can be used for a sooner recognition of diastolic dysfunction (Lin et al., 2020).

Kim et al. sought to assess the extent of correspondence between echocardiography-derived and CMR-derived left atrial strain. They have also evaluated the capability of peak atrial longitudinal strain to detect diastolic dysfunction and to predict atrial fibrillation and congestive heart failure after myocardial infarction. The study cohort consisted of 257 patients. Peak atrial longitudinal strain was lower among patients with diastolic dysfunction as well as among patients with heart failure hospitalizations. Both echocardiography and CMR-derived peak atrial longitudinal strain scored the arrhythmic risk (Kim et al., 2020).

Anyhow, the magnitude of left atrial reservoir impairment corresponds to the degree of diastolic dysfunction, irrespective of ejection fraction, evidences supported also by a recent analysis of SOCRATES-PRESERVED and SOCRATES-REDUCED (Frydas et al., 2020). Left atrial strain shows promises for the evaluation and gradation of diastolic dysfunction, especially in patients in the indeterminate range, warranting however for more research and for validation with larger studies. Normal reference values have not been fully settled and except for age, the factors affecting left atrial strain are only partially understood (Sun et al., 2020).

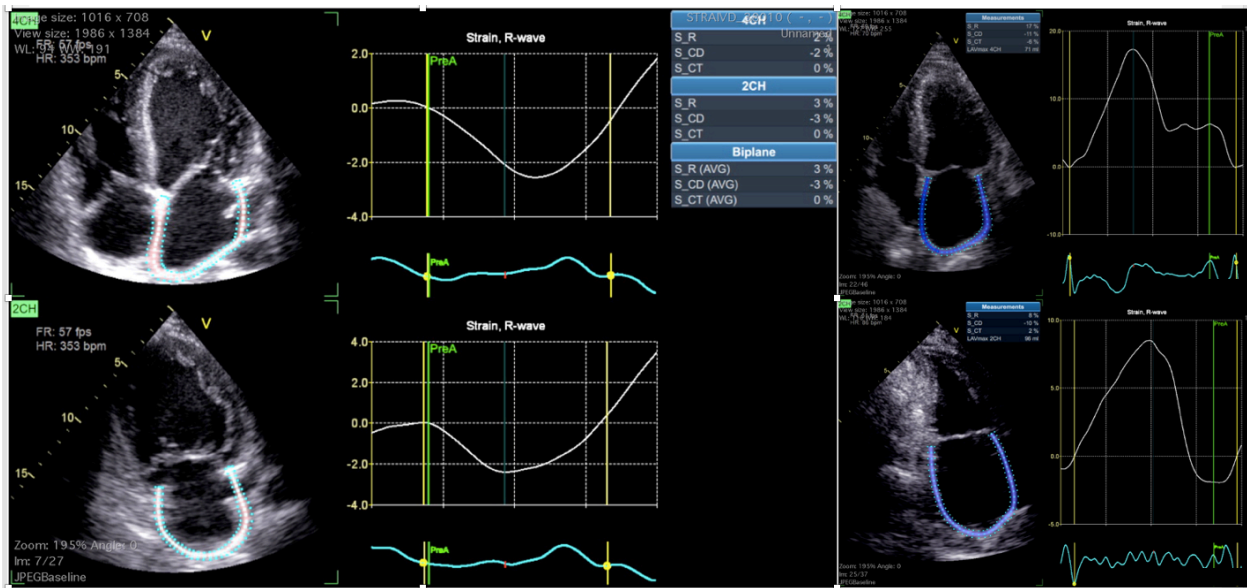


Figure 21. Strain echocardiographic evaluation of left atrial function via speckle tracking echocardiography

In the light of the above-mentioned data, I aim to conduct a clinical, prospective, observational study as a means to examine the potency of left atrial strain to predict the development of diastolic dysfunction after an acute myocardial infarction (primary outcome) as well as the emergences of atrial fibrillation, pulmonary hypertension and heart failure (secondary outcomes). Patients from the Cardiology Clinic of the Institute of Cardiovascular Diseases “Prof. Dr. George I.M. Georgescu”, Iasi, Romania, will be enrolled within 14 days after the onset of the acute event.

An initial, exhaustive, echocardiographic assessment of left ventricular diastolic function will be performed, mainly consisting of:

- Mitral valve inflow pattern (E/ A ratio, deceleration time of early mitral inflow- DT);
- Mitral annular velocities in Tissue Doppler Imaging (E/E' ratio);
- Isovolumic relaxation time (IVRT);
- Color M- Mode (propagation velocity);
- Pulmonary venous flow (Ar-A duration);
- Left atrial size.

Likewise, the 2D echocardiographic appraisal of left ventricular systolic function will be included in the echocardiographic examination protocol. Left ventricular ejection fraction (LVEF) will be measured using the biplane Simpson method as well as the Teicholz formula, where applicable. Only patients in sinus rhythm at the time of the initial evaluation and with no evidence of a diastolic dysfunction greater than grade 1, will be enrolled for further analysis. Left atrial strain will be additionally examined among these subjects with the help of modern speckle tracking echocardiography. Deformation of the atrial wall will be assessed during all three individual

phases: reservoir strain (LASr), conduit strain (LAScd) and contraction strain (LASc). Following this first visit, the patients recruited in the study will be clinically, electrocardiographically, biologically (BNP, NTproBNP) and echocardiographically investigated at 1 month, 3 months, 12 months and respectively 2 years post myocardial infarction.

Subjects will be systematically scrutinized for the occurrence of the following events:

- Diastolic dysfunction of grade 2 or 3;
- Pulmonary hypertension;
- Atrial fibrillation;
- Overt heart failure.

After the completion of all follow-up visits, the relationship between initial changes in absolute values of left atrial strain and the occurrence within 2 years of any of the above mentioned adverse events will be thoroughly analyzed. In other words, the main objective of the study will be to size up the predictive power of the left atrial strain in the onset of diastolic dysfunction, pulmonary hypertension, atrial fibrillation and heart failure after an acute myocardial infarction.

Myocardial infarction with non-obstructive coronary arteries

Myocardial infarction with non-obstructive coronary arteries, commonly known as MINOCA is a puzzling entity that has been increasingly recognized in the past decades. It accounts for 6-8% of all cases of acute infarction and is much more frequent among women, as well as in subjects presenting with NSTEMI (Thygesen et al., 2018; Lindahl et al., 2017; Pasupathy et al., 2015; Smilowitz et al., 2017).

In order to frame the diagnosis of MINOCA, the cooccurrence of the following three criteria is required:

1. Myocardial infarction;
2. No stenosis greater than 50% in a major epicardial coronary artery on angiography;
3. No other obvious cause that could explain the acute presentation (Agewall et al., 2017).

A variety of conditions can result in MINOCA, identifying the cause and consequently establishing the optimal therapeutic approach being the main challenges with this syndrome (Tamis-Holland et al., 2019). Recently, a revision of the terminology has been proposed with the interest of avoiding confusions about the underlying mechanisms. The term TP-NOCA (troponin-positive nonobstructive coronary arteries) comprises not only MINOCA, but also myocardial diseases (such as myocarditis) and non-cardiac disorders (e.g. pulmonary embolism, renal impairment) (Pasupathy et al., 2017). The idea behind the usage of this broader label mainly consists on the fact that elevations in the troponin levels can have either ischemic or nonischemic basis. Accordingly, the term MINOCA should be employed only when there is an ischemic mechanism responsible for the acute presentation. With the aim of facilitating its comprehension, Tamis-Holland et al. developed a clinical algorithm for the diagnosis of MINOCA, that ingeniously uses the “traffic light” sequence (Tamis-Holland et al., 2019).

Correspondingly, the exclusion of other triggers of the acute presentation involves performing a cardiac MRI. Cardiac magnetic resonance can distinguish between ischemic and nonischemic

grounds. The addition of high-resolution late gadolinium enhancement resulted in a reconsideration of the final diagnosis in 45 (26%) patients with MINOCA included in a recent analysis (Lintingre et al., 2020).

Subendocardial late gadolinium enhancement is the hallmark of an infarct pattern and thereupon MINOCA causes can be considered if the CMR acquisitions support the diagnosis of an infarct. Plaque disruption with thrombus formation and instantaneous thrombolysis, coronary artery embolism, coronary artery vasospasm and spontaneous coronary artery dissection are frequent causes of myocardial infarction with non-obstructive coronary arteries (Blankstein et al., 2019).

In addition, CMR findings seem to have not only a high diagnostic value, but also a prognostic one, when combined with conventional risk factors, such as ST-segment elevation on electrocardiogram. However, these observations need further validation through large, multicenter prospective trials (Dastidar et al., 2019). As cardiac magnetic resonance imaging has become broadly available, its integration in the “working diagnosis” of MINOCA is imperative. In order to identify the clear substrat of MINOCA, extra investigations are nevertheless needed (Ferreira, 2019). For instance, invasive imaging studies, such as intravascular ultrasound (IVUS) and optical coherence tomography (OCT) may be helpful in identifying plaque disruption in patients with MINOCA and, thus no signs of obstructive coronary artery disease.

Gerbaud et al. underwent a prospective, 2-center analysis of patients with MINOCA and suspected epicardial causes who benefited of both CMR and OCT imaging. Subjects that had coronary vasospasm during the methylexergonovine provocation test were excluded from the study. The final study population consisted of 40 eligible individuals.

By combining optical coherence tomography with cardiac magnetic resonance the exact mechanism was distinguished in 100% of cases. Of note, 23 subjects (57.5%) had the diagnosis endorsed by both CMR and OCT findings, 8 patients had an unequivocal diagnosis of myocardial infarction established only by CMR and in 9 cases (22.5%) the underlying cause was detected only by OCT (Gerbaud et al., 2020).

Coronary vasospasm is another major cause of MINOCA that needs to be taken into consideration when assessing the etiology as calcium channel blockers can alleviate symptoms and result in better clinical outcomes (Kaski, 2018).

As reported by Montone et al. the implementation of provocative tests with acetylcholine or ergonovine in patients with MINOCA and presumed coronary vasomotor disorders did not carry additional risk and helped recognizing the cause in 46.2% subjects enrolled in their study. On top of these, the patients with a positive response to acetylcholine or ergonovine spasm provocation tests appear to have a poorer prognosis and a higher incidence of adverse outcomes (Montone et al., 2018).

One more cause of MINOCA that has to be thoroughly scrutinized is spontaneous coronary artery dissection (SCAD), particularly type 1 and type 2. It stands to reason that intravascular imaging, such as IVUS and OCT is critical for detection (Collet et al., 2020).

Microvascular dysfunction can supplementary contribute to the pathogenesis of MINOCA, little information with regard to its significance being available so far (Tamis-Holland et al., 2019). Invasive evaluation of coronary microcirculation resourcefully integrates the capability of angiography to exclude obstructive lesions with diverse catheter-based procedures. A reduction of the coronary flow reserve in response to adenosine heavily supports the presence of microvascular dysfunction when corroborated with clinical data. The index of microcirculatory resistance is of further contribution (Taqueti and Di Carli, 2018).

Finally yet importantly, in a detailed systematic review, comprising 28 publications on MINOCA, thrombophilia disorders were reported in 14% of patients (Pasupathy et al., 2015).

If the optimal therapeutic approach of acute myocardial infarction and obstructive coronary artery disease is well documented, insufficient information exist in the field of MINOCA, with no prospective randomized, controlled trials conducted so far.

A cause-target therapy seems therefore to be an appropriate choice, with aspirin being the mainstay in plaque erosion or rupture and calcium channel blockers in epicardial coronary vasospasm. The management of microvascular dysfunction and spontaneous coronary artery dissection is more problematic as, once more, there are no randomized studies addressing these issues in MINOCA population (Tamis-Holland et al., 2019).

Lindahl et al. conducted a large-scale observational study that aimed to assess the efficacy of conventional secondary prevention treatments in MINOCA population. 9136 patients with myocardial infarction with nonobstructive coronary arteries recorded in the SWEDEHEART registry (the Swedish Web-system for Enhancement and Development of Evidence-based care in Heart disease Evaluated According to Recommended Therapy) were included in this analysis. The treatment with statins and renin-angiotensin system blockers resulted in considerable lower rates of adverse events during a follow-up period of 4.1 years, thus suggesting a long-term beneficial effect of these therapeutic agents. In subjects treated with beta-blockers a trend toward a positive effect was observed seeing that the reduction in the number of MACE (major adverse cardiac event) was not statistically significant. For patients treated with dual antiplatelet therapy no beneficial impact on outcomes was noticed. Once again, more research and adequately configured randomized clinical trials to validate these data are needed (Lindahl et al., 2017).

In essence, I believe that researchers should join forces and that the shortcomings of myocardial infarction with nonobstructive coronary arteries have to be tackled by every tertiary center. In this respect, I plan to found a national multicenter registry of MINOCA patients, which, from my perspective, would be of tremendous contribution. Another future research direction I look forward is that of evaluating the arrhythmic risk and implicitly the risk of sudden cardiac death among MINOCA subjects, limited data being available so far.

Thereby, I intend to conduct a prospective study on patients with MINOCA investigated through invasive coronary angiography within the Cardiology Clinic of the Institute of Cardiovascular Diseases “Prof. Dr. George I.M. Georgescu”, Iasi, Romania.

During the index hospitalization, the echocardiographic evaluation will be focused on the following:

- the measurement of left ventricular ejection fraction (biplane Simpson method);
- the assessment of mitral annular plane systolic excursion (MAPSE);
- the assessment of tricuspid annular plane systolic excursion (TAPSE);
- the measurement of peak myocardial systolic velocity (S') with the help of Tissue Doppler Imaging;
- the evaluation of global longitudinal strain (GLS) through the use of speckle-tracking echocardiography;
- the appreciation of left ventricular diastolic function based on peak E-wave velocity, E/A ratio, tricuspid regurgitant jet velocity, left atrial volume index and E/e' ratio.

Within 40 days of the acute event, all patients will benefit of 24-hour Holter ECG monitoring and cardiac magnetic resonance imaging. CMR scan will be performed with the purpose of confirming MINOCA, thus of ruling out an alternative diagnosis (especially myocarditis). CMR has the additional advantage of identifying the extent and the transmural of the fibrotic scar. The arrhythmic substrate is typically located at the border zone of the myocardial scar tissue and is well characterised by the late gadolinium enhancement technique. Furthermore, late gadolinium enhancement is a forceful predictor of outcomes, superior to ventricular volumes and ejection fraction.

Patients will be clinically and echocardiographically evaluated at 3 months, 6 months, 12 months and 2 years after the acute event. At each site visit, they will supplementary benefit of 24-hour Holter ECG monitoring. The primary objective will be to evaluate the risk of major arrhythmic events (nonsustained ventricular tachycardia, sustained ventricular tachycardia, ventricular fibrillation) and the risk of sudden cardiac death within MINOCA population.

The secondary objectives will be to determine the cumulative incidence of reinfarction, to examine the etiology of reinfarction (either coronary artery disease or recurrent MINOCA) and to judge the prognostic value of CMR imaging (the amount of LGE and the risk of ventricular arrhythmias or sudden cardiac death).

As the cooccurrence of sudden cardiac death and MINOCA has not been adequately studied, a prompt recognition of patients with MINOCA at high risk of major arrhythmic events not only represents a giant challenge, but it also carries a critical therapeutic value.

III. 4. FINAL REMARKS

The background in which I plan to continue my career is based on values as feedback, objectivity, sincerity, communication and teamwork. I aim to achieve as many of the didactic and scientific imperatives that are in my responsibility as a doctor, teacher, researcher and colleague. I aim to strengthen my level of enthusiasm and efficiency, to create lasting relationships with all colleagues in the academic community, to promote community ideas, transparency and feedback, to develop modern and competitive teaching content.

This habilitation thesis will offer me the opportunity to train PhD candidates, being an excellent motivation to continue my development in the academic, professional and research field.

SECTION IV. REFERENCES

1. Abedi SA, Tarzamni MK, Nakhjavani MR, Bohlooli A. Effect of renal transplantation on coronary artery calcification in hemodialysis patients. *Transpl Proc.* 2009; 41(7):2829–2831.
2. Abhayaratna WP, Seward JB, Appleton CP, Douglas PS, Oh JK, Tajik AJ, et al. Left atrial size: physiologic determinants and clinical applications. *J Am Coll Cardiol* 2006; 47: 2357-2363.
3. Abudiab MM, Chebrolu LH, Schutt RC, Nagueh SF, Zoghbi WA. Doppler echocardiography for the estimation of LV filling pressure in patients with mitral annular calcification. *JACC Cardiovasc Imaging.* 2017;10(12):1411–1420.
4. Afsar B, Turkmen K, Covic A, Kanbay M. An update on coronary artery disease and chronic kidney disease. *Int J Nephrol.* 2014; 2014:767424.
5. Agarwal S, Tuzcu EM, Desai MY, et al. Updated meta-analysis of septal alcohol ablation versus myectomy for hypertrophic cardiomyopathy. *J Am Coll Cardiol.* 2010;55(8):823-834.
6. Agewall S, Beltrame JF, Reynolds HR, et al. ESC working group position paper on myocardial infarction with non-obstructive coronary arteries. *Eur Heart J.* 2017;38(3):143-153.
7. Agostoni P, Corra U, Cattadori G, Veglia F, La Gioia R, Scardovi AB, et al., Group MSR. Metabolic exercise test data combined with cardiac and kidney indexes, the MECKI score: a multiparametric approach to heart failure prognosis. *Int J Cardiol* 2013; 167 (6):2710-2718.
8. Ahmadian A, Pawar S, Govender P, Berman J, Ruberg FL, Miller EJ. The response of FDG uptake to immunosuppressive treatment on FDG PET/CT imaging for cardiac sarcoidosis. *J Nucl Cardiol.* 2017;24(2):413-424.
9. Akyol S, Cortuk M, Baykan AO, Kiraz K, Borekci A, Seker T, et al. Biventricular Myocardial Performance Is Impaired in Proportion to Severity of Obstructive Sleep Apnea. *Tex Heart Inst J* 2016; 43:119-125.
10. Ali OM, Sayed AA, Mohammed WS, Mohammed RR. Cardiovascular System Affection and Its Relation to First-Year Mortality in Patients Initiating Maintenance Hemodialysis. *Int J Gen Med* 2020; 13:379-385.
11. Ali ZA, Karimi Galougahi K, Nazif T, et al. Imaging and physiology-guided percutaneous coronary intervention without contrast administration in advanced renal failure: a feasibility, safety, and outcome study. *Eur Heart J.* 2016; 37(40):3090–3095.
12. Aljaroudi WA, Desai MY, Tang WH, Phelan D, Cerqueira MD, Jaber WA. Role of imaging in the diagnosis and management of patients with cardiac amyloidosis: state of the art review and focus on emerging nuclear techniques. *J Nucl Cardiol.* 2014;21(2):271-283.

13. Altekin RE, Karakas MS, Yanikoglu A, Ozel D, Ozbudak O, Demir I, et al. Determination of right ventricular dysfunction using the speckle tracking echocardiography method in patients with obstructive sleep apnea. *Cardiol J* 2012; 19:130-139.
14. Altekin RE, Yanikoglu A, Karakas MS, Ozel D, Yildirim AB, Kabukcu M. Evaluation of subclinical left ventricular systolic dysfunction in patients with obstructive sleep apnea by automated function imaging method; an observational study. *Anadolu Kardiyol Derg* 2012; 12:320-330.
15. Ambrosy AP, Fonarow GC, Butler J, Chioncel O, Greene SJ, Vaduganathan M, et al. The global health and economic burden of hospitalizations for heart failure: lessons learned from hospital- ized heart failure registries. *J Am Coll Cardiol*. 2014;63:1123–33.
16. Andersen OS, Smiseth OA, Dokainish H, et al. Estimating Left Ventricular Filling Pressure by Echocardiography. *J Am Coll Cardiol*. 2017; 69(15):1937-1948.
17. Araujo AQ, Arteaga E, Ianni BM, Buck PC, Rabello R, Mady C. Effect of Losartan on left ventricular diastolic function in patients with nonobstructive hypertrophic cardiomyopathy. *Am J Cardiol*. 2005;96(11):1563-1567.
18. Artunc F, Mueller C, Breidthardt T, et al. Sensitive troponins--which suits better for hemodialysis patients? Associated factors and prediction of mortality. *PLoS One* 2012; 7(10):e47610.
19. Arundel C, Sheriff H, Bearden DM, Morgan CJ, Heidenreich PA, Fonarow GC, Butler J, Allman RM, Ahmed A. Discharge home health services referral and 30-day all-cause readmission in older adults with heart failure. *Arch Med Sci* 2018; 14(5):995-1002.
20. Arvidsson S, Henein MY, Wikström G, Suhr OB, Lindqvist P. Right ventricular involvement in transthyretin amyloidosis. *Amyloid*. 2018;25(3):160-166.
21. Authors/Task Force members, Elliott PM, Anastakis A, et al. 2014 ESC Guidelines on diagnosis and management of hypertrophic cardiomyopathy: the Task Force for the Diagnosis and Management of Hypertrophic Cardiomyopathy of the European Society of Cardiology (ESC). *Eur Heart J*. 2014;35(39):2733-2779.
22. Avanesov M, Münch J, Weinrich J, et al. Prediction of the estimated 5-year risk of sudden cardiac death and syncope or non-sustained ventricular tachycardia in patients with hypertrophic cardiomyopathy using late gadolinium enhancement and extracellular volume CMR. *Eur Radiol*. 2017;27(12):5136-5145.
23. Ayyala US, Nair AP, Padilla ML. Cardiac sarcoidosis. *Clin Chest Med*. 2008;29(3):493-ix.
24. Azzalini L, Mitomo S, Hachinohe D, Regazzoli D, Colombo A. Zero- contrast percutaneous coronary intervention guided by dextran-based optical coherence tomography. *Can J Cardiol*. 2018; 34(3):342. e1–e3.
25. Badano LP, Muraru D, Ciambellotti F, et al. Assessment of left ventricular diastolic function by three-dimensional transthoracic echocardiography. *Echocardiography*. 2020; 10.1111/echo.14782.

26. Baguet JP, Barone-Rochette G, Levy P, Vautrin E, Pierre H, Ormezzano O, et al. Left ventricular diastolic dysfunction is linked to severity of obstructive sleep apnoea. *Eur Respir J* 2010; 36:1323-1329.
27. Banerjee A, Davenport A. Changing patterns of pericardial disease in patients with end-stage renal disease. *Hemodial Int* 2006; 0: 249-255.
28. Banypersad SM, Fontana M, Maestrini V, et al. T1 mapping and survival in systemic light-chain amyloidosis. *Eur Heart J*. 2015;36(4):244-251.
29. Barssoum K, Altibi AM, Rai D, et al. Speckle tracking echocardiography can predict subclinical myocardial involvement in patients with sarcoidosis: A meta-analysis. *Echocardiography*. 2020;10.1111/echo.14886.
30. Beauchamp, Alison, Sheppard et al. Health Literacy of Patients Attending Cardiac Rehabilitation. *J Cardiopulm Rehabil Prev*. 2020;40 (4)249-254.
31. Bedetti G, Gargani L, Sicari R, Gianfaldoni ML, Molinaro S, Picano E. Comparison of prognostic value of echographic [corrected] risk score with the thrombolysis in myocardial infarction (TIMI) and global registry in acute coronary events (GRACE) risk scores in acute coronary syndrome. *Am J Cardiol* 2010; 106:1709–1716
32. Beiert T, Straesser S, Malotki R, Stockigt F, Schrickel JW, Andrie RP. Increased mortality and ICD therapies in ischemic versus non-ischemic dilated cardiomyopathy patients with cardiac resynchronization having survived until first device replacement. *Arch Med Sci*. 2019;15(4):845-856.
33. Bejar D, Colombo PC, Latif F, Yuzefpolskaya M. Infiltrative Cardiomyopathies. *Clin Med Insights Cardiol*. 2015;9(Suppl 2):29-38. Published 2015 Jul 8.
34. Benjamin EJ, Muntner P, Alonso A, Bittencourt MS, Callaway CW, Carson AP, et al., American Heart Association Council on E, Prevention Statistics C, Stroke Statistics S. Heart Disease and Stroke Statistics-2019 Update: A Report From the American Heart Association. *Circulation* 2019;139(10):e56-e528.
35. Biagini E, Spirito P, Rocchi G, et al. Prognostic implications of the Doppler restrictive filling pattern in hypertrophic cardiomyopathy. *Am J Cardiol*. 2009;104(12):1727-1731.
36. Birnie DH, Kandolin R, Nery PB, Kupari M. Cardiac manifestations of sarcoidosis: diagnosis and management. *Eur Heart J*. 2017;38(35):2663-2670.
37. Birnie DH, Nery PB, Ha AC, Beanlands RS. Cardiac Sarcoidosis. *J Am Coll Cardiol*. 2016;68(4):411-421.
38. Birnie DH, Sauer WH, Bogun F, et al. HRS expert consensus statement on the diagnosis and management of arrhythmias associated with cardiac sarcoidosis. *Heart Rhythm*. 2014;11(7):1305-1323.
39. Blankstein R, Madamanchi C. Myocardial Infarction With Nonobstructive Coronary Arteries: Getting to the Heart of the Matter. *JACC Cardiovasc Imaging*. 2020; 13(9):1914-1916.
40. Bodez D, Ternacle J, Guellich A, et al. Prognostic value of right ventricular systolic function in cardiac amyloidosis. *Amyloid*. 2016;23(3):158-167.

41. Bois JP, Geske JB, Foley TA, Ommen SR, Pellikka PA. Comparison of Maximal Wall Thickness in Hypertrophic Cardiomyopathy Differs Between Magnetic Resonance Imaging and Transthoracic Echocardiography. *Am J Cardiol.* 2017;119(4):643-650.
42. Bokhari S, Shahzad R, Castaño A, Maurer MS. Nuclear imaging modalities for cardiac amyloidosis. *J Nucl Cardiol.* 2014;21(1):175-184.
43. Boldrini M, Cappelli F, Chacko L, et al. Multiparametric Echocardiography Scores for the Diagnosis of Cardiac Amyloidosis. *JACC Cardiovasc Imaging.* 2020;13(4):909-920.
44. Boorsma EM, Ter Maaten JM, Damman K, et al. Congestion in heart failure: a contemporary look at physiology, diagnosis and treatment. *Nat Rev Cardiol.* 2020;17(10):641-655.
45. Boriani G, Savelieva I, Dan GA, et al. Chronic kidney disease in patients with cardiac rhythm disturbances or implantable electrical devices: clinical significance and implications for decision making—a position paper of the European Heart Rhythm Association endorsed by the Heart Rhythm Society and the Asia Pacific Heart Rhythm Society. *Europace.* 2015;17(8):1169–1196.
46. Boynton SJ, Geske JB, Dispenzieri A, et al. LGE Provides Incremental Prognostic Information Over Serum Biomarkers in AL Cardiac Amyloidosis. *JACC Cardiovasc Imaging.* 2016;9(6):680-686.
47. Bradbury BD, Fissell RB, Albert JM, et al. Predictors of early mortality among incident US hemodialysis patients in the Dialysis Outcomes and Practice Patterns Study (DOPPS). *Clin J Am Soc Nephrol* 2007; 2(1):89-99.
48. Braunauer K, Dünge HD, Belyavskiy E, et al. Potential usefulness and clinical relevance of a novel left atrial filling index to estimate left ventricular filling pressures in patients with preserved left ventricular ejection fraction. *Eur Heart J Cardiovasc Imaging.* 2020; 21(3):260-269.
49. Braunwald E, Lambrew CT, Rockoff SD, Ross J Jr, Morrow AG. Idiopathic Hypertrophic subaortic stenosis. A description of the disease based upon an analysis of 64 patients. *Circulation.* 1964;30:3-119.
50. Brooks D, Horner L, Kozar C, et al. Obstructive sleep apnea as a cause of systemic hypertension: evidence from a canine model. *J Clin Invest* 1997; 99:106–109.
51. Brownrigg J, Lorenzini M, Lumley M, Elliott P. Diagnostic performance of imaging investigations in detecting and differentiating cardiac amyloidosis: a systematic review and meta-analysis. *ESC Heart Fail.* 2019;6(5):1041-1051.
52. Bruder O, Wagner A, Jensen CJ, et al. Myocardial scar visualized by cardiovascular magnetic resonance imaging predicts major adverse events in patients with hypertrophic cardiomyopathy. *J Am Coll Cardiol.* 2010;56(11):875-887.
53. Buessler A, Chouihed T, Duarte K, Bassand A, Huot-Marchand M, Gottwalles Y, et al. Accuracy of Several Lung Ultrasound Methods for the Diagnosis of Acute Heart Failure in the ED: A Multicenter Prospective Study. *Chest* 2020;157 (1):99-110.

54. Buja A, Solinas G, Visca M, Federico B, Gini R, Baldo V, Francesconi P, Sartor G, Bellentani M, Damiani G. Prevalence of Heart Failure and Adherence to Process Indicators: Which Socio-Demographic Determinants are Involved? *Int J Environ Res Public Health* 2019;13(2):238.
55. Buonauro A, Galderisi M, Santoro C, Canora A, Bocchino ML, Lo Iudice F, et al. Obstructive sleep apnoea and right ventricular function: A combined assessment by speckle tracking and three-dimensional echocardiography. *Int J Cardiol.* 2017; 243:544-9.
56. Bush, Montika, Kucharska N et al. Effect of Initiating Cardiac Rehabilitation After Myocardial Infarction on Subsequent Hospitalization in Older Adults. *J Cardiopulm Rehabil Prev.* 2020;40(2):87-93.
57. Byrkjeland R, Njerve I, Anderssen S et al. Effects of exercise training on HbA1c and VO₂peak in patients with type 2 diabetes and coronary artery disease: a randomised clinical trial. *Diabetes Vasc Dis Res.* 2015;12(5):325–33.
58. Byrne D, Walsh JP, Daly C, et al. Improvements in cardiac function detected using echocardiography in patients with hereditary haemochromatosis. *Ir J Med Sci.* 2020;189(1):109-117.
59. Cacoub P, Chapelon-Abric C, Resche-Rigon M, Saadoun D, Desbois AC, Biard L. Cardiac sarcoidosis: A long term follow up study. *PLoS One.* 2020;15(9):e0238391.
60. Cameli M, Mondillo S, Righini FM, et al. Left ventricular deformation and myocardial fibrosis in patients with advanced heart failure requiring transplantation. *J Cardiac Fail.* 2016; 22(11):901–907.
61. Canepa M, Fonseca C, Chioncel O, Laroche C, Crespo-Leiro MG, Coats AJS, Mebazaa A, Piepoli MF, Tavazzi L, Maggioni AP, Investigators EHLTR. Performance of Prognostic Risk Scores in Chronic Heart Failure Patients Enrolled in the European Society of Cardiology Heart Failure Long-Term Registry. *JACC Heart Fail* 2018; 6 (6):452-462.
62. Cardim N, Galderisi M, Edvardsen T, et al. Role of multimodality cardiac imaging in the management of patients with hypertrophic cardiomyopathy: an expert consensus of the European Association of Cardiovascular Imaging Endorsed by the Saudi Heart Association. *Eur Heart J Cardiovasc Imaging.* 2015;16(3):280.
63. Castano A, Haq M, Narotsky DL, et al. Multicenter Study of Planar Technetium 99m Pyrophosphate Cardiac Imaging: Predicting Survival for Patients With ATTR Cardiac Amyloidosis. *JAMA Cardiol.* 2016;1(8):880-889.
64. Cetin S, Vural MG, Gunduz H, Akdemir R, Firat H. Epicardial fat thickness regression with continuous positive airway pressure therapy in patients with obstructive sleep apnea: assessment by two-dimensional echocardiography. *Wien Klin Wochenschr* 2016; 128:187-192.
65. Chacko L, Martone R, Cappelli F, Fontana M. Cardiac Amyloidosis: Updates in Imaging. *Curr Cardiol Rep.* 2019;21(9):108.
66. Charra B, Laurent G, Chazot C, et al. Clinical assessment of dry weight. *Nephrol Dial Transplant* 1996; 11(Suppl 2):16–19.

67. Chawla LS, Herzog CA, Costanzo MR, Tumlin J, Kellum JA, McCullough PA, et al. Proposal for a functional classification system of heart failure in patients with end-stage renal disease: proceedings of the acute dialysis quality initiative (ADQI) XI workgroup. *J Am Coll Cardiol* 2014;63(13):1246-52.
68. Chazot C, Wabel P, Chamney P, Moissl U, Wieskotten S, Wizemann V. Importance of normohydration for the long-term survival of haemodialysis patients. *Nephrol Dial Transplant* 2012;27(6):2404-2410.
69. Cheng H, Zhao S, Jiang S, et al. The relative atrial volume ratio and late gadolinium enhancement provide additive information to differentiate constrictive pericarditis from restrictive cardiomyopathy. *J Cardiovasc Magn Reson*. 2011;13(1):15.
70. Cheriex EC, Leunissen KML, Janssen JHA, et al. Echography of the inferior vena cava is a simple and reliable tool for estimation of 'dry weight' in haemodialysis patients. *Nephrol Dial Transplant* 1989; 4: 563–568.
71. Chertow GM, Levin NW, Beck GJ et al. In-center hemodialysis six times per week versus three times per week. *N Engl J Med* 2010; 363(24):2287–2300.
72. Cheung AK, Sarnak MJ, Yan G, Berkoben M, Heyka R, Kaufman A, et al. Cardiac diseases in maintenance hemodialysis patients: results of the HEMO Study. *Kidney Int* 2004;65(6):2380-9.
73. Chin CY, Matsumura M, Maehara A, et al. Coronary plaque characteristics in hemodialysis-dependent patients as assessed by optical coherence tomography. *Am J Cardiol*. 2017;119(9):1313–1319.
74. Cho GY, Hwang IC. Left Atrial Strain Measurement: A New Normal for Diastolic Assessment? *JACC Cardiovasc Imaging*. 2020; S1936-878X(20)30428-9.
75. Choi MJ, Kim JK, Kim SG, et al. Left atrial volume index is a predictor of silent myocardial ischemia in high-risk patients with end-stage renal disease. *Int J Cardiovasc Imaging*. 2013; 29(7):1433–1439.
76. Cicco S, Solimando AG, Buono R, et al. Right Heart Changes Impact on Clinical Phenotype of Amyloid Cardiac Involvement: A Single Centre Study. *Life (Basel)*. 2020;10(10):247.
77. Coats CJ, Rantell K, Bartnik A, et al. Cardiopulmonary Exercise Testing and Prognosis in Hypertrophic Cardiomyopathy. *Circ Heart Fail*. 2015;8(6):1022-1031.
78. Coiro S, Simonovic D, Deljanin-Ilic M, Duarte K, Carluccio E, Cattadori G, Girerd N, Ambrosio G. Prognostic Value of Dynamic Changes in Pulmonary Congestion During Exercise Stress Echocardiography in Heart Failure With Preserved Ejection Fraction. *Circ Heart Fail* 2020; 13 (6):e006769.
79. Collet JP, Thiele H, Barbato E, et al. 2020 ESC Guidelines for the management of acute coronary syndromes in patients presenting without persistent ST-segment elevation. *Eur Heart J*. 2020; ehaa575.
80. Collier P, Phelan D, Klein A. A Test in Context: Myocardial Strain Measured by Speckle-Tracking Echocardiography. *J Am Coll Cardiol*. 2017;69(8):1043-1056.

81. Contal C, O'Quigley J . An application of changepoint methods in studying the effect of age on survival in breast cancer. *Comput Stat Data Anal* 1999; 30(3):253–270.
82. Conte MR, Bongioanni S, Chiribiri A, et al. Late gadolinium enhancement on cardiac magnetic resonance and phenotypic expression in hypertrophic cardiomyopathy. *Am Heart J*. 2011;161(6):1073-1077.
83. Cosyns B, Plein S, Nihoyanopoulos P, et al. European Association of Cardiovascular Imaging (EACVI) position paper: Multimodality imaging in pericardial disease. *Eur Heart J Cardiovasc Imaging*. 2015;16(1):12-31.
84. Covic A, Ciumanghel AI, Siritopol D, Kanbay M, Dumea R, Gavrilovici C, Nistor I. Value of bioimpedance analysis estimated "dry weight" in maintenance dialysis patients: a systematic review and meta-analysis. *Int Urol Nephrol*. 2017; 49(12):2231-2245.
85. Covic AC, Buimistriuc LD, Green D, Stefan A, Badarau S, Kalra PA. The prognostic value of electrocardiographic estimation of left ventricular hypertrophy in dialysis patients. *Ann Noninvasive Electrocardiol* 2013;18(2):188-198.
86. Cozzolino M, Galassi A, Pivari F, et al. The cardiovascular burden in end-stage renal disease. *Contrib Nephrol* 2017; 191: 44–57.
87. Cozzolino M, Mangano M, Stucchi A, Ciceri P, Conte F, Galassi A. Cardiovascular disease in dialysis patients. *Nephrol Dial Transplant* 2018; 33(suppl_3): iii28-iii34.
88. Crandall ED, Staub NC, Goldberg HS, et al. Recent developments in pulmonary edema. *Ann Intern Med* 1983; 99: 808–822.
89. Curtis JP, Sokol SI, Wang Y, et al. The association of left ventricular ejection fraction, mortality, and cause of death in stable outpatients with heart failure. *J Am Coll Cardiol*. 2003;42(4):736–742.
90. Dabestani A, Mahan G, Gardin JM, Takenaka K, Burn C, Allfie A, Henry WL Evaluation of pulmonary artery pressure and resistance by pulsed Doppler echocardiography. *Am J Cardiol* 1987; 59:662–668.
91. Damy T, Jaccard A, Guellich A, et al. Identification of prognostic markers in transthyretin and AL cardiac amyloidosis. *Amyloid*. 2016;23(3):194-202.
92. Dasgupta NR, Rissing SM, Smith J, Jung J, Benson MD. Inotersen therapy of transthyretin amyloid cardiomyopathy. *Amyloid*. 2020;27(1):52-58.
93. Dastidar AG, Baritussio A, De Garate E, et al. Prognostic Role of CMR and Conventional Risk Factors in Myocardial Infarction With Nonobstructed Coronary Arteries. *JACC Cardiovasc Imaging*. 2019; 12(10):1973-1982.
94. David S, Kämpers P, Seidler V, Biertz F, Haller H, Fliser D. Diagnostic value of N-terminal pro-B-type natriuretic peptide (NT-proBNP) for left ventricular dysfunction in patients with chronic kidney disease stage 5 on haemodialysis. *Nephrol Dial Transplant* 2008; 23(4):1370-1377.
95. Davies SJ, Davenport A. The role of bioimpedance and biomarkers in helping to aid clinical decisionmaking of volume assessments in dialysis patients. *Kidney Int* 2014; 86(3):489–96.

96. Debonnaire P, Thijssen J, Leong DP, et al. Global longitudinal strain and left atrial volume index improve prediction of appropriate implantable cardioverter defibrillator therapy in hypertrophic cardiomyopathy patients. *Int J Cardiovasc Imaging*. 2014;30(3):549-558.
97. Debska-Slizien A, Dudziak M, Kubasik A, Jackowiak D, Zdrojewski Z, Rutkowski B. Echocardiographic changes in left ventricular morphology and function after successful renal transplantation. *Transpl Proc*. 2000; 32(6):1365–1366.
98. Deng Y, Pandit A, Heilman RL, Chakkera HA, Mazur MJ, Mookadam F. Left ventricular torsion changes post kidney transplantation. *J Cardiovasc Ultrasound*. 2013;21(4):171–176.
99. Desai MY, Bhonsale A, Patel P, et al. Exercise echocardiography in asymptomatic HCM: exercise capacity, and not LV outflow tract gradient predicts long-term outcomes. *JACC Cardiovasc Imaging*. 2014;7(1):26-36.
100. DeVore AD, McNulty S, Alenezi F, et al. Impaired left ventricular global longitudinal strain in patients with heart failure with preserved ejection fraction: insights from the RELAX trial. *Eur J Heart Fail*. 2017;19(7):893–900.
101. Di Bella G, Minutoli F, Mazzeo A, et al. MRI of cardiac involvement in transthyretin familial amyloid polyneuropathy. *AJR Am J Roentgenol*. 2010;195(6):W394-W399.
102. Di Carli MF, Geva T, Davidoff R. The Future of Cardiovascular Imaging. *Circulation*. 2016;133(25):2640-2661.
103. Di Nunzio D, Recupero A, de Gregorio C, Zito C, Caretj S, Di Bella G. Echocardiographic Findings in Cardiac Amyloidosis: Inside Two-Dimensional, Doppler, and Strain Imaging. *Curr Cardiol Rep*. 2019;21(2):7.
104. Di Stefano C, Bruno G, Arciniegas Calle MC, et al. Diagnostic and predictive value of speckle tracking echocardiography in cardiac sarcoidosis. *BMC Cardiovasc Disord*. 2020;20(1):21.
105. Di Tanna GL, Wirtz H, Burrows KL, Globe G. Evaluating risk prediction models for adults with heart failure: A systematic literature review. *PLoS One* 2020; 15 (1):e0224135.
106. Díez-López C, Comín-Colet J, González-Costello J. Iron overload cardiomyopathy: from diagnosis to management. *Curr Opin Cardiol*. 2018;33(3):334-340.
107. Dimitrow PP, Bober M, Michałowska J, Sorysz D. Left ventricular outflow tract gradient provoked by upright position or exercise in treated patients with hypertrophic cardiomyopathy without obstruction at rest. *Echocardiography*. 2009;26(5):513-520.
108. Dobrowolski P, Florczak E, Klisiewicz A, Prejbisz A, Rybicka J, Sliwinski P, et al. Pulmonary artery dilation indicates severe obstructive sleep apnea in patients with resistant hypertension: the Resist-POL Study. *Pol Arch Med Wewn* 2016; 126:222-229.
109. Domenech P, Perez T, Saldarini A, Uad P, Musso CG. Kidney-lung pathophysiological crosstalk: its characteristics and importance. *Int Urol Nephrol*. 2017; 49(7):1211-1215.
110. Dorbala S, Cuddy S, Falk RH. How to Image Cardiac Amyloidosis: A Practical Approach. *JACC Cardiovasc Imaging*. 2020;13(6):1368-1383.

111. Dorbala S, Vangala D, Semer J, et al. Imaging cardiac amyloidosis: a pilot study using ¹⁸F-florbetapir positron emission tomography. *Eur J Nucl Med Mol Imaging*. 2014;41(9):1652-1662.
112. Dundon BK, Pisaniello AD, Nelson AJ, et al. Dobutamine stress cardiac MRI for assessment of coronary artery disease prior to kidney transplantation. *Am J Kidney Dis*. 2015; 65(5):808–809.
113. Dungu JN, Valencia O, Pinney JH, et al. CMR-based differentiation of AL and ATTR cardiac amyloidosis. *JACC Cardiovasc Imaging*. 2014;7(2):133-142.
114. Dunlay SM, Roger VL. Understanding the epidemic of heart failure: past, present, and future. *Current Heart Failure Reports* 2014; 11 (4):404-415.
115. Dursunoglu D, Dursunoglu N, Evrengul H, Ozkurt S, Kuru O, Kilic M, et al. Impact of obstructive sleep apnoea on left ventricular mass and global function. *Eur Respir J* 2005; 26(2):283-288.
116. Dwyer KH, Merz AA, Lewis EF, Claggett BL, Crousillat DR, Lau ES, Silverman MB, Peck J, Rivero J, Cheng S, Platz E. Pulmonary Congestion by Lung Ultrasound in Ambulatory Patients With Heart Failure With Reduced or Preserved Ejection Fraction and Hypertension. *J Card Fail*. 2018; 24(4):219-226.
117. Enia G, Torino C, Panuccio V, et al. Asymptomatic pulmonary congestion and physical functioning in hemodialysis patients. *Clin J Am Soc Nephrol* 2013; 8(8):1343-1348.
118. Escher F, Senoner M, Doerler J, et al. When and how do patients with cardiac amyloidosis die?. *Clin Res Cardiol*. 2020;109(1):78-88.
119. Falk RH, Plehn JF, Deering T, et al. Sensitivity and specificity of the echocardiographic features of cardiac amyloidosis. *Am J Cardiol*. 1987;59(5):418-422.
120. Falk RH. Diagnosis and management of the cardiac amyloidoses. *Circulation*. 2005;112(13):2047-2060.
121. Fan JL, Su B, Zhao X, Zhou BY, Ma CS, Wang HP, Hu SD, Zhou YF, Ju YJ, Wang MH. Correlation of left atrial strain with left ventricular end-diastolic pressure in patients with normal left ventricular ejection fraction. *Int J Cardiovasc Imaging*. 2020; 36(9):1659-1666.
122. Farshid A, Pathak R, Shadbolt B, Arnolda L, Talaulikar G. Diastolic function is a strong predictor of mortality in patients with chronic kidney disease. *BMC Nephrol*. 2013; 14:280.
123. Feng D, Edwards WD, Oh JK, et al. Intracardiac thrombosis and embolism in patients with cardiac amyloidosis *Circulation*. 2007;116(21):2420-2426.
124. Ferrario M, Moissl U, Garzotto F, Cruz DN, Clementi A, Brendolan A, et al. Effects of fluid overload on heart rate variability in chronic kidney disease patients on hemodialysis. *BMC Nephrol* 2014; 15:26.
125. Ferreira VM. CMR Should Be a Mandatory Test in the Contemporary Evaluation of "MINOCA". *JACC Cardiovasc Imaging*. 2019; 12(10):1983-1986.
126. Fine NM, White JA, Jimenez-Zepeda V, Howlett JG. Determinants and Prognostic Significance of Serial Right Heart Function Changes in Patients With Cardiac Amyloidosis. *Can J Cardiol*. 2020;36(3):432-440.

127. Finocchiaro G, Haddad F, Knowles JW, et al. Cardiopulmonary responses and prognosis in hypertrophic cardiomyopathy: a potential role for comprehensive noninvasive hemodynamic assessment. *JACC Heart Fail.* 2015;3(5):408-418.
128. Foley RN, Parfrey PS, Harnett JD, Kent GM, Martin CJ, Murray DC, et al. Clinical and echocardiographic disease in patients starting end-stage renal disease therapy. *Kidney Int* 1995; 47(1):186-92.
129. Foley RN, Parfrey PS, Harnett JD, Kent GM, Murray DC, Barre PE. The prognostic importance of left ventricular geometry in uremic cardiomyopathy. *JASN* 1995; 5(12):2024–31.
130. Foley RN, Parfrey PS, Morgan J, et al. Effect of hemoglobin levels in hemodialysis patients with asymptomatic cardiomyopathy. *Kidney Int* 2000; 58(3):1325–1335
131. Fontana M, Banyersad SM, Treibel TA, et al. Differential Myocyte Responses in Patients with Cardiac Transthyretin Amyloidosis and Light-Chain Amyloidosis: A Cardiac MR Imaging Study. *Radiology.* 2015;277(2):388-397.
132. Fontana M, Pica S, Reant P, et al. Prognostic Value of Late Gadolinium Enhancement Cardiovascular Magnetic Resonance in Cardiac Amyloidosis. *Circulation.* 2015;132(16):1570-1579.
133. Frassi F, Gargani L, Gligorova S, Ciampi Q, Mottola G, Picano E. Clinical and echocardiographic determinants of ultrasound lung comets. *Eur J Echocardiogr* 2007; 8(6):474-479.
134. Freitas P, Ferreira AM, Arteaga-Fernández E, et al. The amount of late gadolinium enhancement outperforms current guideline-recommended criteria in the identification of patients with hypertrophic cardiomyopathy at risk of sudden cardiac death. *J Cardiovasc Magn Reson.* 2019;21(1):50.
135. Frydas A, Morris DA, Belyavskiy E, et al. Left atrial strain as sensitive marker of left ventricular diastolic dysfunction in heart failure. *ESC Heart Fail.* 2020; 7(4):1956-1965.
136. Fujikura K, Peltzer B, Tiwari N, et al. Reduced global longitudinal strain is associated with increased risk of cardiovascular events or death after kidney transplant. *Int J Cardiol.* 2018; 272:323–328.
137. Fung JW, Li TS, Choy DK, Yip GW, Ko FW, Sanderson JE, et al. Severe obstructive sleep apnea is associated with left ventricular diastolic dysfunction. *Chest* 2002; 121:422- 429.
138. Gargani L, Frassi F, Soldati G, Tesorio P, Gheorghide M, Picano E. Ultrasound lung comets for the differential diagnosis of acute cardiogenic dyspnoea: a comparison with natriuretic peptides. *Eur J Heart Fail* 2008;10(1):70-77.
139. Gargani L. Lung ultrasound: a new tool for the cardiologist. *Cardiovasc Ultrasound* 2011; 9:6.
140. Gargiulo R, Suhail F, Lerma EV. Cardiovascular disease and chronic kidney disease. *Dis Mon* 2015; 61(9):403-13.

141. Gastl M, Gotschy A, von Spiczak J, et al. Cardiovascular magnetic resonance T2* mapping for structural alterations in hypertrophic cardiomyopathy. *Eur J Radiol Open*. 2019;6:78-84.
142. Gastl M, Gruner C, Labucay K, et al. Cardiovascular magnetic resonance T2* mapping for the assessment of cardiovascular events in hypertrophic cardiomyopathy. *Open Heart*. 2020;7(1):e001152.
143. Gattis WA, O'Connor CM, Gallup DS, Hasselblad V, Gheorghide M, Investigators I-H, Coordinators. Predischarge initiation of carvedilol in patients hospitalized for decompensated heart failure: results of the Initiation Management Predischarge: Process for Assessment of Carvedilol Therapy in Heart Failure (IMPACT-HF) trial. *J Am Coll Cardiol*. 2004; 43(9):1534-1541.
144. GBDS. Global Burden of Disease, 2018.
145. Gerbaud E, Arabucki F, Nivet H, et al. OCT and CMR for the Diagnosis of Patients Presenting With MINOCA and Suspected Epicardial Causes. *JACC Cardiovasc Imaging*. 2020; S1936-878X(20)30634-3.
146. Gerber Y, Weston SA, Redfield MM, Chamberlain AM, Manemann SM, Jiang R, Killian JM, Roger VL. A contemporary appraisal of the heart failure epidemic in Olmsted County, Minnesota, 2000 to 2010. *JAMA Internal Medicine* 2015; 175 (6):996-1004.
147. Gersh BJ, Maron BJ, Bonow RO, et al. 2011 ACCF/AHA guideline for the diagnosis and treatment of hypertrophic cardiomyopathy: executive summary: a report of the American College of Cardiology Foundation/American Heart Association Task Force on Practice Guidelines. *Circulation*. 2011;124(24):2761-2796.
148. Gertz MA, Dispenzieri A. Systemic Amyloidosis Recognition, Prognosis, and Therapy: A Systematic Review. *JAMA*. 2020;324(1):79-89.
149. Geske JB, Ommen SR, Gersh BJ. Hypertrophic Cardiomyopathy: Clinical Update. *JACC Heart Fail*. 2018;6(5):364-375.
150. Gheorghide M, Konstam MA, Burnett JC, Jr., Grinfeld L, Maggioni AP, Swedberg K, Udelson JE, Zannad F, Cook T, Ouyang J, Zimmer C, Orlandi C, Efficacy of Vasopressin Antagonism in Heart Failure Outcome Study With Tolvaptan I. Short-term clinical effects of tolvaptan, an oral vasopressin antagonist, in patients hospitalized for heart failure: the EVEREST Clinical Status Trials. *JAMA*. 2007; 297(12):1332-1343.
151. Giakoumis A, Berdoukas V, Gotsis E, Aessopos A. Comparison of echocardiographic (US) volumetry with cardiac magnetic resonance (CMR) imaging in transfusion dependent thalassemia major (TM). *Cardiovasc Ultrasound*. 2007;5:24.
152. Gillmore JD, Maurer MS, Falk RH, et al. Nonbiopsy Diagnosis of Cardiac Transthyretin Amyloidosis. *Circulation*. 2016;133(24):2404-2412.
153. Gimeno JR, Tomé-Esteban M, Lofiego C, et al. Exercise-induced ventricular arrhythmias and risk of sudden cardiac death in patients with hypertrophic cardiomyopathy. *Eur Heart J*. 2009;30(21):2599-2605.

154. Global, regional, and national age-sex-specific mortality and life expectancy, 1950-2017: a systematic analysis for the Global Burden of Disease Study 2017. *Lancet* (London, England) 2018; 392(10159):1684-735.
155. Grace, Sherry L, Tan et al. Feasibility of Assessing 2 Cardiac Rehabilitation Quality Indicators. *J Cardiopulm Rehabil Prev.* 2016;36(2):112-116.
156. Graham-Brown MP, March DS, Churchward DR, et al. Novel cardiac nuclear magnetic resonance method for noninvasive assessment of myocardial fibrosis in hemodialysis patients. *Kidney Int.* 2016; 90(4):835-844.
157. Graham-Brown MP, Rutherford E, Levelt E, et al. Native T1 mapping: inter-study, inter-observer and inter-center reproducibility in hemodialysis patients. *J Cardiovasc Magn Reson.* 2017; 19(1):21.
158. Grambsch PM, Therneau TM, Fleming TR. Diagnostic plots to reveal functional form for covariates in multiplicative intensity models. *Biometrics.* 1995; 51(4):1469-1482.
159. Green JJ, Berger JS, Kramer CM, Salerno M. Prognostic value of late gadolinium enhancement in clinical outcomes for hypertrophic cardiomyopathy. *JACC Cardiovasc Imaging.* 2012;5(4):370-377.
160. Greulich S, Deluigi CC, Gloekler S, et al. CMR imaging predicts death and other adverse events in suspected cardiac sarcoidosis. *JACC Cardiovasc Imaging.* 2013;6(4):501-511.
161. Guidry UC, Mendes LA, Evans JC, Levy D, O'Connor GT, Larson MG, Gottlieb DJ, Benjamin EJ. Echocardiographic features of the right heart in sleep-disordered breathing: the Framingham Heart Study. *Am J Respir Crit Care Med.* 2001 Sep 15; 164(6):933-8.
162. Gustafsson M, Alehagen U, Johansson P. Imaging Congestion With a Pocket Ultrasound Device: Prognostic Implications in Patients With Chronic Heart Failure. *J Card Fail.* 2015; 21(7):548-554.
163. Guttmann OP, Rahman MS, O'Mahony C, Anastasakis A, Elliott PM. Atrial fibrillation and thromboembolism in patients with hypertrophic cardiomyopathy: systematic review. *Heart.* 2014;100(6):465-472.
164. Güvenç TS, Hüseyinoğlu N, Özben S, Kul Ş, Çetin R, Özen K, Doğan C, Balci B. Right ventricular geometry and mechanics in patients with obstructive sleep apnea living at high altitude. *Sleep Breath.* 2016; 20(1):5-13.
165. Habib G, Bucciarelli-Ducci C, Caforio ALP, et al. Multimodality Imaging in Restrictive Cardiomyopathies: An EACVI expert consensus document In collaboration with the "Working Group on myocardial and pericardial diseases" of the European Society of Cardiology Endorsed by The Indian Academy of Echocardiography. *Eur Heart J Cardiovasc Imaging.* 2017;18(10):1090-1121.
166. Halliday BP, Gulati A, Ali A, et al. Association Between Midwall Late Gadolinium Enhancement and Sudden Cardiac Death in Patients With Dilated Cardiomyopathy and Mild and Moderate Left Ventricular Systolic Dysfunction. *Circulation.* 2017;135(22):2106-2115.

167. Hamidi S, Kojuri J, Attar A, Roozbeh J, Moaref A, Nikoo MH. The effect of kidney transplantation on speckled tracking echocardiography findings in patients on hemodialysis. *J Cardiovasc Thorac Res*. 2018;10(2):90–94.
168. Hammerstingl C, Schueler R, Wiesen M, Momcilovic D, Pabst S, Nickenig G, et al. Impact of untreated obstructive sleep apnea on left and right ventricular myocardial function and effects of CPAP therapy. *PLoS One* 2013; 8:e76352.
169. Hassan HC, Howlin K, Jefferys A, et al. High-sensitivity troponin as a predictor of cardiac events and mortality in the stable dialysis population. *Clin Chem* 2014; 60(2):389-398.
170. Haugaa KH, Smedsrud MK, Steen T, et al. Mechanical dispersion assessed by myocardial strain in patients after myocardial infarction for risk prediction of ventricular arrhythmia. *JACC Cardiovasc Imaging*. 2010; 3(3):247–256.
171. Haydar AA, Hujairi NM, Covic AA, Pereira D, Rubens M, Goldsmith DJ. Coronary artery calcification is related to coronary atherosclerosis in chronic renal disease patients: a study comparing EBCT-generated coronary artery calcium scores and coronary angiography. *Nephrol Dial Transplant*. 2004;19(9):2307–2312.
172. Heidenreich PA, Albert NM, Allen LA, Bluemke DA, Butler J, Fonarow GC, et al. American Heart Association Advocacy Coordinating C, Council on Arteriosclerosis T, Vascular B, Council on Cardiovascular R, Intervention, Council on Clinical C, Council on E, Prevention, Stroke C. Forecasting the impact of heart failure in the United States: a policy statement from the American Heart Association. *Circ Heart Fail*. 2013; 6(3):606-619.
173. Helal I, Belhadj R, Mohseni A, et al. Clinical significance of N-terminal Pro-B-type natriuretic peptide (NT-proBNP) in hemodialysis patients. *Saudi J Kidney Dis Transpl* 2010; 21(2):262-268.
174. Henry RM, Kostense PJ, Bos G, Dekker JM, Nijpels G, Heine RJ, et al. Mild renal insufficiency is associated with increased cardiovascular mortality: The Hoorn Study. *Kidney Int* 2002;62(4):1402-7.
175. Hensen LCR, Goossens K, Delgado V, et al. Prevalence of left ventricular systolic dysfunction in pre-dialysis and dialysis patients with preserved left ventricular ejection fraction. *Eur J Heart Fail*. 2018; 20(3):560–568.
176. Hensen LCR, Goossens K, Delgado V, Rotmans JJ, Jukema JW, Bax JJ. Prognostic implications of left ventricular global longitudinal strain in predialysis and dialysis patients. *Am J Cardiol*. 2017;120(3):500–504.
177. Hensen LCR, Goossens K, Podlesnikar T, et al. Left ventricular mechanical dispersion and global longitudinal strain and ventricular arrhythmias in predialysis and dialysis patients. *J Am Soc Echocardiogr*. 2018;31(7):777–783.
178. Heran B, Chen J, Ebrahim S et al. Exercise-based cardiac rehabilitation for coronary heart disease. *Cochrane Database Syst Rev*. 2011;(7).

179. Hickson LJ, Negrotto SM, Onuigbo M, et al. Echocardiography Criteria for Structural Heart Disease in Patients With End-Stage Renal Disease Initiating Hemodialysis. *J Am Coll Cardiol*. 2016; 67(10):1173–1182.
180. Hill NR, Fatoba ST, Oke JL, Hirst JA, O’Callaghan CA, Lasserson DS, et al. Global prevalence of chronic kidney disease—a systematic review and meta-analysis. *PLoS One* 2016; 11(7): e0158765.
181. Hinojar R, Varma N, Child N, et al. T1 Mapping in Discrimination of Hypertrophic Phenotypes: Hypertensive Heart Disease and Hypertrophic Cardiomyopathy: Findings From the International T1 Multicenter Cardiovascular Magnetic Resonance Study. *Circ Cardiovasc Imaging*. 2015;8(12):e003285.
182. Holtstrand Hjälms H, Fu M, Hansson PO, Zhong Y, Caidahl K, Mandalenakis Z, Morales D, Ergatoudes C, Rosengren A, Grote L, Thunström E. Association between left atrial enlargement and obstructive sleep apnea in a general population of 71-year-old men. *J Sleep Res* 2018; 27:252-258.
183. Hong YJ, Jeong MH, Choi YH, et al. Effect of renal function on ultrasonic coronary plaque characteristics in patients with acute myocardial infarction. *Am J Cardiol*. 2010; 105(7):936–942.
184. Horwich TB, Fonarow GC, Hamilton MA, MacLellan WR, Woo MA, Tillisch JH. The relationship between obesity and mortality in patients with heart failure. *J Am Coll Cardiol* 2001; 38 (3):789-795.
185. Howlett JG. Should we perform a heart failure risk score? *Circ Heart Fail* 2013; 6 (1):4-5.
186. <https://www.fmc-au.com/therapy-systems-and-services/analysis-systems/bcm>. [cited 2019 December 22]; Available from:
187. Huitema MP, Grutters JC, Rensing BJWM, Reesink HJ, Post MC. Pulmonary hypertension complicating pulmonary sarcoidosis. *Neth Heart J*. 2016;24(6):390-399
188. Hung KC, Lee CH, Chen CC, et al. Advanced left ventricular diastolic dysfunction in uremic patients with type 2 diabetes on maintenance hemodialysis. *Circulation* 2012; 76(10): 2380e5.
189. Hung SC, Kuo KL, Peng CH, Wu CH, Wang YC, Tarn DC. Association of fluid retention with anemia and clinical outcomes among patients with chronic kidney disease. *J Am Heart Assoc* 2015; 4 (1):e001480.
190. Hur E, Usta M, Toz H, et al. Effect of fluid management guided by bioimpedance spectroscopy on cardiovascular parameters in hemodialysis patients: a randomized controlled trial. *Am J Kidney Dis* 2013;61(6):957-965.
191. Ichida M, Nishimura Y, Kario K. Clinical significance of left ventricular apical aneurysms in hypertrophic cardiomyopathy patients: the role of diagnostic electrocardiography. *J Cardiol*. 2014;64(4):265-272.
192. Iio K, Nagasawa Y, Kimura T, et al. Assessment of coronary stenosis by a 16-slice MDCT scanner in asymptomatic diabetic patients starting dialysis therapy. *Nephron Clin Pract*. 2008;109(2):c72–c79.

193. Imai Y, Tanaka N, Usui Y, Usui Y, Takahashi N, Kurohane S, Takei Y, et al. Severe obstructive sleep apnea increases left atrial volume independently of left ventricular diastolic impairment. *Sleep Breath* 2015; 19:1249-1255.
194. Infante JR, Moreno M, Rayo JI, Serrano J, Dominguez ML, Garcia L. High liver FDG uptake on PET/CT in patient with lymphoma diagnosed with hereditary hemochromatosis. *Clin Nucl Med*. 2015;40(6):538-539.
195. Inker LA, Astor BC, Fox CH, Isakova T, Lash JP, Peralta CA, Kurella Tamura M, Feldman HI. KDOQI US commentary on the 2012 KDIGO clinical practice guideline for the evaluation and management of CKD. *Am J Kidney Dis* 2014; 63(5):713-35.
196. Ito K, Minamimoto R, Morooka M, Kubota K. A case of secondary hemochromatosis with high uptake of liver in F-18 FDG PET/CT imaging. *Clin Nucl Med*. 2011;36(7):606-608.
197. Jaeger JQ, Mehta RL. Assessment of dry weight in hemodialysis: an overview. *J Am Soc Nephrol* 1999; 10: 392–403.
198. Jain A, Scott C, Chen HH. The renal-cardiac connection in subjects with preserved ejection fraction: a population based study. *ESC Heart Fail*. 2017;4(3):266–273.
199. Jambrik Z, Monti S, Coppola V, Agricola E, Mottola G, Miniati M, Picano E. Usefulness of ultrasound lung comets as a nonradiologic sign of extravascular lung water. *Am J Cardiol*. 2004; 93(10):1265-1270.
200. Javaheri S, Barbe F, Campos-Rodriguez F, et al. Sleep Apnea: Types, Mechanisms, and Clinical Cardiovascular Consequences. *J Am Coll Cardiol*. 2017;69(7):841-858.
201. Jenkins C, Bricknell K, Hanekom L, Marwick TH. Reproducibility and accuracy of echocardiographic measurements of left ventricular parameters using real-time three-dimensional echocardiography. *J Am Coll Cardiol*. 2004;44(4):878–886.
202. Jurcut R, Giusca S, La Gerche A, Vasile S, Gingham C, Voigt JU. The echocardiographic assessment of the right ventricle: What to do in 2010? *Eur J Echocardiogr* 2010; 11:81–96.
203. Jurcuț R, Onciul S, Adam R, et al. Multimodality imaging in cardiac amyloidosis: a primer for cardiologists. *Eur Heart J Cardiovasc Imaging*. 2020;21(8):833-844.
204. Kagioka Y, Yasuda M, Okune M, et al. Right ventricular involvement is an important prognostic factor and risk stratification tool in suspected cardiac sarcoidosis: analysis by cardiac magnetic resonance imaging. *Clin Res Cardiol*. 2020;109(8):988-998.
205. Kalam K, Otahal P, Marwick TH. Prognostic implications of global LV dysfunction: a systematic review and meta-analysis of global longitudinal strain and ejection fraction. *Heart*. 2014;100(21):1673–1680.
206. Kamano C, Osawa H, Hashimoto K, et al. N-Terminal pro-brain natriuretic peptide as a predictor of heart failure with preserved ejection fraction in hemodialysis patients without fluid overload. *Blood Purif*. 2012; 33(1-3):37-43.
207. Kanda H, Hirasaki Y, Iida T, et al. Effect of fluid loading on left ventricular volume and stroke volume variability in patients with end-stage renal disease: a pilot study. *Ther Clin Risk Manag*. 2015; 11:1619–1625.

208. Kansal MM, Lester SJ, Surapaneni P, et al. Usefulness of two-dimensional and speckle tracking echocardiography in "Gray Zone" left ventricular hypertrophy to differentiate professional football player's heart from hypertrophic cardiomyopathy. *Am J Cardiol.* 2011;108(9):1322-1326.
209. Karamitsos TD, Piechnik SK, Banypersad SM, et al. Noncontrast T1 mapping for the diagnosis of cardiac amyloidosis. *JACC Cardiovasc Imaging.* 2013;6(4):488-497.
210. Karimi Galougahi K, Zalewski A, Leon MB, Karpaliotis D, Ali ZA. Optical coherence tomography-guided percutaneous coronary intervention in preterminal chronic kidney disease with no radiocontrast administration. *Eur Heart J.* 2016; 37(13):1059.
211. Kaski JC. Provocative tests for coronary artery spasm in MINOCA: necessary and safe?. *Eur Heart J.* 2018; 39(2):99-101.
212. Kato TS, Daimon M, Satoh T. Use of Cardiac Imaging to Evaluate Cardiac Function and Pulmonary Hemodynamics in Patients with Heart Failure. *Curr Cardiol Rep.* 2019;21(6):53.
213. Kawai H, Sarai M, Kato Y, et al. Diagnosis of isolated cardiac sarcoidosis based on new guidelines. *ESC Heart Fail.* 2020;7(5):2662-2671.
214. Kawasaki M, Takatsu H, Noda T, et al. In vivo quantitative tissue characterization of human coronary arterial plaques by use of integrated backscatter intravascular ultrasound and comparison with angioscopic findings. *Circulation.* 2002; 105(21):2487–2492.
215. KDOQI Clinical Practice Guidelines and Clinical Practice Recommendations for 2006 Updates: Hemodialysis Adequacy, Peritoneal Dialysis Adequacy and Vascular Access. *Am J Kidney Dis* 2006; 48(suppl 1): S1–S322.
216. Keijsers RG, Grutters JC, Thomeer M, et al. Imaging the inflammatory activity of sarcoidosis: sensitivity and inter observer agreement of (67)Ga imaging and (18)F-FDG PET. *Q J Nucl Med Mol Imaging.* 2011;55(1):66-71.
217. Khor YM, Cuddy S, Falk RH, Dorbala S. Multimodality Imaging in the Evaluation and Management of Cardiac Amyloidosis. *Semin Nucl Med.* 2020;50(4):295-310.
218. Kim IY, Kim MJ, Lee DW, et al. Cardiac valve calcification is associated with presence and severity of coronary artery disease in patients with predialysis chronic kidney disease. *Clin Exp Nephrol.* 2015;19(6):1090–1097.
219. Kim J, Yum B, Palumbo MC, et al. Left Atrial Strain Impairment Precedes Geometric Remodeling as a Marker of Post-Myocardial Infarction Diastolic Dysfunction. *JACC Cardiovasc Imaging.* 2020; S1936-878X(20)30617-3.
220. Kim JS, Judson MA, Donnino R, et al. Cardiac sarcoidosis. *Am Heart J.* 2009;157(1):9-21.
221. Kim JS, Yang JW, Yoo JS, Choi SO, Han BG. Association between E/e' ratio and fluid overload in patients with predialysis chronic kidney disease. *PLoS ONE.* 2017;12(9):e0184764.

222. Kirolos I, Yakoub D, Pendola F et al. Cardiac physiology in post myocardial infarction patients: the effect of cardiac rehabilitation programs-a systematic review and update meta-analysis. *Ann Transl Med.* 2019;7(17):416.
223. Kis E, Ablonczy L, Reusz GS. Cardiac magnetic resonance imaging of the myocardium in chronic kidney disease. *Kidney Blood Press Res.* 2018; 43(1):134–142.
224. Kittleson MM, Maurer MS, Ambardekar AV, et al. Cardiac Amyloidosis: Evolving Diagnosis and Management: A Scientific Statement From the American Heart Association. *Circulation.* 2020;142(1):e7-e22.
225. Klarich KW, Attenhofer Jost CH, Binder J, et al. Risk of death in long-term follow-up of patients with apical hypertrophic cardiomyopathy. *Am J Cardiol.* 2013;111(12):1784-1791.
226. Klein AL, Hatle LK, Taliercio CP, et al. Prognostic significance of Doppler measures of diastolic function in cardiac amyloidosis. A Doppler echocardiography study. *Circulation.* 1991;83(3):808-816.
227. Knight DS, Zumbo G, Barcella W, et al. Cardiac Structural and Functional Consequences of Amyloid Deposition by Cardiac Magnetic Resonance and Echocardiography and Their Prognostic Roles. *JACC Cardiovasc Imaging.* 2019;12(5):823-833.
228. Kohler M, Blair E, Risby P, et al. The prevalence of obstructive sleep apnoea and its association with aortic dilatation in Marfan’s syndrome. *Thorax* 2009; 64:162-166.
229. Korcarz CE, Benca R, Barnet JH, Stein JH. Treatment of Obstructive Sleep Apnea in Young and Middle-Aged Adults: Effects of Positive Airway Pressure and Compliance on Arterial Stiffness, Endothelial Function, and Cardiac Hemodynamics. *J Am Heart Assoc* 2016; 5:e002930.
230. Korcarz CE, Peppard PE, Young TB, Chapman CB, Hla KM, Barnet JH, et al. Effects of Obstructive Sleep Apnea and Obesity on Cardiac Remodeling: The Wisconsin Sleep Cohort Study. *Sleep* 2016; 39:1187-1195.
231. Kotecha T, Martinez-Naharro A, Treibel TA, et al. Myocardial Edema and Prognosis in Amyloidosis. *J Am Coll Cardiol.* 2018;71(25):2919-2931.
232. Kouranos V, Tzelepis GE, Rapti A, et al. Complementary Role of CMR to Conventional Screening in the Diagnosis and Prognosis of Cardiac Sarcoidosis. *JACC Cardiovasc Imaging.* 2017;10(12):1437-1447.
233. Kovacs A, Tapolyai M, Celeng C, et al. Impact of hemodialysis, left ventricular mass and FGF-23 on myocardial mechanics in end-stage renal disease: a three-dimensional speckle tracking study. *Int J Cardiovasc Imaging.* 2014; 30(7):1331–1337.
234. Kramer A, Stel VS, Caskey FJ, et al. Exploring the association between macroeconomic indicators and dialysis mortality. *Clin J Am Soc Nephrol.* 2012; 7(10):1655-1663.
235. Kramer CM, Appelbaum E, Desai MY, et al. Hypertrophic Cardiomyopathy Registry: The rationale and design of an international, observational study of hypertrophic cardiomyopathy. *Am Heart J.* 2015;170(2):223-230.

236. Kremastinos DT, Farmakis D. Iron overload cardiomyopathy in clinical practice. *Circulation*. 2011;124(20):2253-2263.
237. Krenning BJ, Voormolen MM, Geleijnse ML, et al. Three-dimensional echocardiographic analysis of left ventricular function during hemodialysis. *Nephron Clin Pract*. 2007;107(2):c43–c49.
238. Krishnasamy R, Isbel NM, Hawley CM, et al. The association between left ventricular global longitudinal strain, renal impairment and all-cause mortality. *Nephrol Dial Transplant*. 2014;29(6):1218–1225.
239. Kume T, Uemura S. Current clinical applications of coronary optical coherence tomography. *Cardiovasc Interv Ther*. 2018; 33(1):1–10.
240. Kurmann R, Mankad SV, Mankad R. Echocardiography in Sarcoidosis. *Curr Cardiol Rep*. 2018;20(11):118.
241. Kusunose K, Fujiwara M, Yamada H, et al. Deterioration of biventricular strain is an early marker of cardiac involvement in confirmed sarcoidosis. *Eur Heart J Cardiovasc Imaging*. 2020;21(7):796-804.
242. Kyriakou P, Mouselimis D, Tsarouchas A, et al. Diagnosis of cardiac amyloidosis: a systematic review on the role of imaging and biomarkers. *BMC Cardiovasc Disord*. 2018;18(1):221.
243. Lang RM, Badano LP, Mor-Avi V, Afilalo J, Armstrong A, Ernande L, Flachskampf FA, Foster E, Goldstein SA, Kuznetsova T, Lancellotti P, Muraru D, Picard MH, Rietzschel ER, Rudski L, Spencer KT, Tsang W, Voigt JU. Recommendations for cardiac chamber quantification by echocardiography in adults: an update from the American Society of Echocardiography and the European Association of Cardiovascular Imaging. *Eur Heart J Cardiovasc Imaging*. 2015;16(3):233-270.
244. Lang RM, Bierig M, Devereux RB, Flachskampf FA, Foster E, Pellikka PA, et al. Recommendations for chamber quantification: a report from the American Society of Echocardiography's Guidelines and Standards Committee and the Chamber Quantification Writing Group, developed in conjunction with the European Association of Echocardiography, a branch of the European Society of Cardiology. *J Am Soc Echocardiogr* 2005;18(12):1440-1463.
245. Law WP, Wang WY, Moore PT, Mollee PN, Ng AC. Cardiac Amyloid Imaging with 18F-Florbetaben PET: A Pilot Study. *J Nucl Med*. 2016;57(11):1733-1739.
246. Lee CHK, Leow LC, Song PR, Li H, Ong TH. Acceptance and Adherence to Continuous Positive Airway Pressure Therapy in patients with Obstructive Sleep Apnea (OSA) in a Southeast Asian privately funded healthcare system. *Sleep Sci*. 2017; 10(2):57-63.
247. Lee JE, Lee YK, Choi EJ, Nam JS, Choi BW, Kim BS. Usefulness of multidetector row computed tomography for predicting cardiac events in asymptomatic chronic kidney disease patients at the initiation of renal replacement therapy. *ScientificWorldJournal*. 2013; 2013:916354.

248. Lee SP, Park K, Kim HK, Kim YJ, Sohn DW. Apically displaced papillary muscles mimicking apical hypertrophic cardiomyopathy. *Eur Heart J Cardiovasc Imaging*. 2013;14(2):128-134.
249. Lesyuk W, Kriza C, Kolominsky-Rabas P. Cost-of-illness studies in heart failure: a systematic review 2004-2016. *BMC Cardiovascular Disorders* 2018; 18 (1):74.
250. Leung DY, Ng ACT. Emerging clinical role of strain imaging in echocardiography. *Heart Lung Circ* 2010; 19:161–174.
251. Levey AS, Stevens LA, Schmid CH, Zhang YL, Castro AF, 3rd, Feldman HI, Kusek JW, Eggers P, Van Lente F, Greene T, Coresh J, Ckd EPI. A new equation to estimate glomerular filtration rate. *Ann Intern Med*. 2009;150(9):604-612.
252. Levey AS, Stevens LA, Schmid CH, Zhang YL, Castro AF, 3rd, Feldman HI, Kusek JW, Eggers P, Van Lente F, Greene T, Coresh J, Ckd EPI. A new equation to estimate glomerular filtration rate. *Ann Intern Med* 2009; 150 (9):604-612.
253. Levin A, Lamb EJ, White CT, Stevens PE, Bilous RW, Coresh J, De Francisco ALM, De Jong PE, Griffith KE, Hemmelgarn BR, Iseki K, Levey AS, Riella MC, Shlipak MG, Wang H, Winearls CG. Kidney disease: Improving global outcomes (KDIGO) CKD work group. KDIGO 2012 clinical practice guideline for the evaluation and management of chronic kidney disease. *Kidney Int Suppl Kidney International Supplements*. 2013; 3(1):1-150.
254. Levin NW, Zhu F, Keen M. Interdialytic weight gain and dry weight. *Blood Purif* 2001; 19: 217–221.
255. Levy WC, Mozaffarian D, Linker DT, Sutradhar SC, Anker SD, Cropp AB, Anand I, Maggioni A, Burton P, Sullivan MD, Pitt B, Poole-Wilson PA, Mann DL, Packer M. The Seattle Heart Failure Model: prediction of survival in heart failure. *Circulation* 2006; 113 (11):1424-1433.
256. Leyba K, Wagner B. Gadolinium-based contrast agents: why nephrologists need to be concerned. *Curr Opin Nephrol Hypertens*. 2019; 28(2):154–162.
257. Li J, Li A, Wang J, Zhang Y, Zhou Y. Early left ventricular dysfunction detected by speckle tracking in long-term hemodialysis patients with valvular calcification. *Cardiorenal Med*. 2019;9(1):22–30.
258. Lichtenstein D, Mezière G. A lung ultrasound sign allowing bedside distinction between pulmonary edema and COPD: the comet-tail artifact. *Intensive Care Med* 1998; 24(12):1331–1334.
259. Lichtenstein DA, Mezière GA. Relevance of lung ultrasound in the diagnosis of acute respiratory failure: the BLUE protocol. *Chest* 2008; 134(1):117–125.
260. Lin J, Ma H, Gao L, et al. Left atrial reservoir strain combined with E/E' as a better single measure to predict elevated LV filling pressures in patients with coronary artery disease. *Cardiovasc Ultrasound*. 2020; 18(1):11.

261. Lindahl B, Baron T, Erlinge D, et al. Medical Therapy for Secondary Prevention and Long-Term Outcome in Patients With Myocardial Infarction With Nonobstructive Coronary Artery Disease. *Circulation*. 2017;135(16):1481-1489.
262. Lintingre PF, Nivet H, Clément-Guinaudeau S, et al. High-Resolution Late Gadolinium Enhancement Magnetic Resonance for the Diagnosis of Myocardial Infarction With Nonobstructed Coronary Arteries. *JACC Cardiovasc Imaging*. 2020; 13(5):1135-1148.
263. Liu H, Pozios I, Haileselassie B, et al. Role of Global Longitudinal Strain in Predicting Outcomes in Hypertrophic Cardiomyopathy. *Am J Cardiol*. 2017;120(4):670-675.
264. Liu S, Zhang DL, Guo W, Cui WY, Liu WH. Left ventricular mass index and aortic arch calcification score are independent mortality predictors of maintenance hemodialysis patients. *Hemodial Int* 2012;16(4):504-511.
265. Lofaro D, Jager KJ, Abu-Hanna A, Groothoff JW, Arikoski P, Hoecker B, Roussey-Kesler G, Spasojevic B, Verrina E, Schaefer F, van Stralen KJ, Registry EE-E. Identification of subgroups by risk of graft failure after paediatric renal transplantation: application of survival tree models on the ESPN/ERA-EDTA Registry. *Nephrol Dial Transplant* 2016; 31 (2):317-324.
266. Lofman I, Szummer K, Dahlstrom U, Jernberg T, Lund LH. Associations with and prognostic impact of chronic kidney disease in heart failure with preserved, mid-range, and reduced ejection fraction. *Eur J Heart Fail*. 2017; 19(12):1606–1614.
267. London GM, Pannier B, Guerin AP, Blacher J, Marchais SJ, Darne B, et al. Alterations of left ventricular hypertrophy in and survival of patients receiving hemodialysis: follow-up of an interventional study. *JASN*. 2001; 12(12):2759–67
268. London GM. Cardiovascular disease in chronic renal failure: pathophysiologic aspects. *Seminars in Dialysis* 2003; 16: 85-94.
269. Longhi S, Guidalotti PL, Quarta CC, et al. Identification of TTR-related subclinical amyloidosis with 99mTc-DPD scintigraphy. *JACC Cardiovasc Imaging*. 2014;7(5):531-532.
270. Lu DY, Hailesealassie B, Ventoulis I, et al. Impact of peak provoked left ventricular outflow tract gradients on clinical outcomes in hypertrophic cardiomyopathy. *Int J Cardiol*. 2017;243:290-295.
271. Lu DY, Hailesealassie B, Ventoulis I, et al. E/e' ratio and outcome prediction in hypertrophic cardiomyopathy: the influence of outflow tract obstruction. *Eur Heart J Cardiovasc Imaging*. 2018;19(1):101-107.
272. Ma Y, Zhang B, Zhang Y, Dong Y, Zhang R. Ultrasonic image analysis of longitudinal strain in uremic patients with preserved left ventricular ejection fraction. *Biomed Eng Online*. 2018;17(1):112.
273. Machek P, Jirka T, Moissl U, Chamney P, Wabel P. Guided optimization of fluid status in haemodialysis patients. *Nephrol Dial Transplant* 2010; 25(2):538–544
274. Magri D, Limongelli G, Re F, et al. Cardiopulmonary exercise test and sudden cardiac death risk in hypertrophic cardiomyopathy. *Heart*. 2016;102(8):602-609.

275. Magri D, Re F, Limongelli G, et al. Heart Failure Progression in Hypertrophic Cardiomyopathy - Possible Insights From Cardiopulmonary Exercise Testing. *Circ J*. 2016;80(10):2204-2211.
276. Maher ER, Young G, Smyth-Walsh B, Pugh S, Curtis JR. Aortic and mitral valve calcification in patients with end-stage renal disease. *Lancet*. 1987; 2(8564):875–877.
277. Mahshid M, Paul O, Caroline C et al. Cardiac Rehabilitation Quality Improvement. *J Cardiopulm Rehabil Prev*. 2019;39(2):226-234.
278. Makavos G, Kairis C, Tselegkidi ME, et al. Hypertrophic cardiomyopathy: an updated review on diagnosis, prognosis, and treatment. *Heart Fail Rev*. 2019;24(4):439-459.
279. Malfatto G, Revera M, Branzi G et al. A brief period of intensive cardiac rehabilitation improves global longitudinal strain and diastolic function after a first uncomplicated myocardial infarction. *Acta Cardiologica*. 2017;72(3):284-291.
280. Mallamaci F, Benedetto FA, Tripepi R, et al. Detection of pulmonary congestion by chest ultrasound in dialysis patients. *JACC Cardiovasc Imaging* 2010; 3(6):586–594
281. Mancia G, Fagard R, Narkiewicz K, Redon J, Zanchetti A, Bohm M, et al. 2013 ESH/ESC Guidelines for the management of arterial hypertension: the Task Force for the management of arterial hypertension of the European Society of Hypertension (ESH) and of the European Society of Cardiology (ESC). *Journal of hypertension*. 2013; 31(7):1281-1357.
282. Mandoli GE, Sisti N, Mondillo S, Cameli M. Left atrial strain in left ventricular diastolic dysfunction: have we finally found the missing piece of the puzzle?. *Heart Fail Rev*. 2020; 25(3):409-417.
283. Marian AJ, Braunwald E. Hypertrophic Cardiomyopathy: Genetics, Pathogenesis, Clinical Manifestations, Diagnosis, and Therapy. *Circ Res*. 2017;121(7):749-770.
284. Mariani J Jr, Guedes C, Soares P, et al. Intravascular ultrasound guidance to minimize the use of iodine contrast in percutaneous coronary intervention: the MOZART (Minimizing cOntrast utiliZation With IVUS Guidance in coRonary angioplasTy) randomized controlled trial. *JACC Cardiovasc Interv*. 2014; 7(11):1287–1293.
285. Marie B, Iris U, Nienketer H et al. Association Between Exercise Capacity and Health-Related Quality of Life During and After Cardiac Rehabilitation in Acute Coronary Syndrome Patients: A Substudy of the OPTICARE Randomized Controlled Trial. *American Heart Journal*. 2020;101(4):50-657.
286. Maron BJ, Epstein SE. Clinical significance and therapeutic implications of the left ventricular outflow tract pressure gradient in hypertrophic cardiomyopathy. *Am J Cardiol*. 1986;58(11):1093-1096.
287. Maron BJ, Gardin JM, Flack JM, Gidding SS, Kurosaki TT, Bild DE. Prevalence of hypertrophic cardiomyopathy in a general population of young adults. Echocardiographic analysis of 4111 subjects in the CARDIA Study. Coronary Artery Risk Development in (Young) Adults. *Circulation*. 1995;92(4):785-789.

288. Maron BJ, Ommen SR, Semsarian C, Spirito P, Olivotto I, Maron MS. Hypertrophic cardiomyopathy: present and future, with translation into contemporary cardiovascular medicine. *J Am Coll Cardiol*. 2014;64(1):83-99.
289. Maron BJ, Rowin EJ, Casey SA, Maron MS. How Hypertrophic Cardiomyopathy Became a Contemporary Treatable Genetic Disease With Low Mortality: Shaped by 50 Years of Clinical Research and Practice. *JAMA Cardiol*. 2016;1(1):98-105.
290. Maron BJ. Clinical Course and Management of Hypertrophic Cardiomyopathy. *N Engl J Med*. 2018;379(7):655-668.
291. Maron MS, Finley JJ, Bos JM, et al. Prevalence, clinical significance, and natural history of left ventricular apical aneurysms in hypertrophic cardiomyopathy. *Circulation*. 2008;118(15):1541-1549.
292. Maron MS, Maron BJ, Harrigan C, et al. Hypertrophic cardiomyopathy phenotype revisited after 50 years with cardiovascular magnetic resonance. *J Am Coll Cardiol*. 2009;54(3):220-228.
293. Maron MS, Maron BJ. Clinical Impact of Contemporary Cardiovascular Magnetic Resonance Imaging in Hypertrophic Cardiomyopathy. *Circulation*. 2015;132(4):292-298.
294. Maron MS, Olivotto I, Betocchi S, et al. Effect of left ventricular outflow tract obstruction on clinical outcome in hypertrophic cardiomyopathy. *N Engl J Med*. 2003;348(4):295-303.
295. Maron MS, Olivotto I, Zenovich AG, et al. Hypertrophic cardiomyopathy is predominantly a disease of left ventricular outflow tract obstruction. *Circulation*. 2006;114(21):2232-2239.
296. Martindale JL, Wakai A, Collins SP, Levy PD, Diercks D, Hiestand BC, Fermann GJ, deSouza I, Sinert R. Diagnosing Acute Heart Failure in the Emergency Department: A Systematic Review and Meta-analysis. *Acad Emerg Med*. 2016; 23(3):223-242.
297. Martinez-Naharro A, Abdel-Gadir A, Treibel TA, et al. CMR-Verified Regression of Cardiac AL Amyloid After Chemotherapy. *JACC Cardiovasc Imaging*. 2018;11(1):152-154.
298. Martinez-Naharro A, Baksi AJ, Hawkins PN, Fontana M. Diagnostic imaging of cardiac amyloidosis. *Nat Rev Cardiol*. 2020;17(7):413-426.
299. Martinez-Naharro A, Treibel TA, Abdel-Gadir A, et al. Magnetic Resonance in Transthyretin Cardiac Amyloidosis. *J Am Coll Cardiol*. 2017;70(4):466-477.
300. Masri A, Pierson LM, Smedira NG, et al. Predictors of long-term outcomes in patients with hypertrophic cardiomyopathy undergoing cardiopulmonary stress testing and echocardiography. *Am Heart J*. 2015;169(5):684-692.e1.
301. Mathew AT, Fishbane S, Obi Y, Kalantar-Zadeh K. Preservation of residual kidney function in hemodialysis patients: reviving an old concept. *Kidney Int*. 2016; 90(2):262–271.
302. Matsuo H, Dohi K, Machida H, Takeuchi H, Aoki T, Nishimura H, et al. Echocardiographic Assessment of Cardiac Structural and Functional Abnormalities in

- Patients With End-Stage Renal Disease Receiving Chronic Hemodialysis. *Circ J* 2018; 82(2):586-95.
303. Maurer MS, Bokhari S, Damy T, et al. Expert Consensus Recommendations for the Suspicion and Diagnosis of Transthyretin Cardiac Amyloidosis. *Circ Heart Fail*. 2019;12(9):e006075.
304. Maurer MS, Elliott P, Comenzo R, Semigran M, Rapezzi C. Addressing Common Questions Encountered in the Diagnosis and Management of Cardiac Amyloidosis. *Circulation*. 2017;135(14):1357-1377.
305. McClelland RL, Jorgensen NW, Budoff M, et al. 10-year coronary heart disease risk prediction using coronary artery calcium and traditional risk factors: derivation in the MESA (Multi-Ethnic Study of Atherosclerosis) with validation in the HNR (Heinz Nixdorf Recall) Study and the DHS (Dallas Heart Study). *J Am Coll Cardiol*. 2015; 66(15):1643–1653.
306. McCullough PA. Cardiovascular disease in chronic kidney disease from a cardiologist's perspective. *Curr Opin Nephrol Hypertens* 2004;13: 591-600.
307. McGee WT, Mailloux P, Jodka P, et al. The pulmonary artery catheter in critical care. *Semin Dial* 2006; 19: 480–491.
308. McGill D, Talaulikar G, Potter JM, Koerbin G, Hickman PE. Over time, high-sensitivity TnT replaces NTproBNP as the most powerful predictor of death in patients with dialysis-dependent chronic renal failure. *Clin Chim Acta* 2010; 411:936–939.
309. Mees EJ. Volaemia and blood pressure in renal failure: have old truths been forgotten? *Nephrol Dial Transplant* 1995; 10:1297–1298.
310. Mehta D, Lubitz SA, Frankel Z, et al. Cardiac involvement in patients with sarcoidosis: diagnostic and prognostic value of outpatient testing. *Chest*. 2008;133(6):1426-1435.
311. Mentias A, Raeisi-Giglou P, Smedira NG, et al. Late Gadolinium Enhancement in Patients With Hypertrophic Cardiomyopathy and Preserved Systolic Function. *J Am Coll Cardiol*. 2018;72(8):857-870.
312. Michalska-Kasiczak M, Bielecka-Dabrowa A, von Haehling S, Anker SD, Rysz J, Banach M. Biomarkers, myocardial fibrosis and co-morbidities in heart failure with preserved ejection fraction: an overview. *Arch Med Sci* 2018;14(4):890-909.
313. Miglioranza MH, Gargani L, Sant'Anna RT, et al. Lung ultrasound for the evaluation of pulmonary congestion in outpatients: a comparison with clinical assessment, natriuretic peptides, and echocardiography. *JACC Cardiovasc Imaging* 2013; 6(11):1141–1151.
314. Miglioranza MH, Picano E, Badano LP, Sant'Anna R, Rover M, Zaffaroni F, Sicari R, Kalil RK, Leiria TL, Gargani L. Pulmonary congestion evaluated by lung ultrasound predicts decompensation in heart failure outpatients. *Int J Cardiol*. 2017; 240:271-278.
315. Milani P, Basset M, Russo F, Foli A, Palladini G, Merlini G. The lung in amyloidosis. *Eur Respir Rev*. 2017;26(145):170046.

316. Mitsutake R, Niimura H, Miura S, et al. Clinical significance of the coronary calcification score by multidetector row computed tomography for the evaluation of coronary stenosis in Japanese patients. *Circ J*. 2006; 70(9):1122–1127.
317. Mohamed-Salem L, Santos-Mateo JJ, Sanchez-Serna J, et al. Prevalence of wild type ATTR assessed as myocardial uptake in bone scan in the elderly population. *Int J Cardiol*. 2018;270:192-196.
318. Mohty D, Petitalot V, Magne J, et al. Left atrial function in patients with light chain amyloidosis: A transthoracic 3D speckle tracking imaging study. *J Cardiol*. 2018;71(4):419-427.
319. Mohty D, Pradel S, Magne J, et al. Prevalence and prognostic impact of left-sided valve thickening in systemic light-chain amyloidosis. *Clin Res Cardiol*. 2017;106(5):331-340.
320. Moissl U, Arias-Guille'n M, Wabel P, et al. Bioimpedance guided fluid management in hemodialysis patients. *Clin J Am Soc Nephrol* 2013; 8(9):1575–1582.
321. Moissl U, Bosaeus I, Lemmey A. Validation of a 3C model for determination of body fat mass. *J Am Soc Nephrol* 2007; 18: 257A
322. Moissl UM, Wabel P, Chamney PW, Bosaeus I, Levin NW, Bosy-Westphal A, et al. Body fluid volume determination via body composition spectroscopy in health and disease. *Physiol Meas*. 2006;27(9):921-933.
323. Montone RA, Niccoli G, Fracassi F, et al. Patients with acute myocardial infarction and non-obstructive coronary arteries: safety and prognostic relevance of invasive coronary provocative tests. *Eur Heart J*. 2018; 39(2):91-98.
324. Mor-Avi V, Yodwut C, Jenkins C, et al. Real-time 3D echocardiographic quantification of left atrial volume: multicenter study for validation with CMR. *JACC Cardiovasc Imaging*. 2012 ;5(8):769-777.
325. Moța E, Popa SG, Moța M, Mitrea A, Penescu M, Tuță L, et al. Prevalence of chronic kidney disease and its association with cardio-metabolic risk factors in the adult Romanian population: the PREDATORR study. *Int Urol Nephrol* 2015; 47(11): 1831-1838.
326. Muchtar E, Blauwet LA, Gertz MA. Restrictive Cardiomyopathy: Genetics, Pathogenesis, Clinical Manifestations, Diagnosis, and Therapy. *Circ Res*. 2017;121(7):819-837.
327. Muehlberg F, Toepper A, Fritschi S, Prothmann M, Schulz-Menger J. Magnetic Resonance Imaging Applications on Infiltrative Cardiomyopathies. *J Thorac Imaging* 2016; 31: 336–347.
328. Munnur RK, Nerlekar N, Wong DT. Imaging of coronary atherosclerosis in various susceptible groups. *Cardiovasc Diagn Ther*. 2016;6(4):382–395.
329. Murtagh G, Laffin LJ, Beshai JF, et al. Prognosis of myocardial damage in sarcoidosis patients with preserved left ventricular ejection fraction: risk stratification using cardiovascular magnetic resonance. *Circ Cardiovasc Imaging* 2016; 9: e003738.
330. Nagueh SF, Smiseth OA, Appleton CP, Byrd BF, 3rd, Dokainish H, Edvardsen T, et al. Recommendations for the Evaluation of Left Ventricular Diastolic Function by Echocardiography: An Update from the American Society of Echocardiography and the

- European Association of Cardiovascular Imaging. *Eur Heart J Cardiovasc Imaging*. 2016;17(12):1321-60.
331. Niederau C, Fischer R, Pürschel A, Stremmel W, Häussinger D, Strohmeyer G. Long-term survival in patients with hereditary hemochromatosis. *Gastroenterology*. 1996;110(4):1107-1119.
332. Nienhuis HL, Bijzet J and Hazenberg BP. The prevalence and management of systemic amyloidosis in Western countries. *Kidney Dis* 2016; 2: 10–19.
333. Nijenkamp LLAM, Bollen IAE, van Velzen HG, et al. Sex Differences at the Time of Myectomy in Hypertrophic Cardiomyopathy. *Circ Heart Fail*. 2018;11(6):e004133.
334. Nishimura RA, Seggewiss H, Schaff HV. Hypertrophic Obstructive Cardiomyopathy: Surgical Myectomy and Septal Ablation. *Circ Res*. 2017;121(7):771-783.
335. Nistri S, Olivotto I, Maron MS, et al. β Blockers for prevention of exercise-induced left ventricular outflow tract obstruction in patients with hypertrophic cardiomyopathy. *Am J Cardiol*. 2012;110(5):715-719.
336. Noble VE, Murray AF, Capp R, et al. Ultrasound assessment for extravascular lung water in patients undergoing hemodialysis. Time course for resolution. *Chest* 2009; 135: 1433–1439.
337. Nochioka K, Quarta CC, Claggett B, et al. Left atrial structure and function in cardiac amyloidosis. *Eur Heart J Cardiovasc Imaging*. 2017;18(10):1128-1137.
338. O'Mahony C, Jichi F, Pavlou M, et al. A novel clinical risk prediction model for sudden cardiac death in hypertrophic cardiomyopathy (HCM risk-SCD). *Eur Heart J*. 2014;35(30):2010-2020.
339. Obokata M, Reddy YNV, Borlaug BA. Diastolic Dysfunction and Heart Failure With Preserved Ejection Fraction: Understanding Mechanisms by Using Noninvasive Methods. *JACC Cardiovasc Imaging*. 2020; 13(1 Pt 2):245-257.
340. Oda S, Kidoh M, Nagayama Y, et al. Trends in Diagnostic Imaging of Cardiac Amyloidosis: Emerging Knowledge and Concepts. *Radiographics*. 2020;40(4):961-981.
341. Oda S, Takashio S, Nagamatsu S, et al. Myocardial extracellular volume quantification using CT for the identification of occult cardiac amyloidosis in patients with severe aortic stenosis referred for transcatheter aortic valve replacement. *Amyloid*. 2019;26(2):97-98.
342. Oh JK, Miranda WR, Bird JG, Kane GC, Nagueh SF. The 2016 Diastolic Function Guideline: Is it Already Time to Revisit or Revise Them?. *JACC Cardiovasc Imaging*. 2020; 13(1 Pt 2):327-335.
343. Oh JK. Echocardiography as a noninvasive Swan-Ganz catheter. *Circulation* 2005; 111: 3192-3194.
344. Ohira H, Birnie DH, Pena E, et al. Comparison of (18)F-fluorodeoxyglucose positron emission tomography (FDG PET) and cardiac magnetic resonance (CMR) in corticosteroid-naïve patients with conduction system disease due to cardiac sarcoidosis. *Eur J Nucl Med Mol Imaging*. 2016;43(2):259-269.

345. Ohlmeier C, Mikolajczyk R, Frick J, Prutz F, Haverkamp W, Garbe E. Incidence, prevalence and 1-year all-cause mortality of heart failure in Germany: a study based on electronic healthcare data of more than six million persons. *Clin Res Cardiol* 2015;104(8):688-696.
346. Oldenburg O, Wellmann B, Buchholz A, et al. Nocturnal hypoxaemia is associated with increased mortality in stable heart failure patients. *Eur Heart J*. 2016;37(21):1695-1703.
347. Oliveira W, Campos O, Cintra F, Matos L, Vieira ML, Rollim B, et al. Impact of continuous positive airway pressure treatment on left atrial volume and function in patients with obstructive sleep apnoea assessed by real-time three-dimensional echocardiography. *Heart* 2009; 95:1872-1878.
348. Oliveira W, Poyares D, Cintra F, Vieira ML, Fischer CH, Moises V, Tufik S, Carvalho A, Campos O. Impact of continuous positive airway pressure treatment on right ventricle performance in patients with obstructive sleep apnoea, assessed by three-dimensional echocardiography. *Sleep Med*. 2012; 13(5):510-6.
349. Olivotto I, Cecchi F, Gistri R, et al. Relevance of coronary microvascular flow impairment to long-term remodeling and systolic dysfunction in hypertrophic cardiomyopathy. *J Am Coll Cardiol*. 2006;47(5):1043-1048.
350. Olivotto I, Hellawell JL, Farzaneh-Far R, et al. Novel Approach Targeting the Complex Pathophysiology of Hypertrophic Cardiomyopathy: The Impact of Late Sodium Current Inhibition on Exercise Capacity in Subjects with Symptomatic Hypertrophic Cardiomyopathy (LIBERTY-HCM) Trial. *Circ Heart Fail*. 2016;9(3):e002764.
351. Omrani H, Rai A, Daraei Z, Sadeghi M. Study of echocardiographic changes after kidney transplantation in end-stage renal disease patients. *Med Arch*. 2017;71(6):408–411.
352. Onofriescu M, Hogas S, Voroneanu L, Apetrii M, Nistor I, Kanbay M, Covic AC. Bioimpedance-guided fluid management in maintenance hemodialysis: a pilot randomized controlled trial. *Am J Kidney Dis*. 2014; 64(1):111-118.
353. Onofriescu M, Sîriopol D, Voroneanu L, et al. Overhydration, cardiac function and survival in hemodialysis patients. *PLoS One* 2015; 10(8):e0135691.
354. Orie M, Hirata K, Tanimoto T, et al. Myocardial Damage Detected by Two-Dimensional Speckle-Tracking Echocardiography in Patients with Extracardiac Sarcoidosis: Comparison with Magnetic Resonance Imaging. *J Am Soc Echocardiogr*. 2015;28(6):683-691.
355. Orimoloye OA, Kambhampati S, Hicks AJ, 3rd, Al Rifai M, Silverman MG, Whelton S, et al. Higher cardiorespiratory fitness predicts long-term survival in patients with heart failure and preserved ejection fraction: the Henry Ford Exercise Testing (FIT) Project. *Arch Med Sci*. 2019;15(2):350-358.
356. Ortiz A, Covic A, Fliser D, et al. Epidemiology, contributors to, and clinical trials of mortality risk in chronic kidney failure. *Lancet* 2014; 383(9931):1831–1843.
357. Ortiz A, Massy ZA, Fliser D, et al. Clinical usefulness of novel prognostic biomarkers in patients on hemodialysis. *Nat Rev Nephrol* 2011; 8(3):141–150

358. Osborne DR, Acuff SN, Stuckey A, Wall JS. A Routine PET/CT Protocol with Streamlined Calculations for Assessing Cardiac Amyloidosis Using (18)F-Florbetapir. *Front Cardiovasc Med*. 2015;2:23.
359. Osborne MT, Hulten EA, Singh A, et al. Reduction in ¹⁸F-fluorodeoxyglucose uptake on serial cardiac positron emission tomography is associated with improved left ventricular ejection fraction in patients with cardiac sarcoidosis. *J Nucl Cardiol*. 2014;21(1):166-174.
360. Ozkececi G, Ulasli SS, Akci O, Dural IE, Avsar A, Unlu M, et al. Assessment of pulmonary arterial stiffness in obstructive sleep apnea. *Int J Cardiovasc Imaging* 2016; 32:799-805.
361. Pabst S, Hammerstingl C, Hundt F, et al. Pulmonary hypertension in patients with chronic kidney disease on dialysis and without dialysis: results of the PEPPER-study. *PLoS ONE*. 2012;7(4):e35310.
362. Pagourelis ED, Duchenne J, Mirea O, et al. The Relation of Ejection Fraction and Global Longitudinal Strain in Amyloidosis: Implications for Differential Diagnosis. *JACC Cardiovasc Imaging*. 2016;9(11):1358-1359.
363. Palka P, Lange A, Atherton J, Stafford WJ, Burstow DJ. Biventricular diastolic behaviour in patients with hypertrophic and hereditary hemochromatosis cardiomyopathies. *Eur J Echocardiogr*. 2004;5(5):356-366.
364. Paneni F, Gregori M, Ciavarella GM, et al. Relation between right and left ventricular function in patients undergoing chronic dialysis. *J Cardiovasc Med (Hagerstown)*. 2013;14(4):289–295.
365. Paneni F, Gregori M, Ciavarella GM, et al. Right ventricular dysfunction in patients with end-stage renal disease. *Am J Nephrol*. 2010;32(5):432–438.
366. Paoletti E, De Nicola L, Gabbai FB, et al. Associations of left ventricular hypertrophy and geometry with adverse outcomes in patients with CKD and hypertension. *Clin J Am Soc Nephrol*. 2016;11(2):271–279.
367. Paraskevaidis IA, Farmakis D, Papadopoulos C, et al. Two-dimensional strain analysis in patients with hypertrophic cardiomyopathy and normal systolic function: a 12-month follow-up study. *Am Heart J*. 2009;158(3):444-450.
368. Parfrey PS, Harnett JD, Foley RN, et al. Impact of renal transplantation on uremic cardiomyopathy. *Transplantation*. 1995;60(9):908–914.
369. Parisi V, Paolillo S, Rengo G, Formisano R, Petraglia L, Grieco F, et al. Sleep-disordered breathing and epicardial adipose tissue in patients with heart failure. *Nutr Metab Cardiovasc Dis* 2018; 28:126-132.
370. Park CS, Lee SE, Cho HJ, Kim YJ, Kang HJ, Oh BH, Lee HY. Body fluid status assessment by bio-impedance analysis in patients presenting to the emergency department with dyspnea. *Korean J Intern Med*. 2018; 33(5):911-921.
371. Park JJ, Park JH, Hwang IC, Park JB, Cho GY, Marwick TH. Left Atrial Strain as a Predictor of New-Onset Atrial Fibrillation in Patients With Heart Failure. *JACC Cardiovasc Imaging*. 2020; S1936-878X(20)30436-8.

372. Park M, Hsu CY, Li Y, et al. Associations between kidney function and subclinical cardiac abnormalities in CKD. *J Am Soc Nephrol*. 2012;23(10):1725–1734.
373. Park SJ, Miyazaki C, Bruce CJ, et al. Left ventricular torsion by two-dimensional speckle tracking echocardiography in patients with diastolic dysfunction and normal ejection fraction. *J Am Soc Echocardiogr* 2008; 21:1129–1137.
374. Parker J, Brooks D, Kozar L, et al. Acute and chronic effects of airway obstruction on canine left ventricular performance. *Am J Respir Crit Care Med* 1999; 160:1888–1896.
375. Parrinello G, Paterna S, Di Pasquale P, Torres D, Fatta A, Mezzero M, Scaglione R, Licata G. The usefulness of bioelectrical impedance analysis in differentiating dyspnea due to decompensated heart failure. *J Card Fail*. 2008;14(8):676-686.
376. Pasupathy S, Air T, Dreyer RP, Tavella R, Beltrame JF. Systematic review of patients presenting with suspected myocardial infarction and non-obstructive coronary arteries. *Circulation*. 2015; 131: 861–70.
377. Pasupathy S, Tavella R, Beltrame JF. Myocardial Infarction With Nonobstructive Coronary Arteries (MINOCA): The Past, Present, and Future Management. *Circulation*. 2017; 135(16):1490-1493.
378. Patel MB, Mor-Avi V, Murtagh G, et al. Right Heart Involvement in Patients with Sarcoidosis. *Echocardiography*. 2016;33(5):734-741.
379. Patel MR, Cawley PJ, Heitner JF, et al. Detection of myocardial damage in patients with sarcoidosis. *Circulation*. 2009;120(20):1969-1977.
380. Patrick R, Kristian B, Mark J. Efficacy of exercise-based cardiac rehabilitation post-myocardial infarction: A systematic review and meta-analysis of randomized controlled trials. *American Heart Journal*. 2011;162(4):571-584.
381. Paudel K, Kausik T, Visser A, Ramballi C, Fan SL. Comparing lung ultrasound with bioimpedance spectroscopy for evaluating hydration in peritoneal dialysis patients. *Nephrology (Carlton)* 2015; 20(1):1–5.
382. Pecoits-Filho R, Barberato SH. Echocardiography in chronic kidney disease: diagnostic and prognostic implications. *Nephron Clin Pract* 2010;114(4):c242-7.
383. Peña-García JI, Shaikh SJ, Villacis-Nunez DS, Gurram MK. Pericardial Effusion in Systemic Sarcoidosis: A Rare Manifestation of Cardiac Sarcoid. *Heart Views*. 2019;20(2):56-59
384. Pencina MJ, D'Agostino RB Sr, Steyerberg EW. Extensions of net reclassification improvement calculations to measure usefulness of new biomarkers. *Stat Med* 2011; 30(1):11–21.
385. Pencina MJ, D'Agostino RB. Overall C as a measure of discrimination in survival analysis: model specific population value and confidence interval estimation. *Stat Med* 2004; 23(13):2109–2123.
386. Peng W, Li Z, Xu H, et al. Assessment of right ventricular dysfunction in end-stage renal disease patients on maintenance haemodialysis by cardiac magnetic resonance imaging. *Eur J Radiol*. 2018; 102:89–94.

387. Penicka M, Gregor P, Kerekes R, et al. The effects of candesartan on left ventricular hypertrophy and function in nonobstructive hypertrophic cardiomyopathy: a pilot, randomized study. *J Mol Diagn.* 2009;11(1):35-41.
388. Pennell DJ, Udelson JE, Arai AE, et al. Cardiovascular function and treatment in β -thalassemia major: a consensus statement from the American Heart Association. *Circulation.* 2013;128(3):281-308.
389. Pereira NL, Grogan M, Dec GW. Spectrum of Restrictive and Infiltrative Cardiomyopathies: Part 1 of a 2-Part Series. *J Am Coll Cardiol.* 2018;71(10):1130-1148.
390. Pereira NL, Grogan M, Dec GW. Spectrum of Restrictive and Infiltrative Cardiomyopathies: Part 2 of a 2-Part Series. *J Am Coll Cardiol.* 2018;71(10):1149-1166.
391. Perez IE, Garcia MJ, Taub CC. Multimodality Imaging in Cardiac Sarcoidosis: Is There a Winner?. *Curr Cardiol Rev.* 2016;12(1):3-11.
392. Perry R, Selvanayagam JB. Echocardiography in Infiltrative Cardiomyopathy. *Heart Lung Circ.* 2019; 28(9):1365-1375.
393. Philips B, Madhavan S, James CA, et al. Arrhythmogenic right ventricular dysplasia/cardiomyopathy and cardiac sarcoidosis: distinguishing features when the diagnosis is unclear. *Circ Arrhythm Electrophysiol.* 2014;7(2):230-236.
394. Picano E, Frassi F, Agricola E, Gligorova S, Gargani L, Mottola G. Ultrasound lung comets: a clinically useful sign of extravascular lung water. *J Am Soc Echocardiogr* 2006; 19(3):356–363.
395. Picano E, Gargani L, Gheorghide M. Why, when, and how to assess pulmonary congestion in heart failure: pathophysiological, clinical, and methodological implications. *Heart Fail Rev* 2010; 15(1):63–72.
396. Pierre-Louis B, Prasad A, Frishman WH. Cardiac manifestations of sarcoidosis and therapeutic options. *Cardiol Rev.* 2009;17(4):153-158.
397. Pinedo M, Villacorta E, Tapia C, et al. Inter- and intra-observer variability in the echocardiographic evaluation of right ventricular function. *Rev Esp Cardiol* 2010; 63: 802–809.
398. Pinney JH, Whelan CJ, Petrie A, et al. Senile systemic amyloidosis: clinical features at presentation and outcome. *J Am Heart Assoc.* 2013;2(2):e000098.
399. Platz E, Lewis EF, Uno H, Peck J, Pivetta E, Merz AA, Hempel D, Wilson C, Frasure SE, Jhund PS, Cheng S, Solomon SD. Detection and prognostic value of pulmonary congestion by lung ultrasound in ambulatory heart failure patients. *Eur Heart J.* 2016; 37(15):1244-1251.
400. Platz E, Merz AA, Jhund PS, Vazir A, Campbell R, McMurray JJ. Dynamic changes and prognostic value of pulmonary congestion by lung ultrasound in acute and chronic heart failure: a systematic review. *Eur J Heart Fail.* 2017;19(9):1154-1163.

401. Polikandrioti M, Panoutsopoulos G, Tsami A, Gerogianni G, Saroglou S, Thomai E, Leventzonis I. Assessment of quality of life and anxiety in heart failure outpatients. *Arch Med Sci Atheroscler Dis*. 2019; 4:e38-e46.
402. Ponikowski P, Anker SD, AlHabib KF, Cowie MR, Force TL, Hu S, Jaarsma T, Krum H, Rastogi V, Rohde LE, Samal UC, Shimokawa H, Budi Siswanto B, Sliwa K, Filippatos G. Heart failure: preventing disease and death worldwide. *ESC Heart Fail* 2014; 1(1):4-25.
403. Ponikowski P, Voors AA, Anker SD, et al. 2016 ESC Guidelines for the diagnosis and treatment of acute and chronic heart failure: The Task Force for the diagnosis and treatment of acute and chronic heart failure of the European Society of Cardiology (ESC) Developed with the special contribution of the Heart Failure Association (HFA) of the ESC. *Eur Heart J*. 2016;37(27):2129-2200.
404. Popović ZB, Kwon DH, Mishra M, et al. Association between regional ventricular function and myocardial fibrosis in hypertrophic cardiomyopathy assessed by speckle tracking echocardiography and delayed hyperenhancement magnetic resonance imaging. *J Am Soc Echocardiogr*. 2008;21(12):1299-1305.
405. Pothineni N, Gondi S, Kovelamudi S. Cardiac rehabilitation after percutaneous coronary intervention – Evidence and barriers. *Heart and Mind Journal*. 2018;2(1):1-4.
406. Potter EL, Ramkumar S, Kawakami H, Yang H, Wright L, Negishi T, Marwick TH. Association of Asymptomatic Diastolic Dysfunction Assessed by Left Atrial Strain With Incident Heart Failure. *JACC Cardiovasc Imaging*. 2020; S1936-878X(20)30427-7.
407. Prati F, Di Vito L, Biondi-Zoccai G, et al. Angiography alone versus angiography plus optical coherence tomography to guide decision-making during percutaneous coronary intervention: the Centro per la Lotta contro l'Infarto-Optimisation of Percutaneous Coronary Intervention (CLI-OPCI) study. *Euro Intervention*. 2012; 8(7):823–829.
408. Puntmann VO, Isted A, Hinojar R, Foote L, Carr-White G, Nagel E. T1 and T2 Mapping in Recognition of Early Cardiac Involvement in Systemic Sarcoidosis. *Radiology*. 2017;285(1):63-72.
409. Quarta CC, Solomon SD, Uraizee I, et al. Left ventricular structure and function in transthyretin-related versus light-chain cardiac amyloidosis. *Circulation*. 2014;129(18):1840-1849.
410. Raggi P. Cardiovascular disease: coronary artery calcification predicts risk of CVD in patients with CKD. *Nat Rev Nephrol*. 2017;13(6):324–326.
411. Raimann JG, Zhu F, Wang J, Thijssen S, Kuhlmann MK, Kotanko P, Levin NW, Kaysen GA. Comparison of fluid volume estimates in chronic hemodialysis patients by bioimpedance, direct isotopic, and dilution methods. *Kidney Int*. 2014; 85(4):898-908.
412. Raimondi PM, Lisker J, Rini JN, et al. Myocardial hypoattenuation in cardiac sarcoidosis: CT correlation with CMR, PET and SPECT. *Clin Imaging*. 2020;67:136-142.
413. Raina S, Lensing SY, Nairooz RS, et al. Prognostic Value of Late Gadolinium Enhancement CMR in Systemic Amyloidosis. *JACC Cardiovasc Imaging*. 2016;9(11):1267-1277.

414. Ramchand J, Fava AM, Chetrit M, Desai MY. Advanced imaging for risk stratification of sudden death in hypertrophic cardiomyopathy. *Heart*. 2020;106(11):793-801.
415. Ramirez R, Trivieri M, Fayad ZA, Ahmadi A, Narula J, Argulian E. Advanced Imaging in Cardiac Sarcoidosis. *J Nucl Med*. 2019;60(7):892-898.
416. Rammos A, Meladinis V, Vovas G, Patsouras D. Restrictive Cardiomyopathies: The Importance of Noninvasive Cardiac Imaging Modalities in Diagnosis and Treatment-A Systematic Review. *Radiol Res Pract*. 2017; 2017:2874902.
417. Rapezzi C, Arbustini E, Caforio AL, et al. Diagnostic work-up in cardiomyopathies: bridging the gap between clinical phenotypes and final diagnosis. A position statement from the ESC Working Group on Myocardial and Pericardial Diseases. *Eur Heart J*. 2013;34(19):1448-1458.
418. Raphael CE, Cooper R, Parker KH, et al. Mechanisms of Myocardial Ischemia in Hypertrophic Cardiomyopathy: Insights From Wave Intensity Analysis and Magnetic Resonance. *J Am Coll Cardiol*. 2016;68(15):1651-1660.
419. Rattanasompattikul M, Feroze U, Molnar MZ, et al. Charlson comorbidity score is a strong predictor of mortality in hemodialysis patients. *Int Urol Nephrol* 2012; 44(6):1813-1823.
420. Rattazzi M, Bertacco E, Del Vecchio A, Puato M, Faggin E, Pauletto P. Aortic valve calcification in chronic kidney disease. *Nephrol Dial Transplant*. 2013; 28(12):2968–2976.
421. Rausch K, Scalia GM, Sato K, et al. Left atrial strain imaging differentiates cardiac amyloidosis and hypertensive heart disease. *Int J Cardiovasc Imaging*. 2020;10.1007/s10554-020-01948-9.
422. Reddan DN, Szczech LA, Hasselblad V, et al. Intradialytic blood volume monitoring in ambulatory hemodialysis patients: a randomized trial. *J Am Soc Nephrol* 2005;16(7):2162-2169.
423. Ribeiro Neto ML, Jellis C, Hachamovitch R, et al. Performance of diagnostic criteria in patients clinically judged to have cardiac sarcoidosis: Is it time to regroup?. *Am Heart J*. 2020;223:106-109.
424. Ribeiro S, Ramos A, Brandao A, et al. Cardiac valve calcification in haemodialysis patients: role of calcium-phosphate metabolism. *Nephrol Dial Transplant*. 1998;13(8):2037–2040.
425. Rickham PP. Human Experimentation. Code of Ethics of the World Medical Association. Declaration of Helsinki. *Br Med J*. 1964; 2(5402):177.
426. Rickham PP. Human Experimentation. Code of Ethics of the World Medical Association. Declaration of Helsinki. *Br Med J* 1964; 2 (5402):177.
427. Roes SD, Mollema SA, Lamb HJ, van der Wall EE, de Roos A, Bax JJ. Validation of echocardiographic two-dimensional speckle tracking longitudinal strain imaging for viability assessment in patients with chronic ischemic left ventricular dysfunction and comparison with contrast-enhanced magnetic resonance imaging. *Am J Cardiol*. 2009;104(3):312–317.

428. Roger VL, Weston SA, Redfield MM, Hellermann-Homan JP, Killian J, Yawn BP, Jacobsen SJ. Trends in heart failure incidence and survival in a community-based population. *JAMA*. 2004; 292(3):344-350.
429. Romero-Corral A, Somers VK, Pellikka PA, Olson EJ, Bailey KR, Korinek J, et al. Decreased right and left ventricular myocardial performance in obstructive sleep apnea. *Chest* 2007; 132:1863-1870.
430. Rowin EJ, Maron BJ, Haas TS, et al. Hypertrophic Cardiomyopathy With Left Ventricular Apical Aneurysm: Implications for Risk Stratification and Management [published correction appears in *J Am Coll Cardiol*. 2017 Mar 28;69(12):1652]. *J Am Coll Cardiol*. 2017;69(7):761-773.
431. Rowin EJ, Maron BJ, Maron MS. The Hypertrophic Cardiomyopathy Phenotype Viewed Through the Prism of Multimodality Imaging: Clinical and Etiologic Implications. *JACC Cardiovasc Imaging*. 2020;13(9):2002-2016.
432. Rowin EJ, Maron BJ, Olivotto I, Maron MS. Role of Exercise Testing in Hypertrophic Cardiomyopathy. *JACC Cardiovasc Imaging*. 2017;10(11):1374-1386.
433. Rozwadowska K, Daniłowicz-Szymanowicz L, Fijałkowski M, et al. Can two-dimensional speckle tracking echocardiography be useful for left ventricular assessment in the early stages of hereditary haemochromatosis?. *Echocardiography*. 2018;35(11):1772-1781.
434. Rozwadowska K, Raczak G, Sikorska K, Fijałkowski M, Kozłowski D, Daniłowicz-Szymanowicz L. Influence of hereditary haemochromatosis on left ventricular wall thickness: does iron overload exacerbate cardiac hypertrophy?. *Folia Morphol (Warsz)*. 2019;78(4):746-753.
435. Rutherford E, Talle MA, Mangion K, et al. Defining myocardial tissue abnormalities in end-stage renal failure with cardiac magnetic resonance imaging using native T1 mapping. *Kidney Int*. 2016; 90(4):845–852.
436. Ryszard P, Jadwiga W. Cardiac rehabilitation following myocardial infarction. *Cardiology Journal*. 2008;15(5):481-7.
437. Sado DM, White SK, Piechnik SK, et al. Identification and assessment of Anderson-Fabry disease by cardiovascular magnetic resonance noncontrast myocardial T1 mapping. *Circ Cardiovasc Imaging*. 2013;6(3):392-398.
438. Sakai K, Ikari Y, Nanasato M, et al. Impact of intravascular ultrasound-guided minimum-contrast coronary intervention on 1-year clinical outcomes in patients with stage 4 or 5 advanced chronic kidney disease. *Cardiovasc Interv Ther*. 2018;1–8.
439. Sánchez D, Juan C, Camargo S et al. The Effects of Maintenance Cardiac Rehabilitation. *J Cardiopulm Rehabil Prev*. 2020;40(4):224-244.
440. Sanchez F, Gutierrez JM, Kha LC, et al. Pathological entities that may affect the lungs and the myocardium. Evaluation with chest CT and cardiac MR. *Clin Imaging*. 2020;70:124-135.
441. Sánchez-de-la-Torre M, Campos-Rodriguez F, Barbé F. Obstructive sleep apnoea and cardiovascular disease. *Lancet Respir Med*. 2013;1(1):61-72.

442. Sanner B, Konermann M, Saturnm A, Müller HJ, Zidek W. Right ventricular function in patients with obstructive sleep apnea. *Eur Respir J* 1997; 10:2079-2083.
443. Sano K, Kawasaki M, Ishihara Y, et al. Assessment of vulnerable plaques causing acute coronary syndrome using integrated backscatter intravascular ultrasound. *J Am Coll Cardiol*. 2006;47(4):734–741.
444. Sarnak MJ, Levey AS, Schoolwerth AC, et al. Kidney disease as a risk factor for development of cardiovascular disease: a statement from the American Heart Association Councils on Kidney in Cardiovascular Disease, High Blood Pressure Research, Clinical Cardiology, and Epidemiology and Prevention. *Circulation* 2003; 108(17): 2154–2169.
445. Sawyer AM, Gooneratne NS, Marcus CL, Ofer D, Richards KC, Weaver TE. A systematic review of CPAP adherence across age groups: clinical and empiric insights for developing CPAP adherence interventions. *Sleep Med Rev*. 2011;15(6):343-56.
446. Schiano-Lomoriello V, Galderisi M, Mele D, et al. Longitudinal strain of left ventricular basal segments and E/e' ratio differentiate primary cardiac amyloidosis at presentation from hypertensive hypertrophy: an automated function imaging study. *Echocardiography*. 2016;33(9):1335-1343.
447. Schieda N, Blaichman JI, Costa AF, et al. Gadolinium-based contrast agents in kidney disease: a comprehensive review and clinical practice guideline issued by the canadian association of radiologists. *Can J Kidney Health Dis*. 2018; 5:2054358118778573.
448. Schnell F, Donal E, Bernard-Brunet A, et al. Strain analysis during exercise in patients with left ventricular hypertrophy: impact of etiology. *J Am Soc Echocardiogr*. 2013;26(10):1163-1169
449. Seferović PM, Polovina M, Bauersachs J, et al. Heart failure in cardiomyopathies: a position paper from the Heart Failure Association of the European Society of Cardiology. *Eur J Heart Fail*. 2019;21(5):553-576.
450. Seidel H, Ball J, Dains J. In: Schrefer S (ed) *Mosby's Guide to Physical Examination*. 3rd edn.,1995, p 419.
451. Sekiguchi H, Schenck LA, Horie R, et al. Critical care ultrasonography differentiates ARDS, pulmonary edema, and other causes in the early course of acute hypoxemic respiratory failure. *Chest* 2015;148(4):912-918.
452. Selvaraj S, Shah SJ, Ommerborn MJ, et al. Pulmonary hypertension is associated with a higher risk of heart failure hospitalization and mortality in patients with chronic kidney disease: the jackson heart study. *Circ Heart Fail*. 2017;10(6).
453. Serri K, Reant P, Lafitte M, et al. Global and regional myocardial function quantification by two-dimensional strain: application in hypertrophic cardiomyopathy. *J Am Coll Cardiol*. 2006;47(6):1175-1181.
454. Seward JB, Casaclang-Verzosa G. Infiltrative cardiovascular diseases: cardiomyopathies that look alike. *J Am Coll Cardiol*. 2010;55(17):1769-1779

455. Sharkey RA, Mulloy EM, O'Neill SJ. The acute effects of oxygen and carbon dioxide on renal vascular resistance in patients with an acute exacerbation of COPD. *Chest*. 1999;115(6):1588-1592.
456. Sharma A, Lavie CJ, Borer JS, Vallakati A, Goel S, Lopez-Jimenez F, Arbab-Zadeh A, Mukherjee D, Lazar JM. Meta-analysis of the relation of body mass index to all-cause and cardiovascular mortality and hospitalization in patients with chronic heart failure. *Am J Cardiol* 2015; 115 (10):1428-1434.
457. Sharma R, Chemla E, Tome M, Mehta RL, Gregson H, Brecker SJ, et al. Echocardiography-based score to predict outcome after renal transplantation. *Heart* 2007; 93: 464-469.
458. Sherrid MV, Wever-Pinzon O, Shah A, Chaudhry FA. Reflections of inflections in hypertrophic cardiomyopathy. *J Am Coll Cardiol*. 2009;54(3):212-219.
459. Shigemoto E, Iwata A, Futami M, et al. Influence of chronic kidney disease on coronary plaque components in coronary artery disease patients with both diabetes mellitus and hypertension. *Heart Vessels*. 2019; 34(7):1065–1075.
460. Shivalkar B, Van de Heyning C, Kerremans M et al. Obstructive sleep apnea syndrome: more insights on structural and functional cardiac alterations, and the effects of treatment with continuous positive airway pressure. *J Am Coll Cardiol* 2006; 47:1433-1439.
461. Shizukuda Y, Bolan CD, Tripodi DJ, et al. Does oxidative stress modulate left ventricular diastolic function in asymptomatic subjects with hereditary hemochromatosis?. *Echocardiography*. 2009;26(10):1153-1158.
462. Silberberg JS, Barre PE, Prichard SS, Sniderman AD. Impact of left ventricular hypertrophy on survival in end-stage renal disease. *Kidney Int* 1989; 36(2):286–90.
463. Silbiger JJ. Pathophysiology and Echocardiographic Diagnosis of Left Ventricular Diastolic Dysfunction. *J Am Soc Echocardiogr*. 2019; 32(2):216-232.e2.
464. Sinha AD, Light RP, Agarwal R. Relative plasma volume monitoring during hemodialysis aids the assessment of dry weight. *Hypertension* 2010; 55: 305–311.
465. Siritopol D, Hogas S, Voroneanu L, et al. Predicting mortality in haemodialysis patients: a comparison between lung ultrasonography, bioimpedance data and echocardiography parameters. *Nephrol Dial Transplant* 2013; 28(11):2851–2859.
466. Siritopol D, Siritopol M, Mihaila M, Rusu F, Sascău R, Costache I, Vasiliu V, Bucur A, Neamtu A, Popa R, Cianga P, Kanbay M, Covic A. Prognostic value of lung ultrasonography and bioimpedance spectroscopy in patients with heart failure and reduced ejection fraction. *Arch Med Sci* 2020; 1-9.
467. Siritopol D, Siritopol M, Stuard S, Voroneanu L, Wabel P, Moissl U, Voiculescu D, Covic A. An analysis of the impact of fluid overload and fluid depletion for all-cause and cardiovascular mortality. *Nephrol Dial Transplant* 2019; 34(8):1385-1393.
468. Siritopol D, Voroneanu L, Hogas S, et al. Bioimpedance analysis versus lung ultrasonography for optimal risk prediction in hemodialysis patients. *Int J Cardiovasc Imaging* 2016; 32(2):263–270.

469. Smedema JP, van Geuns RJ, Ainslie G, Ector J, Heidbuchel H, Crijns HJGM. Right ventricular involvement in cardiac sarcoidosis demonstrated with cardiac magnetic resonance. *ESC Heart Fail.* 2017;4(4):535-544.
470. Smilowitz NR, Mahajan AM, Roe MT, Hellkamp AS, Chiswell K, Gulati M, Reynolds HR. Mortality of myocardial infarction by sex, age, and obstructive coronary artery disease status in the ACTION Registry- GWTG (Acute Coronary Treatment and Intervention Outcomes Network Registry-Get With the Guidelines). *Circ Cardiovasc Qual Outcomes.* 2017; 10:e003443.
471. Smiseth OA. Evaluation of left ventricular diastolic function: state of the art after 35 years with Doppler assessment. *J Echocardiogr.* 2018; 16(2):55-64.
472. So A, Lee TY, Tzemos N. Myocardial Perfusion and Scar Assessment in Cardiac Sarcoidosis With Functional Computed Tomography Imaging. *Circ Cardiovasc Imaging.* 2020;13(4):e010046.
473. Sorajja P, Allison T, Hayes C, Nishimura RA, Lam CS, Ommen SR. Prognostic utility of metabolic exercise testing in minimally symptomatic patients with obstructive hypertrophic cardiomyopathy. *Am J Cardiol.* 2012;109(10):1494-1498.
474. Souza FL, Monteiro Junior F, Salgado Filho N. Effect of kidney transplantation on cardiac morphology and function. *Jornal brasileiro de nefrologia* 2012 ; 34(1):94–100.
475. Sperry BW, Reyes BA, Ikram A, et al. Tenosynovial and Cardiac Amyloidosis in Patients Undergoing Carpal Tunnel Release. *J Am Coll Cardiol.* 2018;72(17):2040-2050.
476. Spinelli A, Vinci B, Tirella A, Matteucci M, Gargani L, Ahluwalia A, Domenici C, Picano E, Chiarelli P. Realization of a poro-elastic ultrasound replica of pulmonary tissue. *Biomatter.* 2012; 2(1):37-42.
477. Spirito P, Autore C, Rapezzi C, et al. Syncope and risk of sudden death in hypertrophic cardiomyopathy. *Circulation.* 2009;119(13):1703-1710.
478. Spudich JA. Three perspectives on the molecular basis of hypercontractility caused by hypertrophic cardiomyopathy mutations. *Pflugers Arch.* 2019;471(5):701-717.
479. Stolfo D, Albani S, Savarese G, et al. Risk of sudden cardiac death in New York Heart Association class I patients with dilated cardiomyopathy: A competing risk analysis. *Int J Cardiol.* 2020;307:75-81.
480. Sun BJ, Park JH, Lee M, Choi JO, Lee JH, Shin MS, Kim MJ, Jung HO, Park JR, Sohn IS, Kim H, Kim HK, Cho GY, Park JS, Shim CY, Shin SH, Kim KH, Kim WS, Park SW. Normal Reference Values for Left Atrial Strain and Its Determinants from a Large Korean Multicenter Registry. *J Cardiovasc Imaging.* 2020; 28(3):186-198.
481. Sun M, Cao X, Guo Y, et al. Long-term impacts of hemodialysis on the right ventricle: assessment via 3-dimensional speckle-tracking echocardiography. *Clin Cardiol.* 2018;41(1):87–95.
482. Sun M, Kang Y, Cheng L, et al. Global longitudinal strain is an independent predictor of cardiovascular events in patients with maintenance hemodialysis: a prospective study using

- three-dimensional speckle tracking echocardiography. *Int J Cardiovasc Imaging*. 2016;32(5):757–766.
483. Suzuki J, Shimamoto R, Nishikawa J, et al. Morphological onset and early diagnosis in apical hypertrophic cardiomyopathy: a long term analysis with nuclear magnetic resonance imaging [published correction appears in *J Am Coll Cardiol* 1999 May;33(6):1750]. *J Am Coll Cardiol*. 1999;33(1):146-151.
484. Tamis-Holland JE, Jneid H, Reynolds HR, et al. Contemporary Diagnosis and Management of Patients With Myocardial Infarction in the Absence of Obstructive Coronary Artery Disease: A Scientific Statement From the American Heart Association. *Circulation*. 2019; 139(18):e891-e908.
485. Tamulenaite E, Zvirblyte R, Ereminiene R, Ziginskiene E, Ereminiene E. Changes of left and right ventricle mechanics and function in patients with end-stage renal disease undergoing haemodialysis. *Medicina (Kaunas)*. 2018;54(5):87.
486. Tang M, Batty JA, Lin C, Fan X, Chan KE, Kalim S. Pulmonary hypertension, mortality, and cardiovascular disease in CKD and ESRD patients: a systematic review and meta-analysis. *Am J Kidney Dis*. 2018;72(1):75–83.
487. Tang R, Wang JT, Wang L, et al. Impact of Patient Preparation on the Diagnostic Performance of 18F-FDG PET in Cardiac Sarcoidosis: A Systematic Review and Meta-analysis. *Clin Nucl Med*. 2016;41(7):e327-e339.
488. Taqueti VR, Di Carli MF. Coronary Microvascular Disease Pathogenic Mechanisms and Therapeutic Options: JACC State-of-the-Art Review. *J Am Coll Cardiol*. 2018; 72(21):2625-2641.
489. Tayebi-Khosroshahi H, Abbasnezhad M, Habibzadeh A, Bakhshandeh M, Chaichi P. Left ventricle hypertrophy, dilatation and ejection fraction changes before and after kidney transplantation. *Cardiol Res*. 2013;4(1):31–34.
490. Taylor CJ, Ryan R, Nichols L, Gale N, Hobbs FR, Marshall T (2017) Survival following a diagnosis of heart failure in primary care. *Family Practice* 2017; 34 (2):161-168.
491. Teare D. Asymmetrical hypertrophy of the heart in young adults. *Br Heart J*. 1958;20(1):1-8.
492. Teekakirikul P, Zhu W, Huang HC, Fung E. Hypertrophic Cardiomyopathy: An Overview of Genetics and Management. *Biomolecules*. 2019;9(12):878.
493. Tei C, Dujardin KS, Hodge DO, Kyle RA, Tajik AJ, Seward JB. Doppler index combining systolic and diastolic myocardial performance: clinical value in cardiac amyloidosis. *J Am Coll Cardiol*. 1996;28(3):658-664.
494. Ternacle J, Krapf L, Mohty D, et al. Aortic Stenosis and Cardiac Amyloidosis: JACC Review Topic of the Week. *J Am Coll Cardiol*. 2019;74(21):2638-2651.
495. Thomas L, Muraru D, Popescu BA, et al. Evaluation of Left Atrial Size and Function: Relevance for Clinical Practice. *J Am Soc Echocardiogr*. 2020; 33(8):934-952.
496. Thygesen K, Alpert JS, Jaffe AS, et al. Fourth Universal Definition of Myocardial Infarction (2018). *J Am Coll Cardiol*. 2018; 72(18):2231-2264.

497. To AC, Dhillon A, Desai MY. Cardiac magnetic resonance in hypertrophic cardiomyopathy. *JACC Cardiovasc Imaging*. 2011;4(10):1123-1137.
498. Toepfer CN, Wakimoto H, Garfinkel AC, et al. Hypertrophic cardiomyopathy mutations in *MYBPC3* dysregulate myosin. *Sci Transl Med*. 2019;11(476):eaat1199.
499. Tonelli M, Wiebe N, Culleton B, et al. Chronic kidneydisease and mortality risk: a systematic review. *J Am Soc Nephrol* 2006; 17(7):2034–2047.
500. Tower-Rader A, Kramer CM, Neubauer S, Nagueh SF, Desai MY. Multimodality Imaging in Hypertrophic Cardiomyopathy for Risk Stratification. *Circ Cardiovasc Imaging*. 2020;13(2):e009026.
501. Tower-Rader A, Mohananey D, To A, Lever HM, Popovic ZB, Desai MY. Prognostic Value of Global Longitudinal Strain in Hypertrophic Cardiomyopathy: A Systematic Review of Existing Literature. *JACC Cardiovasc Imaging*. 2019;12(10):1930-1942.
502. Treibel TA, Bandula S, Fontana M, et al. Extracellular volume quantification by dynamic equilibrium cardiac computed tomography in cardiac amyloidosis. *J Cardiovasc Comput Tomogr*. 2015;9(6):585-592.
503. Tripepi G, Benedetto FA, Mallamaci F, Tripepi R, Malatino L, Zoccali C. Left atrial volume monitoring and cardiovascular risk in patients with end-stage renal disease: a prospective cohort study. *J Am Soc Nephrol*. 2007;18(4):1316–1322.
504. Tripepi G, Mattace-Raso F, Mallamaci F, et al. Biomarkers of left atrial volume: a longitudinal study in patients with end stage renal disease. *Hypertension*. 2009; 54(4):818–824.
505. Tsang TSM, Barnes ME, Gersh BJ, Bailey KR, Seward JB. Left atrial volume as a morphophysiologic expression of left ventricular diastolic dysfunction and relation to cardiovascular risk burden. *Am J Cardiol*. 2002; 90(12):1284-9.
506. Tuohy CV, Kaul S, Song HK, Nazer B, Heitner SB. Hypertrophic cardiomyopathy: the future of treatment. *Eur J Heart Fail*. 2020;22(2):228-240.
507. Urbano-Moral JA, Rowin EJ, Maron MS, Crean A, Pandian NG. Investigation of global and regional myocardial mechanics with 3-dimensional speckle tracking echocardiography and relations to hypertrophy and fibrosis in hypertrophic cardiomyopathy. *Circ Cardiovasc Imaging*. 2014;7(1):11-19.
508. Valocikova I, Vachalcova M, Valocik G, et al. Incremental value of global longitudinal strain in prediction of all-cause mortality in predialysis and dialysis chronic kidney disease patients. *Wien Klin Wochenschr*. 2016;128(13–14):495–503.
509. Varghese MJ, Sharma G, Shukla G, Seth S, Mishra S, Gupta A, Bahl VK. Longitudinal ventricular systolic dysfunction in patients with very severe obstructive sleep apnea: A case control study using speckle tracking imaging. *Indian Heart J* 2017; 69:305-310.
510. Velangi PS, Chen KA, Kazmirczak F, et al. Right Ventricular Abnormalities on Cardiovascular Magnetic Resonance Imaging in Patients With Sarcoidosis. *JACC Cardiovasc Imaging*. 2020;13(6):1395-1405

511. Venkatachalam S, Wu G, Ahmad M. Echocardiographic assessment of the right ventricle in the current era: Application in clinical practice. *Echocardiography*. 2017; 34(12):1930-47.
512. Verdiani V, Lastrucci V, Nozzoli C. Worsening renal function in patients hospitalized with acute heart failure: risk factors and prognostic significances. *Int J Nephrol*. 2010; 2011:785974.
513. Vergaro G, Aimo A, Barison A, et al. Keys to early diagnosis of cardiac amyloidosis: red flags from clinical, laboratory and imaging findings. *Eur J Prev Cardiol*. 2020;27(17):1806-1815.
514. Veselka J, Anavekar NS, Charron P. Hypertrophic obstructive cardiomyopathy. *Lancet*. 2017;389(10075):1253-1267.
515. Vitarelli A, D’Orazio S, Caranci F, et al. Left ventricular torsion abnormalities in patients with obstructive sleep apnea syndrome: an early sign of subclinical dysfunction. *Int J Cardiol* 2013; 165:512–518. [SEP]
516. Voigt JU, Mălăescu GG, Haugaa K, Badano L. How to do LA strain. *Eur Heart J Cardiovasc Imaging*. 2020; 21(7):715-717.
517. Volpicelli G, Elbarbary M, Blaivas M, Lichtenstein DA, Mathis G, Kirkpatrick AW, et al., International Liaison Committee on Lung Ultrasound for International Consensus Conference on Lung U. International evidence-based recommendations for point-of-care lung ultrasound. *Intensive care medicine*.2012; 38(4):577-591.
518. Voroneanu L, Sิริopol D, Nistor I, et al. Superior predictive value for NTproBNP compared with high sensitivity cTnT in dialysis patients: a pilot prospective observational study. *Kidney Blood Press Res* 2014; 39(6):636-647.
519. Vural MG, Cetin S, Keser N, Firat H, Akdemir R, Gunduz H. Left ventricular torsion in patients with obstructive sleep apnoea before and after continuous positive airway pressure therapy: assessment by two-dimensional speckle tracking echocardiography. *Acta Cardiol* 2017; 72:638-647.
520. Wabel P, Chamney P, Moissl U, Jirka T. Importance of whole-body bioimpedance spectroscopy for the management of fluid balance. *Blood Purif*. 2009; 27(1):75-80.
521. Wabel P, Moissl U, Chamney P, Jirka T, Machek P, Ponce P, et al. Towards improved cardiovascular management: the necessity of combining blood pressure and fluid overload. *Nephrol Dial Transplant* 2008; 23(9):2965–71.
522. Wachter R, Luthje L, Klemmstein D, Luers C, Stahrenberg R, Edelmann F, et al. Impact of obstructive sleep apnoea on diastolic function. *Eur Respir J* 2013; 41:376-383.
523. Wald R, Goldstein MB, Wald RM, et al. Correlates of left ventricular mass in chronic hemodialysis recipients. *Int J Cardiovasc Imaging* 2014;30(2):349-356.
524. Wang AY, Wang M, Woo J, Lam CW, Li PK, Lui SF, et al. Cardiac valve calcification as an important predictor for all-cause mortality and cardiovascular mortality in long-term peritoneal dialysis patients: a prospective study. *J Am Soc Nephrol* 2003; 14:159-168.

525. Wang J, Khoury DS, Yue Y, et al. Preserved left ventricular twist and circumferential deformation, but depressed longitudinal and radial deformation in patients with diastolic heart failure. *Eur Heart J* 2008; 29:1283–1289.
526. Wang L, Yuan J, Zhang SJ, et al. Myocardial T1 rho mapping of patients with end-stage renal disease and its comparison with T1 mapping and T2 mapping: a feasibility and reproducibility study. *J Magn Reson Imaging*. 2016; 44(3):723–731.
527. Wang Y, Xiong L, Xu Q, et al. Association of left ventricular systolic dysfunction with mortality in incident peritoneal dialysis patients. *Nephrology*. 2018;23(10):927–932.
528. Weaver TE, Grunstein RR. Adherence to continuous positive airway pressure therapy: the challenge to effective treatment. *Proc Am Thorac Soc*. 2008; 5(2):173-8.
529. Weissler-Snir A, Allan K, Cunningham K, et al. Hypertrophic Cardiomyopathy-Related Sudden Cardiac Death in Young People in Ontario. *Circulation*. 2019;140(21):1706-1716.
530. Weng Z, Yao J, Chan RH, et al. Prognostic Value of LGE-CMR in HCM: A Meta-Analysis. *JACC Cardiovasc Imaging*. 2016;9(12):1392-1402.
531. Wigle ED. Cardiomyopathy: The diagnosis of hypertrophic cardiomyopathy. *Heart*. 2001;86(6):709-714.
532. Wizemann V, Wabel P, Chamney P, Zaluska W, Moissl U, Rode C, Malecka-Masalska T, Marcelli D. The mortality risk of overhydration in haemodialysis patients. *Nephrol Dial Transplant* 2009; 24 (5):1574-1579.
533. Wong C, Chen S, Iyngkaran P. Cardiac Imaging in Heart Failure with Comorbidities. *Curr Cardiol Rev*. 2017;13(1):63-75.
534. Xiao Y, Wang LP, Yang YK, et al. Clinical Profile and Prognosis of Left Ventricular Apical Aneurysm in Hypertrophic Cardiomyopathy. *Am J Med Sci*. 2016;351(1):101-110.
535. Yafasova A, Fosbøl EL, Schou M, et al. Long-Term Adverse Cardiac Outcomes in Patients With Sarcoidosis. *J Am Coll Cardiol*. 2020;76(7):767-777.
536. Yamamoto H, Yokochi T. Transthyretin cardiac amyloidosis: an update on diagnosis and treatment. *ESC Heart Fail*. 2019;6(6):1128-1139.
537. Yamazaki M, Ogawa T, Tamei N, Ando Y, Nitta K. Relation of N-terminal pro-B-type natriuretic peptide (NT-proBNP) and left atrial volume index to left ventricular function in chronic hemodialysis patients. *Heart Vessels* 2011;26(4):421-427.
538. Yanagiuchi T, Tada N, Haga Y, et al. Utility of preprocedural multidetector computed tomography in alcohol septal ablation for hypertrophic obstructive cardiomyopathy. *Cardiovasc Interv Ther*. 2019;34(4):364-372.
539. Yang H, Carasso S, Woo A, et al. Hypertrophy pattern and regional myocardial mechanics are related in septal and apical hypertrophic cardiomyopathy. *J Am Soc Echocardiogr*. 2010;23(10):1081-1089.
540. Yang NI, Wang CH, Hung MJ, et al. Real-time three-dimensional echocardiography provides advanced haemodynamic information associated with intradialytic hypotension in patients with autonomic dysfunction. *Nephrol Dial Transplant*. 2010; 25(1):249–254.

541. Yang SQ, Han LL, Dong XL, Wang CY, Xia H, Liu P, et al. Mal-effects of obstructive sleep apnea on the heart. *Sleep Breath* 2012; 16:717-722.
542. Yang WI, Shim CY, Kim YJ, et al. Left atrial volume index: a predictor of adverse outcome in patients with hypertrophic cardiomyopathy. *J Am Soc Echocardiogr.* 2009;22(12):1338-1343.
543. Yazaki Y, Isobe M, Hiroe M, et al. Prognostic determinants of long-term survival in Japanese patients with cardiac sarcoidosis treated with prednisone. *Am J Cardiol.* 2001;88(9):1006-1010
544. Yigla M, Fruchter O, Aharonson D, et al. Pulmonary hypertension is an independent predictor of mortality in hemodialysis patients. *Kidney Int* 2009; 75(9): 969-975.
545. Yigla M, Nakhoul F, Sabag A, et al. Pulmonary hypertension in patients with end-stage renal disease. *Chest.* 2003;123(5):1577–1582.
546. Young T, Palta M, Dempsey J, Skatrud J, Weber S, Badr S. The occurrence of sleep-disordered breathing among middle-aged adults. *N Engl J Med* 1993; 328:1230-1235.
547. Youssef G, Leung E, Mylonas I, et al. The use of 18F-FDG PET in the diagnosis of cardiac sarcoidosis: a systematic review and metaanalysis including the Ontario experience. *J Nucl Med.* 2012;53(2):241-248.
548. Yu WC, Lin YP, Chuang SY, Lin IF, Chenb CH. Cardiovascular determinants of prognosis in normotensive hemodialysis patients. *BMC nephrology* 2012; 13:115.
549. Zakhama L, Herbegue B, Abouda M et al. Impact of obstructive sleep apnea on the right ventricle. *Tunis Med* 2016; 94:612-615.
550. Zhang YM, Lu Y, Tang Y, et al. The effects of different initiation time of exercise training on left ventricular remodeling and cardiopulmonary rehabilitation in patients with left ventricular dysfunction after myocardial infarction. *Disabil Rehabil.* 2016; 38(3):268-276.
551. Zhao L, Tian Z, Fang Q. Risk Factors and Prognostic Role of Left Atrial Enlargement in Patients with Cardiac Light-Chain Amyloidosis. *Am J Med Sci.* 2016;351(3):271-278.
552. Zhou NW, Shu XH, Liu YL, Shen H, Li WJ, Gong X, et al. A Novel Method for Sensitive Determination of Subclinical Left-Ventricular Systolic Dysfunction in Subjects With Obstructive Sleep Apnea. *Respir Care* 2016; 61:366-375.
553. Zlotnick DM, Axelrod DA, Chobanian MC, et al. Non-invasive detection of pulmonary hypertension prior to renal transplantation is a predictor of increased risk for early graft dysfunction. *Nephrol Dial Transplant* 2010; 25(9): 3090-3096.
554. Zoccali C, Benedetto FA, Mallamaci F, et al. Left ventricular mass monitoring in the follow-up of dialysis patients: prognostic value of left ventricular hypertrophy progression. *Kidney Int* 2004; 65(4):1492–1498.
555. Zoccali C, Benedetto FA, Mallamaci F, et al. Prognostic impact of the indexation of left ventricular mass in patients undergoing dialysis. *J Am Soc Nephrol* 2001; 12(12):2768–2774.

556. Zoccali C, Benedetto FA, Mallamaci F, et al. Prognostic value of echocardiographic indicators of left ventricular systolic function in asymptomatic dialysis patients. *J Am Soc Nephrol*. 2004;15(4):1029–1037.
557. Zoccali C, Torino C, Tripepi R, et al. Pulmonary congestion predicts cardiac events and mortality in ESRD. *J Am Soc Nephrol* 2013; 24: 639–646.
558. Zolty R, Hynes PJ, Vittorio TJ. Severe left ventricular systolic dysfunction may reverse with renal transplantation: uremic cardiomyopathy and cardio-renal syndrome. *Am J Transplant*. 2008;8(11):2219–2224.
559. Zou Y, Song L, Wang Z, et al. Prevalence of idiopathic hypertrophic cardiomyopathy in China: a population-based echocardiographic analysis of 8080 adults. *Am J Med*. 2004;116(1):14-18.